2 Anatomy

GROSS ANATOMY AND OVERVIEW

The auditory system comprises the ears and their connections to and within the central nervous system. From the standpoint of physical layout, the auditory system may be divided into the outer, middle, and inner ears; the auditory nerve; and the central auditory pathways. This section provides a very brief and simplified overview of the auditory system, in the hope that a brief glance at the forest will help the student avoid being blinded by the trees. Before proceeding, those not familiar with anatomical terminology should review the pictures in Fig. 2.1 and the definitions in Table 2.1, which summarize some of the terms used to describe the orientation of anatomical structures and the relationships among them.

The major divisions of the ear are shown in Fig. 2.2, and their relative positions within the head are given in Fig. 2.3. The **outer ear** is made up of the pinna (auricle) and ear canal (external auditory meatus). The eardrum (tympanic membrane) separates the outer and middle ears and is generally considered to be part of the latter. The **middle ear** also includes the tympanic (middle ear) cavity; the ossicular chain with its associated muscles, tendons, and ligaments; and the eustachian (auditory) tube. The **inner ear** begins at the oval window. It includes the sensory organs of hearing (the cochlea) and of balance (the semicircular canals, utricle, and saccule). While the balance system is certainly important, the concern here is hearing, and accordingly the balance apparatus is mentioned only insofar as it is directly associated with the auditory system.

The inner ear, beyond the oval window, is composed of the vestibule, the cochlea, and the vestibular apparatus. A membranous duct is continuous throughout these. In the cochlea, it separates the perilymph-filled scala vestibuli and scala tympani above and below from the endolymph-filled scala media between them. The scala media contains the organ of Corti, whose hair cells are the sensory receptors for hearing. When stimulated, the hair cells initiate activity in the auditory nerve fibers with which they are in contact. The **auditory nerve** leaves the inner ear through the internal auditory canal (internal auditory meatus), enters the brain at the angle of the pons and cerebellum, and terminates in the brainstem at the cochlear nuclei. We are now in the central auditory system.

TEMPORAL BONE

The ear is contained within the **temporal bone.** Knowledge of the major landmarks of this bone is thus important in understanding the anatomy and spatial orientation of the ear. The right and left temporal bones are two of the 22 bones that make up the skull. Eight of these bones (including the two temporal bones) contribute to the cranium, and the remaining 14 bones form the facial skeleton. Figure 2.4 gives a lateral (side) view of the skull, emphasizing the temporal bone. The temporal bone forms the inferior portion of the side of the skull. It is bordered by the mandible, zygomatic parietal, sphenoid, and occipital bones. The temporal bone itself is divided into five anatomical divisions: the squamous, mastoid, petrous, and tympanic portions, and the anteroinferiorly protruding styloid process. These parts of the temporal bone, as well as its major landmarks, are shown in Fig. 2.5.

The **squamous portion** is the fan-shaped part of the temporal bone. It is quite thin, often to the point of being translucent. Its inferior surface forms the roof and part of the posterior wall of the ear canal. The **zygomatic process** protrudes forward from the squamous portion to meet the zygomatic bone. The fan-shaped squamous plate is also in contact with the sphenoid bone anteriorly and with the parietal bone superiorly and posteriorly. The mandible attaches to the temporal bone just anterior to the ear canal, near the base of the zygomatic process, forming the **temporomandibular joint.**

The **mastoid portion** lies behind and below the squamous and forms the posterior aspect of the temporal bone. The mastoid portion attaches to the parietal bone superiorly and to the occipital bone posteriorly. It projects downward to form the **mastoid process**, which appears as a somewhat cone-shaped extension below the base of the skull. The mastoid process contains interconnecting air cells of variable size, shape, and number. Continuous with these air cells is a cavity known as the **tympanic antrum**, which lies anterosuperior to the mastoid process. The antrum also connects with the **epitympanic recess (attic)** of the middle ear via the **aditus ad antrum**. The antrum is bordered inferiorly by the mastoid process, superiorly by the thin bony plate called the **tegmen tympani**, medially by the wall of the lateral **semicircular canal**, and laterally by the squamous part.

The **tympanic portion** of the temporal bone forms the floor as well as the anterior and inferoposterior walls of the ear canal. It is bordered superiorly by the squamous and petrous portions and by the mastoid process posteriorly. The lower part of the tympanic portion partially covers the **styloid process**, which is a thin, cylinder-like anteroinferior projection from the base of the temporal bone. The styloid process, which varies in length from as little as 5 mm to as much as 50 mm, is generally considered to be a separate portion of the temporal bone. Although it does not contribute to the hearing mechanism, per se, the styloid process is important as a connecting point for several muscles involved in speech production.

The **petrous portion** houses the sensory organs of hearing and balance and contains the **internal auditory canal**. It is medially directed and is fused at its base to the tympanic and squamous portions. The mastoid lies posterior to the petrous portion, and in fact develops from it postnatally. The details

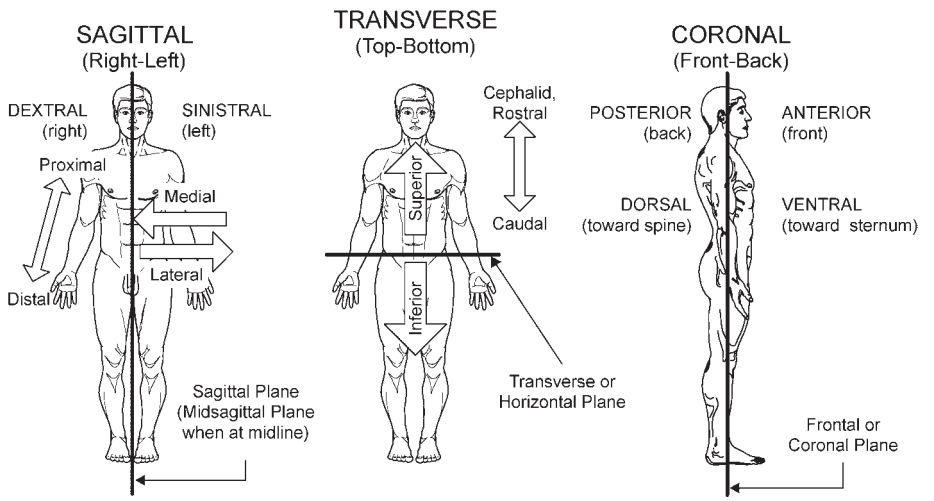

Figure 2.1 Commonly used anatomical orientations and directions. *Source*: From Gelfand (2001), *Essentials of Audiology, Second Edition*, by permission of Thieme Medical Publishers.

of the petrous portion are equivalent to those of the inner ear, discussed below.

OUTER AND MIDDLE EAR

Pinna

The **pinna** (**auricle**) is the external appendage of the ear. It is an irregularly shaped ovoid of highly variable size, which folds over the side of the head posteriorly, superiorly, and inferiorly. It is basically composed of skin-covered elastic cartilage, although it contains some grossly undifferentiated muscles that are of a completely vestigial nature in humans. The pinna has a number of extrinsic muscles as well, which are also essentially vestigial in humans.

The landmarks of the pinna are shown in Fig. 2.6. Most of its perimeter is demarcated by a ridge-like rim called the **helix**.

Table 2.1 Summary of Commonly Used Terms Describing Anatomical Planes, Orientations, and Directions

Term	Definition
Anterior	Front
Caudal	Toward the tail
Cephalad	Toward the head
Contralateral	Opposite side of the body
Coronal plane	Vertical plane separating the structure into front and back; frontal plane
Cranial	Toward the head
Dextral	Right
Distal	Away or further from a reference point (e.g., midline of the body)
Dorsal	Toward the spine (posterior in humans)
Homolateral	Same side of the body
Inferior	Below
Ipsilateral	Same side of the body
Lateral	Away from the midline (toward the side)
Medial	Toward the midline
Midsagittal plane	Sagittal plane at the midline
Posterior	Back
Proximal	Toward, closer to a reference point (e.g., midline of the body)
Rostral	Toward the head (toward the beak)
Sagittal plane	Vertical plane separating the structure into right and left
Sinistral	Left
Superior	Above
Transverse plane	Horizontal plane separating the structure into top and bottom; axial plane
Ventral	Toward the sternum (anterior in humans)

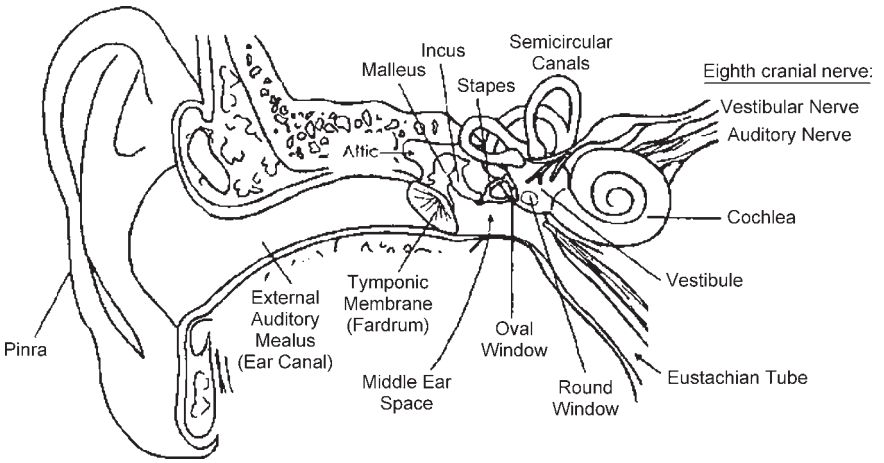

Figure 2.2 Cross-sectional view of the human ear.

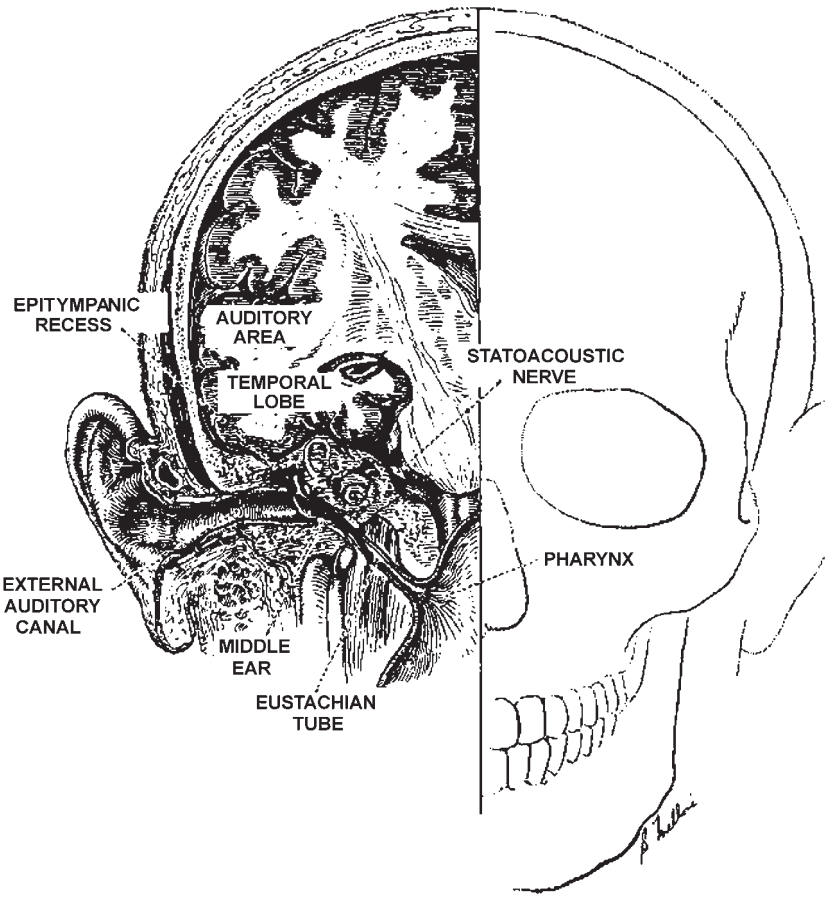

Figure 2.3 Structures of the ear in relation to the head. *Source*: Courtesy of Abbott Laboratories.

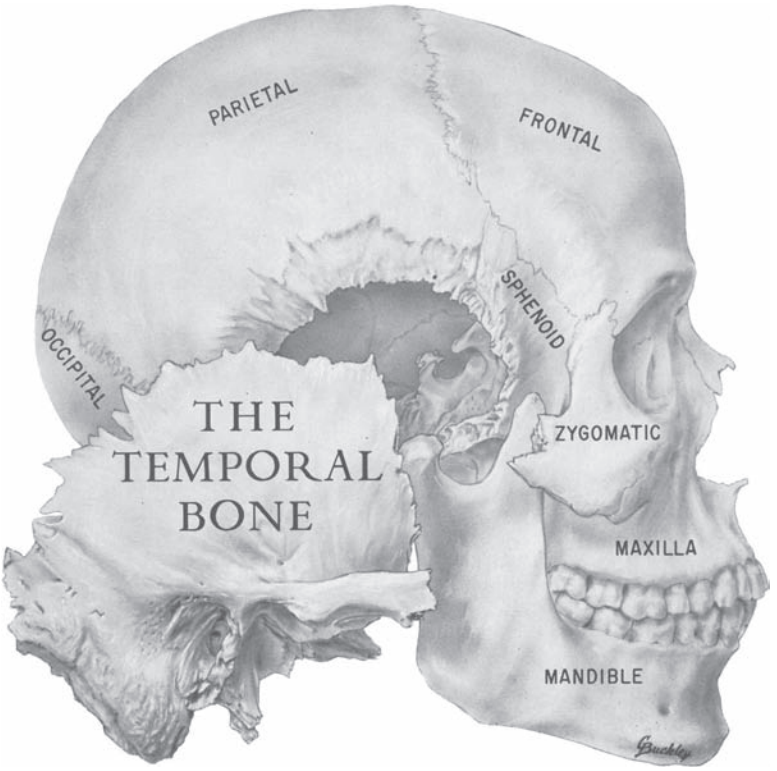

Figure 2.4 Lateral view of the skull emphasizing the position of the temporal bone. *Source*: From Anson and Donaldson (1967). *The Surgical Anatomy of the Temporal Bone and Ear*, Copyright © 1967 by W.B. Saunders, with permission.

If we first follow the helix posteriorly from the top of the ear, we see that it curves widely back and down to end in the **earlobe (lobule)** at the bottom of the pinna. Unlike the rest of the pinna, the lobe does not have any cartilage. Starting again from the apex of the helix, we see that it proceeds anteriorly and downward, and then turns posteriorly in a rather sharp angle to form the **crus of the helix**, which is an almost horizontal shelf at about the center of the pinna. The **scaphoid fossa** is a depression lying between the posterior portion of the helix posteriorly and a ridge called the **antihelix** anteriorly.

The **antihelix** is a ridge that runs essentially parallel to the posterior helix. Its upper end bifurcates to form two crura, a rather wide **superoposterior crus** and a narrower **anterior crus**, which ends under the angle where the helix curves backward. A triangular depression is thus formed by the two crura of the antihelix and the anterior part of the helix, and is called the **triangular fossa**. From the crura, the antihelix curves downward and then forward, and ends in a mound-like widening, the **antitragus.** Opposite and anterior to the antitragus is a backward-folding ridge called the **tragus**. The inferoanterior acute angle formed by the tragus and antitragus is called the **intertragal incisure**. The tragus, the antitragus, and the crus of the helix border a relatively large and cup-shaped depression called the **concha**. Sebaceous glands are present in the skin of the concha as well as in the ear canal. At the bottom of the concha, protected by the tragus, is the entrance to the ear canal.

Ear Canal

The **ear canal (external auditory meatus)** leads from the concha to the eardrum and varies in both size and shape. The outer portion of the canal, about one-third of its length, is cartilaginous; the remaining two-thirds is **bony.** The canal is by no means straight; rather it is quite irregular in its course. It takes on a somewhat S-shaped form medially. It curves first anterosuperiorly, then posterosuperiorly, and finally anteroinferiorly. It is for this reason that the pinna must be pulled up and back in order for one to see the eardrum.

The ear canal has a diameter of about 0.7 cm at its entrance, with an average horizontal diameter of 0.65 cm and a mean vertical diameter of 0.9 cm (Wever and Lawrence, 1954). As would be expected from its irregular course, the length of the canal is not uniform. Instead, it is approximately 2.6 cm long posterosuperiorly and about 3.1 cm long inferoanteriorly (Donaldson and Miller, 1973). Also contributing to the greater length of the lower part of the ear canal is the oblique orientation of the eardrum as it sits in its **annulus** at the end of the canal.

The canal is lined with tight-fitting skin that is thicker in the cartilaginous segment than in the bony part. **Ceruminous (wax)**

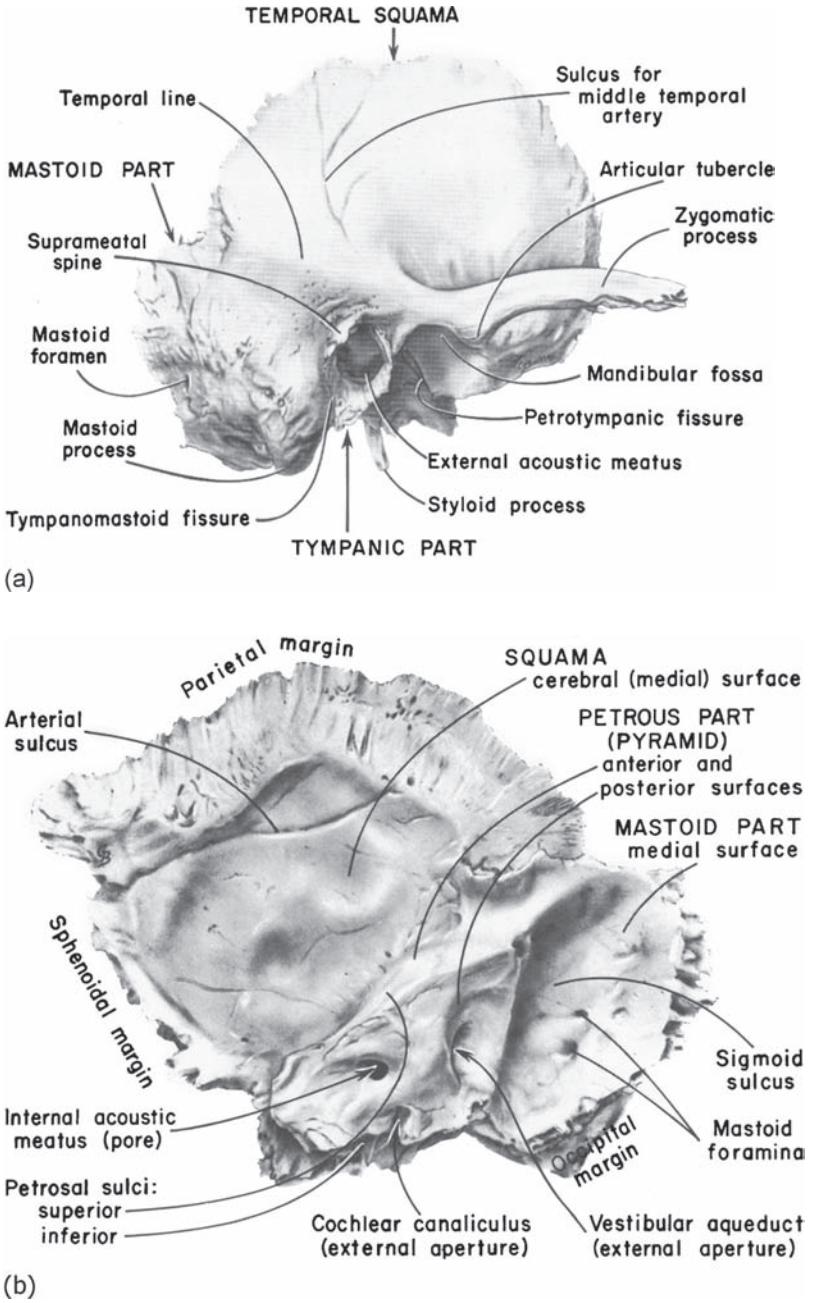

Figure 2.5 Lateral (a) and medial (b) aspects of view of the temporal bone. *Source*: From Anson and Donaldson (1967). *The Surgical Anatomy of the Temporal Bone and Ear*, Copyright © 1967 by W.B. Saunders, with permission.

and **sebaceous (oil) glands** are plentiful in the cartilaginous segment and are also found on the posterior and superior walls of the bony canal. The wax and oil lubricate the canal and help to keep it free of debris and foreign objects. Tiny hairs similarly contribute to the protection of the ear from invasion.

Eardrum

The canal terminates at the **eardrum (tympanic membrane)**, which tilts laterally at the top, so as to sit in its annulus at an angle of about 55° to the ear canal (see Fig. 2.1). The membrane is quite thin and translucent, with an average thickness of approximately

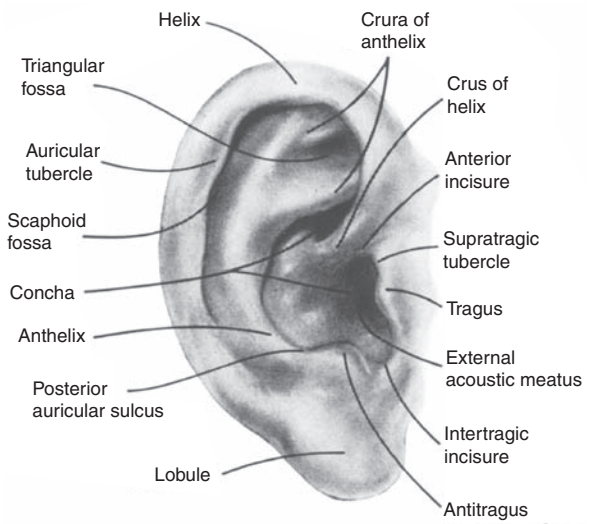

Figure 2.6 Landmarks of the pinna. *Source*: From Anson and Donaldson (1967). *The Surgical Anatomy of the Temporal Bone and Ear*, Copyright © 1967 by W.B. Saunders, with permission.

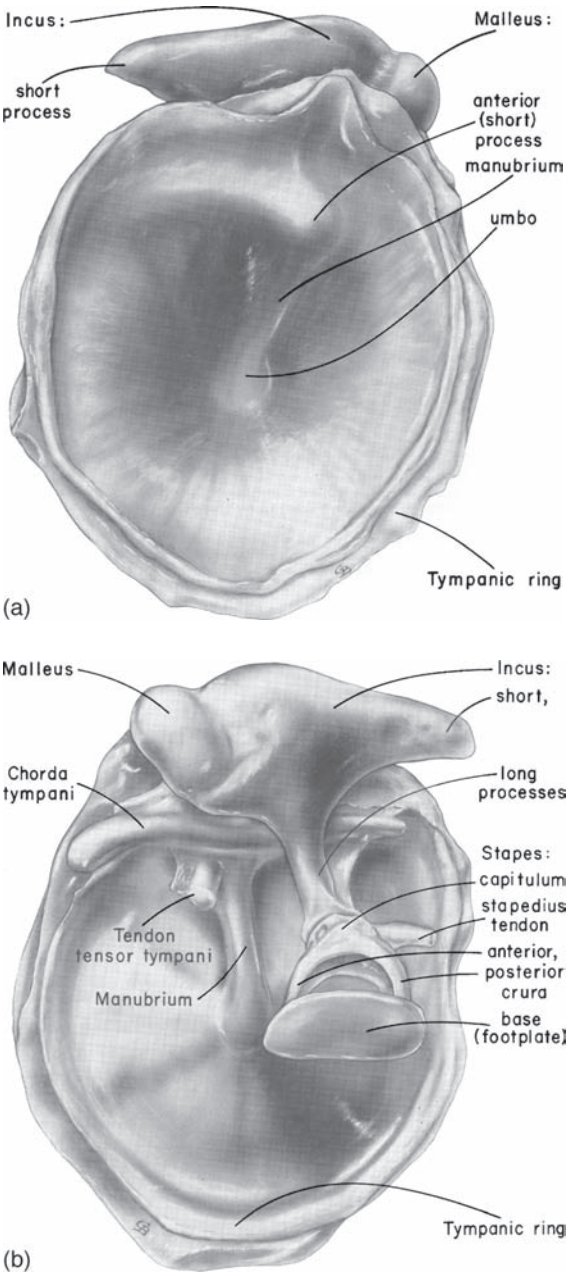

Figure 2.7 Lateral (a) and medial (b) aspects of the tympanic membrane and its connections to the ossicular chain. *Source*: From Anson and Donaldson (1967). *The Surgical Anatomy of the Temporal Bore and Ear*, Copyright © 1967 by W.B. Saunders, with permission.)

0.074 mm (Donaldson and Miller, 1973). It is elliptical in shape, with a vertical diameter of about 0.9 to 1.0 cm and a horizontal cross section of approximately 0.8 to 0.9 cm. The eardrum is concave outward, and the peak of this broad cone is known as the **umbo.** This inward displacement is associated with the drum's attachment to the **manubrium** of the **malleus**, the tip of which corresponds to the umbo (Fig. 2.7). In contact with the drum, the malleus continues upward in a direction corresponding to the 1-o'clock position in the right ear and the 11-o'clock position in the left. The **malleal prominence** of the malleus is formed by the lateral process of the malleus, from which run the **malleal folds**, which divide the drum into the **pars flaccida** above and the **pars tensa** below.

The eardrum is made up of four layers. The outermost layer is continuous with the skin of the ear canal, and the most medial layer is continuous with the mucous membrane of the middle ear. The pars flaccida is composed solely of these two layers. The pars tensa has two additional layers: a layer of radial fibers just medial to the skin layer, and a layer of nonradial fibers between the radial and mucous membrane layers.

Tympanic Cavity

The **middle ear cavity** or **tympanum** may be thought of schematically as a six-sided box or room. The lateral wall is the eardrum, and opposite to it the promontory of the basal cochlear turn forms the medial wall. Figure 2.8 shows such a schematic conceptualization of the right middle ear. The view is as though the lateral wall of the room (the eardrum, shown with the malleus attached to it) had been folded downward to reveal its contents. The front of the head would be toward the right in the drawing and the back of the head would be toward the left.

The roof of the middle ear is formed by the **tegmen tympani**, which separates the middle ear from the middle cranial fossa above. The floor of the tympanum separates it from the jugular bulb. In the anterior wall is the opening to the **eustachian tube**, and above it the canal for the tensor tympani muscle. The canal

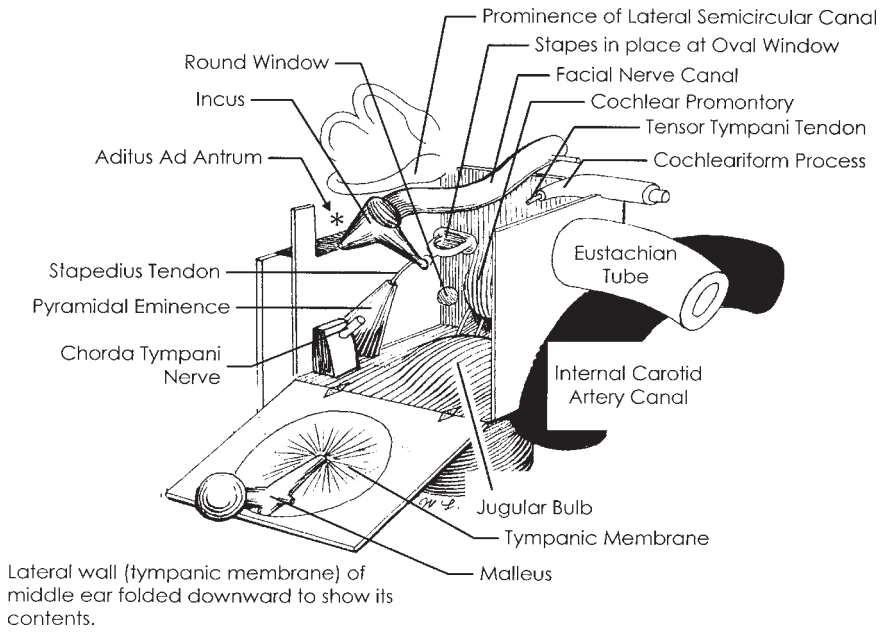

Figure 2.8 Schematic representation of the middle ear as though it were a room with its lateral wall (including the tympanic membrane with the malleus attached) folded downward. *Source*: Adapted from Proctor (1989), *Surgical Anatomy of the Temporal Bone*, by permission of Thieme Medical Publishers.

of the internal carotid artery lies behind the anterior wall, posteroinferior to the tubal opening. The posterior wall contains the **aditus ad antrum**, through which the upper portion of the middle ear called the **epitympanic recess or attic** communicates with the **mastoid antrum**. The posterior wall also contains the **fossa incudis**, a recess that receives the short process of the incus, and the **pyramidal eminence**, which houses the **stapedial muscle**. The **stapedial tendon** exits from the pyramidal prominence at its apex.

Returning to the medial wall, we see that the **oval window** is located posterosuperiorly to the **promontory**, while the **round window** is posteroinferior to the latter. Superior to the oval window lies the **facial canal prominence** with the **cochleariform process** on its anterior aspect. The **tendon** of the **tensor tympani muscle** bends around the cochleariform process to proceed laterally to the malleus.

The **eustachian tube**, also known as the **auditory tube**, serves to equalize the air pressure on both sides of the eardrum as well as allow for drainage of the middle ear by serving as a portal into the nasopharynx. Its principal features are highlighted in relation to the structures of the ear in Fig. 2.9. From its opening in the middle ear, the eustachian tube courses medially, downward at an angle of approximately 45°, and forward to exit into the nasopharynx via a prominence called the **torus tubarius.** The overall length of the tube is about 3.5 cm. The lateral first third of the eustachian tube beginning at the middle ear is surrounded by bone, whereas the remainder is enclosed within an incomplete ring of hook-shaped elastic cartilage, as illustrated in Fig. 2.9. The meeting of the **bony and cartilaginous portions** is called the **isthmus.** At this point, the lumen of the tube may be as little as 1.0 to 1.5 mm compared to a diameter of about 3.0 to 6.0 mm at its opening into the middle ear. The cartilaginous part of the eustachian tube is normally closed (Fig. 2.10a), and it opens reflexively by action of the **tensor palatini muscle**, which

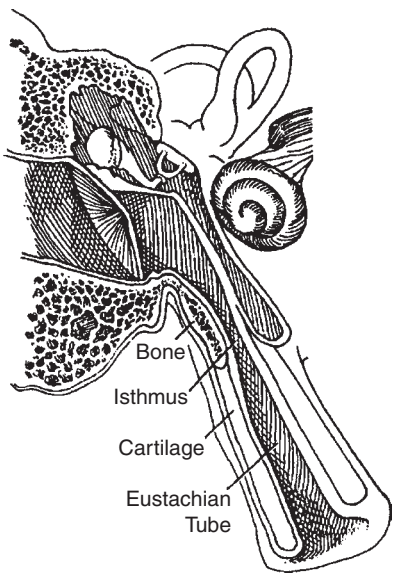

Figure 2.9 Orientation of the eustachian tube with respect to the ear. *Source*: Adapted from Hughes (1985), *Textbook of Otology*, by permission of Thieme Medical Publishers.

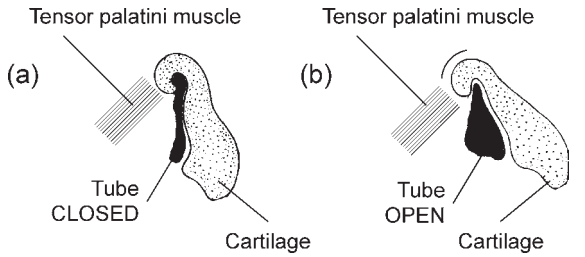

Figure 2.10 (a) Cross-section of the hook-shaped cartilage in the normally closed state of the tube. (b) Opening of the tube by action of the tensor palatini muscles, which uncurls the hook-shaped cartilage. *Source*: Adapted from Gelfand (2001), *Essentials of Audiology, Second Edition*, by permission of Thieme Medical Publishers.

uncurls the normally hook-shaped cartilages (Fig. 2.10b) in response to swallowing, yawning, sneezing, or shouting.

Ossicular Chain

Sound energy impinging upon the eardrum is conducted to the inner ear by way of the ossicles, which are the smallest bones in the body. There are three ossicles in each ear, the **malleus, incus, and stapes**; they are collectively referred to as the **ossicular chain**. Schematic illustrations of these bones are shown with the ossicular chain in place in Fig. 2.11. (Different and somewhat more life-like perspectives of the ossicles may also be seen in Fig. 2.7.) Instead of being attached to the other bones of the skull, the ossicular chain is *suspended* in the middle ear by a series of ligaments, by the tendons of the two intratympanic muscles, and by the attachments of the malleus to the eardrum and of the stapes to the oval window.

The malleus is commonly called the hammer, although it more closely resembles a mace. It is the largest of the ossicles, being about 8 to 9 mm long and weighing approximately 25 mg. The head of the malleus is located in the epitympanic space, to which it is connected by its superior ligament. Laterally, the **manubrium** (handle) is embedded between the mucous membrane and fibrous layers of the eardrum. The anterior process of the malleus projects anteriorly from the top of the manubrium just below the neck. It attaches to the tympanic notch by its anterior ligament, which forms the axis of mallear movement. The malleus is connected to the tensor tympani muscle via a tendon, which inserts at the top of the manubrium.

The **incus** bears a closer resemblance to a tooth with two roots than to the more commonly associated anvil. It weighs approximately 30 mg and has a length of about 5 mm along its short process and about 7 mm along its long process. Its body is connected to the posteromedial aspect of the mallear head within the epitympanic recess. The connection is by a saddle joint, which was originally thought to move by a cog-like mechanism when the malleus was displaced (Helmholtz, 1868). However, subsequent research demonstrated that these

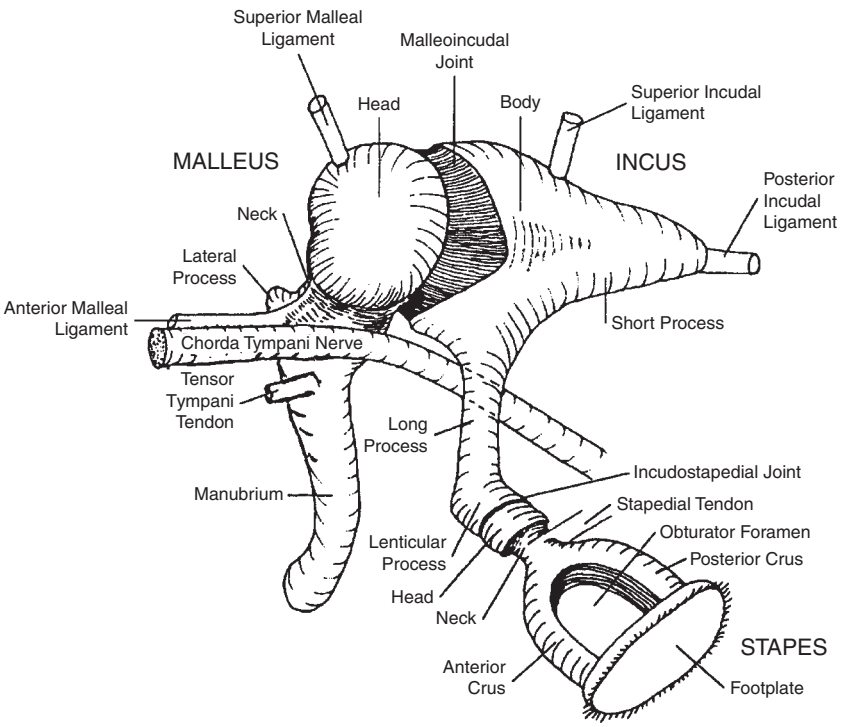

Figure 2.11 Schematic representation of the ossicular chain. *Source*: Adapted from Tos (1995), *Manual of Middle Ear Surgery*, *Vol 2*, by permission of Thieme Medical Publishers.

two bones move as a unit rather than relative to one another (Wever and Lawrence, 1954). The short process of the incus connects via its posterior ligaments to the fossa incudis on the posterior wall of the tympanic cavity. Its long process runs inferiorly, parallel to the manubrium. The end of the long process then bends medially to articulate with the head of the stapes in a true ball-and-socket joint.

The **stapes** (stirrup) is the smallest of the ossicles. It is about 3.5 mm high, and the footplate is about 3 mm long by 1.4 mm wide. It weighs on the order of 3 to 4 mg. The head of the stapes connects to the footplate via two crura. The anterior crus is straighter, thinner, and shorter than the posterior crus. The **footplate**, which encases the very fine stapedial membrane, is attached to the oval window by the annular ligament. The stapedius tendon inserts on the posterior surface of the neck of the stapes and connects the bone to the stapedius muscle.

Intratympanic Muscles

The middle ear contains two muscles, the tensor tympani and the stapedius (Figs. 2.7 and 2.8). The **stapedius muscle** is the smallest muscle in the body, with an average length of 6.3 mm and a mean cross-sectional area of 4.9 mm^2 (Wever and Lawrence, 1954). This muscle is completely encased within the pyramidal eminence on the posterior wall of the tympanic cavity and takes origin from the wall of its own canal. Its tendon exits through the apex of the pyramid and courses horizontally to insert on the posterior aspect of the neck of the stapes. Contraction of the stapedius muscle thus pulls the stapes posteriorly. The stapedius is innervated by the stapedial branch of the **seventh cranial (facial) nerve**.

The **tensor tympani muscle** has an average length of 25 mm and a mean cross-sectional area of approximately 5.85 mm^2 (Wever and Lawrence, 1954). The tensor tympani occupies an *osseous semicanal* on the anterior wall of the tympanum, just superior to the eustachian tube, from which it is separated by a thin bony shelf. The muscle takes origin from the cartilage of the auditory tube, from the walls of its own canal, and from the part of the sphenoid bone adjacent to the canal. Emerging from the canal, the tendon of the tensor tympani hooks around the **cochleariform process**, and inserts on the top of the manubrium of the malleus. Contraction of the tensor tympani thus pulls the malleus anteromedially, at a right angle to the uninterrupted motion of the ossicles. The tensor tympani muscle is innervated by the tensor tympani branch of the otic ganglion of the **fifth cranial (trigeminal) nerve**.

Both intratympanic muscles are completely encased within bony canals and attach to the ossicular chain by way of their respective tendons. Bekesy (1936) pointed out that this situation reduces the effects that muscular contractions might have upon the transmission of sound through the middle ear system. Contraction of either muscle increases the stiffness of the ossicular chain as well as of the eardrum. The stapedius muscle pulls posteriorly whereas the tensor tympani pulls anteromedially so that they might initially be thought to be antagonists. However, the effect of these muscles is to lessen the amount of energy conducted by the ossicular chain, and they thus function as synergists with respect to hearing.

Of particular interest in this context is the **acoustic reflex**, which is the response of the intratympanic muscles to intense sound stimulation. It is generally accepted that the acoustic reflex *in humans is* due mainly, if not exclusively, to contraction of the *stapedius* muscle. In contrast, auditory activation of the tensor tympani muscle in humans occurs only for extremely intense sounds, as part of a *startle* response. The acoustic reflex arc is described in the context of the auditory pathways later in this chapter.

INNER EAR

Osseous and Membranous Labyrinths

The inner ear structures are contained within a system of spaces and canals, the **osseous** or **bony labyrinth**, in the petrous portion of the temporal bone. As shown in Fig. 2.12, these spaces and canals are grossly divided into three sections: the vestibule, the cochlea, and the semicircular canals. The oval window accepts the footplate of stapes and opens medially into the **vestibule**, which is about 4 mm in diameter and is somewhat ovoid in shape. The snail-shaped **cochlea** lies anterior and slightly inferior to the vestibule and is approximately 5 mm high and 9 mm in diameter at its base. Posterior to the vestibule are the three **semicircular canals**, lying at right angles to one another, each about 1 mm in diameter. The general shape of the bony labyrinth is followed by the enclosed **membranous labyrinth**, which contains the *end organs* of hearing and balance. The membranous labyrinth and its principal structures are illustrated in Fig. 2.13.

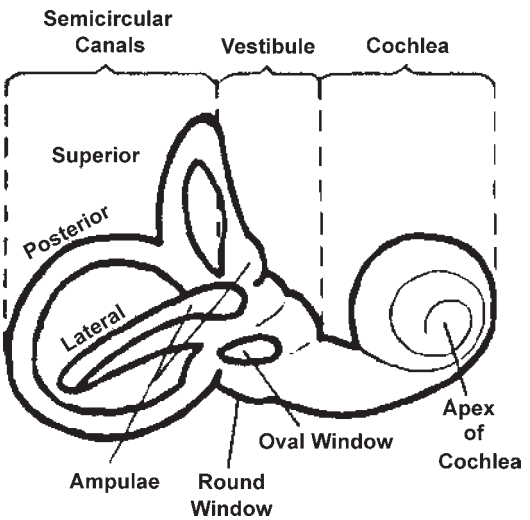

Figure 2.12 The osseous (bony) labyrinth.

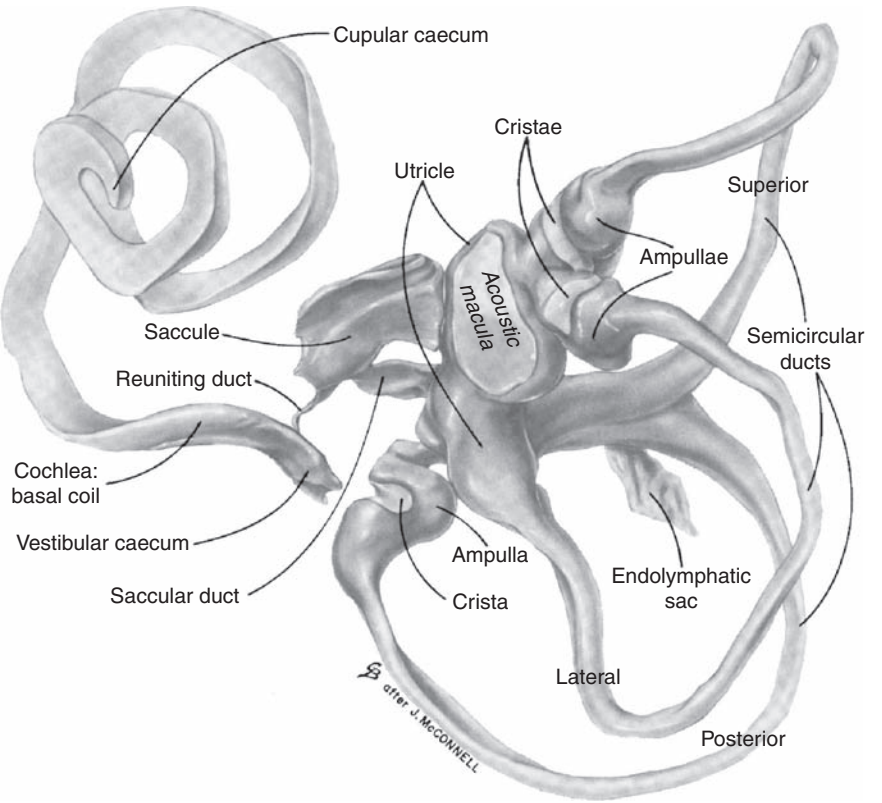

Figure 2.13 The membranous labyrinth. *Source*: From Donaldson and Miller (1973), Anatomy of the ear, in *Otolaryngology*, *Vol. 1*, Paparella and Schurnrick (eds.), Copyright © 1973 by W.B. Saunders (with permission).

Inner Ear Fluids

The spaces between the bony walls of the osseous labyrinth and the membranous labyrinth are filled with a fluid called **perilymph** or **perilymphatic fluid**, and the membranous labyrinth itself is mostly filled with **endolymph** or **endolymphatic fluid**.[1] Because they are located outside of any cells, perilymph and endolymph are referred to as **extracellular fluids**. In contrast, fluids contained within cells are called **intracellular fluids**. Smith Lowry, and Wu (1954) found that perilymph is chemically similar to other extracellular fluids (e.g., cerebrospinal fluid and blood serum) in the sense that it has a very high concentration of sodium and a very low concentration of potassium. Oddly, they found that endolymph has just the opposite concentrations—it is high in potassium but low in sodium. In fact, endolymph has the distinction of being the only extracellular fluid in the body with this characteristic. Subsequent research has not only confirmed the different compositions of perilymph and endolymph, but has also richly expanded our knowledge about their composition and properties, relationships to other fluids and structures, as well as their roles in the cochlea.

The spaces within the organ of Corti itself are filled with perilymph-like fluid that diffuses across the basilar membrane from the scala tympani.[2] As a result, the cochlear hair cells and other structures within the organ of Corti are bathed in a sodium-rich fluid (Slepecky, 1996; Wangemann and Schacht, 1996). Tight junctions among the cells forming the reticular lamina (discussed below) isolate the endolymph above from the organ of Corti below.

The origins of perilymph and endolymph have been the subject of controversy. Perilymph appears to be a derivative of the cerebrospinal fluid and/or the cochlear blood supply, and several lines of evidence have suggested that endolymph components may be derived from perilymph rather than from the blood. Overall, modern experiments disproved early ideas that these fluids are secreted at one site and flow longitudinally to another location, replacing them with the concept that the compositions of the inner ear fluids are maintained locally within the

[1] A third inner ear fluid called **intrastrial fluid** is found in the stria vascularis (see, e.g., Wangemann and Schacht, 1996).

[2] It was previously thought that the organ of Corti contained a distinct sodium-rich fluid called "cortilymph."

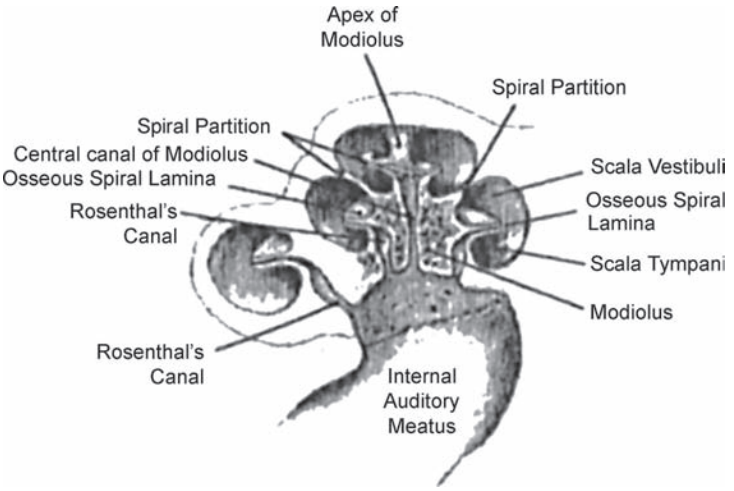

Figure 2.14 The modiolus. *Source*: Adapted from Proctor (1989), *Surgical Anatomy* of *the Ear and Temporal Bone*, by permission of Thieme Medical Publishers.

cochlea (e.g., Ohyama et al., 1998; Salt, 2001; Salt et al., 1986). Informative reviews are provided by Wangemann and Schacht (1996), Salt (2001), and Rask-Andersen, Schrott-Fisher, Pfaller, and Glueckert (2006).

The **cochlear aqueduct** leads from the vicinity of the round window in the scala tympani to the subarachnoid space medial to the dura of the cranium. Although the aqueduct leads from the perilymph-filled scala to the cerebrospinal fluid-filled subarachnoid space, it is not patent in many humans. Thus, it is doubtful that there is any real interchange between these two fluid systems. The **endolymphatic duct** leads from the membranous labyrinth within the vestibule to the **endolymphatic sac**. The sac is located partially between the layers of the dura in the posterior cranial fossa and partly in a niche in the posterior aspect of the petrous portion of the temporal bone.

Vestibular Organs

Returning to the structures of the inner ear, the vestibule contains two **vestibular** or **balance organs**, which are concerned with linear acceleration and gravity effects. These organs are the **utricle and saccule**. The **semicircular canals**, located behind the vestibule, widen anteriorly into five sac-like structures, which open into the somewhat elongated utricle. These widenings are the **ampullae**, and they contain the sensory receptors for rotational acceleration. (The interested reader is referred to any of the fine books listed in the References section for a detailed discussion of the balance system.) The most important connection between the areas of hearing and balance is the **ductus reuniens**, which joins the membranous labyrinth between the cochlea and the utricle.

Cochlea

The **cochlea** is the part of the inner ear concerned with hearing. An extensive albeit rather advanced review of cochlear anatomy and physiology may be found in Dallos, Popper, and Fay (1996). The human cochlea is about 35 mm long and forms a somewhat cone-shaped spiral with about 2 3/4 turns. It is widest at the base, where the diameter is approximately 9 mm, and tapers toward the apex. It is about 5 mm high. The **modiolus** is the core, which forms the axis of the cochlear spiral, as illustrated in Fig. 2.14. Through the modiolus course the auditory nerve and the blood vessels that supply the cochlea. The osseous spiral lamina is a bony ramp-like shelf that goes up the cochlea around the modiolus much like the spiral staircase of a lighthouse, as illustrated in Fig. 2.15. Notice how the basilar membrane is attached to the osseous spiral lamina medially, as it proceeds up the cochlea. Figure 2.16 illustrates how the osseous spiral lamina

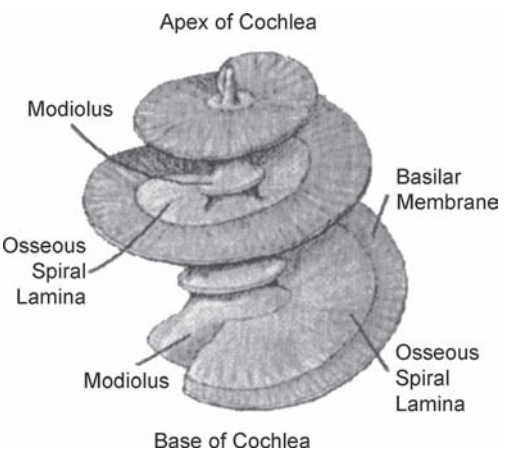

Figure 2.15 The osseous spiral lamina coils around the modiolus like the spiral staircase of a lighthouse. Notice how the basilar membrane is attached to osseous spiral lamina. *Source*: Adapted from Proctor (1989), *Surgical Anatomy of the Ear and Temporal Bone*, by permission of Thieme Medical Publishers.

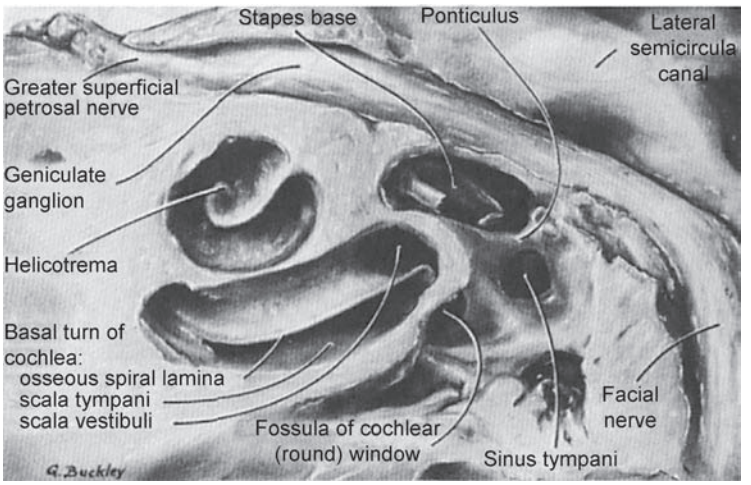

Figure 2.16 The osseous spiral lamina, scala vestibuli, scala tympani, and helicotrema. *Source*: From Anson and Donaldson (1967), *The Surgical Anatomy of the Temporal Bone and Ear*, Copyright © 1967, by W.B. Saunders with permission.

separates the scala vestibuli above from the scala tympani below. It also shows the orientation of the helicotrema at the apical turn, and the relationship between the round window and the scala tympani at the base of the cochlea.

It is easier to visualize the cochlea by imagining that the spiral has been uncoiled, as in Fig. 2.17. In this figure, the base of the cochlea is shown at the left and the apex at the right. We see three chambers: the **scala media**, **scala vestibuli**, and **scala tympani**. The scala media is self-contained and separates the other two. The scalae vestibuli and tympani, on the other hand, communicate with one another at the apex of the cochlea, through an opening called the **helicotrema**. The scala media is enclosed within the membranous labyrinth and contains endolymph, while the other two contain perilymph. The scala vestibuli is in contact with the stapes at the oval window, while the scala tympani has a membrane-covered contact with the middle ear at the round window. The scala media is separated from the scala vestibuli above by **Reissner's membrane**, and from the scala tympani below by the **basilar membrane**. Reissner's membrane is only two cells thick and separates perilymph above from endolymph below without influencing the mechanical properties of the cochlea. In contrast, the basilar membrane plays a major role in cochlear functioning. Bekesy (1960/1989) reported that the basilar membrane is approximately 32 mm long, and that it tapers from about 0.5 mm wide at the apex to about 0.1 mm wide near the stapes at its base. Figures 2.15 and 2.17 illustrate how the basilar membrane gets progressively wider going from the base to the apex. Furthermore, it is thicker at the base than at the apex. Central to its role in cochlear functioning, the basilar membrane is stiffest at its base and becomes progressively less stiff toward the apex (Bekesy, 1960/1989).

The structures and orientation of the **scala media** are shown schematically in Fig. 2.18. The scala media is attached medially to the osseous spiral lamina, just described, and laterally to the outer wall of the cochlea by a fibrous connective tissue

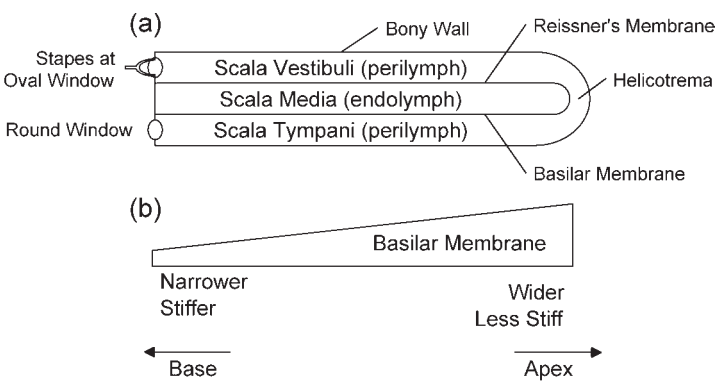

Figure 2.17 Schematic representations of the uncoiled cochlea. (a) Side view showing the three chambers. (b) Top view looking down on the basilar membrane (cochlear partition).

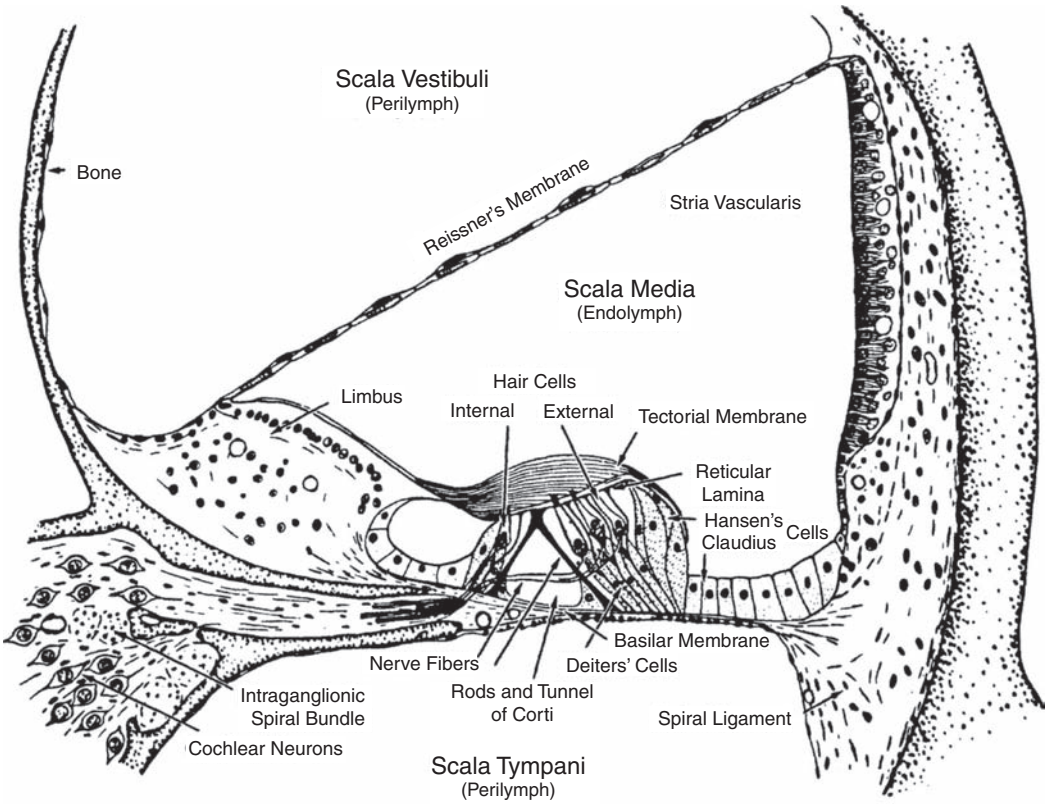

Figure 2.18 Cross-section of the organ of Corti. *Source*: From Davis (1962), with permission.

called the **spiral ligament**. Looking first at the osseous spiral lamina (toward the left in the figure), we see that this bony shelf is actually composed of two plates, separated by a space through which fibers of the auditory nerve pass. These fibers enter via openings called the **habenula perforata**. Resting on the osseous spiral lamina is a thickened band of periosteum, the **limbus**. Reissner's membrane extends from the top of the inner aspect of the limbus to the outer wall of the canal. The side of the limbus facing the organ of Corti is concave outward. The **tectorial membrane** is attached to the limbus at the upper lip of this concave part, forming a space called the **internal spiral sulcus**. The basilar membrane extends from the lower lip of the limbus to the spiral ligament at the outer wall of the duct. The spiral ligament itself has been described in considerable detail (Henson et al., 1984; Morera et al., 1980; Takahashi and Kimura, 1970); it is involved in the metabolic activities of the inner ear in addition to its role as a crucial supporting structure.

The basilar membrane has two sections. The inner section extends from the osseous spiral lamina to the outer pillars and is relatively thin. The remainder is thicker and extends to the spiral ligament. These two sections are called the **zona arcuata** and the **zona pectinata**, respectively. Sitting on the basilar membrane is the end organ of hearing—the organ of Corti. The width, thickness, and orientation of the basilar membrane and the organ of Corti on it vary along the course of the cochlear duct (Lim, 1980).

The **organ of Corti** runs longitudinally along the basilar membrane. Grossly, it is made up of a single row of **inner hair cells (IHCs)**, three rows of **outer hair cells (OHCs)** (though as many as four or five rows have been reported in the apical turn), the **pillar cells** forming the **tunnel of Corti**, and various **supporting cells** (see Slepecky, 1996, for a detailed review). The tunnel pillars contribute considerably to the rigidity of the zona arcuata of the basilar membrane (Miller, 1985).

This tunnel separates the IHCs from the OHCs. Each of the approximately 3500 IHCs is supported by a **phalangeal cell** that holds the rounded base of the IHC as in a cup. There are about 12,000 OHCs, shaped like test tubes, which are supported by **Deiters' cells**. The closeup drawing of the organ of Corti in Fig. 2.19 shows that the IHCs are surrounded by supporting cells. In contrast, the OHCs are attached to the Deiters' cells below and the reticular lamina above, but their sides are not in contact with other cells.

Between the inner and outer hair cells are the tilted and rather conspicuous pillars (rods) of Corti, which come together at their tops to enclose the triangular tunnel of Corti. Fibers of

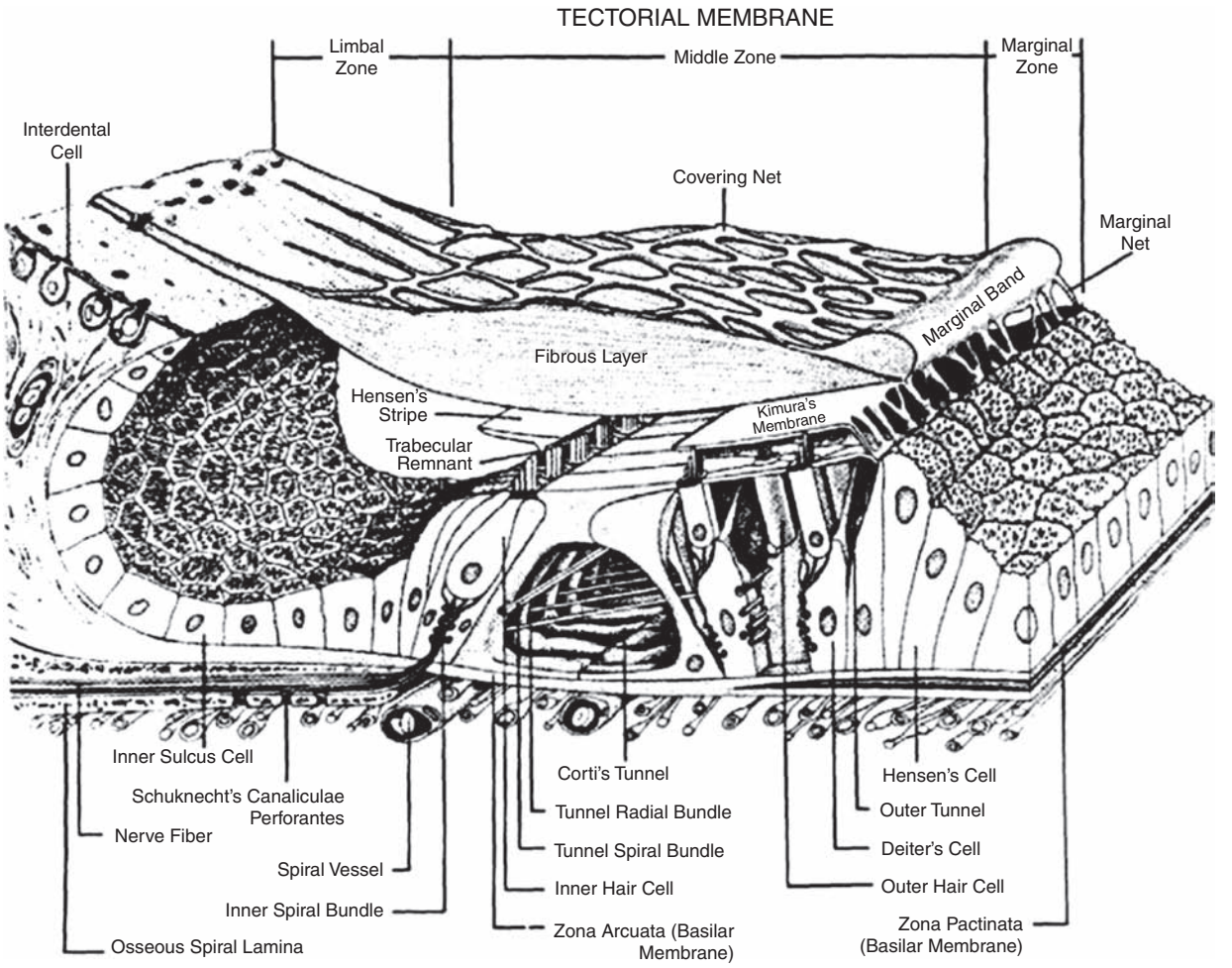

Figure 2.19 Schematic drawing of the organ of Corti and the tectorial membrane. The inner hair cells are surrounded by supporting cells. The outer hair cells attach to the Deiters' cells below and the reticular lamina above, but their lateral aspects do not make contact with other cells. *Source*: From Lim (1980) with permission of *J Acoust Soc Am.*

the eighth cranial (auditory) nerve traverse the tunnel to contact the OHCs. Just lateral to Deiters' cells are several rows of tall, supporting cells called **Hensen's cells**. Lateral to these are the columnar **Claudius cells**, which continue laterally to the spiral ligament and the stria vascularis.

The **reticular lamina** is made up of the tops of the hair cells (cuticular plates; see below) along with the upward-extending processes of the phalangeal and Deiters' cells. *Tight junctions* between the apical parts of these cells provide a barrier that isolates the endolymph-filled portions of the scala media from the structures and spaces of the organ of Corti. The distinctive surface pattern of the reticular lamina is shown in Fig. 2.20. The pillar cells maintain a strong structural attachment between the reticular lamina above and the basilar membrane below, and thus the reticular lamina provides a source of support for the hair cells at their upper surfaces. This relationship is exemplified in Fig. 2.21, showing the OHCs and Deiters' cells in the reticular lamina, as well as the stereocilia of the hair cells protruding through the lamina.

The **tectorial membrane** (Fig. 2.19) extends from its medial connection to the upper lip of the limbus, courses over the hair cells, and then connects laterally to the Hensen's (and perhaps to the most lateral Deiters') cells by a border or marginal net. Its connection to the limbus is a strong and robust one; however, the attachment of the tectorial membrane to the Hensens cells is quite fragile. The undersurface of the main body of the tectorial membrane (fibrous layer) is marked by Hensen's stripe located above the inner hair cells. Informative reviews of the tectorial membrane are provided by Steel (1983, 1985) and Lim (1986a).

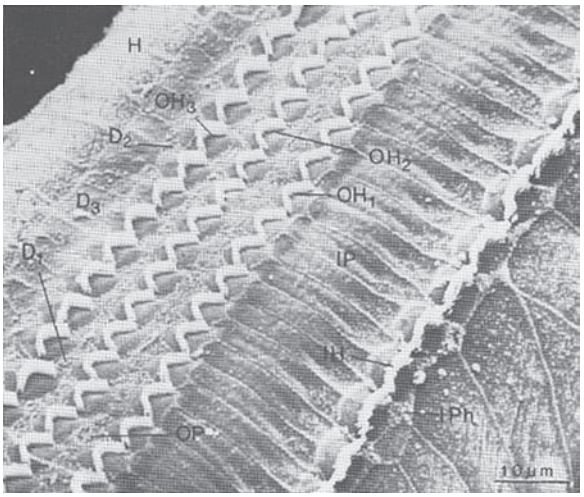

Figure 2.20 The upper surface of the organ of Corti (chinchilla) showing the stereocilia of the inner and outer hair cells protruding through the reticular lamina. The outside aspect (toward the spiral ligament) is at the left, and the medial side (toward the modiolus) is at the right. Landmarks indicated are the Hensen's cells (H), three rows of Deiters' cells (D_1, D_2, D_3), and outer hair cells (OH_1, OH_2, OH_3), outer (OP) and inner (UP) pillar cells, inner hair cells (UH), and inner phalangeal cells (UPh). *Source*: From *Hearing Research* 22, Lim (Functional structure of the organ of Corti: a review, 117–146, © 1986) with kind permission from Elsevier Science Publishers-NL, Sara Burgerhartstraat 25, 1055 KV Amsterdam, The Netherlands.

The tectorial membrane is frequently described as being ribbon-like in appearance, although Fig. 2.19 shows that this is really not the case. Instead, the tectorial membrane has a gelatinous consistency containing various proteins, mainly collagen II, which is arranged in fibers going across the tectorial membrane (Thalmann et al., 1987, 1993). Notice also that it is topped by a covering net. The collagen II provides the tecorial membrane with tensile strength (Zwislocki et al., 1988). The collagen fibers in the part of the tectorial membrane overlying the OHCs become increasingly tightly packed going from the apex toward the base of the cochlea, and its stiffness changes going up the length of the cochlea from stiffest at the base to least stiff at the apex (Gueta et al., 2006, 2007).

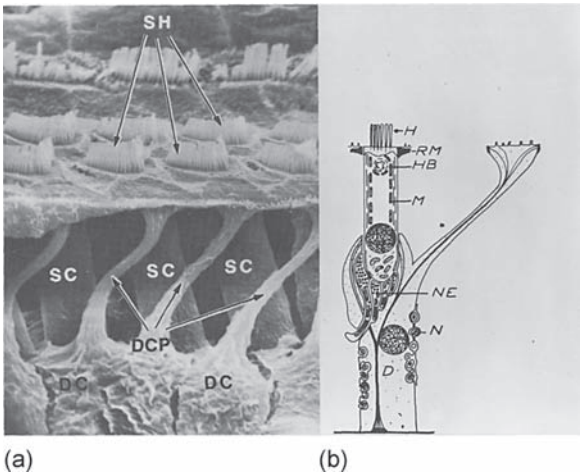

Figure 2.21 Scanning electron micrograph (a) and schematic diagram (b) of Deiters' cells, outer hair cells, and the reticular lamina. *Abbreviations*: DC, Deiters' cell; DCP, phalange of Deiters' cell; SC, sensory (outer hair) cell; SH, sensory hairs (stereocilia). *Source*: From Engstrom and Wersall (1958) by permission of Academic Press.

The **stria vascularis** contains a rich network of capillaries and is attached to the spiral ligament on the lateral wall of the scala media. Structurally, the stria vascularis is composed of three layers having characteristic cell types (e.g., Slepecky, 1996). The hexagonal **marginal cells** face into the scala media. Next are irregular **intermediate cells**, which have projections into the marginal layer. Finally, there are rather flat **basal cells**, which are in contact with the spiral ligament. The stria vascularis maintains the electrochemical characteristics of the endolymph, and in particular is viewed as the source of its high concentration of potassium as well as the endocochlear potential discussed in Chapter 4 (see Wangemann and Schacht, 1996, for an in-depth discussion).

The **blood supply** to the cochlea is well described (see, e.g., Axelsson and Ryan, 2001; Slepecky, 1996). It follows a course of successive arterial branches, going from the **basilar artery** to the **anterior inferior cerebellar artery**, to the **labyrinthine** (**internal auditory**) **artery,** to the **common cochlear artery**, and finally to the **spiral modiolar artery**. As its name implies, the spiral modiolar artery follows a corkscrew-like course up the modiolus from the base to the apex of the cochlea, as shown in Fig. 2.22a. The distribution of the blood supply to the structures in the cochlear duct is illustrated in Fig. 2.22b. Notice that the system involves one branch supplying the spiral ligament above the point of attachment of Reissner's membrane, the capillary network within the stria vascularis, and the spiral prominence, as well as a second branch feeding the limbus and a plexus under the basilar membrane. Venous drainage of the cochlea is into the internal auditory vein.

Hair Cells

There are roughly 12,000 **outer hair cells** (**OHC**) and 3500 **inner hair cells** (**IHC**) in each ear, averaging (with considerable variability among people) about 86 IHCs and 343 OHCs per millimeter of cochlear length (Ulehlova et al., 1987; Wright, 1981; Wright et al., 1987).

The inner and outer hair cells were shown in relation to the cross-section of the organ of Corti in Fig. 2.17. A closer look at these cells is provided in Fig. 2.23. The hair cells are so-named because of the presence of cilia on their upper surfaces. Notice in Fig. 2.23 that the upper surface of each hair cell contains a thickening called the **cuticular plate**, which is topped by three rows of **stereocilia**, as well as a noncuticular area that contains the **basal body** of a rudimentary **kinocilium**.

The structures and interrelationships of the cuticular plate and stereocilia have been described by many researchers

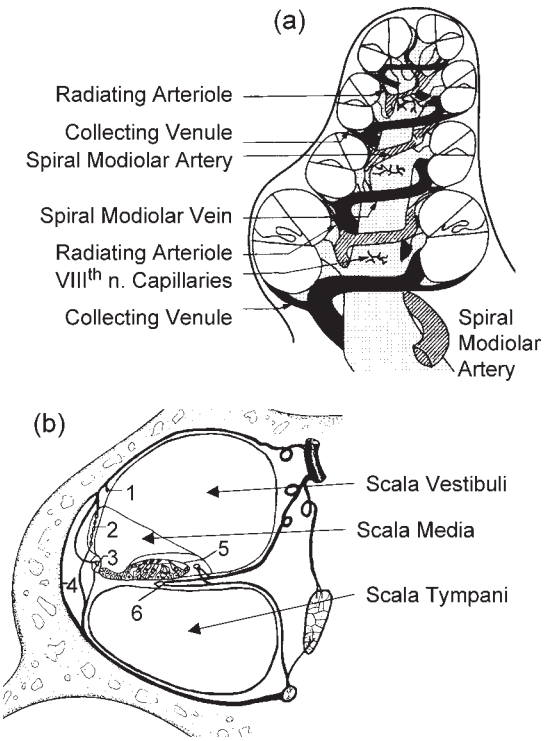

Figure 2.22 Cochlear blood supply: (a) Modiolar view emphasizing the spiral modiolar artery (crosshatched) and the spiral modiolar vein (black). *Source*: Adapted from Axelsson A and Ryan AF (2001), with permission. (b) Cross-sectional view of the cochlear duct emphasizing distribution of blood supply to the spiral ligament above Reissner's membrane (1), stria vascularis (2), spiral prominence (3), limbus (5), and (6) basilar membrane. Also shown are terminal branches to collecting venules (4). *Source*: Adapted from Lawrence (1973), Inner ear physiology, in *Otolaryngology, Vol. 1*, Paparella and Schumrick (eds.), Copyright © 1973 by W.B. Saunders with permission.

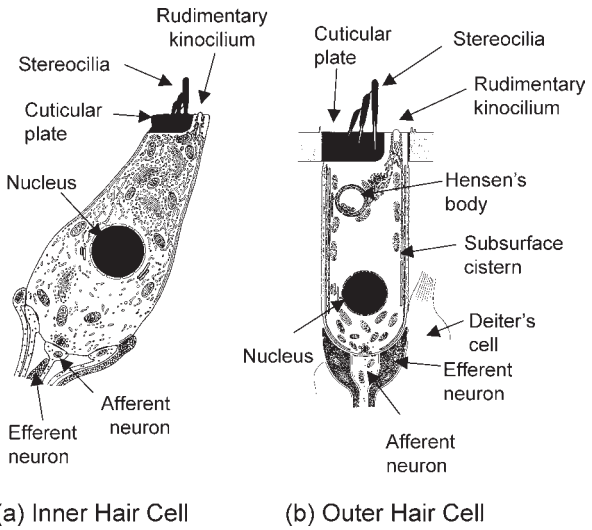

Figure 2.23 Schematic representation of (a) an inner hair cell and (b) an outer hair cell (see text). *Source*: Used with permission from Lim D J (1986b), Effects of noise and ototoxic drugs at the cellular level in the cochlea: A review. *Am J Otolaryngol* 7, 73–99.

(e.g., Crawford and Fettiplace, 1985; Flock and Cheung, 1977; Flock et al., 1981; Hirokawa and Tilney, 1982; Tilney et al., 1980; Tilney and Tilney, 1986). The stereocilia are composed of bundles of actin filaments and are encased in plasma membranes. The actin filaments are extensively cross-linked, and the cuticular plate into which the stereocilia rootlets are planted is similarly made up of a mosaic of cross-linked actin filaments. The filaments of the stereocilia rootlets extend into the cuticular plate, where fine cross bridges also interconnect the rootlet and cuticular plate filaments.

The stereocilia are arranged in a W-shaped pattern on the OHCs and a very wide "U" or "W" shape on the IHCs, as shown in Fig. 2.20. The base of the "W" faces away from the modiolus (or toward the outer wall of the duct). The stereocilia themselves taper toward the base. When the stereocilia are displaced, they remain stiff, bending at the tapered base in response to physical stimulation (Flock et al., 1977; Flock and Strelioff, 1984; Strelioff and Flock, 1984).

Figure 2.24 shows closeup views of the stereocilia bundles from all three rows of OHCs and also for IHCs. The figure highlights the tapering of stereocilia heights from row to row on each hair cell, with the tallest row toward the outer wall of the duct (or away from the modiolus). At least the tallest stereocilia of the OHCs are firmly attached to the undersurface of the tectorial membrane; however, the IHC stereocilia are not attached to Hensen's stripe, or their attachment is tenuous if it does exist (see, e.g., Slepecky, 1996; Steel, 1983, 1985).

The height (length) of the stereocilia increases going from the base (high-frequency end) to the apex (low-frequency end) of the cochlea in many species (Fettiplace and Fuchs, 1999; Lim, 1986b; Saunders et al., 1985; Tilney and Saunders, 1983; Weiss et al., 1976; Wright, 1984). In humans, Wright (1984) found that the longest IHC stereocilia increased linearly from about 4 to 5 μm near the base to about 7 to 8 μm near the apex. The length of the OHC stereocilia also increased with distance up the cochlear duct, although there was more variability and the relationship was not linear.

A particularly interesting aspect of the hair cell stereocilia may be seen in Fig. 2.23. Looking back to this figure, one may notice that the stereocilia are joined by tiny lines. These lines represent filaments that serve as cross-links among the stereocilia. These cross-links occur in both inner and outer hair cells (Flock et al., 1977; Flock and Strelioff, 1984; Furness and Hackney, 1986; Osborne et al., 1988; Pickles et al., 1984; Rhys Evans et al., 1985; Strelioff and Flock, 1984; Vollrath, Kwan, and Corey, 2007). Different types of cross-links occur between the stereocilia of both inner and outer hair cells and are variously named according to their locations and configurations (Figs. 2.25–2.28). Thus, **shaft connectors** go between the main

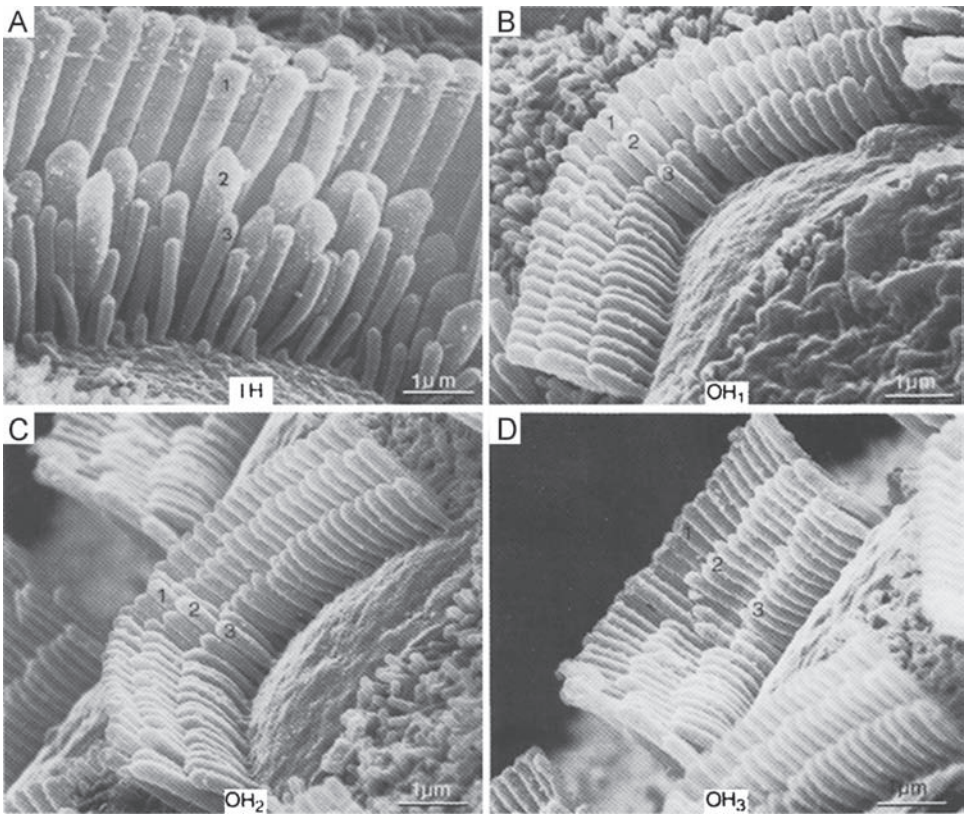

Figure 2.24 Close-up views of the stereocilia bundles of inner (a) and outer (b–d) hair cells demonstrating the decreasing cilia heights from row to row (numbered 1 to 3). *Source*: From *Hearing Research* 22, Lim (Functional structure of the organ of Corti: A review, 117–146, © 1986) with kind permission from Elsevier Science Publishers-NL, Sara Burgerhartstraat 25, 1055 KV Amsterdam, The Netherlands.

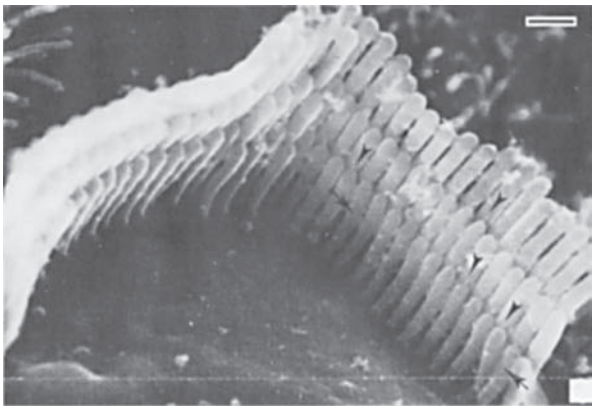

Figure 2.25 Side-to-side (arrows) and tip-links (tip-to-side) cross-links on OHCs. *Source*: From *Hearing Research* 21, Furness and Hackney (High-resolution scanning-electron microscopy of stereocilia using the osmium-thiocarbohydrazide coating technique, © 1986) with kind permission from Elsevier Science Publishers-NL, Sara Burgerhartstraat 25, 1055 KV Amsterdam, The Netherlands.

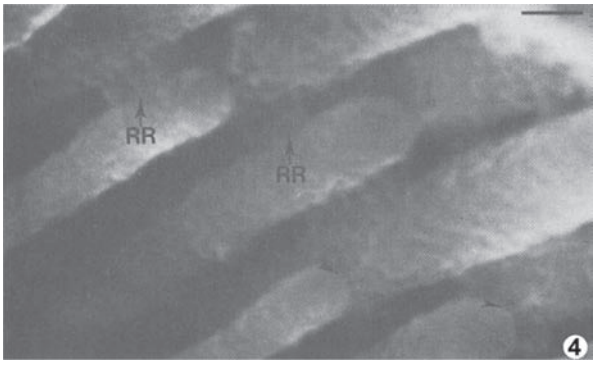

Figure 2.26 Row-to-row cross-links (RR) on OHCs. *Source*: From *Hearing Research* 21, Furness and Hackney (High-resolution scanning-electron microscopy of stereocilia using the osmium-thiocarbohydrazide coating technique, © 1986) with kind permission from Elsevier Science Publishers-NL, Sara Burcrerhartstraat 25, 1055 KV Amsterdam, The Netherlands.

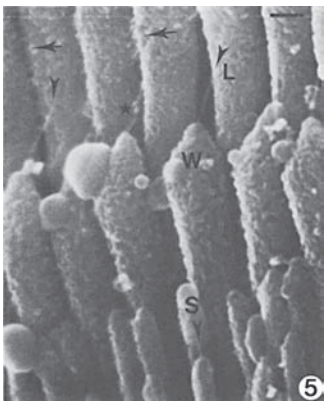

Figure 2.27 Inner hair cell stereocilia showing examples of side-to-side cross links (arrows) and tip-links (arrowheads), which may be relatively long (L) or short (S). *Source*: From *Hearing Research* 21, Furness and Hackney (High-resolution scanning-electron microscopy of stereocilia using the osmium-thiocarbohydrazide coating technique, 1986) with kind permission from Elsevier Science Publishers-NL, Sara Burgerhartstraat 25, 1055 KV Amsterdam, The Netherlands.

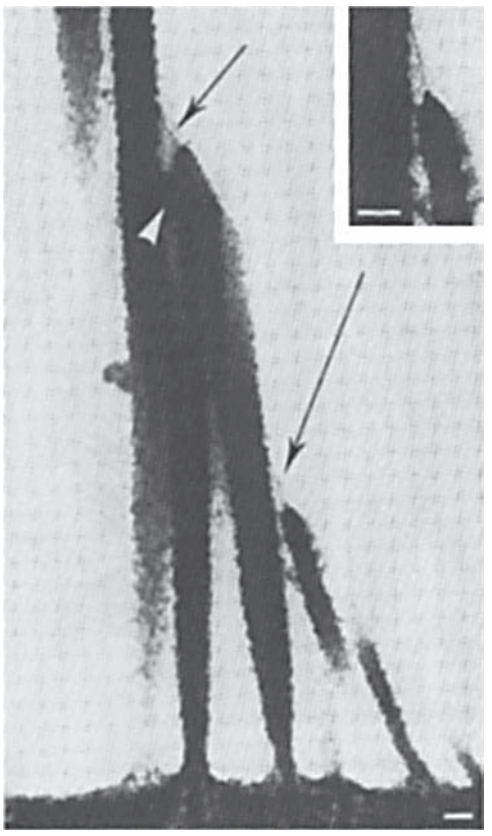

Figure 2.28 Tip-links (arrows) on an outer hair cell. The white arrowhead shows a row-to-row link. *Inset*: close-up of a tip-link. *Source*: From *Hearing Research* 15, Pickles, Comis, and Osborne (Cross links between stereocilia in the guinea pig organ of Corti, and their possible relation to sensory transduction, 103–112, © 1984) with kind permission from Elsevier Science Publishers-NL Sara Burgerhartstraat 25, 1055 KV Amsterdam, The Netherlands.

shafts of the stereocilia; **ankle connectors** are links between the tapered bottoms of the stereocilia; **side-to-side cross-links** join stereocilia that are juxtaposed within the same row; **row-to-row cross-links** go from stereocilia in one row to adjacent ones in the next row.[3] Finally, **tip links** (also known as **tip-to-side** or **upward-pointing cross-links**) go from the tips of stereocilia in a shorter row upward to the sides of the stereocilia in the adjacent taller row and plays a central role in the functioning of the hair cells. As we shall see in Chapter 4, bending of the stereocilia toward the outer wall of the duct stretches these tip links, which in turn open mechanoelectrical transduction pores at the tops of the shorter stereocilia, triggering the hair cell's response (Fettiplace and Hackney, 2006; Vollrath et al., 2007; Beurg et al., 2009).

The structures of the hair cells and their orientation in the organ of Corti reflect their function as sensory receptors, which transduce the mechanical signal carried to them into electrochemical activity. Yet, the contrasting structures and associations of the inner and outer hair cells reflect functional differences between them. Even a casual look at Fig. 2.23 reveals that the test tube–shaped OHCs are very different from the flask-shaped IHCs. Many of these characteristics are associated with the unique property of OHC **electromotility**, their ability to contract and expand, which is central to the active cochlear processes discussed in Chapter 4. For example, OHCs contain **contractile proteins** (e.g., actin, fibrin, myosin, tropomyosin, tubulin) in their cell bodies and cell membranes, stereocilia, and cuticular plates (e.g., Flock, 1980; Flock et al., 1982, 1986; Slepecky, 1996; Slepecky et al., 1988). A more apparent difference pertains to the arrangement of their intracellular structures. Notice that the intracellular structures are distributed throughout the IHC, which is the typical arrangement. In contrast, the nucleus and many organelles in the OHC tend to be concentrated toward the bottom and top of the cell, leaving the cytoplasm between these areas relatively free of cellular structures (Brownell, 1990).

The lateral walls of the OHCs are particularly interesting. They are composed of three layers, as illustrated in Fig. 2.29 (e.g., Brownell and Popel, 1998; Dallos, 1992; Holley, 1996; Slepecky, 1996). The outside layer is the cell's **plasma membrane**, and the inside layer comprises the **subsurface cisternae**. Between them is the **cortical lattice**, which is a matrix composed of parallel rows of actin filaments going circumferentially around the tube-shaped cell, with spectrin cross-links between them. The actin filaments appear to be attached to the outer surface

[3] Horizontal top connectors going between the apical ends of the cilia have been described in the mouse cochlea (Goodyear, Marcotti, Kros, and Richardson, 2005).

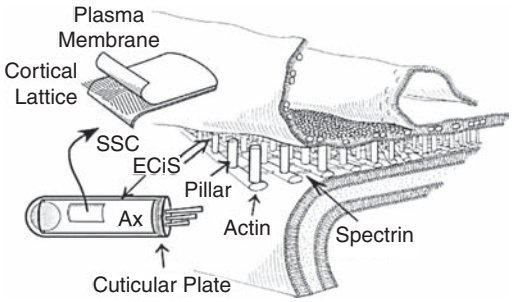

Figure 2.29 The lateral wall of the outer hair cell is composed of the subsurface cisternae on the inside, the plasma membrane on the outside, and a filamentous matrix between them (see text). *Abbreviations*: Ax, axial core of the hair cell; ECiS, extra-cisternal space; SSC, subsurface cisternae. *Source*: Adapted from Brownell and Popel (1998), Electrical and mechanical anatomy of the outer hair cell, in *Psychophysical and Physiological Advances in Hearing*, Palmer et al. (eds.), copyright © 1998 by Whurr, with permission.

of the subsurface cisternae, and they are attached to the plasma membrane by **pillars**. The actin filaments are slanted at about 15° (instead of horizontal) so that they go around the cell in the form of a helix (Fig. 2.30). The OHC's cytoplasm provides positive hydrostatic pressure (turgor) within the cell, and its test tube–like shape is maintained by the tension of the matrix of structures in its lateral walls (Fig. 2.30).

INNERVATION

The sensory hair cells of the cochlea interact with the nervous system by way of the **auditory (cochlear) branch** of the **eighth cranial (vestibulocochlear** or **statoacoustic) nerve**. The auditory nerve was probably first described in the 1500s by Falloppia. However, its structure and connections have become well defined only during the 20th century. A comprehensive discussion of the auditory nerve, its relationship to the cochlea, and its central projections are provided by Ryugo (1992).

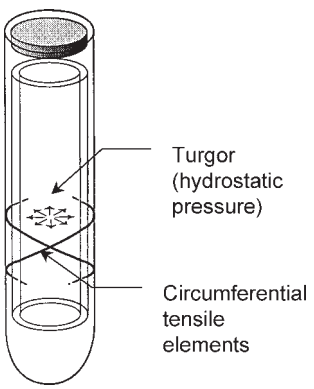

Figure 2.30 Schematic illustration of the hydrostatic pressure (or turgor) of the cytoplasm of an OHC and the matrix of circumferential tensile elements of its lateral walls. *Source*: Adapted from Brownell (1990), with permission.

There are approximately 30,000 neurons in the human auditory nerve, and approximately 50,000 or more cochlear neurons in the cat (Engstrom and Wersall, 1958; Furness and Hackney, 1986). These neurons are primarily afferents, which carry sensory information up from the hair cells, but they also include efferents, which descend from the brainstem to the cochlea. The efferent fibers of the auditory nerve represent the terminal portion of the **olivocochlear bundle**, described later in this chapter. The cell bodies of the afferent auditory neurons constitute the spiral ganglia, residing in Rosenthal's canal in the modiolus. These neurons may be myelinated or unmyelinated before exiting through the habenula perforata, but all auditory nerve fibers are unmyelinated once they enter the organ of Corti. Figure 2.31 shows how the auditory nerve and spiral ganglia relate to a cross section of the cochlear duct.

Most sensory neurons are bipolar, so called because the cell body is located part way along the axon, as illustrated in Fig. 2.32. Auditory neurons are of this general type. More specifically, the cells of the spiral ganglia are composed of at least two distinctive types. Spoendlin (1969, 1971, 1978) demonstrated that approximately 95% of these cells are *relatively large*, *myelinated*, *bipolar* neurons. Spoendlin classified these cells as type I auditory neurons. In contrast, he found that roughly 5% of the spiral ganglion cells were relatively *small*, *unmyelinated*, and tended to be *pseudo-monopolar* in structure. These spiral ganglion cells were classified as type II auditory neurons. These two types of auditory neurons are illustrated in the lower left hand portion in Fig. 2.33.

Upon exiting the habenula perforata into the organ of Corti, the now unmyelinated neural fibers follow different routes to distribute themselves asymmetrically between the inner and outer hair cells, as shown schematically in Figs. 2.33 and 2.34. About 95% of these fibers are inner radial fibers, which course directly out to innervate the *inner* hair cells. The remaining 5%, consist of 2500 to 3000 outer spiral fibers that cross the tunnel of Corti as *basal fibers*, and then turn to follow a route of about 0.6 mm toward the base as the *outer spiral bundle*. These outer spiral fibers then make their way up between the Deiters' cells to synapse with the *outer* hair cells.

Innervation patterns are very different for inner and outer hair cells. Each inner hair cell receives a fairly large number of radial fibers. Each IHC in the cat cochlea receives an exclusive supply of 10 to 30 afferent fibers, with fewer toward the apex and more toward the base (Liberman, Dodds, and Pierce, 1990; Spoendlin, 1978). In contrast, outer spiral bundle gives off collaterals so that each neural fiber innervates several outer hair cells (up to 10 toward the base, and about 10–20 toward the apex), and each OHC receives collaterals from roughly 10 neurons. In humans, IHCs receive about 10 afferents throughout the cochlea, and some fibers branch at their ends to synapse with two or three IHCs instead of to just one (Nadol, 1983a).

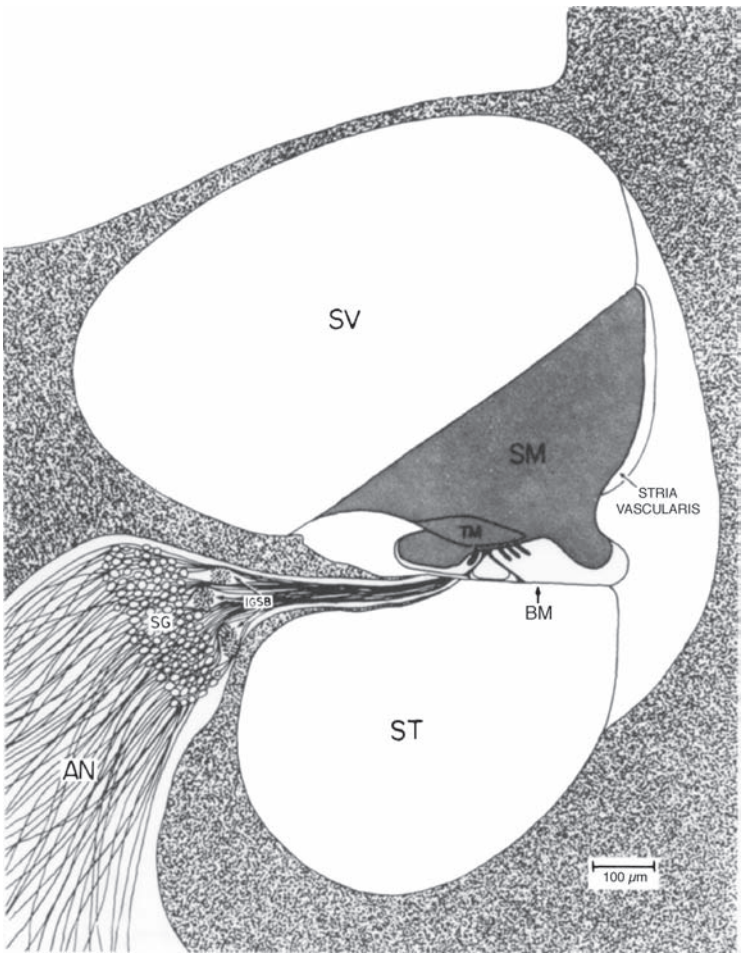

Figure 2.31 Relationship of the auditory nerve to a cross-section of the cochlear duct (cat). *Abbreviations*: AN, auditory nerve; SG, spiral ganglion; IGSB, intraganglionic spiral bundle primarily composed of efferents; TM, tectorial membrane; BM, basilar membrane; SV, SM, ST, scalae vestibuli, media, and tympani, respectively. *Source*: From *Hearing Research* 22, Kiang, Liberman, Sewell, and Guinan (Single unit clues to cochlear mechanisms, 171–182, © 1984) with kind permission from Elsevier Science Publishers-NL, Sara Burgerhartstraat 25, 1055 KV Amsterdam, The Netherlands.

Human OHCs typically receive 4 to 6 afferent fibers (Nadol, 1983b).

Liberman (1982) traced the courses of single auditory neurons by marking them with horseradish peroxidase (HRP). All of the type I auditory neurons he labeled with intracellular injections of HRP could be traced to radial fibers going to IHCs. Kiang et al. (1982) injected HRP into the auditory nerve within the internal auditory canal. They were then able to trace the courses of 50 radial and 11 outer spiral fibers. Their HRP labeling studies confirmed earlier conjectures by Spoendlin (1971, 1978) that the large caliber (over 2 μm), bipolar type I cells continue as radial fibers in the organ of Corti; and that the small caliber (under 1 μm), pseudomonopolar type II cells correspond to the outer spiral fibers (see Figs. 2.32 and 2.33).

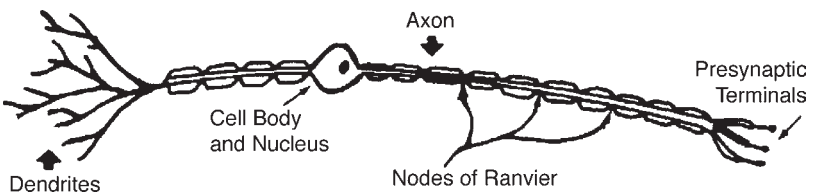

Figure 2.32 Schematic drawing of a typical bipolar sensory neuron.

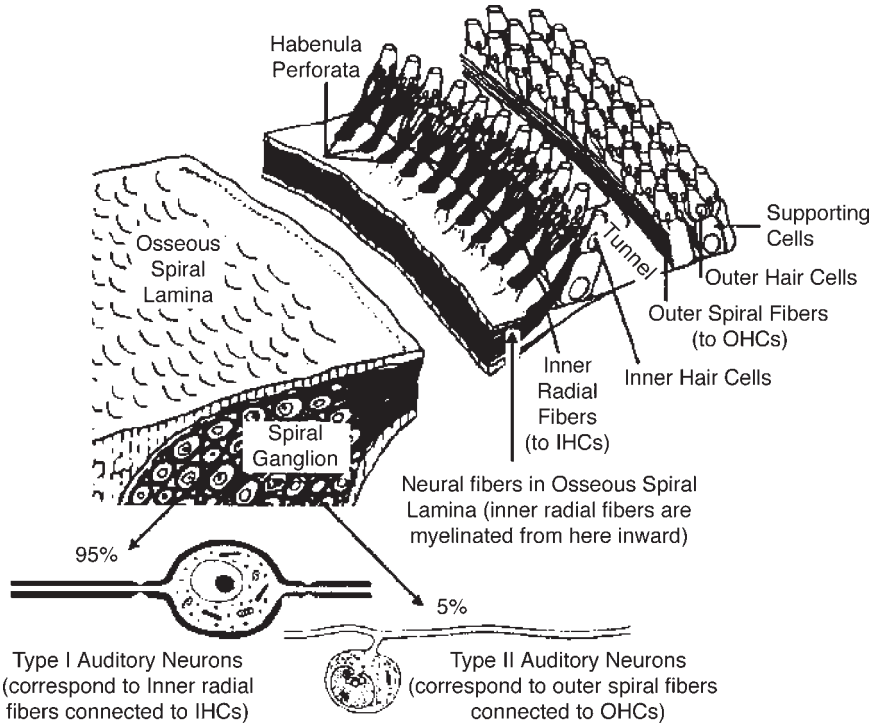

Figure 2.33 The afferent innervation of the organ of Corti. Notice how Type I auditory neurons in the spiral ganglion continue in the organ of Corti as inner radial fibers to inner hair cells, and Type II auditory neurons continue as outer spiral fibers to outer hair cells. Examples of Type I and Type II neurons are illustrated in the lower left-hand section of the drawing. *Source*: Adapted from drawings by Spoendlin H. The afferent innervation of the cochlea, in *Electrical Activity of the Auditory Nervous System*, R.F. Naunton and C. Fernandez (eds.), Copyright © 1978 by Academic Press, with permission.

As illustrated in Fig. 2.35, Liberman and Simmons (1985) demonstrated that a given inner hair cell makes contact with three types of radial fibers, differing in terms of their average diameters, cellular characteristics, and spontaneous firing rates (see Chap. 5). Moreover, these three types of radial fibers attach to the IHC at characteristic locations. The thickest fibers (having the highest spontaneous rates) always attach on the surface of the IHC, which is toward the OHCs. The thinnest and medium thickness fibers (having low and medium spontaneous rates, respectively) attach to the IHC on the surface facing toward the modiolus.

Efferent Innervation of the Hair Cells

Other kinds of neurons are also found in the organ of Corti. Figures 2.34 and 2.36 show that two different types of fibers can be identified with respect to their nerve endings (Engstrom, 1958; Smith and Sjostrand, 1961). One group of cells has smaller nonvesiculated endings. These are afferent (ascending sensory) neurons.

The second group of cells has larger vesiculated endings and is derived from the **efferent** (descending) neurons of the **olivocochlear bundle** (see below). The vesiculated endings contain *acetylcholine*. Various studies found degeneration of these vesiculated units when parts of the descending olivocochlear bundle were cut (Smith and Rasmussen, 1963; Spoendlin and Gacek, 1963). However, no degeneration was found to occur for the nonvesiculated afferent neurons. The endings of the efferent fibers are in direct contact with the OHCs, whereas they terminate on the afferent neural fibers of the IHCs rather than on these sensor cells themselves (Fig. 2.36). This suggests that the efferents act directly upon the OHCs (presynaptically), but that they act upon the associated afferent fibers of the IHCs (postsynaptically). The density of efferent fibers is substantially greater for the OHCs than for the IHCs. Furthermore, there is greater efferent innervation for the OHCs at the base of the cochlea than at the apex, and this innervation of the OHCs also tapers from the first row through the third.

CENTRAL AUDITORY PATHWAYS

The auditory (or cochlear) nerve appears as a twisted trunk—its core is made up of fibers derived from the apex of the cochlea, and its outer layers come from more basal regions. The nerve leaves the inner ear via the internal auditory meatus and enters the brainstem at the lateral aspect of the lower pons. We are now in the **central auditory nervous system**, or the **central auditory pathways**, the major aspects of which are outlined in

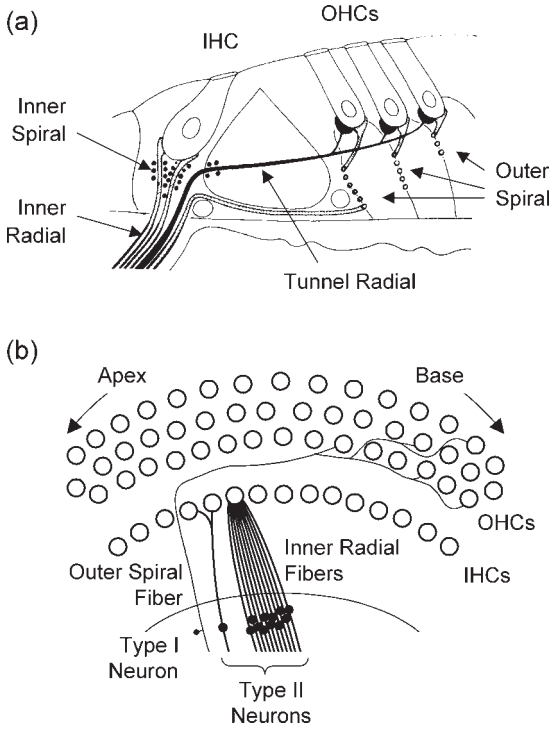

Figure 2.34 (a) Afferent and efferent innervation of the organ of Corti. *Source*: Adapated from Spoendlin (1975) with permission. Efferent fibers are shown in black. (b) Arrangement of Type I and Type II afferent auditory nerve fibers to inner and outer hair cells [based on findings of Spoendlin (1975) and Nadol (1983a)].

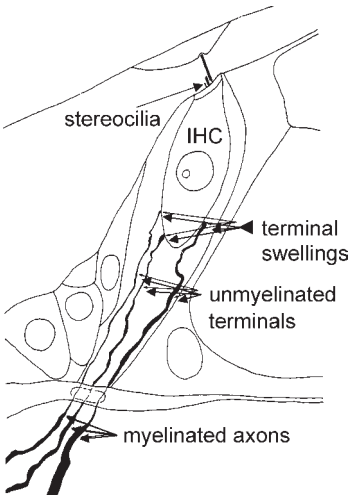

Figure 2.35 The thickest radial fibers attach to the IHC surface facing the OHCs, whereas the thinnest and medium thickness fibers attach on the surface toward the modiolus. *Source*: From Liberman and Simmons (1985), with permission of *J Acoust Soc Am.*

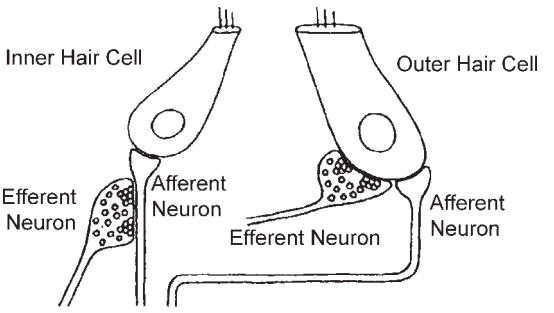

Figure 2.36 Relationship between afferent and efferent neural fibers and the inner and outer hair cells. *Source*: Adapted from Spoendlin (1975), with permission.

this section. Although not addressed here, interested students will find a summary of the neurotransmitters associated with the auditory system in Table 2.2. In addition, many sources are available to those wishing to pursue a more detailed coverage of the anatomy and physiology of the auditory pathways (e.g., Ehret and Romand, 1997; Møller, 2000; Musiek and Baran, 2007; Popper and Fay, 1992; Webster, Popper and Fay, 1992; Altschuler, Bobbin, Clopton, and Hoffman, 1991; Winer, 1992).

Afferent Pathways

The major aspects of the ascending central auditory pathways are shown schematically in Fig. 2.37. The fibers of the auditory nerve constitute the first-order neurons of the ascending central auditory pathways. The number of nerve fibers associated with the auditory system increases dramatically going from the auditory nerve to the cortex. For example, the rhesus monkey has roughly 30,000 cells in its auditory nerve, compared to approximately 10 million at the auditory cortex (Chow, 1951).

Upon entering the brainstem, the auditory nerve fibers synapse with cells in the **cochlear nuclei**, constituting the first level of way stations in the central auditory nervous system. Comprehensive discussions of the cochlear nuclei and their synaptic connections may be found in Cant (1992) and Ryugo (1992). The cochlear nuclei are composed of three main sections: the **anterior ventral cochlear nucleus (AVCN)**, the **posterior ventral cochlear nucleus (PVCN)**, and the **dorsal cochlear nucleus (DCN)**. The incoming type I auditory neurons (originating from the inner hair cells) bifurcate into ascending branches to the AVCN and descending branches to the PVCN and DCN. [Type II auditory neurons also project to the cochlear nuclei, following paths parallel to the type I fibers, but they terminate in different cellular regions (Leak-Jones and Snyder, 1982; Ruggero et al., 1982; Ryugo, 1992).] Auditory neurons arising from the more basal (higher frequency) areas of the cochlea terminate in the dorsomedial parts of the cochlear nuclei, and fibers from the more apical (lower frequency) parts of the cochlea go to the ventrolateral parts of these nuclei. Frequency–place relationships extend throughout the central

Table 2.2 Likely/Possible Neurotransmitters in the Auditory Nervous System

Location	Neurotransmitter(s)	Reference examples
Auditory nerve	Aspartate, glutamate	Wenthold (1978), Romand and Avan (1997)
Cochlear nucleus	Ach, aspartate, GABA, glutamate, glycine	Godfrey et al. (1990), Wenthold et al. (1993), Romand and Avan (1997)
Superior olivary complex	Aspartate (in MSO), GABA, glutamate (in MSO), glutamate decarboxylase, glycine (in LSO)	Wenthold (1991), Helfert and Aschoff (1997)
Lateral lemniscus	GABA, glycine	Helfert and Aschoff (1997)
Inferior colliculus	GABA, glutamate decarboxylase, glycine	Faingold et al. (1989), Wynne et al. (1995)
Medial geniculate	GABA, glutamate	Li et al. (1995), Schwartz et al. (2000)
Auditory cortex	Ach, GABA, glutamate, noradrenoline, serotonin	Metherate and Ashe (1995), Metherate and Hsieh (2003)
Medial olivocochlear bundle	Ach, CGRP, GABA	Sahley et al. (1997)
Lateral olivocochlear bundle	Ach, CGRP, dopamine, dynorphin, enkephalin, GABA, urocortin	Fex and Altschuler (1981), Sahley et al. (1997), Gil-Loyzaga et al. (2000)

Abbreviations: Ach, acetylcholine; CGRP, calcitonin gene-related peptide; GABA, γ-aminobutyric acid; LSO, lateral superior olive; MSO, medial superior olive.

auditory nervous system and are covered in the discussion of *tonotopic organization* in Chapter 6.

Second-order neurons arise from the cochlear nuclei to proceed up the auditory pathways. Some fibers ascend ipsilaterally, but most cross the midline and ascend along the contralateral pathway. The **ventral acoustic stria** arises from the AVCN, forming the **trapezoid body**. The fibers of the trapezoid body *decussate* [cross to the opposite side to synapse with the nuclei of the contralateral superior olivary complex (SOC) or to ascend in the lateral lemniscus]. Other fibers of the trapezoid body terminate at the SOC on the ipsilateral side and at the trapezoid nuclei. The PVCN gives rise to the **intermediate acoustic stria** (of Held), which contralateralizes to ascend in the lateral lemniscus of the opposite side. The **dorsal acoustic stria** (of Monakow) is made up of fibers projecting from the DCN, which cross to the opposite side and ascend in the contralateral lateral lemniscus.

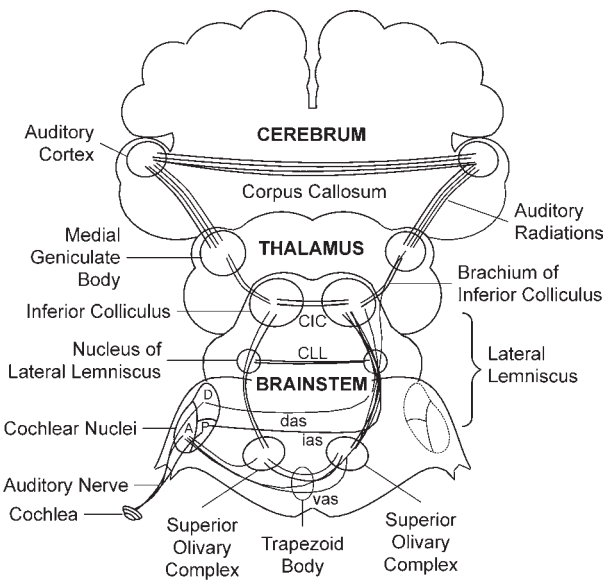

Figure 2.37 Schematic representation of the major aspects of the ascending central auditory pathways. *Abbreviations*: A, anterior ventral cochlear nucleus; P, posterior ventral cochlear nucleus; D, dorsal cochlear nucleus; CIC, commissure of the inferior colliculus; CLL, commissure of the lateral lemniscus; das, dorsal acoustic stria; ias, intermediate acoustic stria; vas, ventral acoustic stria.

The **superior olivary complex** constitutes the next way station in the auditory pathway and is distinguished as the first (lowest) level that receives information originating from both sides of the head (*bilateral representation*). The SOC is made up of the **medial superior olive (MSO)**, the **lateral superior olive (LSO)**, and the **medial nucleus of the trapezoid body (MNTB)**, as well as rather diffuse accumulations of cell bodies known as the **periolivary nuclei** (Helfert and Aschoff, 1997; Moore, 1987, 2000; Schwartz, 1992). Each MSO receives bilateral inputs from the right and left AVCNs, and then projects to the ipsilateral inferior colliculus via the lateral lemniscus on its own side. The LSO also receives inputs directly from the AVCN on the same side as well as from the opposite AVCN via the ipsilateral MNTB. In turn, the LSO projects bilaterally to the inferior colliculi via the lateral lemnisci on both sides. As just implied, the MNTB receives its input from the opposite AVCN and then projects to the LSO on its own side. Although similar to the SOCs of lower mammals, the human SOC has a relatively smaller LSO, more prominent periolovary cell groups, and the TB does not appear to be organized into a identifiable nucleus (Moore, 2000).

The **lateral lemniscus (LL)** is the pathway from the lower nuclei of the auditory pathway just described to the level of the inferior colliculus and has been described in some detail (e.g., Brunso-Bechtold, Thompson, and Masterton, 1981; Ferraro and Minckler, 1977a; Glendenning, Brunso-Bechtold, Thompson, and Masterton, 1981; Helfert and Aschoff, 1997; Moore, 1987; Schwartz, 1992). Each lateral lemniscus includes neural

fibers originating from the cochlear nuclei and superior olivary complexes on both sides, as well as fibers arising from the nuclei of the LL itself. The LL principally includes a **ventral nucleus (VNLL)** and a **dorsal nucleus (DNLL)**, which have typically been described, although an intermediate nucleus has also been described. However, Ferraro and Minckler (1977a) reported that the nuclei of the human LL are somewhat dispersed into scattered cell clusters among the lemniscal fibers, and that a clear-cut demarcation between them could not be found. Communication between the lateral lemnisci of the two sides occurs via the **commissural fibers of Probst**.

The majority of the ascending fibers from the LL project to the **inferior colliculi (IC)**, which are large nuclei on the right and left sides of the midbrain (see, e.g., Ehret and Romand, 1997; Oliver and Huerta, 1992; Oliver and Morest, 1984). The divisions of the IC have been variously described based on different anatomical and physiological methods (e.g., Morest and Olivers, 1984; Rockel and Jones, 1973a, 1973b). The **central nucleus** of the IC is the principal way station for auditory signals arising from the LL, while its **dorsal cortex** and **pericentral** and **external (lateral) nuclei** interact with the central nucleus as well as being involved in many interconnections with other neural systems. Hence, the IC plays a role in multisensory integration. Communication between the inferior colliculi of the two sides occurs via the **commissure of the inferior colliculus**. The auditory pathway continues from the IC to the medial geniculate body (MGB) of the thalamus by way of the **brachium of the inferior colliculus**, which also includes ascending fibers that bypass the IC (Ferraro and Minckler, 1977b). See Oliver and Huerta (1992) for a comprehensive review of the anatomy of the inferior colliculus.

The **medial geniculate body** is the highest subcortical way station of the auditory pathway, which has been described in great detail by Winer (1984, 1985, 1991, 1992). Unlike other way stations along the ascending auditory pathway, all fibers reaching the MGB will synapse here. Moreover, the right and left MGBs are not connected by commissural pathways. Each MGB is composed of **ventral**, **dorsal**, and **medial divisions**, which are relatively similar in humans and other mammals. The ventral division receives auditory signals from the central nucleus of the IC (and nonauditory inputs from the reticular nucleus of the thalamus and the ventrolateral medullary nucleus). It projects mainly to the primary auditory cortex, as well as to some other cortical auditory areas. The dorsal division receives auditory signals from the IC and nonauditory information from a variety of brainstem and thalamic inputs and projects mainly to the auditory association cortex as well as to a wide variety of other cortical sites. The medial division receives a wide range of both auditory inputs (from the IC, perolivary nuclei of the SOC, and the ventral nucleus of the LL) and multisensory nonauditory inputs (from the spinal cord, superior colliculus, vestibular nuclei, and spinal cord), and projects to diverse areas of the cortex, including the somatosensory and prefrontal cortices. The **auditory (geniculocortical** or **thalamocortical)**

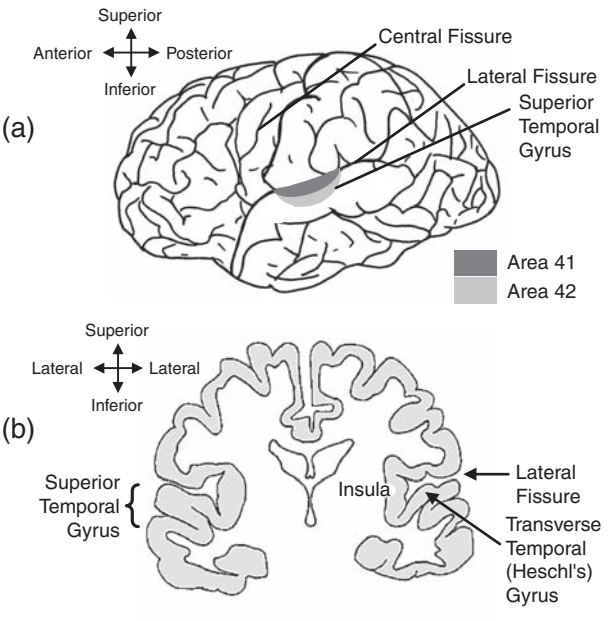

Figure 2.38 Lateral (a) and coronal (b) representations of the human brain illustrating the locations of the primary and secondary auditory areas.

radiations project ipsilaterally from the MGB to the **auditory cortex**, which is located in the temporal lobe.

The **auditory cortex** occupies a band of tissue along the superior border of the temporal lobe just below the **lateral (Sylvian) fissure**, largely involving the **transverse temporal (Heschl's) gyrus** and the posterior two-thirds of the **superior temporal gyrus** (Fig. 2.38) The traditional view of the auditory cortex distinguishes between the primary auditory and auditory association cortices. The **primary auditory cortex** (**koniocortex**), or **area AI**, mainly involves Heschl's gyrus located within the lateral fissure, and roughly corresponds to **area 41** in the classic Brodmann classification system. Area AI is largely surrounded by the **auditory association cortex** (**parakoniocortex**), or **area AII**, which is mainly situated on parts of the posterior transverse and superior temporal gyri, more-or-less corresponding to Brodmann **area 42**. A more precise description of the auditory cortex is still evolving, with current descriptions of the anatomy expressed in terms of **core** regions and secondary **belt** regions (e.g., Galaburda and Sanides, 1980; Hackett, Preuss, and Kaas, 2001; Rivier and Clark, 1997; Wallace, Johnson, and Palmer, 2002). For example, Wallace et al. (2002) integrated their findings with those of Rivier and Clark (1997) to delineate the anatomical regions in the human auditory cortex illustrated in Fig. 2.39. The figure identifies two core regions surrounded by six belt regions. The **core regions** are (filled with dots in the figure) include (a) the primary auditory area (**AI**) involving the posteriomedial two-thirds of Heschl's gyrus, and (b) a narrow lateroposterior area (**LP**) adjacent to it and abutting Heschl's sulcus. The surrounding **belt regions** (filled with lines

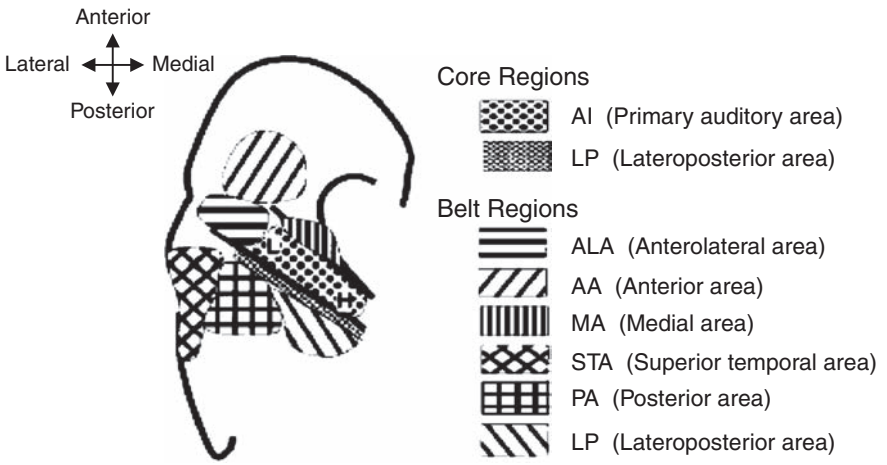

Figure 2.39 The core and belt regions of the human auditory cortex based on the combined findings of Rivier and Clarke (1997) and Wallace et al. (2002). Dots represent core regions; lines and cross-hatching represent belt regions. *Abbreviations*: AI, primary auditory area; LP, lateroposterior area; ALA, anterolateral area; AA, anterior area; MA, medial area; LA, lateral area (lateral to LP); PA, posterior area; STA, superior temporal area; L, responsive to low frequencies; H, responsive to high frequencies. *Source*: From Wallace et al. (2002), Histochemical identification of cortical areas, *Experimental Brain Research*, *Vol 143*, p. 506, Fig. 6A, ©2002, used with kind permission of Springer Science+Business Media.

and cross-hatching in the figure) include the (a) anterolateral (**ALA**) area on the posterior third of Heschl's gyrus, (b) anterior area (**AA**) anterior to area AI, (c) medial area (**MA**) anteromedial to AI, (d) lateral area (**LA**) lateral to LP, (e) posterior area (**PA**) posterior to LP, and (f) a superior temporal area (**STA**).

The fiber connections between the medial geniculate body and auditory cortex have been described based on findings in various animals and humans (e.g., Diamond et al., 1958; Mesulam and Pandya, 1973; Niimi and Matsuoka, 1979; Ravizza and Belmore, 1978; Rose and Woolsey, 1949, 1958; Winer et al., 1977). The principal connections are from the ventral division of the MGB to area AI; however, there are also connections from other parts of the MGB to many of the areas that respond to auditory stimulation, such as areas AII and Ep, among others.

As suggested in the previous paragraph, areas AI and AII are by no means the only cortical locations that respond to sound. Additional cortical auditory areas have been known for some time (e.g., Reale and Imig, 1980; Rose, 1949; Rose and Woolsey, 1958), and are discussed further in Chapter 6. Communication between right and left auditory cortices occurs via the **corpus callosum** (e.g., Karol and Pandya, 1971; Musiek and Baran, 2007; Pandya et al., 1969).

In contrast to the principal afferent auditory pathway from the cochlea to the primary auditory cortex (AI), as in Fig. 2.37, those involving more diverse connections and leading to other areas have been identified as the **nonclassical (adjunct) auditory pathways** (see, Aitkin, 1986; Ehret and Romand, 1997; Møller, 2000). This include the **diffuse system** from IC to the dorsal division of the MGB, and then to auditory association cortex (AII); and the **polysensory system**, which goes from the IC (including visual and somatosensory inputs) to the medial division of the MGB, and then projecting to sites such as the anterior auditory field of the cortex, the thalamic reticular nucleus, and the limbic system.

Acoustic Reflex Arc

The **acoustic reflex** was mentioned earlier in this chapter and is addressed in some detail in Chapter 3. The **acoustic reflex arc** has been described in detail (Borg, 1973; Lyons, 1978) and is shown schematically in Fig. 2.40. The afferent (sensory) leg of the reflex arc is the **auditory nerve**, and the efferent (motor) legs are the **seventh cranial (facial) nerve** to the stapedius muscle and the **fifth cranial (trigeminal) nerve** to the tensor tympani. We will trace the pathways for just the **stapedius reflex**, which constitutes the acoustic reflex in humans (see Chap. 3).

The afferent leg of the reflex goes from the stimulated cochlea via the auditory nerve to the ipsilateral VCN. From

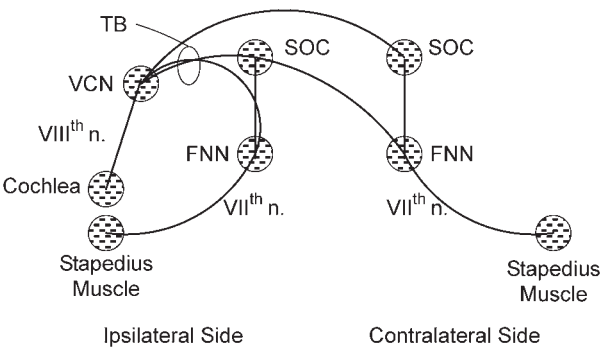

Figure 2.40 Schematic diagram of the crossed and uncrossed acoustic (stapedius) reflex pathways. *Abbreviations*: FNN, facial nerve nucleus; SOC, superior olivary complex; TB, trapezoid body; VCN, ventral cochlear nucleus.

there, second-order neurons pass through the trapezoid body leading to two uncrossed and two crossed pathways. One of the **uncrossed pathways** goes from the VCN to the facial nerve nucleus, from which motor neurons go to the stapedius muscle on the same side. The other uncrossed pathway goes from the VCN to the ipsilateral SOC, from which third-order neurons go to the facial nerve nucleus. From there, motor neurons proceed to the ipsilateral stapedius muscle.

One of the **crossed pathways** goes from the ipsilateral VCN to the ipsilateral SOC, from which third-order neurons cross the midline to the facial nerve nucleus on the opposite side. From there, the facial nerve goes to the stapedius muscle on the side opposite the stimulated ear. The other crossed pathway goes from the ipsilateral VCN to the contralateral SOC, and then to the facial nerve nucleus on that side (opposite to the stimulated cochlea). The facial nerve then proceeds to the stapedius muscle contralateral to the stimulated cochlea.

Efferent Pathways

As described above, descending efferent fibers enter the inner ear and make contact with the OHCs directly and with the IHCs indirectly via synapses with their associated afferent fibers. These fibers are the cochlear terminations of the **olivocochlear bundle (OCB)**. The OCB is sometimes referred to as *Rasmussen's bundle* because it was originally characterized in 1946 by Rasmussen. Since then, the OCB has been described in considerable detail (e.g., DeVenecia, Liberman, Guinan, and Brown, 2005; Guinan, 1996, 2006; Guinan et al., 1983, 1984; Liberman and Brown, 1986; Luk et al., 1974; Robertson, 1985; Strutz and Spatz, 1980; Warr, 1978, 1992).

The general organization of the olivocochlear pathway system is depicted in Fig. 2.41. It is made up of neurons derived from the regions of the **medial superior olive (MSO)** and the **lateral superior olive (LSO)** on both sides. The neurons of the OCB enter the inner ear along with the vestibular branch of the auditory nerve, and then enter the cochlea to distribute themselves to the inner and outer hair cells.

Figure 2.40 shows that we are really dealing with two efferent systems rather than one. The **lateral olivocochlear (LOC) system**, or **uncrossed olivocochlear bundle (UOCB)**, is made up of efferent fibers derived from the vicinity of the lateral superior olive. These unmyelinated, small diameter fibers project to the ipsilateral cochlea, where they synapse with the afferents of the inner hair cells. A comparably small number of myelinated fibers from the ipsilateral medial superior olive go to outer hair cells on the same side.

The **medial olivocochlear (MOC) system** or **crossed olivocochlear bundle (COCB)** involves large-diameter, myelinated neurons originating from the vicinity of the medial superior olive. These cross the midline of the brainstem at the level of the fourth ventricle and eventually terminate directly upon the outer hair cells on the opposite side. (A few unmyelinated fibers from the lateral superior olivary area also cross the midline, going to the contralateral inner hair cells.)

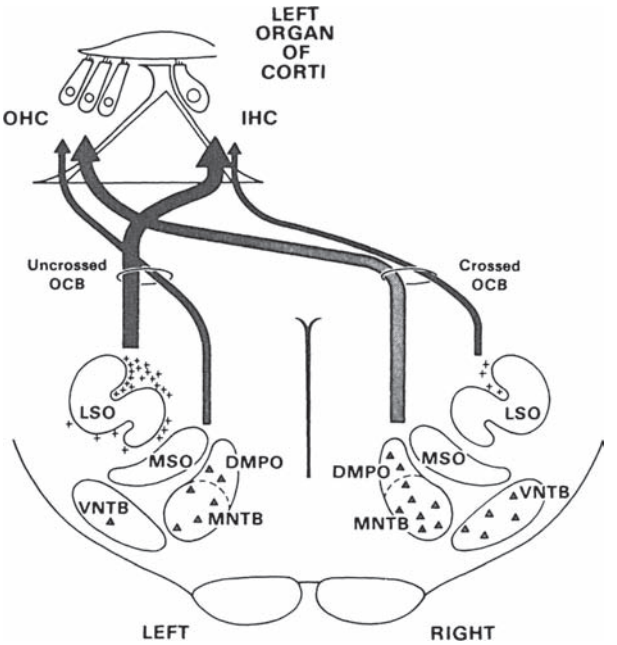

Figure 2.41 Schematic representation of the crossed and uncrossed olivocochlear bundles. As suggested by the wider lines, the crossed OCB goes mainly from the MSO to the contralateral OHCs, and the uncrossed OCB goes mainly from the LSO to the ipsilateral IHCs. *Abbreviations*: OCB, olivocochlear bundle; LSO, lateral superior olive; MSO, medial superior olive; DMPO, dorsal periolivary nucleus; MNTB, medial nucleus of trapezoid body; VNTB, ventral nucleus of trapezoid body; triangles, large OCB neurons; crosses, small OCB neurons. *Source*: Adapted from Warr (1978), The olivocochlear bundle: Its origins and terminations in the cat, in *Evoked Electrical Activity in the Auditory Nervous System*, R.E Naunton and C. Fernandez (eds.), Copyright © 1978 by Academic Press.

In addition to the olivocochlear systems, other efferent connections have been demonstrated coming from the inferior colliculus, the nuclei of the lateral lemniscus, and possibly the cerebellum (e.g., Harrison and Howe, 1974; Huffman and Henson, 1990; Rasmussen, 1967), as well as descending fibers that may also provide cortical feedback and/or control over lower centers including, for example, corticofugal pathways to the inferior colliculus and to the medial geniculate (e.g., Anderson et al., 1980; Diamond et al., 1969; Oliver and Huerta, 1992; Rockel and Jones, 1973a, 1973b; Winer, 1992; Winer et al., 1977).

REFERENCES

Aitkin, J. 1986. *The Auditory Midbrain*. Clifton, NJ: Humana Press.

Anderson, RA, Snyder, RL, Merzenich, MM. 1980. The tonotopic organization of corticocollicular projections from physiologically identified loci in AI, AII, and anterior cortical fields of the cat. *J Comp Neurol* 191, 479–494.

Anson, BJ, Donaldson, JA. 1967. *The Surgical Anatomy of the Temporal Bone and the Ear*. Philadelphia, PA: Saunders.

Axelsson, A, Ryan, AF. 2001. Circulation of the inner ear: I. Comparative study of the vascular anatomy in the mallalian cochlea. In: AF Jahn, J Santos-Sacchi (eds.), *Physiology of the Ear*, 2nd ed. San Diego: Singular, 301–320.

Bekesy, G. 1936. Zur Physik des Mittelohres und uber das Horen bei fehlerhaftem Trommelfell. *Akust Zeitschr* i, 13–23.

Bekesy, G. 1960/1989. *Experiments in Hearing*. New York: McGraw-Hill. [Republished by the Acoustical Society of America].

Beurg, M, Fettiplace, R, Nam, J-H, Ricci, AJ. 2009. Localization of inner hair cell mechanotransducer channels using high-speed calcium imaging. *Nature Neurosci* 12, 553–558.

Borg, E. 1973. On the neuronal organization of the acoustic middle ear reflex: A physiological and anatomical study. *Brain Res* 49, 101–123.

Brodmann, K. 1909. Vergleichende Lokalisantionlehre der Grosshirnrinde in ihren Preinzipien dargestellt auf Grund des Zellenbaues. Leipzig: Barth.

Brownell, WE. 1990. Outer hair cell electromotility and otoacoustic emissions. *Ear Hear* 11, 82–92.

Brownell, WE, Popel, AS. 1998. Electrical and mechanical anatomy of the outer hair cell. In: AR Palmer, A Rees, AQ Summerfield, R Meddis (eds.), *Psychophysical and Physiological Advances in Hearing*. London: Whurr, 89–96.

Brunso-Bechtold, JK, Thompson, GC, Masterton, RB. 1981. HRP study of the organization of the auditory afferents ascending to central nucleus of inferior colliculus in cat. *J Comp Neurol* 197, 705–722.

Cant, NB. 1992. The cochlear nucleus: Neuronal types and their synaptic organization. In: WB Webster, AN Popper, RF Fay (eds.), *The Mammalian Auditory Pathway: Neuroanatomy*. New York: Springer-Verlag, 66–116.

Chow, K. 1951. Numerical estimates of the auditory central nervous system of the monkey. *J Comp Neurol* 95,159–175.

Crawford, AC, Fettiplace, R. 1985. The mechanical properties of ciliary bundles of turtle cochlear hair cells. *J Physiol* 364, 359–379.

Dallos, P. 1992. The active cochlea. *J Neurosci* 12, 4575–4585.

Dallos, P, Popper, AN, Fay, RR (eds.) (1996). *The Cochlea*. New York, NY: Springer-Verlag.

Davis, H. 1962. Advances in the neurophysiology and neuroanatomy of the cochlea. *J Acoust Soc Am* 34, 1377–1385.

DeVenecia, RK, Liberman, MC, Guinan, JJ Jr, Brown, MC. 2005. Medial olivocochlear reflex interneurons are located in the posteroventral cochlear nucleus: A kainic acid lesion study in guinea pigs. *J Comp Neurol* 487, 345–360.

Diamond, IT, Chow, KL, Neff, WD. 1958. Degeneration of caudal medial geniculate body following cortical lesion ventral to auditory area II in the cat. *J Comp Neurol* 109, 349–362.

Diamond, IT, Jones, EG, Powell, TPS. 1969. The projection of the auditory cortex upon the diencephalon and brain stem in the cat. *Brain Res* 15, 305–340.

Donaldson, JA, Miller, JM. 1973. Anatomy of the ear. In: MM Paparella, DA Shumrick (eds.), *Otolaryngology Vol. 1: Basic Sciences and Related Disciplines*. Philadelphia, PA: Saunders, 75–110.

Ehret, G, Romand, R, eds. 1997. *The Central Auditory Pathway*. New York, NY: Oxford University Press.

Engstrom, H. 1958. On the double innervation of the inner ear sensory epithelia. *Acta Otol* 49, 109–118.

Engstrom, H, Wersäll, J. 1953. Structure and innervation of the inner ear sensory epithelia. *Int Rev Cytol* 7, 535–585.

Engstrom, H, Wersall, J. 1958. Structure and innervation of the inner ear sensory epithelia. *Int Rev Cytol* 7, 535–585.

Faingold, CL, Gehlbach, G, Caspary, DM. 1989. On the role of GABA as an inhibitory *neurotransmitter* in *inferior colliculus* neurons: iontophoretic studies. Brain Res 500, 302–312.

Ferraro, JA, Minckler, J. 1977a. The human auditory pathways: A quantitative study: The human lateral lemniscus and its nuclei. *Brain Lang* 4, 277–294.

Ferraro, JA, Minckler, J. 1977b. The human auditory pathways: A quantitative study: The brachium of the inferior colliculus. *Brain Lang* 4, 156–164.

Fettiplace, R, Fuchs, PA. 1999. Mechanisms of hair cell tuning. *Ann Rev Physiol* 61, 809–834.

Fettiplace, R, Hackney, CM. 2006. The sensory and motor roles of auditory hair cells. *Nat Rev Neurosci* 7(1), 19–29.

Fex, J, Altschuler, RA. 1981. Enkephalin-like immuno reactivity of olivocochlear nerve fibers in cochlea of guinea pig and cat. *Proc Natl Acad Sci U S A* 78, 1255–1259.

Flock, A. 1980. Contractile proteins in hair cells. *Hear Res* 2, 411–412.

Flock, A, Bretscher, A, Weber, K. 1982. Immunohistochemical localization of several cytoskeletal proteins in inner ear sensory and supporting cells. *Hear Res* 7, 75–89.

Flock, A, Cheung, HC. 1977. Actin filaments in sensory hairs of inner ear receptor cells. *J Cell Biol* 75, 339–343.

Flock, A, Cheung, HC, Utter, G. 1981. Three sets of actin filaments in sensory hairs of the inner ear: Identification and functional organization determined by gel electrophoresis, immunofluorescence, and electron microscopy. *J Neurocytol* 10, 133–147.

Flock, A, Flock, B, Murray, E. 1977. Studies on the sensory hairs of receptor cells in the inner ear. *Acta Otol* 83, 85–91.

Flock, A, Flock, B, Ulfendahl, M. 1986. Mechanisms of movement in outer hair cells and a possible structural basis. *Arch Otoryhinolaryngol* 243, 83–90.

Flock, A, Strelioff, D. 1984. Studies on hair cells in isolated coils from the guinea pig cochlea. *Hear Res* 15, 11–18.

Frommer, GH. 1982. Observations of the organ of Corti under in vivo-like conditions. *Acta Otol* 94, 451–460.

Furness, DN, Hackney, CM. 1985. Cross links between stereocilia in the guinea pig cochlea. *Hear Res* 18, 177–188.

Furness, DN, Hackney, CM. 1986. High-resolution scanning-electron microscopy of stereocilia using the osmium-thiocarbohydrazide coating technique. *Hear Res* 21, 243–249.

Galaburda, A, Sanides, F. 1980. Cytoarchitectonic organization of the *human auditory* cortex. *J Comp Neurol* 190, 597–610.

Gelfand, SA. 2001. *Essentials of Audiology*, 2nd ed. New York, NY: Thieme Medical Publishers.

Gil-Loyzaga, P, Bartolome, V, Vicente-Torres, A, Carricondo, F. 2000. Serotonergic innervation of the organ of Corti. *Acta Otolaryngol* 120, 128–132.

Glendenning, KK, Brunso-Bechtold, JK, Thompson, GC, Masterton, RB. 1981. Ascending afferents to the nuclei of the lateral lemniscus. *J Comp Neurol* 197, 673–703.

Godfrey, D, Beranek, K, Carlson, L, Parli, J, Dunn, J, and Ross, C. 1990. Contribution of centrifugal innervation to choline acetyltransferase activity in the cat cochlear nucleus. *Hear Res* 49, 259–280.

Goodyear, RJ, Marcotti, W, Kros, CJ, Richardson, GP. 2005. Development and properties of stereociliary link types in hair cells of the mouse cochlea. *J Comp Neurol* 485, 75–85.

Gueta, R, Barlam, D, Shneck, RZ, Rousso, I. 2006. Measurement of the mechanical properties of isolated tectorial membrane using atomic force microscopy. *Proc Natl Acad Sci USA* 103, 14790–14795.

Gueta, R, Tal, E, Silberberg, Y, Rousso, I. 2007. The 3D structure of the tectorial membrane determined by second-harmonic imaging microscopy. *J Struct Biol* 159, 103–110

Guinan, JJ Jr. 1996. Physiology of olivocochlear efferents. In: P Dallos, AN Popper, RR Fay (eds.), *The Cochlea*. New York, NY: Springer-Verlag, 435–502.

Guinan, JJ Jr. 2006. Olivocochlear efferents: Anatomy, physiology, function, and the measurement of efferent effects in humans. *Ear Hear* 27, 589–607.

Guinan, JJ, Warr, WB, Norris, BE. 1983. Differential olivocochlear projections from lateral vs medial zones of the superior olivary complex. *J Comp Neurol* 221, 358–370.

Guinan, JJ, Warr, WB, Norris, BE. 1984. Topographic organization of the olivocochlear projections from the lateral and medial zones of the superior olivary complex. *J Comp Neurol* 226, 21–27.

Hackett, TA, Preuss, TM, Kaas, JH. 2001. Architectonic identification of the core region in auditory cortex of macaques, chimpanzees, and humans. *J Comp Neurol* 441, 197–222.

Harrison, JM, Howe, ME. 1974. Anatomy of the descending auditory system (mammalian). In: WD Keidel, WD Neff (eds.), *Handbook of Sensory Physiology*, V5/1. Berlin, Germany: Springer, 363–388.

Helfert, RH, Aschoff, A. 1997. Superior olivary complex and nuclei of the lateral lemniscus. In: G Ehret, R Romand (eds.), *The Central Auditory System*. New York, NY: Oxford University Press, 193–258.

Helmholtz, H. 1868. Die Mechanik der Gehorknochelchen und des Trommelfells. *Pflugers Arch Physiol* 1, 1–60.

Henson, MM, Henson, OW Jr, Jenkins, DB. 1984. The attachment of the spiral ligament to the cochlear wall: Anchoring cells and the creation of tension. *Hear Res* 16, 231–242.

Hirokawa, N, Tilney, LG. 1982. Interactions between actin filaments and between actin filaments and membranes in quick-frozen and deeply etched hair cells of the chick ear. *J Cell Biol* 95, 249–261.

Holley, MC. 1996. Cochlear mechanics and micromechanics. In: P Dallos, AN Popper, RR Fay (eds.), *The Cochlea*. New York, NY: Springer-Verlag, 386–434.

Holton, T, Hudspeth, AJ. 1983. A micromechanical contribution to cochlear tuning and tonotopic organization. *Science* 222, 508–510.

Huffman, RF, Henson, OW Jr. 1990. The descending auditory pathway and acousticomotor systems: Connections with the inferior colliculus. *Brain Res Rev* 15, 295–323.

Hughes, GB. 1985. *Textbook of Otology*. New York, NY: Thieme Medical Publishers.

Jepsen, O. 1963. Middle-ear muscle reflexes in man. In: J Jerger (ed). *Modern Developments in Audiology*. New York, NY: Academic Press, 194–239.

Karol, EA, Pandya, DN. 1971. The distribution of the corpus callosum in the rhesus monkey. Brain 94, 471–486.

Kiang, NYS, Rho, JM, Northrop, CC, Liberman, MC, Ryugo, DK. 1982. Hair-cell innervation by spiral ganglion cells in adult cats. *Science* 217, 175–177.

Lawrence, M. 1966. Effects of interference with terminal blood supply on the organ of Corti. *Laryngoscope* 76, 1318–1337.

Lawrence, M. 1973. Inner ear physiology. In: MM Paparella, DA Shumrick (eds.), *Otolaryngology Vol. 1: Basic Sciences and Related Disciplines*. Philadelphia, PA: Saunders, 275–298.

Leak-Jones, PA, Synder, RL. 1982. Uptake transport of horseradish peroxidase by cochlear spiral ganglion neurons. *Hearing Res* 8, 199–223.

Li, XF, Phillips, R, LeDouz, JE. 1995. NMDA and non-MNDA receptors contribue to synaptic transmission between the medial geniculate body and the lateral nucleus of the amygdala. *Exp Brain Res* 105, 87–100.

Liberman, MC. 1982. Single-neuron labeling in the cat auditory nerve. *Science* 216, 1239–1241.

Liberman, MC, Brown, MC. 1986. Physiology and anatomy of single olivocochlear neurons in the cat. *Hear Res* 24, 17–36.

Liberman, MC, Dodds, LW, Pierce, S. 1990. Afferent and efferent innervation of the cat cochlea: Quantitative analysis with light and electron microscopy. *J Comp Neurol* 301, 443–460.

Liberman, MC, Simmons, DD. 1985. Applications of neural labeling to the study of the peripheral auditory system. *J Acoust Soc Am* 78, 312–319.

Lim, DJ. 1980. Cochlear anatomy related to cochlear microphonics. A review. *J Acoust Soc Am* 67, 1686–1695.

Lim, DJ. 1986a. Functional structure of the organ of corti: A review. *Hear Res* 22, 117–146.

Lim, DJ. 1986b. Effects of noise and ototoxic drugs at the cellular level in cochlea: A review. *Am J Otol* 7, 73–99.

Lim, DJ, Melnick, W. 1971. Acoustic damage of the cochlea: A scanning and transmission electron microscope observation. *Arch Otol* 94, 294–305.

Luk, GD, Morest, DK, McKenna, NM. 1974. Origins of the crossed olivocochlear bundle shown by an acid phophatase method in the cat. *Ann Otol* 83, 382–392.

Lyons, MJ. 1978. The central location of the motor neurons to the stapedius muscle in the cat. *Brain Res* 143, 437–444.

Mesulam, MM, Pandya, DN. 1973. The projections of the medial geniculate complex within the Sylvian fissure of the rhesus monkey. *Brain Res* 60, 315–333.

Metherate, R, Ashe, JH. 1995. Synaptic interactions involving *acetylcholine*, glutamate, and GABA in rat *auditory cortex*. *Exp Brain Res* 107, 59–72.

Metherate, R, Hsieh, CY. (2003). Regulation of glutamate synapses by nicotinic *acetylcholine* receptors in *auditory cortex*. *Neurobiol Learn Mem* 80, 285–290.

Miller, CE. 1985. Structural implications of basilar membrane compliance measurements. *J Acoust Soc Am* 77, 1465–1474.

Møller, AR. 2000. *Hearing: Its Physiology and Pathophysiology*. San Diego, CA: Academic Press.

Moore, JK. 1987. The human auditory brain stem: A comparative review. *Hear Res* 29, 33–43.

Moore, JK. 2000. Organization of the human superior olivary complex. *Microsc Res Tech* 51, 403–412.

Morera, C, DalSasso, A, Iurato, S. 1980. Submicroscopic structure of the spiral ligament in man. *Rev Laryngol* 101, 73–85.

Morest, DK, Oliver, DL. 1984. The neuronal architecture of the inferior colliculus in the cat: Defining the functional anatomy of the auditory midbrain. *J Comp Neurol* 222, 209–236.

Musiek, FE, Baran, JA. 2007. *The Auditory System: Anatomy, Physiology, and Clinical Correlates*. Boston: Allyn & Bacon.

Nadol, JB Jr. 1983a. Serial section reconstruction of the neural poles of hair cells in the human organ of Corti. I. Inner hair cells. *Laryngoscope* 93, 599–614.

Nadol, JB Jr. 1983b. Serial section reconstruction of the neural poles of hair cells in the human organ of Corti. II. Outer hair cells. *Laryngoscope* 93, 780–791.

Niimi, K, Matsuoka, H. 1979. Thalamocortical organization of the auditory system in the cat studied by retrograde axonal transport of horseradish peroxidase. *Adv Anat Embryol Cell Biol* 57, 1–56.

Ohyama, K, Salt, AN, Thalmann, R. 1998. Volume flow rate of perilymph in the guinea-pig cochlea. *Hear Res* 35, 119–129.

Oliver, DL, Huerta, MF. 1992. Inferior and superior colliculi. In: WB Webster, AN Popper, RF Fay (eds.), *The Mammalian Auditory Pathway: Neuroanatomy*. New York, NY: Springer-Verlag, 168–221.

Oliver, DL, Morest, DK. 1984. The central nucleus of the inferior colliculus in the cat. *J Comp Neurol* 222, 237–264.

Osborne, M, Comis, SD, Pickles, JO. 1988. Further observations on the fine structure of tip links between stereocilia of the guinea pig cochlea. *Hear Res* 35, 99–108.

Pandya, DN, Hallett, M, Mukherjee, S. 1969. Intra- and interhemispheric connections of neocortical auditory system in the rhesus monkey. *Brain Res* 14, 49–65.

Pickles, JO, Comis, SD, Osborne, MR. 1984. Cross links between stereocilia in the guinea-pig organ of Corti, and their possible relation to sensory transduction. *Hear Res* 15, 103–112.

Popper, AN, Fay RF, (eds). 1992. *The Mammalian Auditory Pathway: Neurophysiology*. New York, NY: Springer-Verlag.

Proctor, B. 1989. *Surgical Anatomy of the Ear and Temporal Bone*. New York, NY: Thieme Medical Publishers.

Rask-Andersen, H, Schrott-Fisher, A, Pfaller, K, Glueckert, R. 2006. Perlilymph/modiolar communication routes in the human cochlea. *Ear Hear* 27, 457–465.

Rasmussen, GL. 1946. The olivary peduncle and other fiber projections of the superior olivary complex. *J Comp Neurol* 84, 141–219.

Rasmussen, GL. 1967. Efferent connections of the cochlear nucleus. In: AB Graham (ed.), *Sensorineural Hearing Processes and Disorders*. Boston, MA: Little, Brown.

Ravizza, RJ, Belmore, SM. 1978. Auditory forebrain: Evidence from anatomical and behavioral experiments involving human and animal subjects. In: RB Masterson (ed.), *Handbook of Behavioral Neurobiology*. New York, NY: Plenum Press, 459–501.

Reale, RA, Imig, TJ. 1980. Tonotopic organization in the auditory cortex of the cat. *J Comp Neurol* 192, 265–291.

Rhys Evans, RH, Comis, SD, Osborne, MR, Pickles, JO, Jefferies, DJR. 1985. Cross links between stereocilia in the human organ of Corti. *J Laryngol Otol* 99, 11–20.

Rivier, F, Clarke, S. 1997. Cytochrome oxidase, acetylcholinesterase, and NADPH-diaphorase staining in *human supratemporal* and insular cortex: Evidence for multiple auditory areas. *Neuroimage* 6, 288–304.

Robertson, D. 1985. Brainstem localization of efferent neurons projecting to the guinea pig cochlea. *Hear Res* 20, 79–84.

Rockel, AJ, Jones, EG. 1973a. The neuronal organization of the inferior colliculus of the adult cat. I. The central nucleus. *J Comp Neurol* 147, 22–60.

Rockel, AJ, Jones, EG. 1973b. The neuronal organization of the inferior colliculus of the adult cat: II. The pericentral nucleus. *J Comp Neurol* 147, 301–334.

Romand, R, Avan, P. 1997. Anatomical and functional aspects of the cochlear nucleus. In: G Ehret, R Romand (eds.), *The Central Auditory System*. New York, NY: Oxford University Press, 97–192.

Rose, JE. 1949. The cellular structure of the auditory region of the cat. *J Comp Neurol* 91, 409–439.

Rose, JE, Woolsey, CN. 1949. The relations of thalamic connections, cellular structure and evokable electrical activity in the auditory region of the cat. *J Comp Neurol* 91, 441–466.

Rose, JE, Woolsey, CN. 1958. Cortical connections and functional organization of the thalamic auditory system of the cat. In: HF Harlow, CN Woolsey (eds.), *Biological and Biochemical Bases of Behavior*. Madison, WI: University of Wisconsin Press, 127–150.

Ruggero, MA, Santi, PA, Rich NC. 1982. Type II cochlear ganglion cells in the chinchilla. *Hearing Res* 8, 339–356.

Ryugo, DK. 1992. The auditory nerve: Peripheral innervation, cell body morphology, and central projections. In: WB Webster, AN Popper, RF Fay (eds.), *The Mammalian Auditory Pathway: Neuroanatomy*. New York, NY: Springer-Verlag, 23–65.

Sahley, SL, Nodar, RH, Musiek, FE. 1997. *Efferent Auditory System*. San Diego, CA: Singular.

Salt, AN. 2001. Dynamics of the inner ear fluids. In: AF. Jahn, J Santos-Sacchi (eds.), *Physiology of the Ear*, 2nd ed. San Diego, CA: Singular, 333–355.

Salt, AN, Thalmann, R, Marcus, DC, Bohne, BA. 1986. Direct measurement of longitudinal endolymph flow rate in the guinea pig cochlea. *Hear Res* 23, 141–151.

Saunders, JC, Schneider, ME, Dear, SR. 1985. The structure and function of actin in hair cells. *J Acoust Soc Am* 78, 299–311.

Schwartz, DW, Tennigkeit, F, Puil, E. 2000. Metabotropic transmitter actions in auditory thalamus. *Acta Otolaryngol* 120, 251–254.

Schwartz, IR. 1992. The superior olivary complex and lateral lemniscal nuclei. In: WB Webster, AN Popper, RF Fay (eds.), *The Mammalian Auditory Pathway: Neuroanatomy*. New York, NY: Springer-Verlag, 117–167.

Slepecky, NB. 1996. Structure of the mammalian cochlea. In: P Dallos, AN Popper, RR Fay (eds.), *The Cochlea*. New York, NY: Springer-Verlag, 44–129.

Slepecky, NB, Ulfendahl, M, Flock, A. 1988. Effects of caffeine and tetracaine on outer hair cell shortening suggest intracellular calcium involvement. *Hear Res* 32, 11–32.

Smith, CA, Lowry, OH, Wu, M-L. 1954. The electrolytes of the labyrinthine fluids. *Laryngoscope* 64, 141–153.

Smith, CA, Rasmussen, GL. 1963. Recent observations on the olivocochlear bundle. *Ann Otol* 72, 489–506.

Smith, CA, Sjostrand, F. 1961. Structure of the nerve endings of the guinea pig cochlea by serial sections. *J Ultrasound Res* 5, 523–556.

Spoendlin, H. 1969. Innervation of the organ of Corti of the cat. *Acta Otol* 67, 239–254.

Spoendlin, H. 1971. Degeneration behavior in the cochlear nerve. *Arch Klin Exp Ohren Nasen KehlkopfFeilkd* 200, 275–291.

Spoendlin, H. 1975. Neuroanatomical basis of cochlear coding mechanisms. *Audiology* 14, 383–407.

Spoendlin, H. 1978. The afferent innervation of the cochlea. In: RF Naunton, C Fernandez (eds.), *Evoked Electrical Activity in the Auditory Nervous System*. London, UK: Academic Press, 21–41.

Spoendlin, H. 1979. Neural connection of the outer hair-cell system. *Acta Otol* 87, 381–387.

Spoendlin, H. 1981. Differentiation of cochlear afferent neurons. *Acta Otol* 91, 451–456.

Spoendlin, H. 1982. Innervation of the outer hair cell system. *Am J Otol* 3, 274–278.

Spoendlin, H, Gacek, RR. 1963. Electromicroscopic study of the efferent and afferent innervation of the organ of Corti. *Ann Otol* 72, 660–686.

Steel, KR. 1983. The tectorial membrane of mammals. *Hear Res* 9, 327–359.

Steel, KR. 1985. Composition and properties of mammalian tectorial membrane. In: DG Drescher (ed.), *Auditory Biochemistry*. Springfield, IL: Charles C. Thomas, 351–365.

Strelioff, D, Flock, A. 1984. Stiffness of sensory-cell hair bundles in the isolated guinea pig cochlea. *Hear Res* 15, 19–28.

Strutz, J, Spatz, W. 1980. Superior olivary and extraolivary origin of centrifugal innervation of the cochlea in guinea pig: A horseradish peroxadase studys. *Neurosci Lett* 17, 227.

Takahashi, T, Kimura, RS. 1970. The ultrastructure of the spiral ligament in the Rhesus monkey. *Acta Otol* 69, 46–60.

Thalmann, I, Machiki, K, Calabro, A, Hascall, VC, Thalmann, R. 1993. Uronic acid-containing glycosaminoglycans and keratan sulfate are present in the tectorial membrane of the inner ear: Functional implications. *Arch Biochem Biophys* 307, 391–393.

Thalmann, I, Thallinger, G, Comegys, TH, Crouch, EC, Barret, N, Thalmann, R. 1987. Composition and supramolecular organization of the tectorial membrane. *Laryngoscope* 97, 357–367.

Tilney, LG, DeRosier, DJ, Mulroy, MJ. 1980. The organization of actin filaments in the skeleton of cochlear hair cells. *J Cell Biol* 86. 244–259.

Tilney, LG, Saunders, JC. 1983. Actin filaments, stereocilia, and hair cells of bird cochlea. I. Length, number, width, and distribution of stereocilia of each hair cell are related to the position of the hair cell on the cochlea. *J Cell Biol* 96, 807–821.

Tilney, LG, Tilney, MS. 1986. Functional Organization of the Cytoskeleton. *Hear Res* 22, 55–77.

Tos, M. 1995. *Manual of Middle Ear Surgery: Vol. 2, Mastoid Surgery and Reconstructive Procedures*. New York, NY: Thieme Medical Publishers.

Ulehlova, J, Voldrich, L, Janisch, R. 1987. Correlative study of sensory cell density and cochlear length in humans. *Hear Res* 28, 149–151.

Vollrath, MA, Kwan, KY, Corey, DP. 2007. The micromachinery of mechanotransduction in hair cells. *Ann Rev Neurosci* 30, 339–365.

Wallace, MN, Johnson, PW, Palmer, AR. 2002. Histochemical identification of cortical areas in the *auditory region* of the human brain. *Exp Brain Res* 143, 499–508.

Wangemann, P, Schacht, J. 1996. Cochlear homeostasis. In: P Dallos, AN Popper, RR Fay (eds.), *The Cochlea: Handbook of Auditory Research*. Vol. 8. New York: Springer Verlag, 130–185.

Warr, WB. 1978. The olivocochlear bundle: Its origins and terminations in the cat. In: RF Naunton, C Fernandez (eds.), *Evoked Electrical Activity in the Auditory Nervous System*. New York, NY: Academic Press, 43–65.

Warr, WB. 1992. Organization of the olivocochlear efferent systems in mammals. In: WB Webster, AN Popper, RF Fay (eds.), *The Mammalian Auditory Pathway: Neuroanatomy*. New York, NY: Springer-Verlag, 410–448.

Wbarnes, WT, Magoun, HW, Ranson, SW. 1943. The ascending auditory projection in the brainstem of the monkey. *J Comp Neurol* 79, 129–152.

Webster, WB, Popper, AN, Fay, RF, (eds.). 1992. *The Mammalian Auditory Pathway: Neuroanatomy*. New York, NY: Springer-Verlag.

Weiss, TE, Mulroy, MJ, Turner, RG, Pike, CL. 1976. Tuning of single fibers in the cochlear nerve of the alligator lizards: Relation to receptor morphology. *Brain Res* 115, 71–90.

Wenthold, RJ. 1978. Glutamic acid and apartic acid in subdivisions of the cochlear nucleus after auditory nerve lesion. *Brain Res* 143, 544–548.

Wenthold, RJ. 1991. Neurotransmitters of the brainstem auditory nuclei. In: RA Altschuler, RP Bobbin, BM Clopton, DW Hoffman (eds.), *Neurobiology of Hearing: The Central Auditory System*. New York, NY: Raven, 121–140.

Wenthold, R, Hunter, C, Petralia, R. 1993. Excitatory amino acid in the rat cochlear nucleus. In: M Murchan, J Juis, D Godfrey, F Mugnaina (eds.), *The Mammalian Cochlear Nuclei: Organization and Function*. New York, NY: Plenum, 179–194.

Wever, EG, Lawrence, M. 1954. *Physiological Acoustics*. Princeton, NJ: Princeton University Press.

Winer, JA. 1984. The human medial geniculate body. *Hear Res* 15, 225–247.

Winer, JA. 1985. The medial geniculate body of the cat. *Adv Anat Embryol Cell Biol* 86, 1–98.

Winer, JA. 1991. Anatomy of the medial geniculate body. In: RA Altschuler, RP Bobbin, BM Clopton, DW Hoffman (eds.), *Neurobiology of Hearing, Vol. 2. The Central Auditory System*. New York, NY: Springer-Verlag.

Winer, JA. 1992. The functional architecture of the medial geniculate body and the primary auditory cortex. In: WB Webster, AN Popper, RF Fay (eds.), *The Mammalian Auditory Pathway: Neuroanatomy*. New York, NY: Springer-Verlag, 222–409.

Winer, JA, Diamond, IT, Raczkowski, D. 1977. Subdivisions of the auditory cortex of the cat: The retrograde transport of horseradish peroxidase to the medial geniculate body and posterior thalamic nuclei. *J Comp Neurol* 176, 387–417.

Wright, A. 1981. Scanning electron microscopy of the human cochlea—The organ of Corti. *Arch Otorhinolaryngol* 230,11–19.

Wright, A. 1984. Dimensions of the cochlear stereocilia in man and the guinea pig. *Hear Res* 13, 89–98.

Wright, A, Davis, A, Bredberg, G, Ulehlova, L, Spencer, H. 1987. Hair cell distributions in the normal human cochlea. *Acta Otol Suppl* 444, 1–48.

Wynne, B, Harvey, AR, Robertson, D, and Sirinathsinghji, DJ 1995. *Neurotransmitter* and neuromodulator systems of the rat *inferior colliculus* and auditory brainstem studied by in situ hybridization. *J Chem Neuroanat* 9, 289–300.

Zwislocki, JJ, Chamberlain, SC, Slepecky, NB. 1988. Tectorial membrane 1: Static mechanical properties in vivo. *Hear Res* 33, 207–222.

3 Conductive Mechanism

This chapter deals with the routes over which sound is conducted to the inner ear. The first section is concerned with the usual air conduction path through the outer and middle ear. The second section briefly discusses the bone conduction route. In the last section, we shall address the acoustic reflex.

OUTER EAR

We cannot discuss the contributions of the outer ear *per se* without being aware that the sounds we hear are affected by the entire acoustical path from the sound source to our ears. This path includes the effects of the listener him- or herself. For example, the head casts an acoustical shadow (analogous to an eclipse) when it is between the sound source and the ear being tested. This **head shadow** is significant for frequencies over about 1500 Hz because their wavelengths are small compared to the size of the head. Moreover, the sound entering the ear canal is affected by reflections and diffractions associated with the head, pinna, and torso. Hence, the issue of spatial orientation comes into play, and with it the need for a way to describe the direction of a sound source. Many of these matters are discussed in Chapter 13. For now, it should suffice to know that the *horizontal direction* of a source is given as an angle called **azimuth**, where 0° is straight ahead, 180° is straight back, and 90° is off to one side; and that the *vertical direction* (along the medial plane from front to back) is given by an angle called **elevation**, where 0° is straight ahead, 180° is straight back, and 90° is directly above.

Pinna

The **pinna** has traditionally been credited with funneling sounds into the ear canal and enhancing localization. It has been demonstrated, however, that hearing sensitivity is not affected when the pinna is excluded from sound conduction by bypassing it with tubes into the canal and by filling its depressions (Bekesy and Rosenblith, 1958). Thus, the sound collecting/funneling function is not significant for the human pinna. The pinna's greatest contribution to hearing is actually in the realm of sound source *localization* (see Chap. 13).

The pinna influences localization because its depressions and ridges filter the high-frequency aspects of the signal (over about 4000 Hz) in a way that depends on the direction of the sound (e.g., Shaw, 1997). The spectral variations introduced by the pinna are important directional cues for determining the *elevation* of a sound source and *front/back* distinctions, and contribute to *extracranialization*, or the perception that a sound source is outside of the head (Plenge, 1974 ; Blauert, 1997). Pinna effects are particularly important when one must localize sounds while listening with only one ear (monaurally), because monaural hearing precludes the use of the interaural differences available during binaural hearing, and when the sound source is in the *medial plane* of the head, where interaural differences are minimized because the sound source is equidistant from both ears. These effects are readily shown by increases in the number of localization errors that are made when the various depressions of the pinna are filled (e.g., Gardner and Gardner, 1973 ; Oldfield and Parker, 1984).

Ear Canal

The tympanic membrane is located at the end of the ear canal rather than flush with the surface of the skull. Sounds reaching the eardrum are thus affected by the acoustic characteristics of the ear canal. The ear canal may be conceived of as a tube open at one end and closed at the other. Such a tube resonates at the frequency with a wavelength four times the length of the tube. Because the human ear canal is about 2.3 cm long, its resonance should occur at the frequency corresponding to a wavelength of 9.2 cm, that is, at about 3800 Hz. One could test this hypothesis by directing a known sound into a sound field, and then monitoring the sound pressure at the eardrum of a subject sitting in that sound field. This test has been done in various ways in many studies. Figure 3.1 shows the results of three classic studies in the form of head-related transfer functions (Wiener and Ross, 1946 ; Shaw, 1974 ; Mehrgardt and Mellert, 1977). A **transfer function** shows the relationship between the input to a system and its output. The **head-related transfer function (HRTF)** shows how sounds presented from a particular direction are affected by the entire path from the loudspeaker to the eardrum. The HRTFs in the figure show how sounds presented from a speaker directly in front of the subject (0° azimuth) are affected by the ear canal. The common finding of these functions is a wide resonance peak in from roughly 2000 to 5000 Hz, which is due to the resonance of the ear canal. It does not resemble the sharp resonance of a rigid tube. However, the ear canal is an irregular rather than a simple tube, and the drum and canal walls are absorptive rather than rigid. These factors introduce damping. Group (averaged) data are also shown in the figure. Because resonant frequency depends on canal length, variations in ear canal length among subjects will widen and smooth the averaged function. The important point, however, is that the resonance characteristics of the canal serve to boost the level of sounds in the mid-to-high frequencies by as much as about 15 dB at the eardrum compared to the sound field.

Stinton and Lawton (1989) reported very accurate geometric specifications of the human ear canal based upon impressions taken from cadavers. They found considerable diversity from canal to canal, resulting in differences greater than 20 dB for the higher frequencies, particularly over 10,000 Hz. Considerable variability in the dimensions of the skull, dimensions of pinna structures, etc., which influence HRTFs, has also been reported by Middlebrooks (1999) .

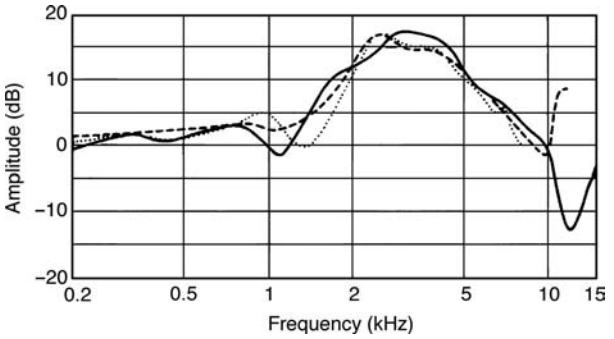

Figure 3.1 Head-related transfer functions for sounds presented from directly in front of the listener (0° azimuth) from three studies [Wiener and Ross (1946), *dotted line*; Shaw (1974), *dashed line*; Mehrgardt and Mellert (1977), *solid line*]. *Source*: From Mehrgardt and Mellert (1977), with permission of *J Acoust. Soc. Am.*

Head-related transfer functions depend on the direction of the sound source. The fundamental nature of this azimuth effect is illustrated for two representative directions in Fig. 3.2. Here, we are concerned with the sound reaching the right eardrum when it is presented from a loudspeaker at an azimuth of 45° to the right compared to being presented from a speaker at 45° to the left. The right ear is the **near ear** when the sound comes from the right (same side of the head), and it is the **far ear** when the sound comes from the left (the opposite side of the head). Note that the sound level increases going from the far ear, and that there are differences in the details of the shapes of the two curves. Physical factors of this type provide the basis for sound localization in space (see Chap. 13).

Middle Ear

Sound reaches the ear by way of the air, a gas. On the other hand, the organ of Corti is contained within the cochlear fluids, which are physically comparable to seawater. The difference between these media is of considerable import to hearing, as the following example will show. Suppose you and a friend are standing in water at the beach. He is speaking, and in the middle of his sentence you dunk your head under the water. However loud and clear your friend's voice was a moment ago, it will be barely, if at all, audible while your head is submerged. Why?

The answer to this question is really quite straightforward. Air offers less opposition, or **impedance**, to the flow of sound energy than does seawater. Because the water's impedance is greater than that of the air, there is an impedance mismatch at the boundary between them. Airborne sound thus meets a substantial increase in the opposition to its flow at the water's surface, and much of the energy is reflected back rather than being transmitted through the water. The impedance mismatch between the air and cochlear fluids has the same effect. The middle ear system serves as an **impedance-matching transformer** that makes it possible for the sound energy to be efficiently transmitted from the air to the cochlea.

As with any other system, the impedance of the conductive system is due to its stiffness, mass, and resistance. Figure 3.3 is a block diagram of the conductive mechanism with respect to its impedance components, based on conceptualizations by

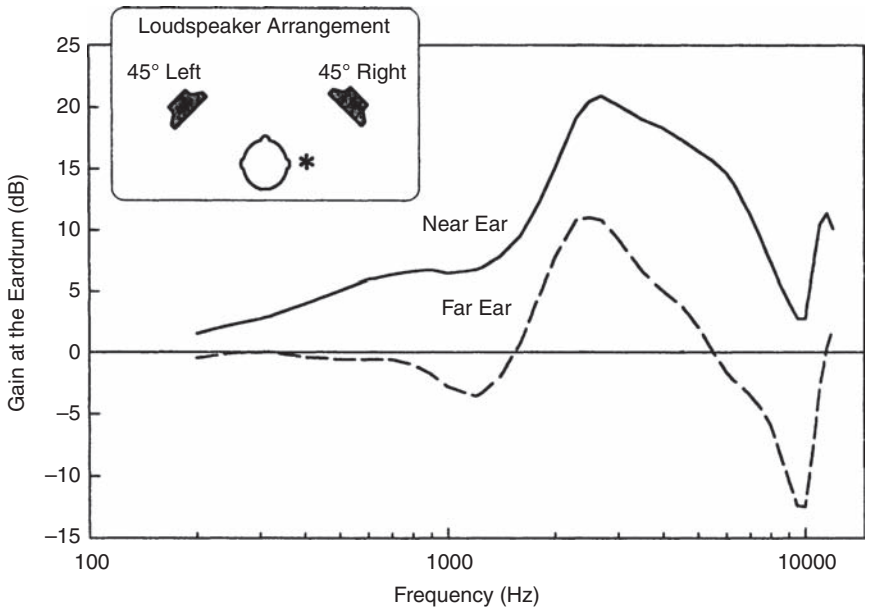

Figure 3.2 Head-related transfer functions resulting from the presentation of sound from loudspeakers located on the same ("near ear") and opposite ("far ear") sides of the head. Insert: loudspeaker arrangement associated with the transfer functions. *Source*: Based on data derived from Shaw (1974) and Shaw and Vaillancourt (1985).

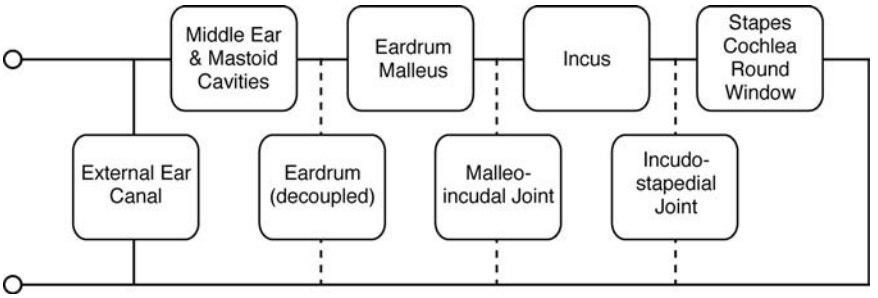

Figure 3.3 Block diagram of the components contributing to the impedance of the ear, based on various diagrams by Zwislocki (1962, 1976) and Bennett (1984).

Zwislocki (1962 , 1976) and Bennett (1984) . The leftmost box, labeled "external ear canal," represents the stiffness reactance contributed by the external auditory meatus. One may think of the upper row of boxes as the line of energy flow from the eardrum to the cochlea, and of the boxes coming down from them via dotted lines as the ways in which energy is shunted from the system. The first box represents the middle ear cavities, which contribute significantly to the stiffness of the system. Actually, the impedance of the middle ear space (including the mastoid air cells) is controlled by compliance up to about 500 Hz, but becomes complicated at higher frequencies (Stepp and Voss, 2005). The next two boxes, "eardrum/malleus" and "eardrum (decoupled)," should be thought of together. The former represents the proportion of sound energy transmitted from the drum to the malleus. It includes the inertia of the malleus; the elasticity of the drum, tensor tympani muscle, and mallear ligaments; and the friction caused by the strain on these structures. "Eardrum (decoupled)" is the proportion of energy diverted from the system when the drum vibrates independently (decoupled from) the malleus, which occurs particularly at high frequencies. The box labeled "incus" is the effective mass of the incus and the stiffness of its supporting ligaments. The energy lost at the two ossicular joints is represented by the boxes labeled "malleoincudal joint" and "incudostapedial joint," which shunt energy off the main line of the diagram. The last box shows the effects of the stapes, cochlea, and round window in series. The attachments of the stapes as well as the round window membrane contribute to the stiffness component. Most of the ear's resistance is attributable to the cochlea. Zwislocki (1975) pointed out that a major effect of this resistance is to smooth out the response of the middle ear by damping the free oscillations of the ossicular chain.

Middle Ear Transformer Mechanism

The ratio between the impedances of the cochlear fluids and the air is approximately 4000:1. To find out how much energy would be transmitted from the air to the cochlea without the middle ear, we apply the simple formula $T = 4r/(r + 1)^2$, where T is transmission and r is the ratio of the impedances. The result is approximately 0.001. In other words, only about 0.1% of the airborne energy would be transmitted to the cochlea, while about 99.9% would be reflected back. This corresponds to a 40-dB drop going from the air to the cochlea.

The middle ear "steps up" the level of airborne sound to overcome the impedance mismatch between the air and cochlear fluids. As we shall see in the next chapter, early place theory held that the middle ear transformer mechanism was the source of various nonlinearities in hearing, such as the perception of combination tones (Helmholtz, 1868). These *distortion products* of the middle ear's hypothetical nonlinear response were ostensibly transmitted to the cochlea, where the nonlinearities were analyzed according to the place principle as though they were present in the original signal. However, Wever and Lawrence (1954) demonstrated that the middle ear mechanism actually performs its function with elegant linearity, and we must accordingly regard it as a linear transformer, and look elsewhere (to the cochlea) for the sources of nonlinear distortions.

Several factors, discussed below, contribute to the transformer function of the middle ear. They include the area ratio of the eardrum to the oval window, the curved-membrane mechanism of the eardrum, and the lever action of the ossicular chain.

Area Ratio

We know that pressure (p) is equal to force (F) per unit area (A), or $p = F/A$. If we therefore exert the same pressure over two areas, one of which is five times larger than the other, then the pressure on the smaller surface will be five times greater. Examples of the fundamental principle are shown in Fig. 3.4a.

Wever and Lawrence (1954) reported that the area of the human eardrum is roughly 64.3 mm^2, whereas Bekesy (1941) estimated its area to be about 85 mm^2. Regardless of which estimate is used, it is clear that the area of the eardrum is substantially larger than that of the oval window, which is commonly accepted to be only 3.2 mm^2. Using the values by Wever and Lawrence for purposes of illustration, the ratio of the area of the eardrum to that of the oval window area would be 64.3/3.2 = 20.1 to 1, as shown in Fig. 3.4b. If we assume that the ossicles act as a simple rigid connection between the two membranes,

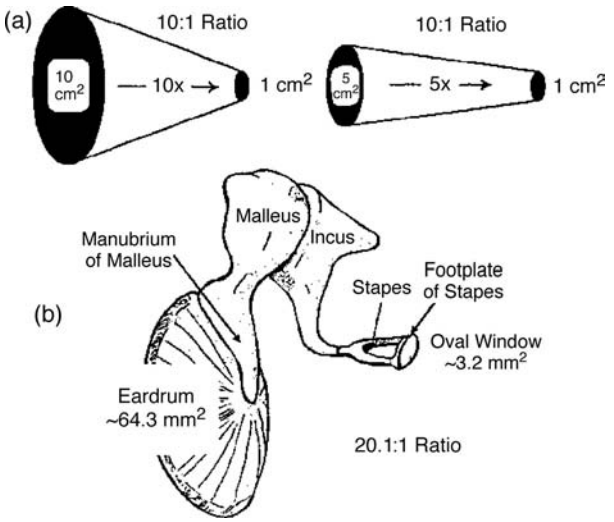

Figure 3.4 (a) Conceptual representation of the area ratio. (b) Determination of the overall area ration using values by Wever and Lawrence (1954), using Bekesy's (1941) values and applying the effective area result in different estimates of the area ratio (see text).

then this area ratio would cause the pressure to be amplified by a factor of 20.1 going from the tympanic membrane to the oval window.

Curved-Membrane Mechanism

Helmholtz (1868) suggested that the eardrum contributes to the effectiveness of the middle ear transformer by a form of lever action, according to the curved-membrane principle (Fig. 3.5). The eardrum's rim is firmly attached to the annulus and curves down to the attachment of the malleus, which is mobile, as in the figure. A given force increment z thus displaces the membrane with greater amplitude than it displaces the manubrium. Because the products of force and distance (amplitude of displacement) on both legs of the lever are equal ($F_1D_1 = F_2D_2$), the smaller distance traveled by the manubrium is accompanied by a much greater force. In this way, Helmholtz proposed that lever action of the eardrum would result in an amplification of force to the ossicles.

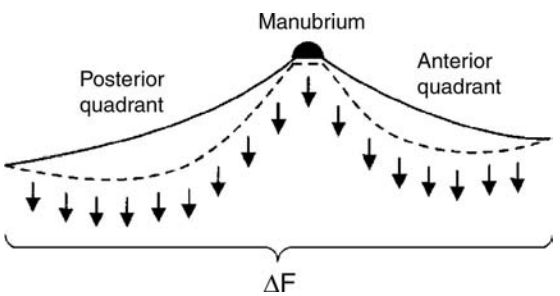

Figure 3.5 The curved-membrane principle (see text). *Source*: Adapted from Tonndorf and Khanna (1970), with permission of *Ann. Otol.*

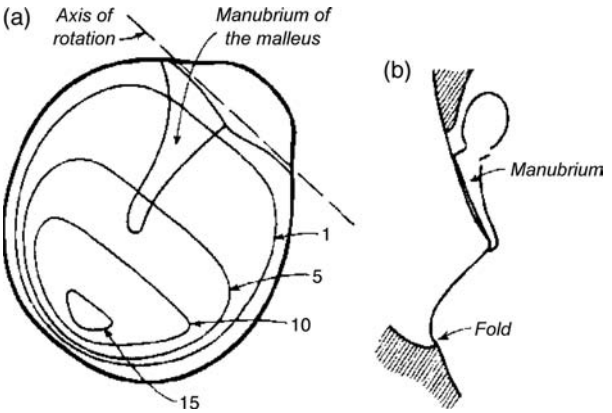

Figure 3.6 (a) Equal relative eardrum displacement contours for a 2000-Hz stimulus. Numbers indicate the relative amplitudes. (b) Cross-section of the tympanic membrane showing a loose-fitting inferior edge. *Source*: From Bekesy (1941).

Subsequent experiments led to the abandonment of this principle, since studies of drum movement were inconsistent with it, and since Helmholtz's results were not replicated (Wever and Lawrence, 1954). Bekesy (1941) used a capacitance probe to measure human eardrum displacement at various frequencies. The capacitance probe used a very fine wire as one plate of a capacitor and the drum surface as the other plate. Sound causes the drum to vibrate, which in turn varies its distance from the wire. If a current is passed through this capacitor, the movement of the drum will affect current flow. Monitoring the current flow at different spots on the drum enabled Bekesy to determine its displacement with considerable accuracy.

Figure 3.6a shows Bekesy's results for a 2000-Hz tone in the form of equal displacement contours. For frequencies up to approximately 2000 Hz, the eardrum moved as a stiff plate or piston, hinged superiorly at the axis of the ossicles. The greatest displacement occurred inferiorly. Bekesy attributed the drum's ability to move in this manner, without significant deformation, to a highly elastic or loose-fitting fold at its inferior edge (Fig. 3.6b). Above about 2000 Hz the tympanic membrane's stiffness broke down, and movement of the manubrium lagged behind that of the membrane rather than being synchronized with it. The stiffly moving portion of the drum had an area of 55 mm^2 out of a total area of 85 mm^2. This area constitutes an **effective area** for the eardrum of about 55 mm^2/85 mm^2 = 65% of its total area. Using Bekesy's values, the ratio of the area of the entire eardrum to the area of the oval window would be 85 mm^2/3.2 mm^2 = 26.6 to 1. However, applying the eardrum's 65% effective area to the overall ratio results in an *effective* area ratio of 26.6 × 0.65 = 17.3 to 1.

The role of the eardrum was reevaluated by Tonndorf and Khanna (1970), who used time-averaged holography to study eardrum movement in the cat. Time-averaged holography is an optical method that reveals equal-amplitude (or isoamplitude) contours as alternating bright and dark lines on a vibrating

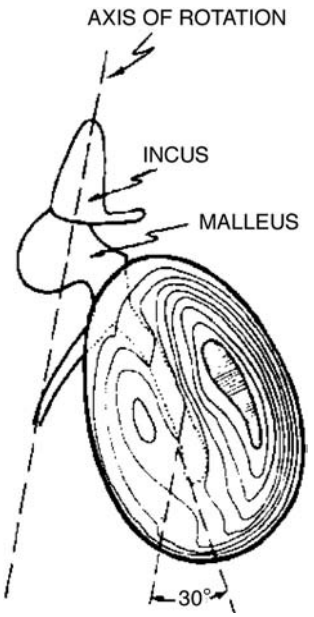

Figure 3.7 Vibration patterns of the cat's eardrum in response to 600-Hz tone. *Source*: From Tonndorf and Khanna (1970), with permission of *Ann. Otol*.

membrane. Figure 3.7 shows the isoamplitude contours for a 600-Hz tone. These contours show that the eardrum actually does not move as a stiff plate. Instead, there are two areas of peak displacement revealing a buckling effect in the eardrum vibration pattern that is consistent with Helmholtz's curved-membrane concept. This mode of vibration is seen up to about 1500 Hz. The pattern becomes more restricted at higher frequencies, and increasingly complex subpatterns occur in the vibrations as frequency rises above 3000 Hz. The curved-membrane principle contributes to the middle ear transformer ratio by a factor of 2.0 based upon the cat data. If we accept an area ratio of 34.6 to 1 for the cat, then the middle ear transfer ratio as of this point becomes $34.6 \times 2.0 = 69.2$ to 1. This value must be multiplied by the level ratio of the ossicles to arrive at the final transformer ratio of the middle ear.

Ossicular Lever

Helmholtz (1868) proposed that nonlinear distortions are introduced by the ossicular chain, and are largely due to what he conceived of as a cogwheel articulation between the malleus and incus. This situation would allow for relative movement in one direction at the malleoincudal joint. The resulting distortions would stimulate the cochlea at places corresponding to the receptors for those frequencies, as though they were present in the original signal. Barany (1938) demonstrated, however, that except during intense stimulation these two bones are rigidly fixed at the malleoincudal joint and move as a unit in response to sound stimulation.

Bekesy (1936) reported that the stapes moves differently in response to moderate and intense stimulation in human cadavers, as illustrated in Fig. 3.8. At moderate intensities, the stapedial footplate rocks with a piston-like motion in the oval window, with greater amplitude anteriorly (Fig. 3.8a). Intense stimulation results in rotation of the footplate around its longitudinal axis (Fig. 3.8b). Rocking of the stapes around the longitudinal axis substantially reduces the energy transmitted to the cochlea. However, Guinan and Peake (1967) have shown that the cat stapes maintains essentially piston-like movements even at very high intensities, at least for low frequencies.

It has been known for a long time that the ossicular chain rotates around its axis, illustrated in Fig. 3.9 (top), which corresponds to a line through the long process of the malleus and the short process of the incus (Barany, 1938). Measurements using advanced optical techniques have revealed that the motion of the malleus is frequency-dependent, so that its vibratory pattern is essentially in one dimension below 2500 Hz, but involves an elliptical path in all three dimensions, as opposed to having a single axis above 2500 Hz (Decraemer, Khanna, and Funnell, 1991, 1994).

The ossicular chain is delicately balanced around its center of gravity so that the inertia of the system is minimal (Barany, 1938). As a result, the ossicular chain acts as a lever about its axis (Fig. 3.9). The malleus constitutes the longer leg of this ossicular lever and the incus constitutes the shorter leg. The lever ratio is on the order of 1.3 to 1 in humans and 2.2 to 1 in cats. However, the actual lever ratio is smaller, because of the interaction of the curvature of the eardrum and the length of the ossicular chain lever (Tonndorf and Khanna, 1970).

Recall that the drum curves more toward the umbo, and may be regarded as a curved string. The transformer ratio of a curved string decreases as the curvature becomes stronger (1/curvature). On the other hand, the transformer ratio of the ossicular lever increases with length. Note in Fig. 3.10 that the ossicular lever is long (with respect to the point of attachment of the malleus on the drum) where the curvature is strong, and that it is short where the curvature is small. This interaction results in an essentially constant lever ratio, with a value of about 1.4 for the cat ossicular chain.

We may now apply the ossicular lever ratio to the intermediate solution of 69.2 obtained so far for the cat's middle ear transfer ratio. The final ratio becomes $69.2 \times 1.4 = 96.9$ to 1. The ratio is converted into decibels as follows: $20 \times \log 96.9 = 39.7$ dB. This value closely approximates the 40-dB loss that results when the cat's middle ear is completely obliterated (Tonndorf, Khanna, and Fingerhood, 1966). Using an effective area ratio of 26.6, an eardrum bucking factor of 2.0 and an ossicular lever ratio of 1.3, the human middle ear transformer ratio may be estimated at approximately $26.6 \times 2 \times 1.3 = 69.2$ to 1, which corresponds to $20 \times \log 69.2 = 36.8$ dB. As illustrated in Fig. 3.11, actual middle ear transformer ratios fall short of these values, and they depend considerably upon frequency. That the actual boost provided by the conductive

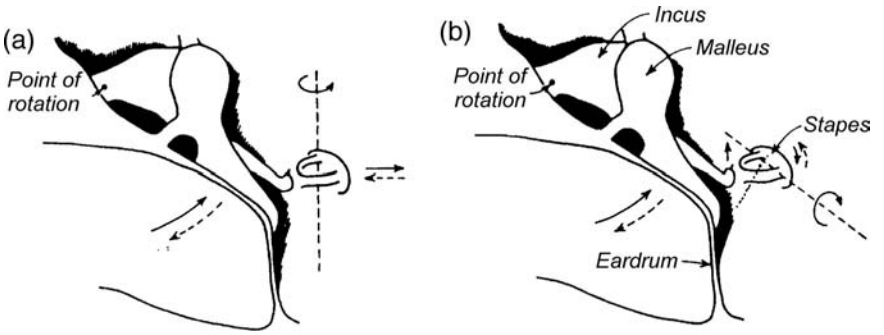

Figure 3.8 The nature of stapes movement in cadavers in response to stimuli presented at (a) moderate levels and (b) very intense levels. *Source*: From Bekesy (1936).

system does not achieve the values based on the calculations is probably due to transmission losses. Rosowski (1991) estimated that the efficiency of the human middle ear system peaks at about 0.4 in the vicinity of 900 Hz, and then decreases for higher frequencies, and averages approximately 0.2 in the cat.

Middle Ear Response

Figure 3.11, based on Nedzelnitsky's (1980) data from cats, provides an example of a middle ear transfer function. The middle ear transfer function makes a substantial contribution to the shapes of minimal audibility curves (see Chap. 9). These curves show the amount of sound energy needed to reach the threshold of hearing as a function of frequency.

Bekesy (1941) reported that the resonant frequency of the middle ear is in the 800 to 1500 Hz region. Recall that resonance occurs when mass and stiffness reactance are equal, canceling out. Impedance is then entirely composed of resistance, and accordingly the opposition to energy flow is minimal at the resonant frequencies. Mϕller (1960)Møller (1960) found the major resonance peak of the middle ear to be about 1200 Hz, with a smaller resonance peak around 800 Hz. Normal ear reactance and resistance values based on 20 studies are summarized in Fig. 3.12 (Margolis, VanCamp, Wilson, and Creten, 1985). Note that the ear's impedance results primarily from negative reactance up to about 800 Hz. This effect is due to the middle ear mechanism itself, which is stiffness controlled below the resonant frequency. There is virtually no reactance between about 800 Hz and roughly 5000–6000 Hz, indicating that energy transmission from the eardrum to the cochlea is maximal in this range. Positive reactance takes over at higher frequencies as a result of the effective mass of the drum and ossicles. We thus expect sound transmission through the middle ear to be frequency-dependent with emphasis on the midfrequencies; and the minimal audibility curves of the ear should reflect this relation.

The cat's middle ear transfer function and behavioral thresholds are compared in Fig. 3.13. The open circles in Fig. 3.13 show the middle ear transfer function based on data from anesthetized cats (Dallos, 1973). The filled circles are the behavioral

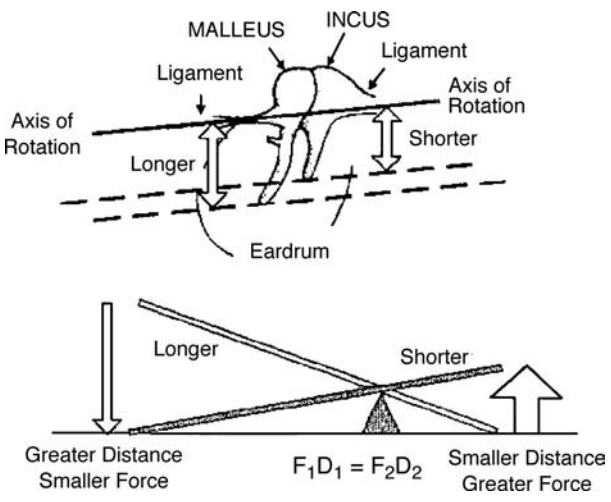

Figure 3.9 The axis of rotation of the ossicular chain and the ossicular lever mechanism. Based in part on drawings by Barany (1938) and Bekesy (1941).

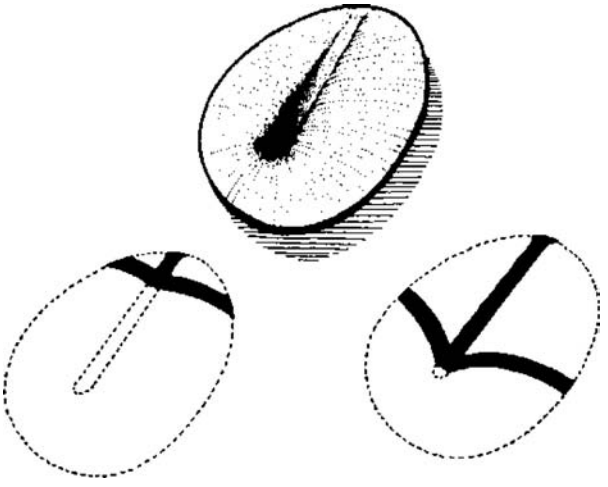

Figure 3.10 The interaction between the length of the ossicular chain and the inverse of the eardrum curvature. *Source*: From Tonndorf and Khanna (1970), with permission of *Ann. Otol.*

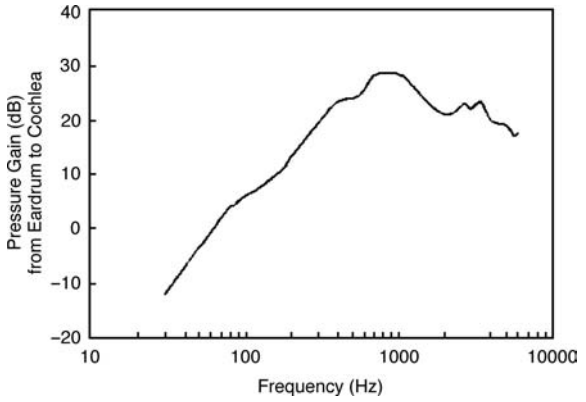

Figure 3.11 The middle ear transfer function from the tympanic membrane to the cochlear fluids as a function of frequency. *Source*: Adapted from Nedzelnitsky (1980), with permission of *J. Acoust. Soc. Am.*

thresholds of waking cats in a sound field (Miller et al., 1963). The binaural threshold and transfer function are generally similar, but the threshold curve is steeper at low frequencies and flatter at high. This may reflect several factors (Simmons, 1964; Wiener et al., 1966; Dallos, 1970, 1973): First, since the thresholds show mean group data, the curve is probably somewhat flattened by the averaging among subjects; the transfer function is from a single representative animal. In addition, there is a peak at around 4000 Hz in the middle ear response of anesthetized animals, which is much smaller when they are awake due to damping of the system by the tonus of the stapedius muscle. A second factor has to do with the effects of head diffraction, the pinna, and the ear canal, as discussed in the section on the outer ear in this chapter. These effects are accounted for by viewing the behavioral thresholds in terms of the sound pressure level (SPL) near the eardrum at threshold, as is shown by the filled triangles in Fig. 3.13. The relationship of the threshold curve to the transfer function is closer when considered in these terms. The disparity between the transfer function and thresholds below about 1000 Hz is reconciled by correcting the transfer function for the input impedance of the cochlea (open triangles).

These factors show a considerable degree of correspondence between the middle ear transfer function and the threshold curve, at least for the cat. Reasonable agreement between the transfer function based upon a model of the middle ear and the threshold curve has also been shown for humans (Zwislocki, 1975). Thus we find that the impedance-matching job of the middle ear is accomplished quite well for the midfrequencies, although the frequency-dependent nature of the middle ear reduces its efficiency at higher and lower frequencies.

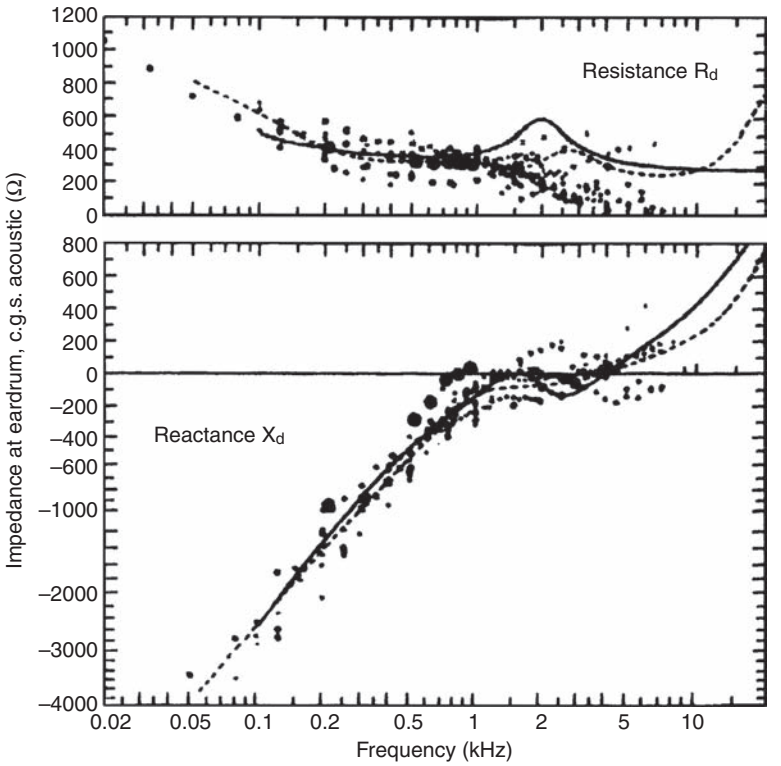

Figure 3.12 Acoustic resistance and reactance as a function of frequency based on 20 studies (see text). *Source*: From Margolis, Van Camp, Wilson, and Creten (1985), with permission.

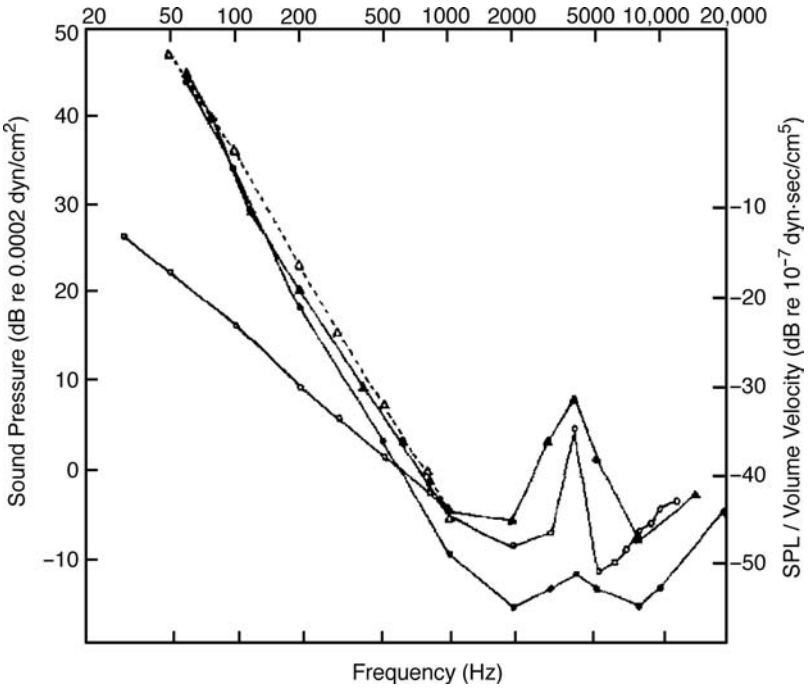

Figure 3.13 Middle ear transfer function (*open circles*) compared to behavioral thresholds (*closed circles*) and sound pressure level (SPL) at the eardrum (*closed triangles*) in cats. *Source*: From Dallos (1973), *The Auditory Periphery*, copyright © 1973 by Academic Press.

BONE CONDUCTION

Until now we have dealt with the usual route from the air to the cochlea. The discussion would be incomplete, however, without at least a brief consideration of bone conduction—the transmission of sound to the cochlea by the bones of the skull. For this to occur, a sound must be strong enough to cause the bones to vibrate, or else the stimulus must be delivered by way of a vibrator applied to the skull. The impedance mismatch between air and bone is even greater than between air and cochlear fluid: An airborne sound must exceed the air conduction threshold by at least 50 to 60 dB before the bone conduction threshold is reached (Bekesy, 1948). Direct stimulation with a vibrator is routinely employed in audiological evaluations to separate hearing losses attributable to the outer and/or middle ear from those due to impairments of the sensorineural mechanisms.

Two classic experiments proved that both air conduction and bone conduction initiate the same traveling waves in the cochlea (see Chap. 4). Bekesy (1932) showed that air- and bone-conduction signals cancel one another when their phases and amplitudes are appropriately adjusted. Lowy (1942) demonstrated that this cancellation occurs in the cochlea, since repetition of the Bekesy experiment on guinea pigs resulted in cancellation of the cochlear microphonic. (The cochlear microphonic is an electrical potential that reflects the activity of the hair cells; see Chap 4.) The implications of these experiments are monumental, since they demonstrate that the final activity in the cochlea is the same regardless of the mode of entry of the sound. Furthermore, this result gives support to the use of bone conduction as an audiological tool, and the results of which can validly be compared with those of air conduction in determining the locus of a lesion (assuming appropriate calibration of both signals).

Bekesy (1932) found that below 200 Hz the human skull vibrates as a unit (Fig. 3.14a). At about 800 Hz, the mode of vibration changes (Fig. 3.14b), and the front and back of the head vibrate in opposite phase to one another, with a nodal line of compression between them. At about 1600 Hz, the head begins to vibrate in four segments (Fig. 3.14c).

Tonndorf and colleagues (1966, 1968) demonstrated that the mechanism of bone conduction includes contributions from the outer, middle, and inner ear. For clarity, let us look at these components, beginning with the inner ear.

Compressional bone conduction is illustrated in Fig. 3.15. Vibration of the temporal bone results in alternate compression and expansion of the cochlear capsule. Because the cochlear fluids are incompressible, there should be bulging at compliant points. Bulging would occur at the oval and round windows without displacement of the cochlear partition if both windows were equally compliant (Fig. 3.15a). However, since the round window is much more compliant than the oval window, compression of the cochlear capsule pushes the fluid in the scala vestibuli downward, displacing the basilar membrane as shown in Fig. 3.15b. This effect is reinforced, since the sum of the

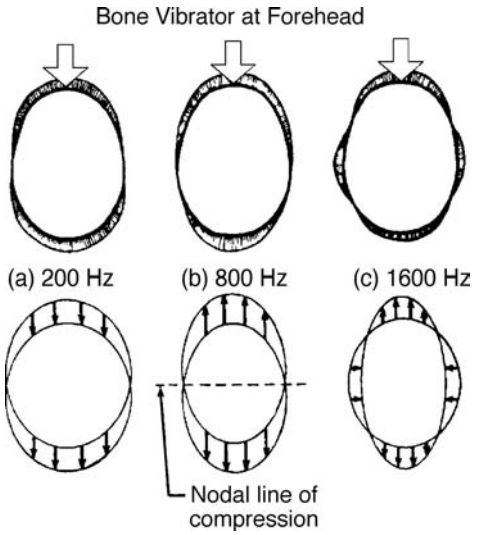

Figure 3.14 Patterns of skull vibration at (a) 200 Hz, (b) 800 Hz, and (c) 1600 Hz, in response to a bone conduction stimulus being applied to the forehead. *Source*: Adapted from Bekesy (1932).

surface area of the vestibule (V in the figure) and the surface area of the scala vestibuli is greater than that of the scala tympani (Fig. 3.15c). The possibility of a "third window" for the release of this pressure is provided by the cochlear aqueduct.

Tonndorf (1962), however, found that the primary mechanism of bone conduction in the inner ear involves distortional vibrations of the cochlear capsule, which are synchronous with the signal (Fig. 3.16). **Distortional bone conduction** occurs because the volume of the scala vestibuli is greater than that of the scala tympani, so that distortions of the cochlear capsule result in compensatory displacements of the cochlear

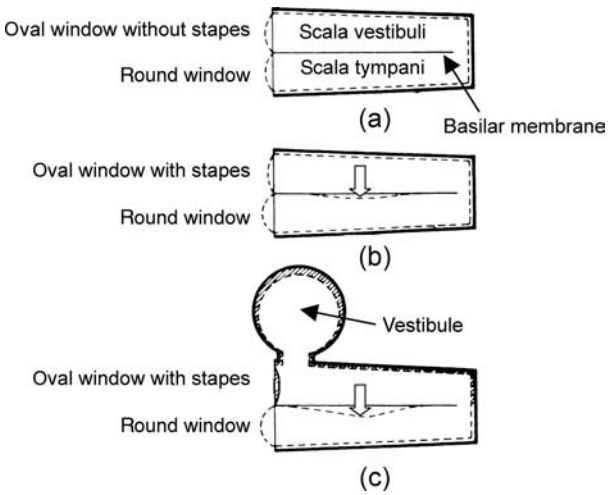

Figure 3.15 Compressional bone conduction (see text). *Source*: Adapted from Bekesy (1932).

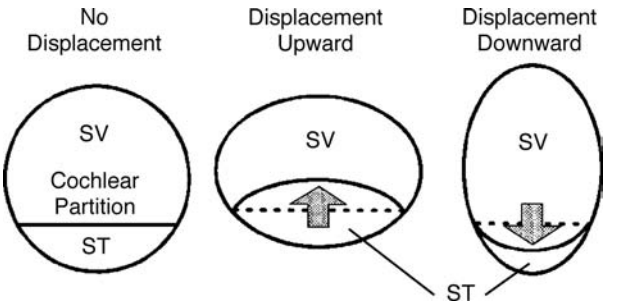

Figure 3.16 Effects of distortional vibrations on displacement of the cochlear partition. *Source*: Adapted from Tonndorf (1962), with permission of *J. Acoust. Soc. Am.*

partition even in the absence of compliant windows. The above-mentioned "windows effects" modify the distortional component.

The contribution of the middle ear to bone conduction is often known as **inertial** or **ossicular-lag bone conduction**, and was demonstrated by Barany (1938). Recall that the ossicles move from side to side rather than front to back. Barany found that for low frequencies bone conduction was maximal when a vibrator was applied to the side of the head and was minimal when it was applied to the forehead. This occurs because the lateral placement vibrates the skull in the direction of ossicular movement (Fig. 3.17a), whereas frontal placement vibrates the skull perpendicular to their movement (Fig. 3.17b). In other words, the signal was transmitted best when it was applied in the direction of rotation of the ossicular chain about its axis. The mechanism is as follows: Because the ossicles are suspended analogously to pendulums, as shown in Fig. 3.17, their inertia causes them to move relative to the skull when the latter is vibrated. Inertial bone conduction, then, stimulates the cochlea by the relative movement of the skull and ossicles, and the effect of which is a rocking motion of the stapes at the oval window.

The middle ear component of bone conduction is of particular interest in otosclerosis, a disorder in which hearing loss

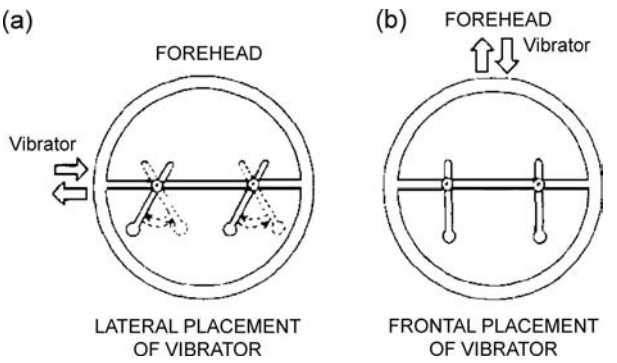

Figure 3.17 Inertial (ossicular lag) bone conduction: (a) lateral placement of the bone vibrator; (b) forehead placement. *Source*: Abstracted from Barany (1938).

results from fixation of the stapes in the oval window. A hearing loss results because the fixated stapedial footplate cannot effectively transmit energy to the cochlea. Although one might expect bone conduction to be impaired at low frequencies, the elevated bone-conduction threshold occurs at about 2000 Hz. This phenomenon is called *Carhart's notch* (Carhart, 1950). Bone conduction is impaired at 2000 Hz, because this is the resonant frequency of the ossicular chain in humans (Tonndorf, 1966).[1]

The contribution of the outer ear to bone conduction is often called osseotympanic bone conduction. It occurs because the vibration of the skull leads to the radiation of sound energy into the ear canal from its walls, and is principally due to vibrations of the cartilaginous portion of the canal (Naunton, 1963; Stenfelt et al., 2003). These radiations then stimulate the eardrum and finally the cochlea along the familiar air-conduction route. The outer ear component is emphasized at low frequencies during occlusion of the cartilaginous part of the ear canal, called the **occlusion effect**. According to Tonndorf (1966), this enhancement of the low frequencies is not appreciated when the ear is unoccluded because the open ear canal acts as a high-pass (low-cut) filter. However, closing off the canal removes the high-pass filter so that the lows are not lost. Another explanation attributes the occlusion effect to differences in the resonances of the ear canal when it is open and closed (Huizing, 1960).

In summary, the bone-conduction mechanism appears to be primarily due to distortion of the inner ear capsule, to the relative movements of the skull and ossicles due to the inertial lag of the latter, and to the sound radiated into the ear canal from its walls. Tonndorf (1966) found in cats that the outer and middle ear components are dominant below about 1000 Hz, but that all three mechanisms are about equally important in the range of 1000 to 6000 Hz, as illustrated in Fig. 3.18. However, findings in human cadavers have suggested that the outer ear component is not significant when the ears are open, although it becomes dominant when the ears are occluded (Stenfelt et al., 2003).

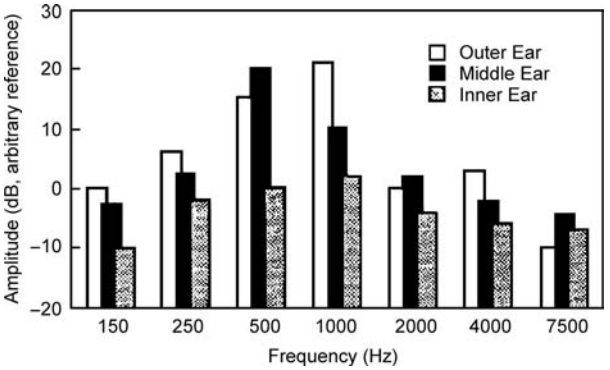

Figure 3.18 The relative contributions of the inner, middle, and outer ear components of bone conduction. *Source*: Adapted from Tonndorf et al. (1966).

THE ACOUSTIC REFLEX

The contraction of the middle ear muscles in response to relatively intense sound stimulation is known as the **acoustic reflex**. Early experiments on dogs revealed bilateral tensor tympani contractions when either ear was stimulated by intense sound (Hensen, 1878; Pollack, 1886). It was later demonstrated that the stapedius muscles also respond bilaterally to sound stimulation in cats and rabbits (Kato, 1913). However, whether the acoustic reflex in humans is due to contractions of one or both of the intratympanic muscles has been the subject of some controversy.

Direct observation through perforated eardrums revealed stapedius muscle contractions in humans as a consequence of intense sound stimulation (Lüscher, 1929; Lindsay et al., 1936; Potter, 1936). Terkildsen (1957, 1960) indirectly examined middle ear muscle activity by monitoring changes in air pressure in the ear canal in response to sound stimulation. Stapedius contraction would result in an outward movement of the drum, while tensor concentration would pull the drum inward (see Chap. 2). The drum movement, in turn, results in changes in ear canal pressure. Terkildsen could thus infer the nature of muscle activity by monitoring the air pressure in the ear canal during sound stimulation. Most of his subjects manifested an outward deflection of the drum, suggesting that the stapedius muscle was active. There were, however, some cases showing tensor activity as well (inward drum displacement). Similar findings were reported by Mendelson (1957, 1961).

Perhaps the greatest contribution to what is known about the acoustic reflex comes from measurements of acoustic impedance at the plane of the eardrum using impedance bridges and subsequent instruments. The mechanical acoustic impedance bridge was first applied to the study of the acoustic reflex by Metz (1946) and was improved upon and made clinically efficient by Zwislocki (1963). An electroacoustic impedance bridge was introduced by Terkildsen and Nielsen (1960). Almost all acoustic reflex research since the introduction of the electroacoustic device has used this method or variations of it. The main principle is straightforward: Because contractions of the intratympanic muscles stiffen the middle ear system (including the drum), the impedance is increased. (The reflex primarily affects the compliance component of impedance rather than resistance, because the system is stiffened.) It is this change in acoustic impedance that is measured by the device.

Let us now consider how the ear's impedance can be used to infer information about the activities of one intratympanic muscle versus the other. In the normal ear, we really cannot tell whether the acoustic reflex is due to contractions of the stapedius and/or of the tensor. However, if the reflex is present

[1] The resonant frequency was about 1500 Hz in temporal bones from cadavers of individuals averaging 74 years old (Stenfelt et al., 2002).

when the stapedius muscle is intact but not when the muscle (or its reflex arc or attachment) is impaired, then we may conclude that the stapedius muscle contributes to the acoustic reflex in humans. The same argument applies to the tensor tympani.

Several studies have demonstrated that the acoustic reflex is absent when there is pathology affecting the stapedius muscle (Jepsen, 1955; Klockhoff, 1961; Feldman, 1967). However, the acoustic reflex was still obtained in two cases of tensor tympani pathology (Jepsen, 1955). It might be added at this point that a measurable tensor tympani reflex is known to occur as part of a startle reaction to very intense sound (Djupesland, 1964), or in response to a jet of air directed into the eye (Klockhoff, 1961). Based on these observations, one is drawn to conclude that in humans the acoustic reflex is a *stapedius* reflex.

Reflex Parameters

Several parameters of the acoustic reflex should be discussed before describing its effect upon energy transmission through the ear, or its suggested roles within the auditory system. The possible relationship between the acoustic reflex and loudness will also be considered.

We have been referring to the acoustic reflex as occurring in response to "intense" sound stimulation. Let us now examine just how intense a sound is needed. With a reasonable amount of variation among studies, the acoustic reflex thresholds in response to pure-tone signals from 250 to 4000 Hz range from 85- to 100-dB SPL (Metz, 1952; Møller, 1962; Jepsen, 1963, Jerger, 1970; Margolis and Popelka, 1975; Wilson and McBride, 1978; Silman, Popelka, and Gelfand, 1978; Gelfand, 1984). The reflex threshold is approximately 20 dB lower (better) when the eliciting stimulus is broadband noise (Peterson and Liden, 1972; Margolis and Popelka, 1975; Silman et al., 1978; Gelfand, 1984). In general, the reflex response is obtained at a lower intensity when it is monitored in the ear being stimulated (the ipsilateral or uncrossed acoustic reflex) instead of in the opposite ear (the contralateral or crossed acoustic reflex) (Møller, 1961; Green and Margolis, 1984). For an extensive discussion of the acoustic reflex threshold and its parameters, see the review by Gelfand (1984).

The lower reflex threshold for broadband noise than for tones suggests that the acoustic reflex is related to the bandwidth of the stimulus. Flottrop et al. (1971) studied this relationship by measuring acoustic reflex thresholds elicited by successively wider bands of noise and complex tones. They found that the increasing bandwidth did not cause the threshold to differ from its value for a pure-tone activator until a certain bandwidth was exceeded. At this point there was a clear-cut break, after which increasing the bandwidth resulted in successively lower reflex thresholds. Similar results were found by Popelka, Karlovich, and Wiley (1974). In addition, Djupesland and Zwislocki (1973) found that increasing the separation in frequency between the two tones in a two-tone complex caused a lowering of the reflex threshold once a particular bandwidth was exceeded. These findings suggest that there is a **critical band** for the acoustic reflex, beyond which widening of the bandwidth results in lower thresholds.

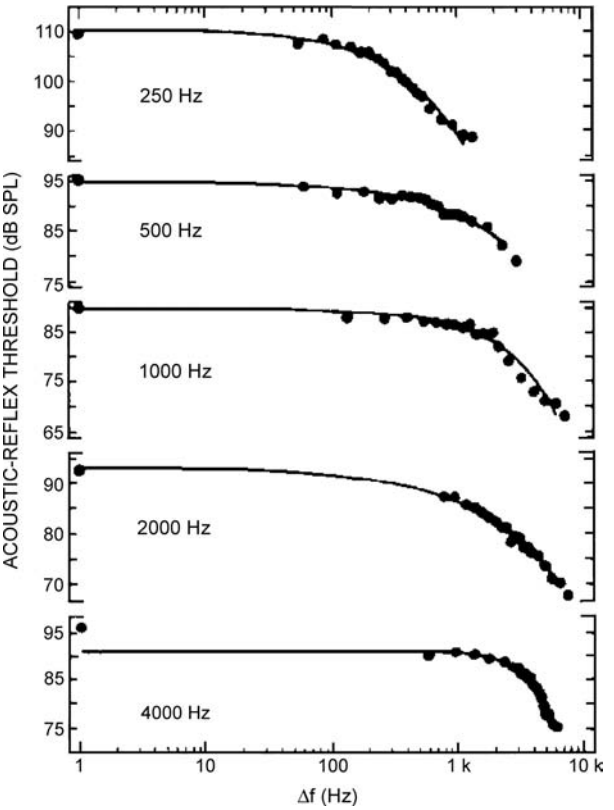

Figure 3.19 Critical bandwidths for acoustic reflex thresholds at center frequencies of 250 to 4000 Hz. Dots to the left of the functions show the corresponding pure-tone reflex thresholds. *Source*: From Popelka et al. (1976), with permission of *J. Acoust. Soc. Am.*

Although the existence of a critical bandwidth was a consistent finding in the noise and two-tone studies, the thresholds were lower for noise. Popelka, Margolis, and Wiley (1976) replicated this work using tone complexes made up of many components that were equally spaced (on a logarithmic scale) in frequency. Their findings, which are shown in Fig. 3.19, confirm the critical band phenomenon. The width of the critical band (shown by the break from the horizontal on each function in Fig. 3.19) increases with center frequency. It is important to note that the critical bandwidth for the acoustic reflex is substantially wider than the psychoacoustic critical bands discussed in chapters that follow. However, Hellmann and Scharf (1984) pointed out that the differences between acoustic reflex and psychoacoustic critical bands may not be as substantial as has been supposed.

The acoustic reflex does not occur instantaneously upon the presentation of the activating signal. Instead, a measurable impedance change is observed after a **latency**, the length of which depends on both the intensity and frequency of the

stimulus. Metz (1951) found that this latency decreased from about 150 ms at 80 dB above the threshold of hearing [dB sensation level (SL)] to 40 m at 100-dB SL in response to a 1000-Hz activating signal. Møller (1958) reported latencies of 25 to 130 ms for 500-Hz and 1500-Hz pure-tones. As a rule, latencies were shorter for 1500 Hz than for 500-Hz tones. Dallos (1964) found a similar inverse relationship between activator intensity and reflex latency for white noise. Hung and Dallos (1972) found that acoustic reflex latencies were shorter for noise signals than for pure-tones, with the longest latencies for tones below 300 Hz. The shortest latencies, on the order of 20 ms, were in response to noise activators.

These measurements were based upon changes in acoustic impedance. However, the latency of the impedance change reflects the *mechanical* response of the middle ear rather than of the *neural transport time* for the reflex arc alone (Borg, 1976). Zakrisson, Borg, and Blom (1974) found that the electromyographic (EMG) response of the stapedius muscle in humans is as short as 12 ms. They also reported that the EMG threshold is about 6 dB lower than that for the impedance change measured as the lowest stimulus level needed to yield 10% of the maximum response. Because we are concerned with the effect of the acoustic reflex on the transmission of energy through the middle ear (at least in this context), we are most interested in the mechanical-response latency. However, one should be aware that changes in muscle potentials occur in the stapedius prior to the measured impedance change.

We have already seen that acoustic reflex latency shortens with increasing stimulus intensity. Similarly, increasing stimulus level also causes an increase in reflex magnitude, which is the amount of impedance change associated with the reflex (Metz, 1951; Møller, 1958; Silman et al., 1978; Gelfand et al., 1981; Silman and Gelfand, 1981; Silman, 1984) and a faster rise time of the reflex response (Dallos, 1964; Hung and Dallos, 1972). The relationship between stimulus level and the resulting reflex magnitude is called the **acoustic reflex growth function**.

The acoustic reflex growth function has been studied in response to pure-tones and wide- and narrowband noise activating signals (Møller, 1962; Dallos, 1964; Hung and Dallos, 1972; Wilson and McBride, 1978; Silman et al., 1978; Gelfand et al., 1981; Silman and Gelfand, 1981; Silman, 1984). The reflex growth functions of four subjects studied by Hung and Dallos (1972) are presented in Fig. 3.20. It illustrates that the growth of acoustic reflex magnitude is essentially linear for pure-tones as high as about 120-dB SPL. The functions for wideband noise are essentially linear up to approximately 110-dB SPL. These data are substantially supported by the other studies cited. Thus, acoustic reflex magnitude tends to increase linearly with a stimulus intensity of 85- to 120-dB SPL for tones and roughly 70- to 110-dB SPL for wideband noise. Saturation occurs at higher levels.

Møller (1961, 1962) reported steeper reflex growth functions with increasing frequency in the 300- to 1500-Hz range. Flottrop et al. (1971) found greater impedance changes at 250 Hz than at 4000 Hz. They also reported that although signals at 1000 and 2000 Hz elicited the same maximum reflex magnitude as at 250 Hz, about 10 dB more (re: reflex threshold) was needed for the two higher frequencies. Furthermore, while some have suggested that a 2000-Hz tone elicits the greatest impedance change (e.g., Kaplan, Gilman, and Dirks, 1977), others suggest that 1000-Hz and wideband stimuli produce maximal responses (Cunningham, 1976; Wilson and McBride, 1978). On the other hand, Borg and Møller (1968) found no significant differences in the slopes of acoustic reflex growth functions in the range from 500 to 3000 Hz in laboratory animals. It thus appears that a clear-cut relationship between activator frequency and reflex magnitude is not fully established.

Temporal summation deals with the relationship between stimulus duration and intensity when the time frame is less than about 1 s (see Chap. 9). It is most easily understood by example. Suppose a subject's threshold for a tone that lasts 200 ms happens to be 18 dB. Will the threshold remain at 18 dB when the same tone is presented for only 20 ms? It is found that when the 20-ms tone is used the threshold changes to 28 dB. (A similar trade-off is needed to maintain the stimulus at a constant loudness. This illustrates the general psychoacoustic observation that when a signal is shortened by a factor of 10 (e.g., from 200 to 20 ms), the signal level must be increased by as much as 10 dB to offset the decade decrease in duration. This relationship is understandably called a **time-intensity trade**.

Temporal summation also occurs for the acoustic reflex (Djupesland and Zwislocki, 1971; Djupesland et al., 1973; Woodford et al., 1975; Jerger et al., 1977; Gelfand et al., 1981). However, it appears that the amount of intensity change needed to counteract a given decrease in stimulus duration is greater for the acoustic reflex than for psychoacoustic phenomena. Figure 3.21 summarizes the general nature of temporal summation for the acoustic reflex (Woodford et al., 1975). Unfortunately, there are rather large differences between the results of various studies reporting the intensity needed to offset a given duration change. For example, decreasing the duration of a 2000-Hz tone from 100 to 10 ms was offset by an increase in stimulus level by about 25 dB in one study (Djupesland and Zwislocki, 1971) as opposed to roughly 15 dB in another (Woodford et al., 1975). In the 500- to 4000-Hz range, Djupesland et al. (1973) studied the time-intensity trade-off relation for the acoustic reflex with one-octave wide noise bands. They used as their comparison point the stimulus level/duration needed to maintain the reflex magnitude at half the maximum impedance change. Djupesland et al. found that a 10-fold decrease in duration was offset by a 20- to 25-dB increase in signal level. In contrast, Gnewikow [1974, cited by Jerger et al. (1977)] found that a 12- to 23-dB intensity increase was needed to offset decade reductions in duration for 500- and 4000-Hz pure-tones. Jerger et al. (1977) found less temporal summation than the other studies, as shown in Fig. 3.22 for 500-, 1000-, 2000-, and 4000-Hz stimuli. Note that the amount of temporal integration increases with frequency, which

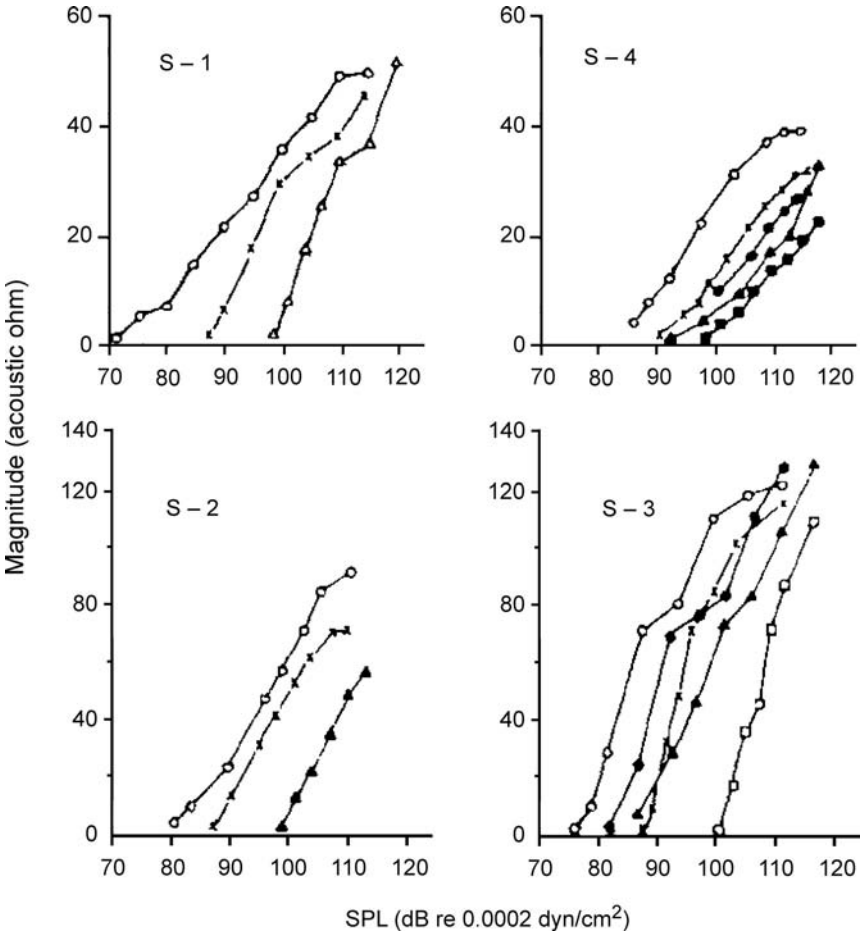

Figure 3.20 Reflex growth functions for wideband noise (*open circles*) and pure-tones (250 Hz, *open squares*; 300 Hz, *filled squares*; 500 Hz, *filled triangles*; 600 Hz, *open tri angles*; 1000 Hz, *crosses*; 1500 Hz, *filled circles*). *Source*: From Hung and Dallos (1972), with permission of *J. Acoust. Soc. Am.*

is a common finding among studies. Jerger et al. (1977) suggested that at least some of the differences are due to problems associated with the "visual detection threshold" (the smallest noticeable impedance change on a meter or oscilloscope), and with "constant percentage of maximum impedance change" methods (Djupesland et al., 1973) of obtaining the data.

Early studies on laboratory animals showed that the degree of muscle contraction due to the acoustic reflex decreases as stimulation is prolonged (Kato, 1913; Lorente de Nó, 1935). This decrease in acoustic reflex magnitude over time is referred to as **reflex decay** or **adaptation**, and it has been found in humans (Dallos, 1964; Borg, 1968; Tietze, 1969a,1969b; Wiley and Karlovich, 1975; Kaplan, Gilman, and Dirks, 1977; Wilson, McCollough, and Lilly, 1984a; Wilson, Shanks, and Lilly 1984b). An extensive review of this topic is provided by Wilson et al. (1984b). In spite of differences among studies, the common finding is that reflex adaptation increases as the frequency of a pure-tone stimulus is raised.

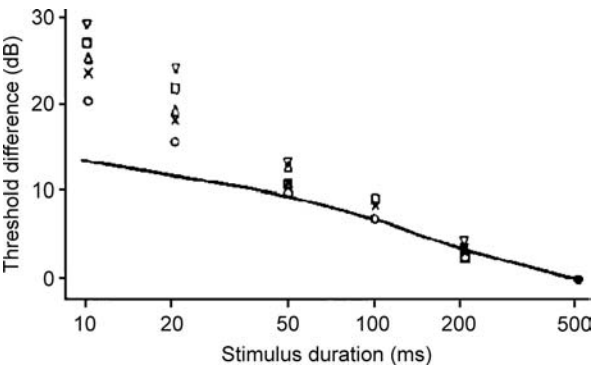

Figure 3.21 Temporal summation for the acoustic reflex threshold. This figure shows the trade-off between activator signal duration and level at 500 Hz (*crosses*), 1000 Hz (*circles*), 2000 Hz (*triangles*), 3000 Hz (*squares*), and 4000 Hz (*inverted triangles*). A typical psychoacoustic temporal summation function is represented by the solid line for comparison. *Source*: From Woodford, Henderson, Hamernick, and Feldman (1975), with permission.

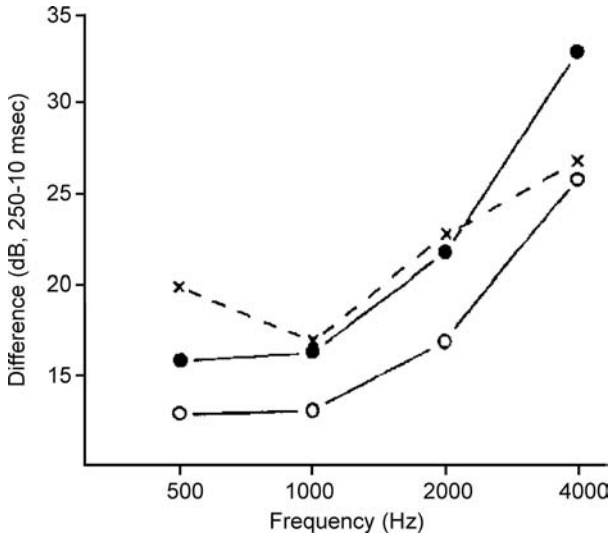

Figure 3.22 Temporal summation for the acoustic reflex at four frequencies obtained by Jerger et al. (1977) (*open circles*), Gnewikow (1974) (*filled circles*), and Woodford et al. (1975) (*crosses*). *Source*: From Jerger, Mauldin, and Lewis (1977). Temporal summation of the acoustic reflex, *Audiology* 16, 177–200 , with permission.

Particular attention should be given to the findings of Kaplan et al. (1977), who studied acoustic reflex adaptation to pure-tones of 500 to 4000 Hz, which were presented at levels of 6, 12, and 18 dB above the reflex threshold. Figure 3.23 summarizes their median data at three sensation levels re: reflex threshold, with stimulus frequency as the parameter. [**Sensation level (SL)** more properly refers to the number of dB above one's threshold of *hearing*. However, in the context of the acoustic reflex, SL is also used to refer to the number of dB above the *reflex* threshold.] There is greater reflex adaptation as frequency increases. Also, adaptation tends to begin sooner after stimulus onset for higher frequencies. These data are normalized in Fig. 3.24, in which the point of greatest impedance change is given a value of 100% and the other points are shown as percentages of the maximum impedance change. In this plot, the data are shown separately at each frequency, with the suprathreshold level as the parameter. In addition to clearly showing the frequency effect, Fig. 3.24 demonstrates that the course of the adaptation function is similar at various levels above reflex threshold, at least up to +18 dB.

Tietze (1969a,1969b) proposed that the course of acoustic reflex adaptation could be described by the time constants of reflex rise time and adaptation. These time constants refer

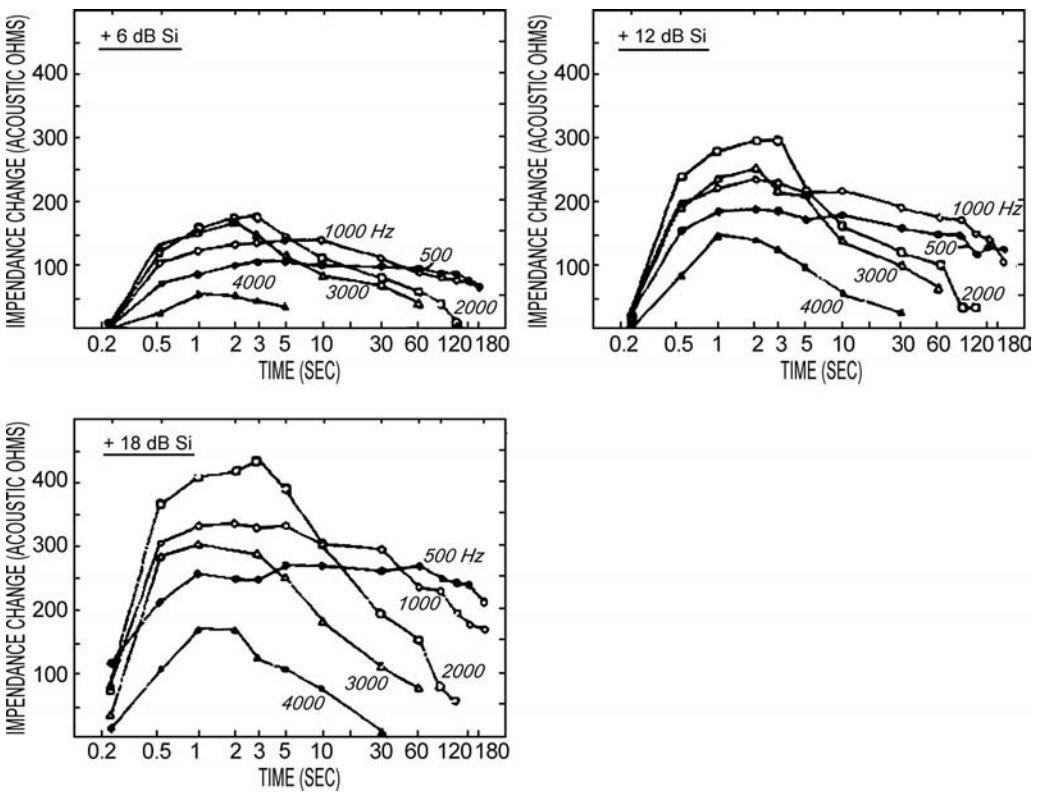

Figure 3.23 Median absolute impedance change (in acoustic ohms) as a function of time for three levels above the acoustic reflex threshold. *Source*: From Kaplan et al. (1977), with permission of *Ann. Otol.*

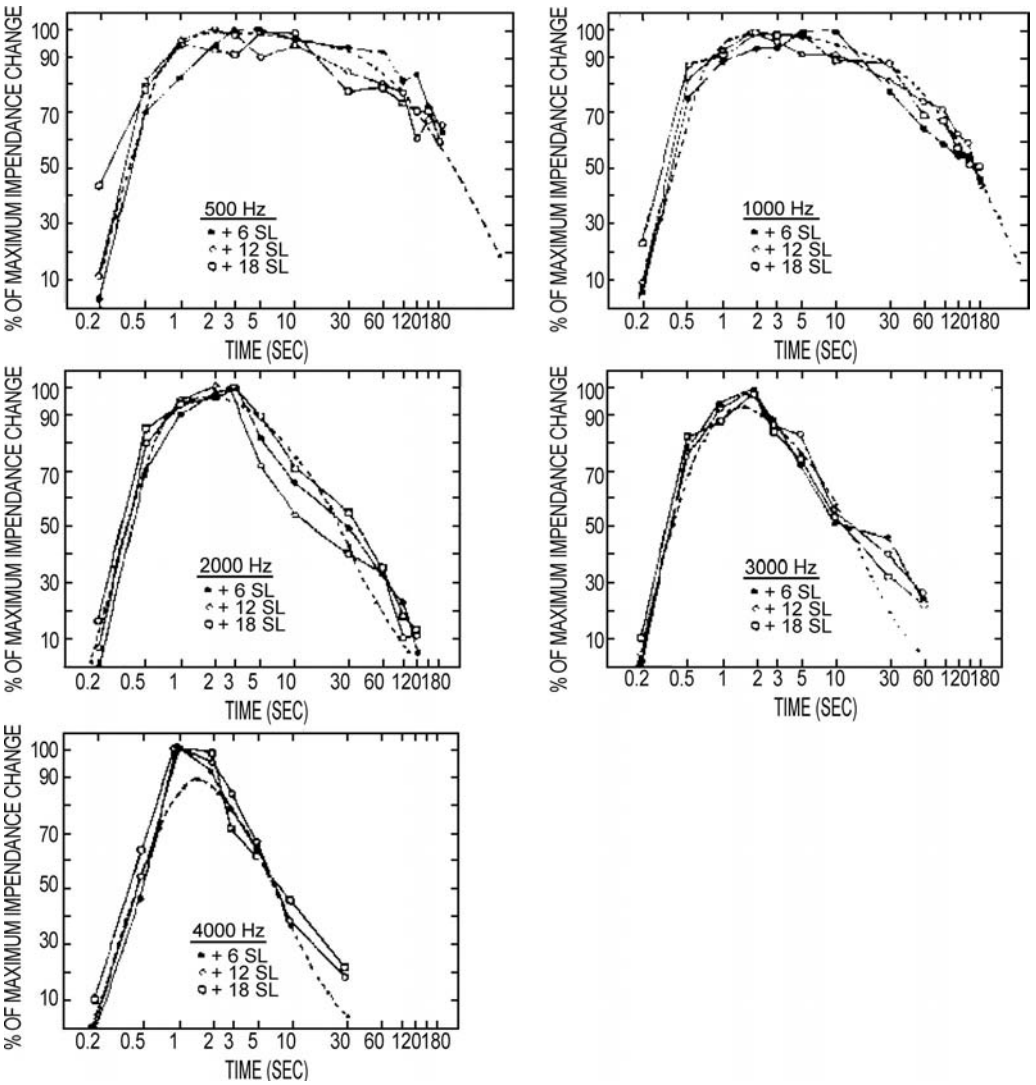

Figure 3.24 Median normalized impedance change (in percent) as a function of time for each frequency. *Source*: From Kaplan et al. (1977), with permission of *Ann. Otol.*

respectively to how long it takes for reflex magnitude to attain 63% of the maximum value (rise) and then to decrease to 63% of it (adaptation); both are measured from the moment of acoustic reflex onset. The time constants are functions of frequency. Tietz's model describes reflex adaptation by the formula

$$\mathrm{Zn} = \frac{1}{1 - \tau_{an}/\tau_{ab}} \left[\exp\left(-t/\tau_{ab}\right) - \exp\left(-t/\tau_{an}\right)\right] \qquad (3.1)$$

where Zn is the normalized maximum impedance change; τ_{an} and τ_{ab} are the time constants of reflex rise and adaptation, respectively; and t is the time (in seconds) of reflex rise from onset. Kaplan et al. (1977) applied this formula to their data, using the ratio τ_{an}/τ_{ab} to generate the dotted lines in Fig. 3.24. (Note that, except at high frequencies where rapid adaptation reduces the maximum impedance change, τ_{an} is generally quite small relative to τ_{ab}.) As Fig. 3.24 shows, the data of Kaplan et al. support the exponential adaptation predicted by Tietze's model.

Loudness is the perceptual correlate of the intensity of the acoustic stimulus (see Chap. 11); other things being equal, loudness increases as stimulus level is increased. An aberration of the intensity–loudness relationship is found in patients with cochlear disorders. Once the signal is increased above the impaired threshold of such an ear, the loudness grows at a faster rate than normal in response to increasing stimulus level. This is called **loudness recruitment**. What has the acoustic reflex to

do with loudness and recruitment? Because both loudness and the acoustic reflex are related to stimulus intensity, at least some association between them is understandable. The question is whether the acoustic reflex is a function of loudness.

Metz (1952) obtained acoustic reflex thresholds at lower SLs from patients with presumably cochlear sensorineural hearing loss than from normal subjects. In other words, the spread between the threshold of hearing and the acoustic reflex threshold was smaller for those with the hearing losses. Because the impaired subjects also had loudness recruitment, Metz proposed that the lower SL of the reflex reflected recruitment. In other words, it was argued that the acoustic reflex was elicited by the loudness of the signal. Jepsen (1963) also attributed acoustic reflex findings in patients with sensorineural hearing losses to be the result of recruitment.

The relationship between loudness and the acoustic reflex, however, is not nearly as clear-cut as these early findings suggest. Ross (1968) compared the equal-loudness and equal-reflex contours of four subjects. The contours were similar for two, while the others had systematic differences between the loudness and acoustic reflex contours (the loudness curves were flatter). Ross suggested that the latter two equal-loudness contours might have been aberrant, but in fact they were quite similar to those reported by Fletcher and Munson (1933), among others.

Margolis and Popelka (1975) compared the loudness of a variety of stimuli set to the acoustic reflex threshold level. There was a range of about 17 dB in the loudness levels, suggesting that the acoustic reflex is not a manifestation of a critical loudness level. Block and Wightman (1977) suggested that the loudness–reflex relationship is supported by their finding of similarly shaped equal-loudness and equal-reflex contours. However, they often found that the same reflex magnitude was elicited by stimulus levels as much as 10 dB apart. Such a spread corresponds to a doubling of loudness (Stevens, 1956); in this light, their findings appear to support rather than refute those of Margolis and Popelka. The substantially wider critical bands for the acoustic reflex than for loudness discussed previously provide a further basis for questioning the concept that the acoustic reflex is loudness-based.

Returning to patient data, Beedle and Harford (1973) found steeper acoustic reflex growth functions for normal ears than for ears with cochlear dysfunction. This result is, of course, inconsistent with a loudness basis for the reflex. The impact of their data, however, was impaired by the fact that their normal subjects averaged 24 years old, compared to 47 years old for the pathological group. The reflex growth functions of age-matched normal and hearing-impaired subjects were studied by Silman, Popelka, and Gelfand (1978). Examples of their findings are shown in Fig. 3.25. If the reflex were loudness-determined, then the function for the impaired groups, although displaced along the intensity axis, would be expected to approach the normal curves at higher stimulus levels. This expectation is based on the notion that loudness recruitment should result in equal loudness for both groups at equal suprathreshold levels. Equal loudness would in turn elicit equal reflex magnitudes at those levels. As Fig. 3.25 shows, this was not the case.

Hellman and Scharf (1984) argued that the case against a loudness–reflex relationship is not as convincing as it might seem. Just two examples will be briefly mentioned. Consider first the material in Fig. 3.25, just discussed. These data could be explained by the fact that both loudness and reflex magnitude increase as power functions of the stimulus level at the SPLs where these functions are obtained. Second, they demonstrated that for given subjects, equally loud sounds elicited equal reflex magnitudes when the criteria were defined precisely. Given that both loudness and the acoustic reflex reflect the neural coding of the stimulus level at the periphery, it is thus understandable that the two phenomena should be related. The controversial and unresolved issue is whether one is dependent upon the other. It is apparent that the acoustic reflex is largely stimulus-dependent. Furthermore, it should not be surprising that the parameters of the reflex response reflect the sensory (and neural) processing of relatively intense stimulation. It is equally apparent that the acoustic reflex is a feedback or control mechanism, although its exact purpose(s) remains unclear. Given these points, what effect does the acoustic reflex have on energy transmission through the conductive mechanism?

Recall that the acoustic reflex stiffens the conductive mechanism so that sound is reflected at the eardrum (Dallos, 1964). Because the effect of stiffness is inversely related to frequency, we would expect the acoustic reflex to affect middle ear transmission most strongly at lower frequencies.

Smith (1943) and Reger (1960) compared the pure-tone thresholds of human subjects to the thresholds during voluntary contractions of the middle ear muscles. Thresholds were shifted by about 20 to 40 dB at 125 to 500 Hz, and by 15 dB at 1000 Hz, and there was little or no change at higher frequencies. While the expected frequency relation is maintained, voluntary contractions may not yield the same transmission loss as the acoustic reflex (Reger, 1960). Perhaps the most impressive data on how the acoustic reflex affects middle ear transmission come from animal studies.

The transmission loss produced by the acoustic reflex has been studied in animals by monitoring the resulting changes in the magnitude of the cochlear microphonic (e.g., Simmons, 1959; Møller, 1964, 1965; Nuttall, 1974). (The cochlear microphonic is an electrical potential of the cochlea, which is proportional to the intensity of the stimulus over a wide dynamic range; it is discussed in the next chapter.) Figure 3.26 shows the changes in the cochlear microphonic magnitude as a function of frequency due to stapedius muscle contraction in the cat, obtained by Møller (1965). He found that impedance change data and cochlear microphonic findings in response to the acoustic reflex were within 5 dB over a substantial portion of the frequency range. The figure shows that the acoustic reflex affects primarily the frequencies below about 2000 Hz. Low-frequency changes have also been reported in response to contractions of the tensor tympani muscle (e.g., Starr, 1969; Nuttall, 1974).

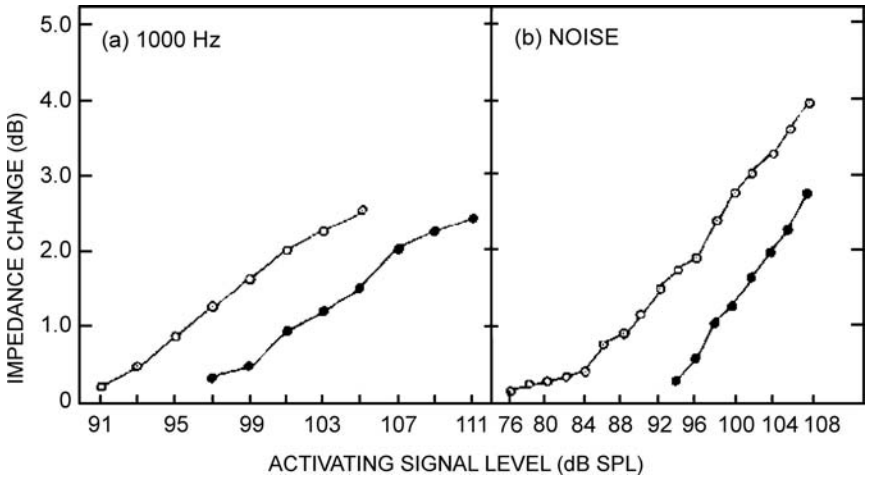

Figure 3.25 Reflex growth as a function of activator level in dB SPL for (a) a 1000-Hz tone and (b) a broadband noise. Open symbols, normal ears; closed symbols, impaired ears. *Source*: Adapted from Silman, Popelka, and Gelfand (1978).

Several studies have addressed the effects of middle ear muscle contractions on absolute thresholds and loudness in humans (Smith, 1946; Loeb and Riopelle, 1960; Morgan and Dirks, 1975; Morgan, Dirks, and Kamm, 1978; Rabinowitz, 1976), albeit with mixed results. For example, Rabinowitz (1976) reported a 10-dB change in the low-frequency transmission characteristics of the middle ear due to the acoustic reflex, but Morgan et al. (1978) found that absolute thresholds were not affected by the acoustic reflex. Morgan and Dirks (1975) found that the acoustic reflex caused a change in the loudness of a test tone presented to the opposite ear when the reflex-eliciting stimulus was greater than 100-dB SPL, but not for lower activator levels.

Middle Ear Muscle Theories

There are many theories and speculations about the purpose of the middle ear muscles and the acoustic reflex. Space and scope preclude more than a cursory review here; and the reader should see the discussions by Simmons (1964); Jepsen (1963); and Borg, Counter, and Rosler (1984).

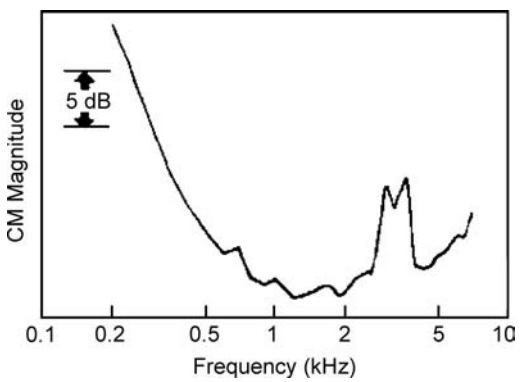

Figure 3.26 Effect of the acoustic reflex on transmission in the cat's middle ear. *Source*: Adapted from Møller (1965), with permission.

Because the reflex is elicited by relatively high stimulus levels and its magnitude grows with increasing stimulus level, one would expect that a primary purpose of the acoustic reflex would be protection of the cochlea from damaging stimulation. This *protection theory* is limited by the latency and adaptation of the reflex, causing it to respond too slowly to sudden sounds, and making it inefficient against prolonged sounds. Nevertheless, protection against injury to hearing is still a beneficial effect of the acoustic reflex, even if it is not the main purpose.

The *accommodation theory* states that the action of the two middle ear muscles modifies the conductive mechanism so as to optimize the absorption of sound energy. According to the *ossicular fixation theory*, the intratympanic muscles help keep the ossicles in proper position and appropriately rigid, particularly at high frequencies, where acceleration is great. Other theories have asserted that these muscles contribute to changes in labyrinthine pressure and to the formation of aural overtones.

Simmons (1964) found a sharp antiresonance peak around 4000 Hz in the middle ear transmission function of cats whose intratympanic muscles were removed, as well as in normal cats under anesthesia. Normal, waking cats whose intratympanic muscles have normal tonus showed greatly reduced dips in this region. In his *perceptual theory*, Simmons reasoned that tonus of the middle ear muscles smoothes the frequency response of the conductive system. He suggested that modulation of muscle tonus would have the effect of enhancing attention by changing the intensity and frequency characteristics of environmental sounds. This modulation would be analogous to the constant motion of the extraocular muscles in vision. Also, several skeletal movements as well as unexpected and novel environmental sounds elicit the acoustic reflex. Because the reflex mainly attenuates low frequencies, and most of an organism's own

physiological noises are low in frequency, such a reflex response would have the effect of reducing the animal's internal noise. A better signal-to-noise ratio would result, which is of obvious importance to the survival of any species, whether predator or prey. This idea agrees with Borg's (1976) position that the qualitative purpose of the acoustic reflex is to attenuate low-frequency sounds, thereby improving the auditory system's dynamic range.

The *desensitization–interference–injury protection theory* proposed by Borg et al. (1984) explained that the middle ear muscles and the acoustic reflex have multiple purposes: (1) Contractions of the intratympanic muscles are elicited by eating, talking, yelling, and other vocalizations. The muscle contractions alleviate *desensitization* because they reduce the noises produced by these activities, which would have otherwise compromised the alertness and the sensitivity to salient aspects of the acoustical environment. (2) *Interference* is reduced because contractions of the middle ear muscles cause the low frequencies to be attenuated, thereby reducing the extent to which they mask the higher frequencies (e.g., reducing the masking produced by one's own speech). (3) Finally, middle ear muscle contractions provide *injury protection* by attenuating intense sounds reaching the inner ear.

REFERENCES

Barany, E. 1938. A contribution to the physiology of bone conduction. *Acta Otol* Suppl 26, 1–223.

Beedle, RK, Harford, ER. 1973. A comparison of acoustic reflex growth in normal and pathological ears. *J Speech Hear Res* 16, 271–280.

Bekesy, G. 1932. Zur Theorie des Hören bei der Schallaufnahme durch Knochenleitung. *Ann Physik* 13, 111–136.

Bekesy, G. 1936. Zur Physik des Mittelohres und über das Hören bei fehlerhaftem Trommelfell. *Akust Zeitschr* 1, 13–23.

Bekesy, G. 1941. Über die Messung der Schwingungsamplitude der Gehörknöchelchen mittels einer kapazitiven Sonde. *Akust Zeitschr* 6, 1–16.

Bekesy, G. 1948. Vibrations of the head in a sound field and its role in hearing by bone conduction. *J Acoust Soc Am* 20, 749–760.

Bekesy, G. 1960/1989. *Experiments in Hearing*. New York, NY: McGraw-Hill. [Republished by the Acoustical Society of America].

Bekesy, G, Rosenblith, WA. 1958. The mechanical properties of the ear. In: SS Stevens (ed.), *Handbook of Experimental Psychology*. New York, NY: Wiley, 1075–1115.

Bennett, M. 1984. Impedance concepts relating to the acoustic reflex. In: S Silman (ed.), *The Acoustic Reflex*. New York, NY: Academic Press, 35–61.

Blauert, J. 1997. *Special Hearing: The Psychophysics of Human Sound Localization*. Revised Edition. Cambridge, MA: MIT Press.

Block, MG, Wightman, FL. 1977. A statistically based measure of the acoustic reflex and its relation to stimulus loudness. *J Acoust Soc Am* 61, 120–125.

Borg, E. 1968. A quantitative study of the effects of the acoustic stapedius reflex on sound transmission through the middle ear. *Acta Otol* 66, 461–472.

Borg, E. 1976. Dynamic characteristics of the intra-aural muscle reflex. In: AS Feldman, LA Wilber (eds.), *Acoustic Impedance and Admittance*. Baltimore: Williams Wilkins, 236–299.

Borg, E, Counter, SA, Rosler, G. 1984. Theories of middle-ear muscle function. In: S Silman (ed.), *The Acoustic Reflex*. New York, NY: Academic Press, 63–99.

Borg, E, Møller, A. 1968. The acoustic middle ear reflex in man and in anesthetized rabbits. *Acta Otol* 65, 575–585.

Bosatra, A, Russolo, M, Silverman, CA. 1984. Acoustic—reflex latency: State of the art. In: S Silman (ed.), *The Acoustic Reflex*. New York, NY: Academic Press, 301–328.

Carhart, R. 1950. Clinical application of bone conduction audiometry. *Arch Otol* 51, 798–808.

Cunningham, D. 1976. Admittance values associated with acoustic reflex decay. *J Acoust Soc Am* 1, 197–205.

Dallos, P. 1964. Dynamics of the acoustic reflex: Phenomenological aspects. *J Acoust Soc Am* 36, 2175–2183.

Dallos, P. 1970. Low-frequency auditory characteristics: Species dependencies. *J Acoust Soc Am* 48, 489–499.

Dallos, P. 1973. *The Auditory Periphery*. New York, NY: Academic Press.

Decraemer, WF, Khanna, SM, Funnell, WRL. 1991. Malleus vibration mode changes with frequency. *Hear Res* 54, 305–318.

Decraemer, WF, Khanna, SM, Funnell, WRL. 1994. A method for determining three-dimensional vibration in the ear. *Hear Res* 77, 19–37.

Djupesland, G. 1964. Middle ear muscle reflexes elicited by acoustic and nonacoustic stimulation. *Acta Otol* Suppl 188, 287–292.

Djupesland, G, Sundby, A, Flottrop, G. 1973. Temporal summation in the acoustic stapedius reflex mechanism. *Acta Otol* 76, 305–312.

Djupesland, G, Zwislocki, J. 1971. Effect on temporal summation on the human stapedius reflex. *Acta Otol* 71, 262–265.

Djupesland, G, Zwislocki, J. 1973. On the critical band in the acoustic stapedius reflex. *J Acoust Soc Am* 54, 1157–1159.

Dutsch, L. 1972. The threshold of the stapedius reflex for pure-tone and noise stimuli. *Acta Otol* 74, 248–251.

Feldman, A. 1967. A report of further impedance studies of the acoustic reflex. *J Speech Hear Res* 10, 616–622.

Fletcher, H, Munson, WA. 1933. Loudness: Its definition, measurement and calculation. *J Acoust Soc Am* 5, 82–108.

Flottrop, G, Djupesland, G, Winther, F. 1971. The acoustic stapedius reflex in relation to critical bandwidth. *J Acoust Soc Am* 49, 457–461.

Gardner, MB, Gardner, RS. 1973. Problems of localization in the medial plane: Effect of pinnae cavity occlusion. *J Acoust Soc Am* 53, 400–408.

Gelfand, SA. 1984. The contralateral acoustic—reflex threshold. In: S Silman (ed.), *The Acoustic Reflex*. New York, NY: Academic Press, 137–186.

Gelfand, SA, Silman, S, Silverman, CA. 1981. Temporal summation in acoustic reflex growth functions. *Acta Otol* 91, 177–182.

Green, KW, Margolis, RH. 1984. The ipsilateral acoustic reflex. In: S Silman (ed.), *The Acoustic Reflex*. New York, NY: Academic Press, 275–299.

Guinan, J, Peake, WT. 1967. Middle ear characteristics of anesthetized cats. *J Acoust Soc Am* 41, 1237–1261.

Hellman, R, Scharf, B. 1984. Acoustic reflex and loudness. In: S Silman (ed.), *The Acoustic Reflex*. New York, NY: Academic Press, 469–516.

Helmholtz, H. 1868. Die Mechanik der Gehorknochelchen und des Trommelfells. *Pflugers Arch Ges Physiol I*, 1–60.

Hensen, V. 1878. Beobachtungen uber die Thatigkeit des Trommellspanners bei Hund und Katze. *Arch Anat Physiol II*, 312–319.

Huizing, EH. 1960. Bone conduction—The influence of the middle ear. Acta Otol Suppl 155, 1–99.

Hung, I, Dallos, P. 1972. Study of the acoustic reflex in human beings: I. Dynamic characteristics. *J Acoust Soc Am* 52, 1168–1180.

Jepsen, O. 1955. *Studies on the acoustic stapedius reflex in man: Measurements of the acoustic impedance of the tympanic membrane in normal individuals and in patients with peripheral facial palsy* [Thesis], Universitetsforlaget, Aarhus, Denmark.

Jepsen, O. 1963. The middle ear muscle reflexes in man. In: J Jerger (ed.), *Modern Developments in Audiology*. New York, NY: Academic Press, 194–239.

Jerger, J. 1970. Clinical experience with impedance audiometry. *Arch Otol* 92, 311–321.

Jerger, J, Mauldin, L, Lewis, N. 1977. Temporal summation of the acoustic reflex. *Audiology* 16, 177–200.

Kaplan, H, Gilman, S, Dirks, D. 1977. Properties of acoustic reflex adaptation. *Ann Otol* 86, 348–356.

Kato, T. 1913. Zur Physiologie der Binnenmuskeln des Ohres. *Pflugers Arch Physiol* 150, 569–625.

Klockhoff, I. 1961. Middle-ear muscle reflexes in man. *Acta Otol Suppl.* 164.

Lindsay, JR, Kobrack, H, Perlman, HB. 1936. Relation of the stapedius reflex to hearing sensitivity in man. *Arch Otol* 23, 671–678.

Loeb, M, Riopelle, AJ. 1960. Influence of loud contralateral stimulation on the threshold and perceived loudness of low-frequency tones. *J Acoust Soc Am* 32, 602–610.

Lorente de Nó, R. 1935. The function of the central acoustic nuclei examined by means of the acoustic reflexes. *Laryngoscope* 45, 573–595.

Lowy, K. 1942. Cancellation of the electrical cochlear response with air- and bone-conduction. *J Acoust Soc Am* 14, 156–158.

Luscher, E. 1929. Die Function des Musculus stapedius beim Menschen. *Zeitschr Hals Nasen Ohrenheilk* 23, 105–132.

Margolis, R, Popelka, G. 1975. Loudness and the acoustic reflex. *J Acoust Soc Am* 58, 1330–1332.

Margolis, RH, Van Camp, J, Wilson, RH, Creten, WL. 1985. Multifrequency tympanometry in normal ears. *Audiology* 24, 44–53.

Mehrgardt, S, Mellert, V. 1977. Transformation characteristics of the external human ear. *J Acoust Soc Am* 61, 1567–1576.

Mendelson, ES. 1957. A sensitive method for registration of human intratympanic muscle reflexes. *J Appl Physiol* 11, 499–502.

Mendelson, ES. 1961. Improved method for studying tympanic reflexes in man. *J Acoust Soc Am* 33, 146–152.

Metz, O. 1946. The acoustic impedance measured on normal and pathological ears. *Acta Otol* 63(Suppl), 3–254.

Metz, O. 1951. Studies on the contraction of the tympanic muscles as indicated by changes in impedance of the ear. *Acta Otol* 39, 397–405.

Metz, O. 1952. Threshold of reflex contractions of muscles of the middle ear and recruitment of loudness. *Arch Otol* 55, 536–593.

Middlebrooks, JC. 1999. Individual differences in external ear transfer functions reduced by scaling in frequency. *J Acoust Soc Am* 106, 1480–1492.

Miller, JD, Watson, CS, Covell, WP. 1963. Deafening effects of noise on the cat. *Acta Otol* 176(Suppl), 1–91.

Møller, A. 1958. Intra-aural muscle contraction in man examined by measuring acoustic impedance of the ear. *Laryngoscope* 68, 48–62.

Møller, A. 1961. Bilateral contraction of the tympanic muscles in man examined by measuring acoustic impedance-change. *Ann Otol* 70, 735–753.

Møller, AR. 1960. Improved technique for detailed measurements of the middle ear impedance. *J Acoust Soc Am* 32, 250–257.

Møller, AR. 1962. The sensitivity of contraction of tympanic muscle in man. *Ann Otol* 71, 86–95.

Møller, AR. 1964. Effects of tympanic muscle activity on movement of the ear drum, acoustic impedance, and cochlear microphonics. *Acta Otol* 58, 525–534.

Møller, AR. 1965. An experimental study of the acoustic impedance and its transmission properties *Acta Otol* 60, 129–149.

Morgan, DE, Dirks, DD. 1975. Influence of middle ear muscle contraction on pure-tone suprathreshold loudness judgments. *J Acoust Soc Am* 57, 411–420.

Morgan, D.E, Dirks, DD, Kamm, C. 1978. The influence of middle-ear contraction on auditory threshold for selected pure-tones. *J Acoust Soc Am* 63,1896–1903.

Nedzelnitsky, V. 1980. Sound pressures in the basal turn of the cat cochlea. *J Acoust Soc Am* 68, 1676–1689.

Naunton, R. 1963. The measurement of hearing by bone conduction. In: J Jerger (ed.), *Modern Developments in Audiology*. New York, NY: Academic Press, 1–29.

Nuttall, AL. 1974. Tympanic muscle effects on middle-ear transfer characteristic. *J Acoust Soc Am* 56, 1239–1247.

Oldfield, SR, Parker, PA. 1984. Acuity of sound localization: A topography of auditory space. II. Pinna cues absent. *Perception* 13, 601–617.

Peterson, JL, Liden, G. 1972. Some static characteristics of the stapedial muscle reflex. *Audiology* 11, 97–114.

Plenge, G. 1974. On the difference between localization and lateralization. *J Acoust Soc Am* 56, 944–951.

Pollack, J. 1886. Uber die Function des Musculus tensor tympani. *Med Jahrbuch* 82, 555–582.

Popelka, G, Karlovich, R, Wiley, T. 1974. Acoustic reflex and critical bandwidth. *J Acoust Soc Am* 55, 883–885.

Popelka, G, Margolis, R, Wiley, T. 1976. Effects of activating signal bandwidth on acoustic-reflex thresholds. *J Acoust Soc Am* 59, 153–159.

Potter, AB 1936. Function of the stapedius muscle. *Ann Otol* 45, 639–643.

Rabinowitz, WM. 1976. *Acoustic-Reflex Effects on the Input Admittance and Transfer Characteristics of the Human Middle-Ear* [unpublished Ph.D. Dissertation]. Cambridge, MA: MIT Press.

Reger, SN. 1960. Effect of middle ear muscle action on certain psycho-physical measurements. *Ann Otol* 69, 1179–1198.

Rosowski, JJ. 1991. The effects of external- and middle-ear filtering on auditory threshold and noise-induced hearing loss. *J Acoust Soc Am* 90, 124–135.

Ross, S. 1968. On the relation between the acoustic reflex and loudness. *J Acoust Soc Am* 43, 768–779.

Shaw, EAG. 1974. Transformation of sound pressure level from the free field to the eardrum in the horizontal plane. *J Acoust Soc Am* 56, 1848–1861.

Shaw, EAG. 1997. Acoustical features of the external ear. In: R Gilkey, T Anderson (eds.), *Binaural and Spacial Hearing in Real and Virtual Environments*. Hillsdale, NJ: Erlbaum, 25–47.

Shaw, EAG, Vaillancourt, MM. 1985. Transformation of sound-pressure level from the free field to the eardrum presented in numerical form. *J Acoust Soc Am* 78, 1120–1123.

Silman, S. 1984. Magnitude and growth of the acoustic reflex. In: S Silman (ed.), *The Acoustic Reflex*. New York, NY: Academic Press, 225–274.

Silman, S, Gelfand, SA. 1981. Effect of sensorineural hearing loss on the stapedius reflex growth function in the elderly. *J Acoust Soc Am* 69, 1099–1106.

Silman, S, Popelka, S, Gelfand, SA. 1978. Effect of sensorineural hearing loss on acoustic stapedius reflex growth functions. *J Acoust Soc Am* 64, 1406–1411.

Simmons, FB 1959. Middle ear muscle activity at moderate sound levels. *Ann Otol* 68, 1126–1143.

Simmons, FB. 1964. Perceptual theories of middle ear function. *Ann Otol* 73, 724–740.

Smith, HD. 1943. Audiometric effects of voluntary contraction of the tensor tympani muscle. *Arch Otol* 38, 369–373.

Smith, HD. 1946. Audiometric effects of voluntary contraction of the tensor tympani muscles. *Arch Otol* 38, 369–372.

Starr, A. 1969. Regulatory mechanisms of the auditory pathway. In: S Locke (ed.), *Modern Neurology*. Boston, MA: Little, Brown.

Stenfelt, S, Hato, N, Goode, RL. 2002. Factors contributing to bone conduction: The middle ear. *J Acoust Soc Am* 111, 947–959.

Stenfelt, S, Wild, T, Hato, N, Goode, RL. 2003. Factors contributing to bone conduction: The outer ear. *J Acoust Soc Am* 113, 902–913.

Stepp, CE, Voss, SE. (2005). Acoustics of the human middle-ear air space. *J Acoust Soc Am* 118, 861–871.

Stevens, SS. 1956. The direct estimation of sensory magnitude—Loudness. *Am J Psychol* 69, 1–25.

Stinton, MR, Lawton, DW. 1989. Specification of the geometry of the human ear canal for the prediction of sound-pressure level distribution. *J Acoust Soc Am* 85, 2492–2530.

Terkildsen, K. 1957. Movements of the eardrum following interaural muscle reflexes. *Arch Otol* 66, 484–488.

Terkildsen, K. 1960. Acoustic reflexes of the human musculus tensor tympani. *Acta Otol* Suppl. 158, 230–236.

Terkildsen, K, Nielsen, SS. 1960. An electroacoustic measuring bridge for clinical use. *Arch Otol* 72, 339–346.

Tietze, G. 1969a. Zum zeitverhalten des akustischen reflexes bei reizung mit dauertonen. *Arch Klin Exp Ohren Nasen Kehlkoopfheilkd* 193, 43–52.

Tietze, G. 1969b. Einge eigenschaften des akustischen reflexes bei reizung mit tonimpulsen. *Arch Klin Exp Ohren Nasen KehlkopfFeilkd* 193, 53–69.

Tonndorf, J. 1962. Compressional bone conduction in cochlear models. *J Acoust Soc Am* 34, 1127–1132.

Tonndorf, J. 1966. Bone conduction: Studies in experimental animals—A collection of papers. *Acta Otol* Suppl 213, 1–32.

Tonndorf, J. 1968. A new concepts of bone conduction. *Arch Otol* 87, 49–54.

Tonndorf, J, Khanna, SM. 1970. The role of the tympanic membrane in middle ear transmission. *Ann Otol* 79, 743–753.

Tonndorf, J, Khanna, SM, Fingerhood, BJ. 1966. The input impedance of the inner ear in cats. *Ann Otol* 75, 752–763.

Wever, EG, Lawrence, M. 1954. *Physiological Acoustics*. Princeton, NJ: Princeton University Press.

Wiener, FN, Pfeiffer, RR, Backus, ASN. 1966. On the pressure transformation by the head and auditory meatus of the cat. *Acta Otol* 61, 255–269.

Wiener, FM, Ross, DA. 1946. The pressure distribution in the auditory canal in a progressive sound field. *J Acoust Soc Am* 18, 401–408.

Wiley, TL, Karlovich, TS. 1975. Acoustic reflex response to sustained signals. *J Speech Hear Res* 18, 148–157.

Wilson, RH, McBride, LM. 1978. Threshold and growth of the acoustic reflex. *J Acoust Soc Am* 63, 147–154.

Wilson, RH, McCollough, JK, Lilly, DJ. 1984a. Acoustic reflex adaptation: Morphology and half-life data for subjects with normal hearing. *J Speech Hear Res* 27, 586–595.

Wilson, RH, Shanks, JE, Lilly, DJ. 1984b. Acoustic-reflex adaptation. In: S Silman (ed.), *The Acoustic Reflex*. New York, NY: Academic Press, 329–386.

Woodford, C, Henderson, D, Hamernick, R, Feldman, A. 1975. Threshold duration function of the acoustic reflex in man. *Audiology* 14, 53–62.

Zakrisson, JE, Borg, E, Blom, S. 1974. The acoustic impedance change as a measure of stapedius muscle activity in man: A methodological study with electromyography. *Acta Otol* 78, 357–364.

Zwislocki, J. 1962. Analysis of the middle-ear function. Part I: Input impedance. *J Acoust Soc Am* 34, 1514–1523.

Zwislocki, J. 1963. An acoustic method for clinical examination of the ear. *J Speech Hear Res* 6, 303–314.

Zwislocki, J. 1975. The role of the external and middle ear in sound transmission. In: DB Tower, EL. Eagles (eds.), *The Nervous System. Vol. 3: Human Communication and Its Disorders.* New York, NY: Raven Press, 45–55.

Zwislocki, J. 1976. The acoustic middle ear function. In: AS Feldman, LA, Wilber (eds.), *Acoustic Impedance and Admittance—The Measurement of Middle Ear Function.* Baltimore, MD: Williams & Wilkins. 66–77.

4 Cochlear Mechanisms and Processes

We have already discussed the manner in which the conductive mechanism influences the signal and transmits it to the inner ear. In this chapter we will concentrate upon the sensory mechanism. The cochlea may be conceived of as a transducer that converts the vibratory stimulus into a form usable by the nervous system. However, this is far from the whole picture. We shall see that the cochlea performs a considerable amount of analysis, that it is the major source of aural distortion, and that it is involved in processes that are active as well as passive.

Before proceeding to examine the processes of the cochlea, it is desirable to briefly review the traditional theories of hearing as well as some principles of sensory receptor action. These two topics provide a useful general framework as well as an important historical perspective within which the student can consider the material that follows.

CLASSICAL THEORIES OF HEARING

The study of the auditory system is practically and historically intertwined with the traditional theories of hearing. Broadly speaking, these theories fall into two general categories—place (resonance) theories and frequency (temporal, periodicity) theories—as well as the combined place-frequency theory. A detailed review of these theories goes beyond the current scope or intent; the student is referred to Wever's classical work *Theory of Hearing Hearing* (1949) for an excellent review of these theories.

Classical Resonance Theory

Although place or resonance theories existed since the beginning of the 1600s, modern versions began with the **resonance theory** proposed by Helmholtz (1870). Helmholtz relied to a large extent upon **Ohm's auditory law** and **Müller's doctrine of specific nerve energies**. Ohm's auditory law states that the ear performs a Fourier analysis upon complex periodic sounds; that is, that it breaks the complex wave down into its components regardless of their phase relationships. A major problem with Ohm's auditory law is that it precludes temporal analysis. We shall see, however, that the auditory system is sensitive to temporal as well as frequency parameters. Müller's doctrine refers to the specificity of the different senses. It state that the neural signal coming from the ear is interpreted as sound whether the actual stimulus was a tone or a blow to the head; the eye elicits a visual image whether the stimulus is light or pressure on the eyeball, etc. The doctrine appears to hold on the periphery, although there are dramatic commonalities among the various senses in terms of their fundamental principles of operation (see section "Action of Sensory Receptors," below) and central mechanisms.

The resonance place theory proposed by Helmholtz assumes that the basilar membrane is composed of a series of tuned segments, each of which resonates in response to a particular frequency. Thus, an incoming stimulus results in the vibration of those parts of the basilar membrane whose natural frequencies correspond to the components of the stimulus. Since these resonators are arranged by place along the cochlear partition, the precise place of the vibrating segment would signal the existence of a component at the natural frequency of that location. Nonlinear distortions introduced by the ear (such as combination tones due to the interaction of two stimulus tones, or harmonics of the stimulus tone) were viewed as being generated by a nonlinear response of the middle ear mechanism. These distortion products are then transmitted to the cochlea, where they cause vibrations at the places whose resonant frequencies correspond to the frequency of the combination tone (or harmonic). The distortion product is thus perceived as though it were present in the original signal.

Such a strict resonance theory is faced with several serious problems. To begin with, in order to account for the sharp frequency tuning of the inner ear, the theory demands that the basilar membrane contains segments that are under differing amounts of tension in a manner analogous to the tension on variously tuned piano strings. However, Bekesy (1948)[1] demonstrated that the basilar membrane is under no tension at all.

A second problem is that resonance theory cannot account for the perception of the "missing fundamental," the phenomenon in which the presence of only the harmonics of tone (e.g., 1100, 1200, and 1300 Hz) results in the perception of the fundamental frequency (100 Hz), even though the latter is not physically present. (The missing fundamental is discussed in Chap. 12.)

Resonance theory is also plagued by the relationship between the sharpness of a system's tuning and the persistence of its response. In order for the ear to achieve the required fine frequency discriminations, the various segments of the basilar membrane must be sharply tuned. In other words, they could each respond only to a very narrow range of frequencies. A segment could not respond to higher or lower frequencies, or else the necessary discriminations would be impossible. The problem is that such a narrowly tuned system must have very low damping—its response will take a relatively long time to die away after the stimulus stops. In other words, if there were sharp tuning of the resonators along the basilar membrane, then their responses would persist long after the stimulus had ceased. This situation would cause an interminable echo in our ears, precluding any functional hearing. On the other hand, if the resonators were less sharply tuned, they would not have the

[1] The student will find much of Bekesy's work is conveniently reproduced in his book, *Experiments in Hearing* (1960/1989).

persistence problem, but they would be unable to support the necessary fine frequency discriminations.

The resonance theory ascribed the perception aural distortions to nonlinear processes taking place in the middle ear. However, as we saw in the last chapter, it is now known that the middle ear operates in a manner that is astoundingly linear. Moreover, we shall see later in this chapter that the inner ear is the site of active processes, and that most nonlinear distortions are attributable to the cochlea.

Traveling Wave Theory

A variety of other place theories followed that of Helmholtz. Of particular interest is the **traveling wave theory** of Nobel laureate Georg von Bekesy. The traveling wave theory has been confirmed by many investigators using a multiplicity of approaches and is discussed later in this chapter.

Classical Temporal Theories

The classical **temporal (frequency) theories** proposed that the peripheral hearing mechanism does not perform a frequency analysis, but rather that it transmits the signal to the central auditory nervous system for processing. Such theories have been referred to as "telephone theories" by analogy with the manner in which a telephone signal is transmitted. Although there are several such theories, Rutherford's (1886) **telephone theory**, proposed not long after Helmholtz described the resonance theory, has been the best known. It proposed that the cochlea is not frequency-sensitive along its length, but rather that all parts respond to all frequencies. The job of the hair cells is simply to transmit all parameters of the stimulus waveform to the auditory nerve, and analysis is performed at higher levels.

Because a neuron can respond only in an all-or-none manner, the only way in which it can of itself transmit frequency information is to discharge the same number of times per second as there are cycles in the stimulus (e.g., it must fire 720 times per second to transmit 720-Hz tone). Classical temporal theory thus presumes that auditory nerve fibers can fire fast enough to represent this information. There is no problem at low frequencies; however, an upper limit on the number of discharges per second is imposed by the absolute refractory period of the neuron. The **absolute refractory period** is the time required after discharging for the cell to re-establish the polarization it needs to fire again; it lasts about 1 ms. The fiber cannot fire during the absolute refractory period, no matter how intensely stimulated. This period is followed by a relative refractory period during which the neuron will respond provided the stimulus is strong enough. The 1-ms absolute refractory period corresponds to a maximum firing rate of 1000 times per second. Thus, simple frequency theory is hard pressed to explain how sounds higher in frequency than about 1000 Hz can be transmitted by the auditory nerve and perceived by the listener.

A second problem of the telephone theories is that damage to the basal part of the cochlea results in high-frequency hearing loss. This is contradictory to frequency theory, which states that the different parts of the cochlea are not differentially sensitive to frequency. Furthermore, we shall see that there is actually a remarkable degree of frequency selectivity along the cochlear partition.

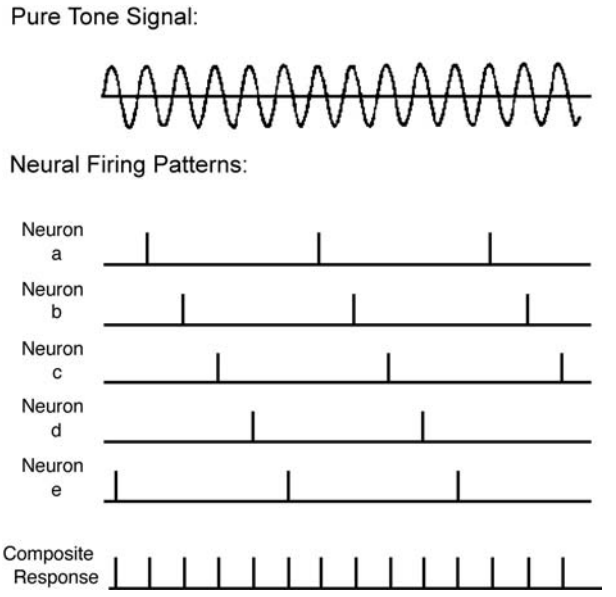

Figure 4.1 Diagrammatic representation of the volley principle (see text). *Source*: Based on various drawings by Wever and colleagues.

We shall see in Chapter 5 that the discharges of auditory nerve fibers do appear to follow the periodicity of the stimulus for frequencies as high as about 4000 to 5000 Hz. However, these responses are probabilistic rather than one-to-one.

Place-Volley Theory

Instead of suggesting that any one neuron must carry the entire information burden, Wever's (1949) **volley principle** states that groups of fibers cooperate to represent the stimulus frequency in the auditory nerve. This is shown in Fig. 4.1. The sinusoid (sound wave) at the top of the figure has a frequency too high to be represented by a series of spike discharges from a single auditory nerve fiber. Instead, fibers work in groups so that in the total response of the group there is a spike corresponding to each cycle of the stimulus. This cooperation is accomplished by having each individual neuron respond to cycles separated by some interval. In Fig. 4.1 this interval is every 5 cycles. Thus, fiber a discharges in response to cycles 1, 6, and 11; fiber b to cycles 2, 7, and 12; fiber c to 3, 8, and 13; etc. The result is that each cycle is represented by a spike in the combined response of the fiber group (bottom line in the figure).

Even at this early point it should be apparent that neither the place nor temporal theory alone can explain the selectivity of the ear. Instead, both mechanisms are operative. A periodicity mechanism is most important for low frequencies, while a place mechanism is paramount for high-frequency

representation (Wever, 1949; Wever and Lawrence, 1954). The question is not one of where the "cutoff points" are, because these do not exist. As we shall see in the following chapters, place coding below approximately 300 to 400 Hz is too broad to reasonably account for frequency discrimination, and periodicity coding is not supported for frequencies above roughly 4000 to 5000 Hz. Frequency coding in the wide range between these two extremes appears to involve the interaction of both mechanisms.

ACTION OF SENSORY RECEPTORS

The auditory system is one of several specialized sensory systems. Although there is specificity of the senses at the periphery, there are nevertheless remarkable similarities among them. The following is a brief overview of sensory receptor action, with particular reference to the ear (Davis, 1961; Grundfest, 1971; Tonndorf, 1975).

Davis (1961) proposed a general plan of sensory action, which is outlined schematically in Fig. 4.2. This model describes how external stimulus energy is transmitted and coded into a form, which is usable by the central nervous system. The **sensory neuron** is common to all sensory systems, although specialized receptor cells (sense organs) and accessory structures may or may not be present, and are different for the various senses. In the ear, the conductive mechanisms and the parts of the cochlea other than the hair cells constitute the accessory structures. The hair cells are the specialized receptors for hearing.

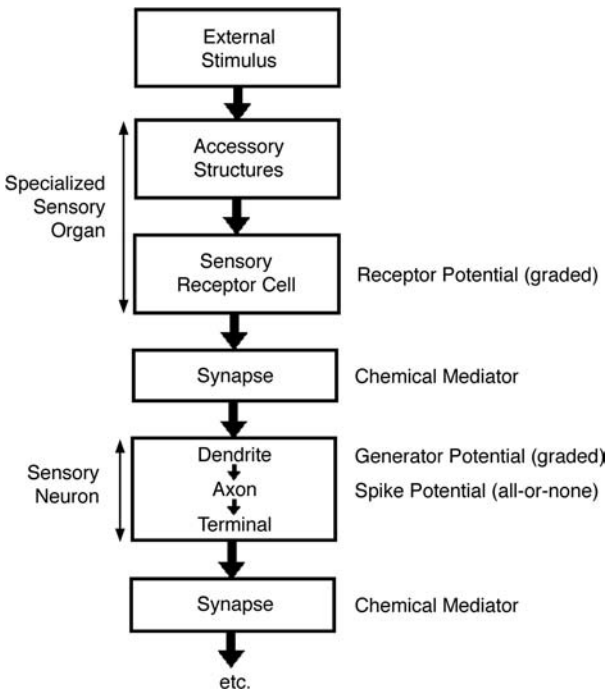

Figure 4.2 General plan of sensory receptor action (efferent feedback not shown) as described by Davis (1961).

The accessory structures assist in the action of the sense organ, but do not actually enter directly into the sensory transduction process per se. In other words, the conductive and cochlear structures help the hair cell to do its job, but are not themselves receptors. In the ear, the accessory structures carry out a large variety of vital functions. They receive, amplify, and analyze the stimulus, and convert it into a form usable by the hair cells. They may also perform feedback and inhibitory functions (under the control of efferent neurons), and protect the sensory receptors from external damage.

The sensory receptor cell transduces the stimulus and transmits it to the afferent neuron, which is an electrochemical event. Electrical potentials associated with this process can be detected within the hair cells and outside of them as receptor potentials. These **receptor potentials** are graded, meaning that their magnitudes depend upon the intensity of the stimulus. The receptor cell also emits a chemical mediator that is transmitted across the synapse between the hair cell and the afferent neuron. It is this chemical mediator that excites the neuron.

Exactly what substance constitutes the **neurotransmitter** from the hair cells to the *afferent* auditory neurons is still not firmly established. However, the amino acid **glutamate** is the most likely candidate. **Acetylcholine** is accepted as the principal *efferent* mediator in the cochlea, although others have also been identified [γ-aminobutyric acid (GABA), calcium gene-related peptide, dynorphin, and enkephalins]. Detailed discussion of neurotransmitters in the cochlea may be found in several informative reviews (Klink, 1986; Eybalin, 1993; Sewell, 1996; Wangemann and Schacht, 1996).

The neuron's dendrite receives an amount of chemical mediator from the hair cell, which elicits a graded **postsynaptic potential**. The postsynaptic potential is called a generator potential because it provides the electrical stimulus that triggers the all-or-none spike discharges from the axon. When the magnitude of the generator potential is great enough, it activates the axon, which in turn produces the **spike potential** (nerve impulse). The material in Chapter 5 on the activity of the auditory nerve is based upon these **action potentials**. This impulse travels down the axon to its terminus, where the presynaptic endings emit a chemical mediator. This chemical mediator crosses the synaptic junction to excite the dendrites of the next neuron, and the process is repeated.

THE TRAVELING WAVE

Classical resonance theory envisioned the basilar membrane to be under varying degrees of tension along its length to account for frequency tuning by place. However, Bekesy (1948) demonstrated that the basilar membrane is not under tension at all. Instead, its elasticity per unit area is essentially uniform, while there is a widening of the basilar membrane with distance along

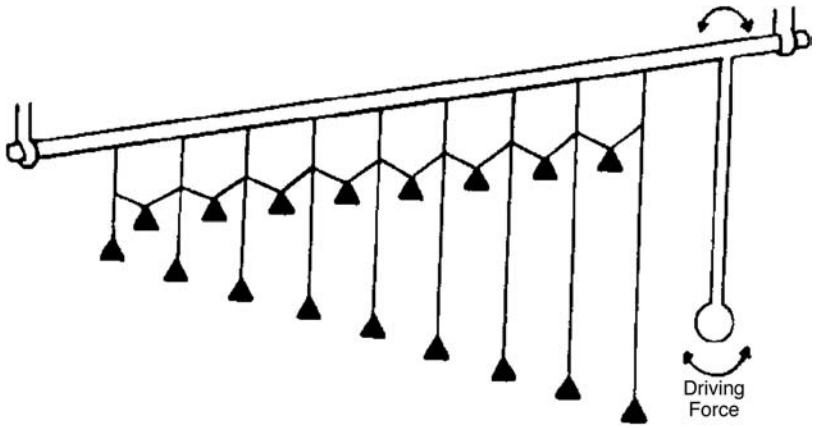

Figure 4.3 Pendulum analogy of traveling wave motion. *Source*: Based on various drawings by Bekesy.

the cochlea from base to apex (see Chap. 2). This widening of the basilar membrane results in a gradation of *stiffness* along the cochlear partition such that the membrane is about 100 times stiffer near the stapes than at the helicotrema (Naidu and Mountain, 1998). Because of this **stiffness gradient**, stimulation of the cochlea results in the formation of a pressure wave that travels from the base to the apex. In fact, this **traveling wave** proceeds toward the helicotrema regardless of where the stimulus is applied.

Before examining the details of the traveling wave, let us explore why it occurs. To begin with, the wavelengths of all audible sounds are much larger than the length of the outstretched cochlea. The result is that the pressure exerted on the cochlear partition is uniform over its length. The stiffness gradient of the basilar membrane causes it to act as a series of low-pass filters. Thus, no matter where applied, successively higher frequencies can only initiate vibrations of the cochlear partition closer and closer to the base, where they fall within the pass-band. Because the partition's impedance is composed of both stiffness and resistive components toward the base, and virtually only resistance toward the apex, the traveling wave is propagated up the partition from places of greater impedance to places of lesser impedance. The speed of the traveling wave decreases with distance from the stapes as it proceeds up the cochlear duct (Bekesy, 1960/1989).

The **pendulum analogy** suggested by Bekesy (1960/1989) should make the nature of the traveling wave clear. Suppose there is a rod to which a series of progressively longer pendulums are attached (Fig. 4.3). Each pendulum has its own natural frequency: the shorter the string, the higher the resonant frequency. We may think of each pendulum as representing a place along the basilar membrane, with the lengths of the pendulum strings corresponding to the stiffness gradient. A driving force is supplied by swinging the heavy pendulum rigidly attached to the rod. If the rod is rotated back and forth at a particular frequency, the resulting stimulus is applied over the entire rod just as the pressure from a sound stimulus is exerted over the entire cochlear duct. The motion of the rod will cause each pendulum to swing at the stimulus frequency. Of course, the closer the natural frequency of a particular pendulum is to the frequency being applied to the rod, the larger will be its amplitude of swing. There will thus be a particular pendulum that swings with maximum amplitude for each frequency applied to the rod, and changing the frequency at which the rod rocks will move the location of maximum swing to the pendulum whose resonant frequency corresponds to the new stimulus frequency. Note at this point that each pendulum is connected to its neighbor so that the vibrations of the pendulums interact. The different string lengths cause phase differences between the pendulums, which produces waves. The result is that a sinusoidal motion applied to the rod causes a wave that travels from shorter (higher frequency) to longer (lower frequency) pendulums, with the maximum of the wave occurring at the pendulum that resonates at the frequency of the stimulus.

Let us now proceed to the vibration pattern of the basilar membrane in response to sinusoidal stimulation. The abscissa in Fig. 4.4 is distance (in mm) from the stapes along the basilar membrane, and the ordinate is amplitude of membrane displacement. Two types of information are shown in this figure.

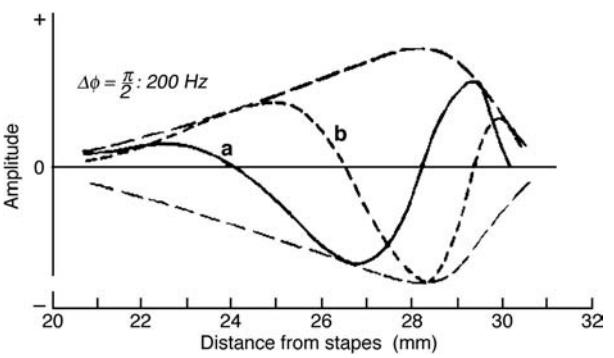

Figure 4.4 Traveling wave pattern for a 200-Hz tone. *Source*: From Bekesy (1947) with permission of *J. Acoust. Soc. Am.*

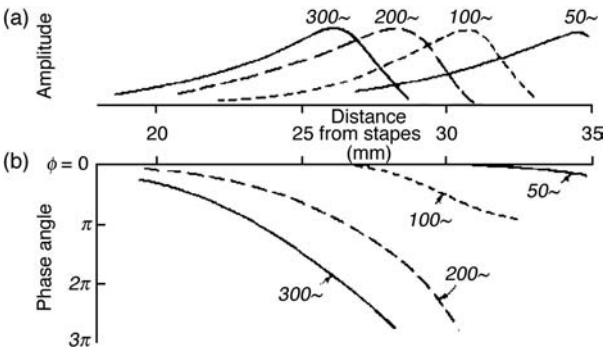

Figure 4.5 Traveling wave envelopes (a) and phase curves (b) for several low frequencies. *Source*: From Bekesy (1947) with permission of *J. Acoust. Soc. Am.*

The outer dashed lines represent the **envelope** of the **traveling wave** as a whole. This envelope outlines the displacement of the cochlear partition during an entire cycle of the wave. Note that the **displacement pattern** builds gradually with distance from the stapes, reaches a maximum in the vicinity of 28 to 29 mm, and then decays rapidly beyond the point of maximal displacement. The **peak** of the **traveling wave envelope** occurs at the place along the basilar membrane where vibration is greatest in response to the stimulus frequency (200 Hz in this case). The traveling wave envelopes for several low frequencies are shown in Fig. 4.5. Observe that these low frequencies result in displacement patterns covering most of the basilar membrane, although the places of maximum vibration move toward the base with increasing frequency. Standing waves do not arise because there are virtually no reflections from the apical end of the cochlear duct. For very low frequencies (50 Hz), the entire membrane vibrates in phase so that no traveling wave arises. For higher frequencies, however, notice that there is an increasing phase lag with distance from the stapes; this lag reflects the increasing propagation time and shortening wavelength as the wave proceeds toward the apex. Bekesy also used **cochlear models** like the one illustrated in Fig. 4.6 to observe the nature of the traveling wave. Models of this type were based on the known properties of the cochlear duct and greatly facilitated experimental manipulations and measurements.

Figure 4.4 also shows the peak-to-peak amplitudes of membrane displacement at two discrete phases of the wave cycle. For simplicity, assume that the solid line a occurs at 0° (time zero) and that the dashed line b occurs at 90° (1/4-cycle later). The difference between the two instantaneous displacements depends on what phase of the cycle the wave is in. A full cycle would include a complex set of **instantaneous displacement** patterns back and forth within the traveling wave envelope, which would begin and end at the solid curve a we have designated as our reference for 0° phase. If one imagines this series of instantaneous displacement curves in rapid succession (as in a motion picture with a successive phase in each frame), then the resulting image would be a traveling wave with a maximum at the place shown by the peak of the envelope.

HAIR CELL ACTIVATION

A primary task is to determine exactly what it is that stimulates the hair cells of the organ of Corti. It is firmly established that hair cells transduce mechanical into electrochemical activity when their stereocilia are bent (e.g., Hudspeth and Corey, 1977; Hudspeth and Jacobs, 1979; Hudspeth, 1982, 1985; Roberts et al., 1988; Pickles and Corey, 1992). Flock (1971) demonstrated that sensory hair cells like those in the cochlea are activated (excited) when their stereocilia are bent in a particular direction, whereas inhibition occurs when they are bent in the opposite direction. *Excitation* is associated with an increase in the firing rate of the auditory neurons connected to the hair cell, and *inhibition* is associated with a decrease in their firing rates (these concepts will become clearer in Chap. 5). The effects of the direction of stereocilia bending are illustrated in Fig. 4.7. Here we see that bending of the stereocilia *toward* the tallest row results in *excitation*, while bending *away* from the tallest row is *inhibitory*. Recall that the tall row of stereocilia (as well as the base of their W- or U-shaped arrangement on the

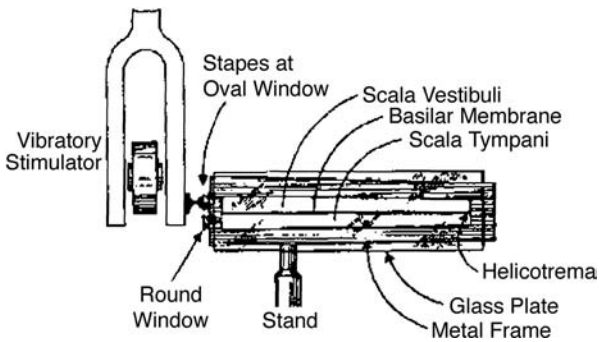

Figure 4.6 An example of a cochlear model used by Bekesy (1928).

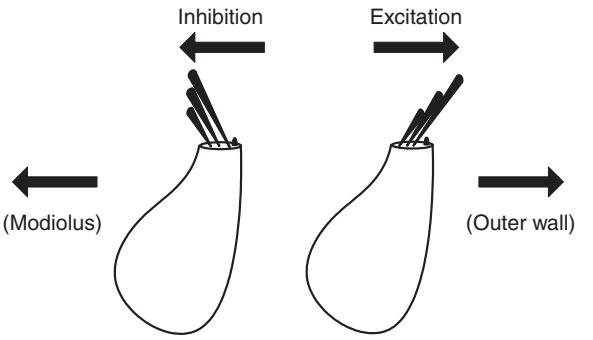

Figure 4.7 Bending of the stereocilia toward the tall row of stereocilia (toward the outer wall of the duct) causes excitation, and bending of the stereocilia away from the tall row (toward the modiolus) causes inhibition.

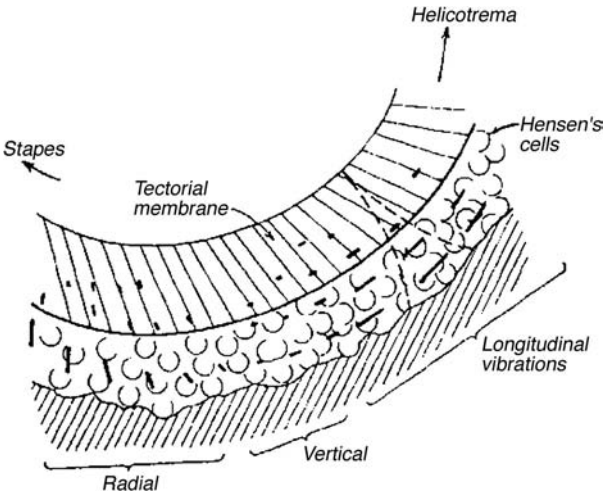

Figure 4.8 Schematic diagram showing radial and longitudinal shearing observed by Bekesy in the vicinity of the traveling wave peak. *Source*: From Bekesy (1953) with permission of *J. Acoust. Soc. Am.*

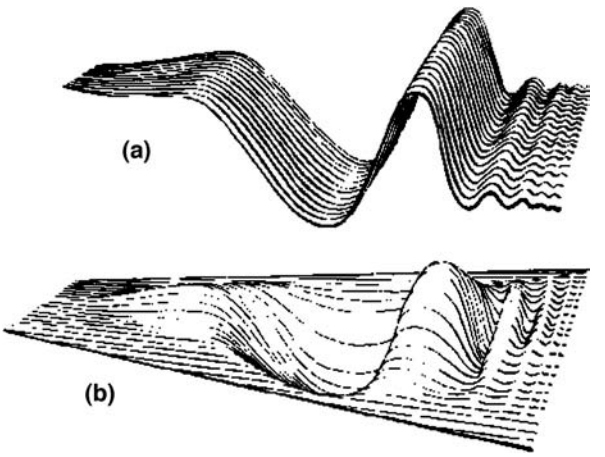

Figure 4.9 Vibration patterns of the basilar membrane that would be expected if it vibrated (a) like an unconstrained ribbon, and (b) when it is constrained by its lateral attachments. *Source*: From Tonndorf (1960) with permission of *J. Acoust. Soc. Am.*

hair cells) is *toward* the *outside* of the cochlear duct, *away* from the *modiolus*. Therefore, from the standpoint of orientation within the cochlea, the process of hair cell activation involves the bending of the stereocilia toward the outer wall or away from the modiolus.

Having established that the mechanical stimulus to the sensory cells is to bend their stereocilia away from the modiolus, we are left with two key questions. First, how does the mechanical activity along the cochlear partition get translated into such bending forces upon the sensory hairs? Second, what is it about the bending of these cilia, which causes the hair cells to become activated?

Bending of the hair cell stereocilia toward and away from the modiolus involves a motion that is *across* the cochlear duct, that is, in the *radial* direction. Yet, the traveling wave runs longitudinally in the direction of the cochlear duct. Bekesy (1953) demonstrated that such radial motion is actually achieved in the vicinity of the traveling wave peak. Specifically, he observed that the nature of the shearing force changes at different locations along the traveling wave envelope. As shown in Fig. 4.8, the shearing vibrations basal to the point of maximal displacement (toward the stapes) were found to be in the radial direction, as required to eventuate the properly oriented stimulation of the stereocilia. The shearing forces apical to the peak of the traveling wave (toward the helicotrema) were in the longitudinal direction, that is, in the direction followed by the cochlear duct.

Tonndorf (1960) explained how this change from longitudinal to radial shearing can come about. Figure 4.9a shows how the basilar membrane might move if it were like a freely vibrating ribbon. Note how the pattern is all in the longitudinal direction. However, this is not the case. Instead, the membrane is actually constrained on both sides by its attachments to the walls of the cochlea. The result is a vibration pattern more like the one depicted in Fig. 4.10b, which is based upon observations of the instantaneous pattern in a cochlear model. Notice that the vibrations under these lateral constraints induce radially directed forces on the basal (high frequency) side of the travel-

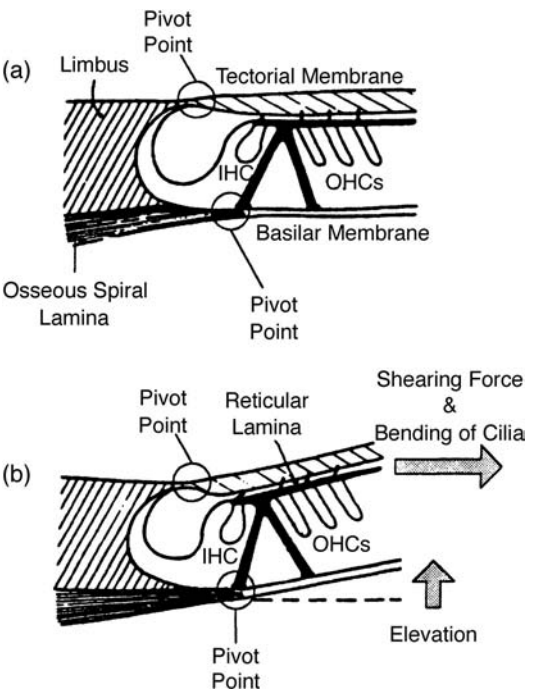

Figure 4.10 Relative positions of the basilar membrane and tectorial membrane (a) at rest, and (b) duration elevation toward the scala vestibuli. *Source*: Based on Davis, 1958. Davis' (1958) model calls for upward deflection to result in outward bending of the stereocilia, as shown in frame (b).

ing wave peak. In the cochlea, these forces would be across the direction of the duct.

Having established a mechanism to generate radial forces, we may focus on how these forces are caused to act upon the hair cells. It has long been established that the bending of the hair cell stereocilia in the proper direction (away from the modiolus) occurs when the cilia are sheared between the tectorial membrane above and the reticular lamina below. Recall here that the hair cells are seated in a complex system of supporting cells on the basilar membrane with the reticular lamina on top and with their cilia associated in various ways with the tectorial membrane (Chap. 2). The shearing effect takes place because the tectorial and basilar membranes are hinged at different points. Specifically, although the basilar membrane extends from the bottom of the osseous spiral lamina, the tectorial membrane is hinged at the upper lip of the limbus. As a result, the axes of rotation are different for these two membranes so that their displacement causes them to move relative to one another. The result is a **shearing force** upon the stereocilia between them.

The essence of the notion just described appears to have been introduced by Kuile in 1900. The most widely accepted mechanism for this concept was proposed by Davis (1958) and is represented schematically in Fig. 4.10. Frame (a) in the figure shows the relative positions of the basilar membrane and tectorial membrane at rest, and frame (b) shows their relative positions when the scala media is deflected upward toward the scala vestibuli. Notice that the membranes are viewed as operating as stiff boards that pivot around the hinge points. The resulting motions shear the cilia so that they bend outward (away from the modiolus) when the membranes are deflected upward (toward scala vestibuli), resulting in depolarization of the hair cell. Interestingly, Manoussaki, Dimitriadis, and Chadwick (2006) recently found that the increasing curvature of the spiral-shaped cochlea acts to concentrate vibrations toward the outer wall of the duct, especially for the low frequencies.

Recall from Chapter 2 that the stereocilia of the **outer hair cells (OHCs)** are firmly attached to the overlying tectorial membrane, whereas the **inner hair cell (IHC)** stereocilia are in contact with the tectorial membrane but are not attached to it (e.g., Steel, 1983). This difference implies alternative means of communicating the movements of the membranes to the stereocilia of the two types of hair cells. To study this, Dallos and associates (1972a) compared the cochlear microphonics generated by the IHCs and OHCs in the guinea pig. (Cochlear microphonics are electrical potentials that reflect cochlear activity and are explained later in this chapter.) It is possible to differentiate the responses of the two cell groups because the normal cochlear microphonic is derived chiefly from the OHCs, and ototoxic drugs tend to obliterate these same cells. Thus, the cochlear microphonic responses of the two cell groups were separated by measuring the responses before and after the animals were injected with an ototoxic drug (kanamycin). The output of the OHCs was found to be proportional to the basilar membrane *displacement*. In contrast, the response of the IHCs was proportional to the *velocity* of basilar membrane displacement. Subsequent studies have confirmed that the IHCs are activated by the *velocity* of basilar membrane movement (Sellick and Russell, 1980; Nuttall et al., 1981; Russell and Sellick, 1983; Dallos, 1984). In other words, the OHCs respond to the *amount* of basilar membrane displacement and the IHCs respond to the *rate* at which the displacement changes.

This difference in the mode of activation is consistent with the different relationships of the inner and outer hair cell stereocilia to the tectorial membrane. Since the OHC cilia attach to the tectorial membrane, an effective stimulus is provided by the relative movement of the reticular and tectorial membranes, which depends on basilar membrane displacement. The IHCs, on the other hand, stand free of the tectorial membrane. Their stimulus is thus provided by the *drag* imposed by the surrounding viscous fluid as the basilar membrane is displaced; the greater the velocity of basilar membrane displacement, the greater the drag exerted upon the cilia.

Suppose that all the necessary events have brought the signal to the relevant location along the organ of Corti, and that whatever relative appropriate movements of the reticular and tectorial membranes have operated in order to impart outward shearing forces upon the hair cells. We already know that the hair cells are activated by the ensuing deflections of their stereocilia away from the modiolus. How does this occur? In other words, what is the process by which the bending of the stereocilia translates into sensory transduction?

MECHANOELECTRICAL TRANSDUCTION

The **transduction process** has been described by Pickles and by Hudspeth and their collaborators (Hudspeth and Corey, 1977; Hudspeth and Jacobs, 1979; Hudspeth, 1982, 1985; Pickles et al., 1984; Roberts et al., 1988; Pickles and Corey, 1992). In addition, the interested student will find several detailed reviews (e.g., Dallos et al., 1996; Geisler, 1998; Robles and Ruggero, 2001; Corey, 2006; Fettiplace and Hackney, 2006; Vollrath, Kwan, and Corey, 2007). Recall from Chapter 2 that the stereocilia bundles are composed of rows of stiff cilia that are cross-linked by fine filaments. One general class of cross-linking fibers connects the stereocilia laterally within and between rows. The other general category involves **tip links**, which are filaments that go upward from the tip of a shorter stereocilium to the side of the adjacent taller stereocilium in the next row (Fig. 4.11).[2] Bending of the stereocilia toward their tallest row (i.e., toward the outer wall of

[2] Tip links are formed by the interaction of cadherin 23 and protocadherin 15 (Kazmierczak, Sakaguchi, Tokita, et al., 2007), but the properties of the transduction channels themselves are still being investigated (Corey, 2006; Vollrath et al., 2007). For a review of the molecular constituents involved in mechanoelectrical transduction, see Vollrath et al. (2007).

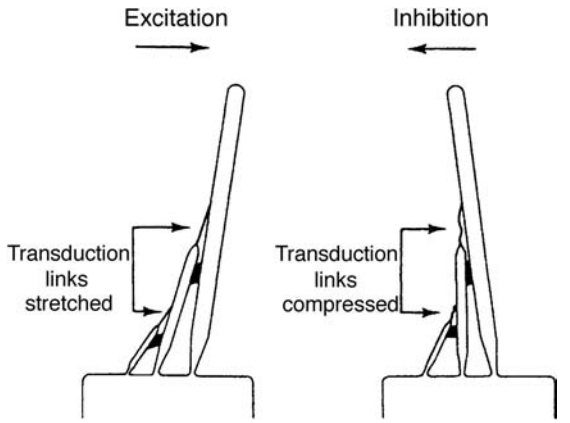

Figure 4.11 Tip links (identified as transduction links), which are upward-pointing (or tip-to-side) filaments between hair cell stereocilia, are shown in relation to the sensory transduction process (see text). *Source*: From *Hearing Research 15*, Pickles, Comis and Osborne (Cross-links between stereocilia in the guinea pig organ of Corti, and their possible relation to sensory transduction, 103–112, © 1984), with kind permission of from Elsevier Science Publishers—NL, Sara Burgerhartstraat 25, 1055 KV Amsterdam, The Netherlands.

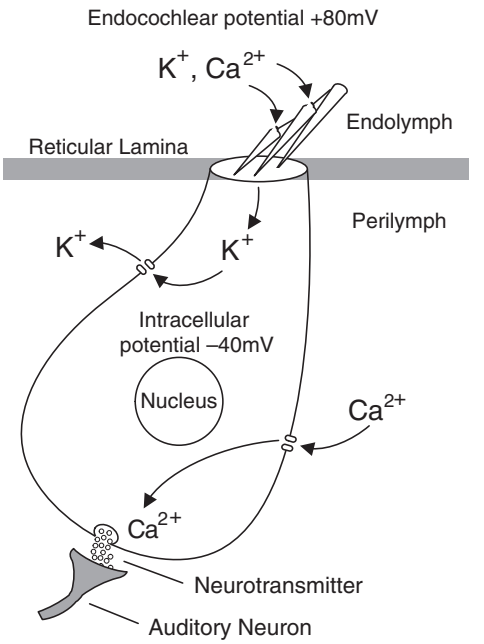

Figure 4.12 Bending of the stereocilia opens their transduction pores, leading to an inflow of potassium (K^+) and calcium (Ca^{2+}) ions. Changes in the receptor potential trigger the inflow of calcium ions (Ca^{2+}), which in turn activate the release of neurotransmitter to the afferent neurons attached to the hair cell.

the duct) is associated with *excitation*. This motion is illustrated in left frame of Fig. 4.11, where we see that it *stretches* the tip links. Bending of the stereocilia in the opposite direction as in the right frame of the figure *compresses* the tip links and is associated with *inhibition*.

Stretching of the tip links causes **pores** known as **mechano-electrical transduction (MET) channels** to open on the tops of the shorter stereocilia, where the links are attached. In contrast, the pores would be closed when opposite bending of the stereocilia compresses the rows together. By analogy, the bending of the stereocilia in one direction or the other in effect pulls or pushes upon the tip link, which in turn opens or closes a "trap door" on the stereocilium. This opening of the MET channel grants access to a channel through which ions may flow. This mechanism may be thought of as being springy so that the pore alternates between being open and closed even when there is no stimulation. When stimulation deflects the stereocilia in the appropriate direction, the filaments are stretched so that the MET channel stays open for a longer proportion of the time, which in turn causes the ion current flow be greater and causes the hair cell to be activated. This mechanism constitutes the **mechanoelectrical transduction** process at the hair cells.

Figure 4.12 illustrates some of the basic electrochemical events associated with the electromechanical transduction process (see, e.g., Kros, 1996; Patuzzi, 1996; Wangemann and Schacht, 1996; Geisler, 1998; Fettiplace and Hackney, 2006; Vollrath et al., 2007). Notice that the endolymph is electrically positive (+80 mV) and the inside of the hair cell is electrically negative (−40 mV), constituting a polarity (voltage difference) of about 120 mV. (Cochlear electrical potentials are discussed further in the next section.) The mechanically gated opening of the transduction channels at the apex of the hair cell leads to an inflow of potassium and calcium ions, constituting a **transduction current**. As a result, the hair cell becomes partially depolarized, and the transmembrane voltage triggers the inflow of calcium ions. In turn, the calcium ions trigger the release of a neurotransmitter from the hair cell to its associated auditory neurons. Thus, sound stimulation is transformed into basilar membrane vibrations, which lead to the opening and closing of MET channels on the stereocilia, and result in electrochemical responses, leading to the representation of the sound in the auditory nerve.

COCHLEAR ELECTRICAL POTENTIALS

Several electrical potentials may be recorded from various parts of the cochlea and its environs. References have already been made to the cochlear microphonic, which is one of these, and to the general conceptualization of the action of sensory receptors. **Resting potentials** are the positive and negative direct current (DC) polarizations of the various tissues and their surrounding fluids. **Receptor potentials** are electrical responses from a receptor cell (e.g., a cochlear hair cell) that result when the cell is stimulated. These may involve alternating current (AC) or DC. Note that the presence of a receptor potential does not necessarily mean that the nervous system is aware of the

stimulus: it reflects the fact that the hair cell itself has responded. It is the transmission of a chemical mediator across the synapse and the resulting neural firing that indicate that the signal has now activated the nervous system. We may conceive of these potentials in terms of whether they are derived from a single cell or from many cells. Compound potentials include the contributions of many cells at various distances from the electrode and may include responses to different phases of the same stimulus (or to different stimuli) at different times and in different ways. Thus, the electrode "sees" a much different picture than it would if it were recording from a single cell.

The method of measurement chosen determines whether single-cell or compound (gross) potentials are recorded. The differences among methods boil down to a dichotomy between microelectrodes and gross electrodes. Basically, *microelectrodes* are electrodes small enough to impale an individual cell so that its activity can be monitored in relative isolation from other cells. Microelectrodes often have diameters much smaller than one micrometer. *Gross electrodes*, on the other hand, are not small enough to enter a cell. They include electrodes ranging in size from those that can be inserted into a nerve bundle (which are sometimes themselves called microelectrodes) to the large surface electrodes used in electroencephalography and other clinical applications. Electrodes are used in two general ways. One method uses a single *active electrode* to measure the electrical activity in an area (relative to a *ground electrode*). On the other hand, *differential electrodes* use two active electrodes, the signals of which are added, subtracted, or averaged, depending upon the specific need.

Resting Potentials

The unusual chemical situation in the cochlear duct was discussed in Chapter 2. Recall that endolymph is high in potassium, and that the proper ionic balance of the cochlear fluids has a profound effect upon the functioning of the organ of Corti.

Bekesy (1952) measured the cochlear resting potentials of the guinea pig by inserting an electrode into the perilymph of the scala vestibuli (which he set as a 0 mV reference), and then advancing it down through the scala media and the organ of Corti, and into the scala tympani. He found a positive 50 to 80 mV resting potential within the scala media. As the electrode was advanced through the organ of Corti, the voltage dropped from about +50 mV to about −50 mV, and then returned to near zero as the electrode passed through the basilar membrane into the perilymph of the scala tympani. Peake, Sohmer, and Weiss (1969) found the scala media potential to be about +100 mV. This *positive* resting potential is called the **endocochlear potential (EP)**, illustrated above the reticular lamina in Fig. 4.12. The stria vascularis is the source of the endocochlear potential (e.g., Tasaki et al., 1954; Tasaki and Spiropoulos, 1959; Konishi et al., 1961; Wangemann and Schacht, 1996).

Tasaki et al. (1954) measured a *negative* resting potential of about −60 to −70 mV in the organ of Corti, which is the **intracellular potential (IP)** of the hair cells (Dallos, 1973). Advances in measurement techniques enabled subsequent studies to provide a more accurate picture of the resting potentials of the inner and outer hair cells (Russell and Sellick, 1978a, 1983; Dallos et al., 1982; Dallos, 1985, 1986; Wangemann and Schacht, 1996). For example, Dallos and colleagues measured the electrical potentials in the upper turns of the guinea pig cochlea by using a precisely controlled microelectrode that was advanced across the organ of Corti below and parallel to the reticular lamina (Dallos et al., 1982; Dallos, 1985, 1986). This approach enabled them to accurately establish intracellular potentials for both inner and outer hair cells, as well as to describe the details of both AC and DC intracellular receptor potentials, addressed below. Based on their data, it would appear that representative values are approximately −40 mV for the IHCs (as in Fig. 4.12) and −70 mV for the OHCs (Dallos, 1985, 1986). The net result of the positive endocochlear potential and negative intracellular potential is an electrical polarity difference of 120 mV or more across the reticular lamina.

Receptor Potentials

The measurement of electrical potentials that depend on the stimulation of the ear has impacted upon virtually all aspects of our understanding of auditory physiology. In this section, we will explore several aspects of the cochlear receptor potentials. The parameters of these potentials to a large extent also describe many other aspects of cochlear physiology, as well.

Cochlear Microphonics

In 1930, Wever and Bray reported that if the electrical activity picked up from the cat's auditory nerve is amplified and directed to a loudspeaker, then one can talk into the animal's ear and simultaneously hear himself over the speaker. This result demonstrated that the electrical potentials being monitored were a faithful representation of the stimulus waveform.

Wever and Bray originally thought that they were monitoring the auditory nerve alone. However, it was soon shown that the auditory nerve action potential was not the only signal being recorded. Instead, the W*ever–Bray effect* is actually due to an AC electrical potential being picked up by the electrodes placed near the nerve (Adrian, 1931; Davis et al., 1934). It was found, for example, that the response was stronger at the round window than at the nerve, and that it was still found even if the nerve was destroyed or anesthetized. Such findings demonstrated that the AC potential which reflects the stimulus with such remarkable fidelity is generated by the cochlea, and Adrian (1931) coined the term **cochlear microphonic (CM)** to describe it.

The relationship between the hair cells and the CM is firmly established (Wever, 1966; Dallos, 1973). Bekesy (1950) demonstrated that CMs are elicited by basilar membrane deflections. A classic study by Tasaki, Davis, and Eldridge (1954) revealed that the CM is generated at the cilia-bearing ends of the hair cells. To locate the generator of the CM, the polarity of the potential was monitored by an electrode that was advanced through

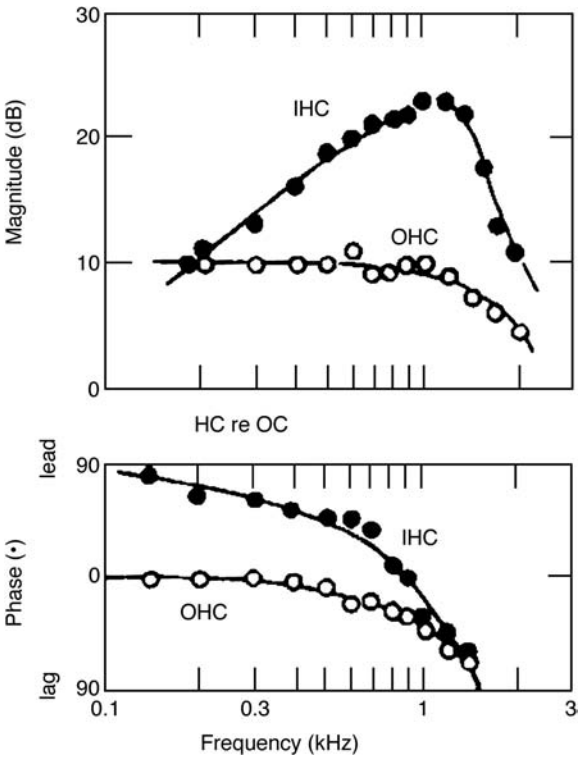

Figure 4.13 Comparison of the magnitudes (*upper graph*) and phases (*lower graph*) of intracellular AC reception potentials within the IHCs and OHCs to those in the organ of Corti outside of the hair cells (hence, HC re OC). Notice that the IHC values change as a function of frequency relative to those in the organ of Corti, whereas those for the OHCs remain relatively constant. *Source*: From *Hearing Research 14*, Dallos (Some electrical circuit properties of the organ of Corti. II. Analysis including reactive elements, 281–291, © 1984), with kind permission of from Elsevier Science Publishers—NL, Sara Burgerhartstraat 25, 1055 KV Amsterdam, The Netherlands.

the cochlea from the scala tympani toward the scala vestibuli. The polarity of the CM reversed when the electrode crossed the reticular lamina, suggesting that this is the location of the CM generator. (The polarity of an electrical potential is out of phase when measured from opposite sides of its generator.) The site of CM polarity reversal was localized to the cilia-bearing ends of the hair cells (at the reticular lamina) because the DC resting potential changed dramatically to the positive EP at this point, indicating that the reticular membrane had been impaled.

Cochlear microphonics are produced by both the inner and outer hair cells, although there is evidence indicating that they reflect a greater contribution by the outer hair cells (Russell and Sellick, 1983; Dallos and Cheatham, 1976; Dallos, 1984, 1985, 1986). Figure 4.13 demonstrates one of the reasons for this conclusion. It shows the intracellular AC receptor potential relative to the AC potential outside of these cells, within the fluid of the organ of Corti. The latter is, of course, the cochlear microphonic. A value of zero implies no difference between what is happening inside and outside of the cell, and any other value indicates the degree to which the intracellular activity differs from what is happening outside. The IHC values change as a function of frequency relative to those in the organ of Corti. However, even though the potentials are about 10 dB greater inside the OHC than outside, there is little change in magnitude or phase as a function of frequency for the AC potentials inside the OHCs compared to the fluids of the organ of Corti. The implication is that the OHCs must be making a principal contribution to the gross AC potential of the cochlea, namely, the cochlear microphonic.

How is the cochlear microphonic generated? The most widely accepted explanation is the **battery** or **variable resistance model** described by Davis (1957, 1965; see Kros, 1996; Wangemann and Schacht, 1996). Figure 4.14 shows a typical version of Davis' model. Think of the sources of the cochlear resting potentials as biological batteries generating a current flowing through the scala media, the basilar membrane, and the scala tympani. One pole of the biological battery goes to the cochlear blood supply, completing the circuit. (Recall at this point that opening of the transduction pores on the stereocilia results in a flow of ions into the cell, constituting a transduction current.) A sound stimulus would then be represented electrically (the CM) if it caused the resistance to current flow to change in accordance with the stimulus waveform. As Davis proposed, this variable resistance is provided by the movements of the hair cell stereocilia, which occur in response to basilar membrane displacement. (Recall now that the transduction pores open when bent one way and close when bent the other way, which modulates the transduction current.) In other words, the movements of the stereocilia modulate the resistance, which in turn sets up an alternating current (AC). This AC potential is monitored as the cochlear microphonic. The amount of current (CM magnitude) depends on the forces exerted upon the cilia, which is ultimately determined by the intensity of the sound stimulus.

The cochlear microphonic is a **graded potential**, which means that its magnitude changes as the stimulus level is raised or lowered. This is shown by the **input-output (I-O) function** of the cochlear microphonic. Figure 4.15 shows an idealized example of a cochlear microphonic I-O function abstracted from several classical sources. Notice that the magnitude of the cochlear microphonic increases linearly over a stimulus range of roughly 60 dB, as shown by the straight line segment of the I-O function (e.g., Wever and Lawrence, 1950, 1954). The hypothetical function in the figure shows the linear response extending down to about 0.4 μV, but CM magnitudes have actually been recorded as small as a few thousandths of a microvolt (Wever, 1966). Saturation occurs as the stimulus level is raised beyond the linear segment of the I-O function, as shown by the flattening of the curve. Increasing amounts of harmonic distortion occur in this region. Raising the intensity of the stimulus even further causes overloading, in which case the overall magnitude of the CM can actually decrease.

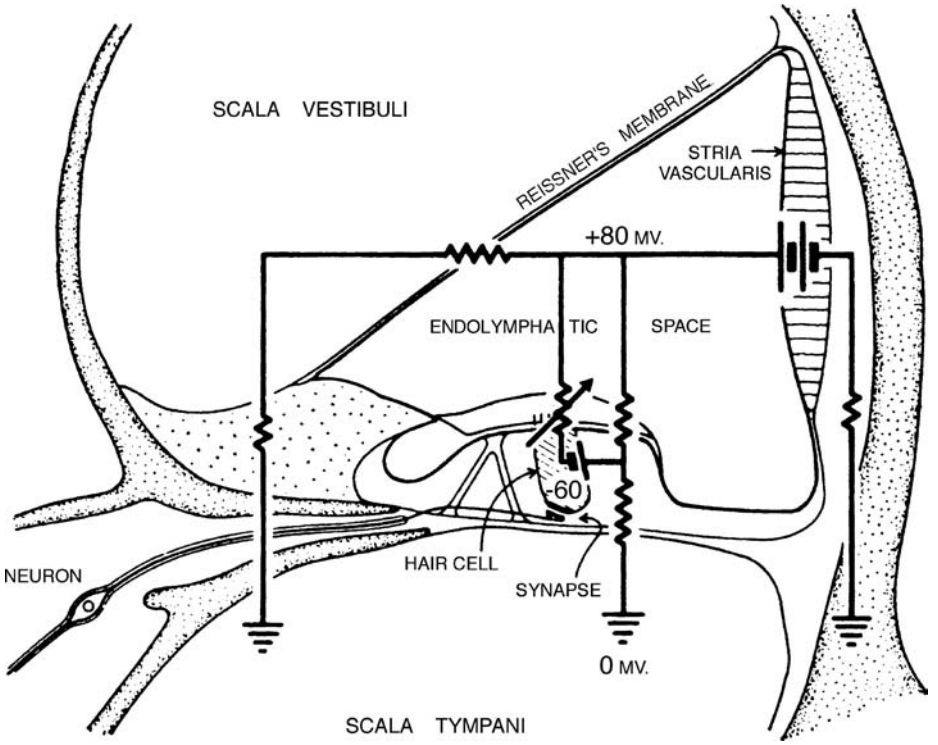

Figure 4.14 An electrical circuit representing the variable resistance model in relation to the major structures of the cochlea. *Source*: From Davis (1965), with permission.

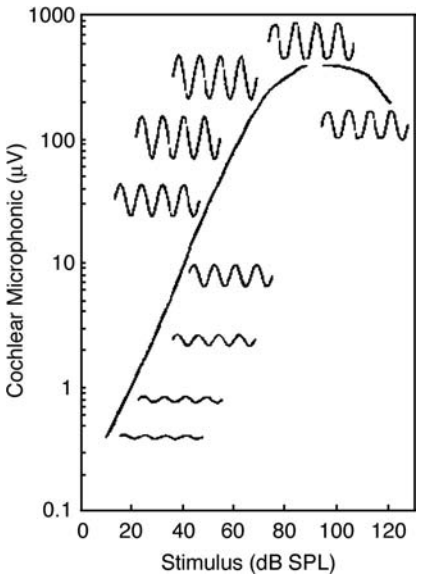

Figure 4.15 An idealized input-output function for cochlear microphonics in response to pure tone stimuli presented at increasing levels. The sine waves represent the cochlear microphonic responses at various points on the function (notice the distortion at high levels). *Source*: Based on various data and figures by Wever and Lawrence (1950, 1954) and Davis and Eldridge (1959).

The graded nature of the cochlear microphonic is also observed in terms of the intracellular AC reception potential, which is its equivalent measured within the hair cells. In fact, because these potentials are recorded *within* a given cell, they enable one to compare the relative thresholds of the inner versus outer hair cells. Using this approach, Dallos (1985) showed that the inner hair cells are on the order of 12 dB more sensitive than the outer hair cells. (This demonstration negated the previously held notion that the OHCs are more sensitive than the IHCs, which was largely based upon studies that measured thresholds following the destruction of OHCs with ototoxic drugs [Davis et al., 1958; Dallos et al., 1972a, 1972b].)

Figure 4.16 shows how the intracellular AC receptor potential changes in magnitude as a function of frequency in response to stimuli that are increased in 20-dB steps. The IHC–OHC sensitivity difference is marked by the comparison of their response magnitudes at the best frequency for the lowest stimulus level (0 dB). (The best, or characteristic, frequency is the one for which the hair cell has the lowest thresholds or the greatest magnitude of response.) The graded nature of the response is revealed by the increasing magnitude of the potential as the stimulus level increases. The slowing down of response growth at higher levels is easily seen in the figure: Even though any two successive stimuli are 20 dB apart, the resulting curves become closer and closer for the higher stimulus levels.

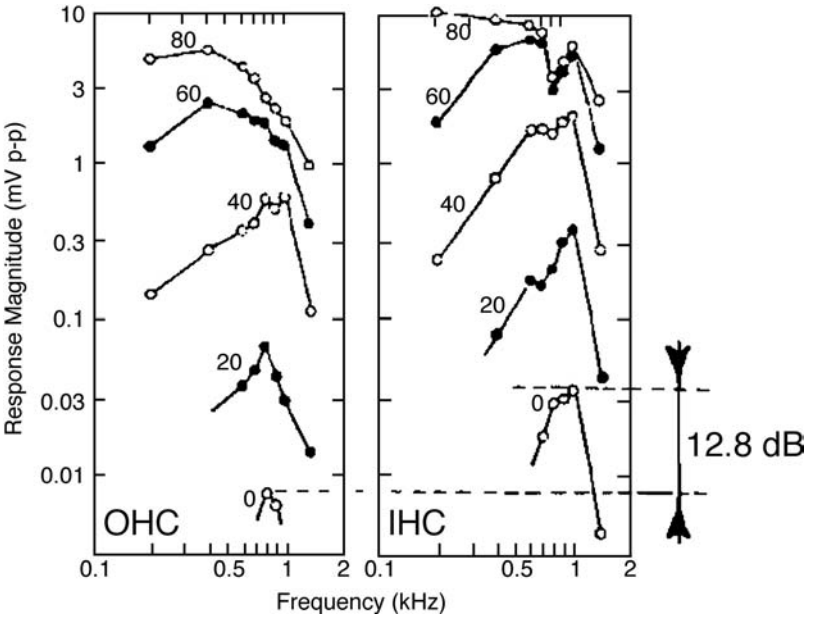

Figure 4.16 Effects of stimulus levels on the magnitude of the intracellular AC receptor potential as a function of frequency for an outer hair cell (*left frame*) and an inner hair cell (*right frame*). *Source*: From *Hearing Research 22*, Dallos (Neurobiology of cochlear inner and outer hair cells: Intracellular recordings, 185–198, © 1986), with kind permission of from Elsevier Science Publishers—NL, Sara Burgerhartstraat 25, 1055 KV Amsterdam, The Netherlands.

Distribution of the Cochlear Microphonic

Recall that large cochlear microphonic responses are recorded from the round window (Wever and Bray, 1930; Wever and Lawrence, 1954; Eggermont et al., 1974). In order to determine what contributes to the round window response, Misrahy et al. (1958) successively destroyed sections of the guinea pig's cochlea, beginning at the apex and working downward, while monitoring the CM in the basal turn. They found that the upper turns did not make significant contributions to the CM in the basal turn. It may thus be concluded that the CM recorded at the round window is for the most part derived from the activity of the basal turn.

Another approach to studying the distribution of the CM is to place electrodes along the cochlea to obtain CMs from more or less restricted locations. The distribution of the CM along the cochlear spiral was first reported with this method by Tasaki, Davis, and Legouix (1952). They inserted pairs of differential electrodes into the scalae tympani and vestibuli of the guinea pig. One electrode pair was placed in each of the four turns. This method allowed them to separate the CM, which is of opposite polarity in the two scalae, from the auditory nerve action potential (AP), which is always negative. (Addition of the out-of-phase signals cancels the CM and enhances the AP, whereas subtraction removes the AP and enhances the CM.) They found that the distribution of the CM was consistent with the propagation pattern of the traveling wave. Low-frequency signals had large CMs at the apical turn and minimal responses at the base, while high frequencies had maximal CMs at the base and no response at the apex (Fig. 4.17). They also found that the velocity of the signal was very high in the first turn of the cochlea and smaller toward the apex.

Honrubia and Ward (1968) used microelectrodes in the scala media to measure the distribution of CM responses along the cochlear duct. The electrodes were precisely placed at intervals determined from place-frequency maps of the cochlear partition. Tones were then presented at fixed intensities, and CM magnitude was measured at various distances along the cochlear duct. For example, the CM was measured at each electrode site in response to a 1200-Hz tone at 78 dB, a 2500-Hz tone at 101 dB, etc. Figure 4.18 shows typical results, with stimulus level as the parameter. Consider first the distribution of CMs at the lowest stimulus levels (most sensitive curves). Consistent with the traveling wave envelope, the peaks of these curves occur closer to the apex as frequency decreases. However, the CM curves do not line up exactly with the basilar membrane displacement curve. This discrepancy is shown clearly in Fig. 4.19, in which the CM curve is wider and less peaked than the basilar membrane tuning curve. The difference occurs because the electrode "sees" CMs generated by thousands of hair cells in its general vicinity rather than by just those at its precise point of insertion (Dallos et al., 1974). In other words, the electrode really monitors a weighted average of many CMs, which has the effect of flattening the curve somewhat.

As shown in Fig. 4.15, CM magnitude increases with stimulus level for each frequency. Also, the place of maximum CM magnitude shifts downward toward the base as intensity increases.

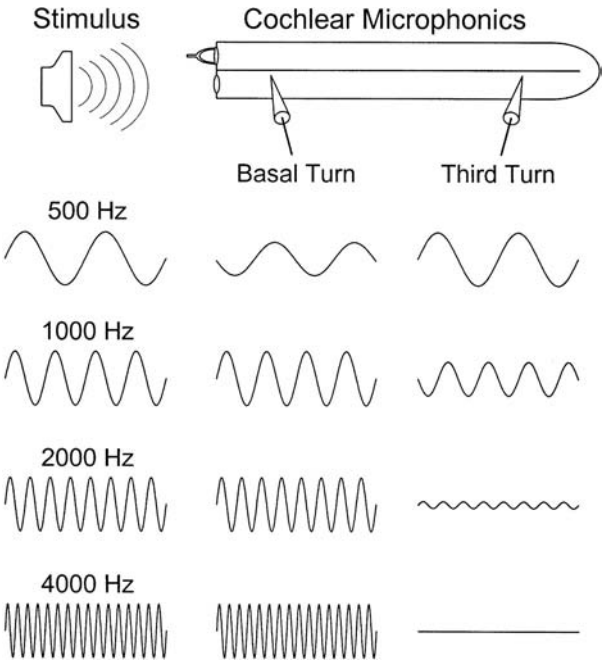

Figure 4.17 Artist's representation of the cochlear microphonics recorded with differential electrodes in the first and third turns of the guinea pig cochlea (*right*) in response to stimuli of various frequencies (*left*).

This may at first seem inconsistent with the place principle. However, the basal shift of maximum CM response is probably due to the wider range over which the more basal generators respond linearly (Dallos, 1973). In other words, as stimulus intensity increases, the CMs from the most sensitive place along the basilar membrane become saturated sooner than do the responses from more basal regions. Thus, CMs generated toward the base continue to increase in magnitude when those from the most sensitive place have already become saturated. The place of maximal CM response therefore shifts downward along the cochlear partition (upward in frequency).

The intracellular AC receptor potential also reveals a changing distribution with respect to frequency when the stimulus level increases, as shown in Fig. 4.16. Here, we see that the tuning of the AC potential is reasonably restricted around the best frequency when the stimulus level is low, and that it becomes wider, extending toward the low frequencies, when the stimulus level becomes greater. In other words, the intracellular AC receptor potential resembles a band-pass filter around the best frequency at low levels of stimulation and a low-pass filter at higher levels (Dallos, 1985).

Summating Potentials

The **summating potential (SP)** was first described by Davis, Fernandez, and McAuliffe (1950) and by Bekesy (1950). Unlike

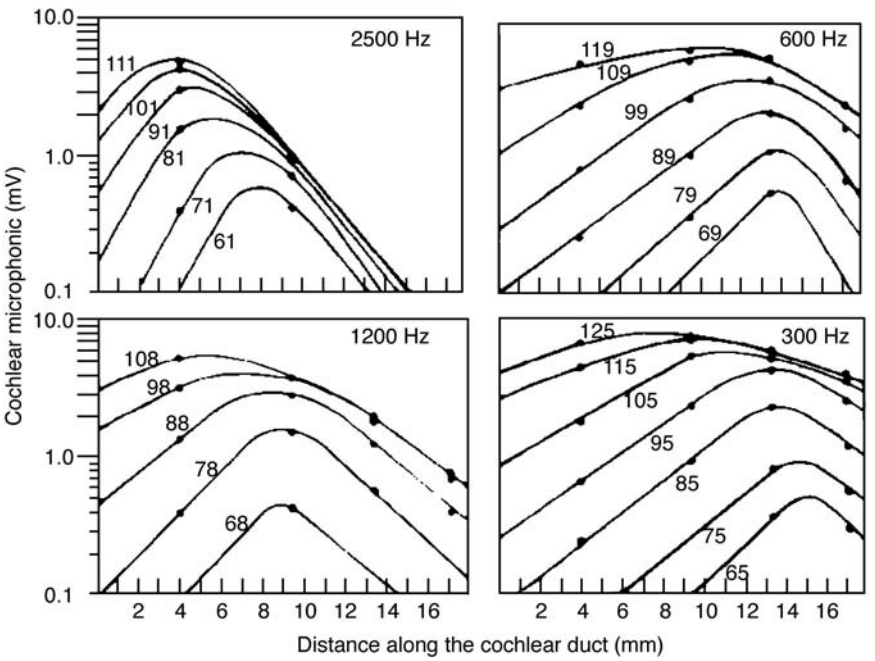

Figure 4.18 Cochlear microphonic magnitude as a function of distance along the basilar membrane for four frequencies presented at various intensities. *Source*: From Honrubia and Ward (1968), with permission of *J. Acoust. Soc. Am.*

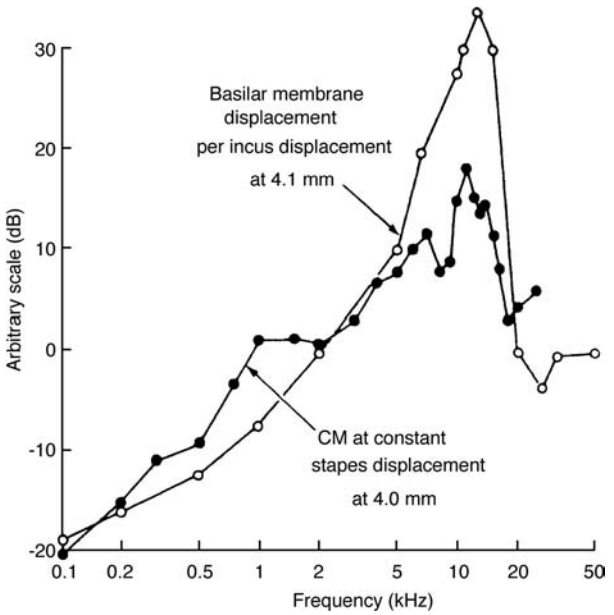

Figure 4.19 Comparison of basilar membrane tuning curves (based on Wilson and Johnstone, 1972) and the CM curve at similar locations in the guinea pig cochlea. *Source*: From Dallos et al. (1974), with permission of *J. Acoust. Soc. Am.*

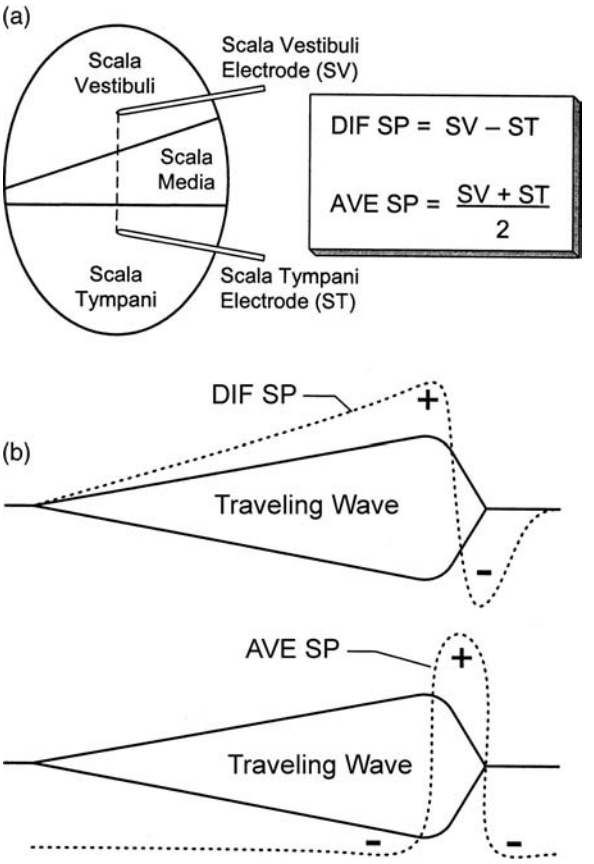

Figure 4.20 (a) Electrode arrangement and calculations used to obtain the DIF and AVE components of the summating potential. (b) Spatial relationships of the AVE SP and the DIF SP to the traveling wave envelope. *Source*: Modified from various drawings by Dallos, with permission.

the CM, which is an AC potential, the SP is a shift in the DC baseline in response to sound stimulation. In other words, the SP is a DC potential. Bekesy originally called this shift the "DC fall." Subsequent research revealed that it may be either a positive or a negative baseline shift (Davis et al., 1958). We will see that SP polarity is associated with the traveling wave envelope and how the potential is recorded. Like the cochlear microphonic, the SP is a graded potential that increases in magnitude as the stimulus level is raised (Davis et al., 1958). Although the origin of the SP was once a matter of debate, it is now well established that it is a *receptor potential* of the hair cells (Dallos and Cheatham 1976; Russell and Sellick, 1977a, 1977b, 1978a, 1978b, 1983; Dallos, 1985, 1986).

Honrubia and Ward (1969b) measured the SP and CM simultaneously in each turn of the guinea pig cochlea using electrodes located in scala media. We have already seen that the envelope of the distribution of CM amplitude along the length of the cochlear duct is a reasonable representation of the traveling wave envelope. Honrubia and Ward found that the SP was positive on the basal side of the CM envelope and negative on its apical side. This suggests that the SP is positive on the basal side of the traveling wave and becomes negative apical to the traveling wave peak.

Dallos and colleagues used a somewhat different recording approach (Dallos, 1973; Dallos et al., 1970, 1972b; Cheatham and Dallos, 1984). This method distinguishes between the average potential of both the scala vestibuli and the scala tympani on the one hand and the potential gradient (difference) across the cochlear partition on the other. This at first complicated distinction is clarified in Fig. 4.20a. One electrode is in the scala vestibuli and the other is in the scala tympani. Each one registers the SP at the same cross-sectional plane along the cochlea, but from opposite sides of the scala media. Subtracting the SP in the scala tympani (ST) from the SP in the scala vestibuli (SV), (SV − ST), gives the potential difference of the SP across the cochlear partition. This difference is called the DIF component. The average (AVE) component is obtained by simply averaging the SPs from both scalae [(SV + ST)/2]. The AVE component thus expresses the common properties (common mode) of the SP on both sides of scala media.

The spatial arrangements of the DIF SP and AVE SP are shown superimposed upon the traveling wave envelope in Fig. 4.20b. Note that the DIF component becomes negative in the vicinity of the peak of the traveling wave envelope, a situation that resembles the spatial distribution of SP+ and SP− discussed above. The polarity of the AVE component is essentially the reverse, being positive around the traveling wave peak and negative

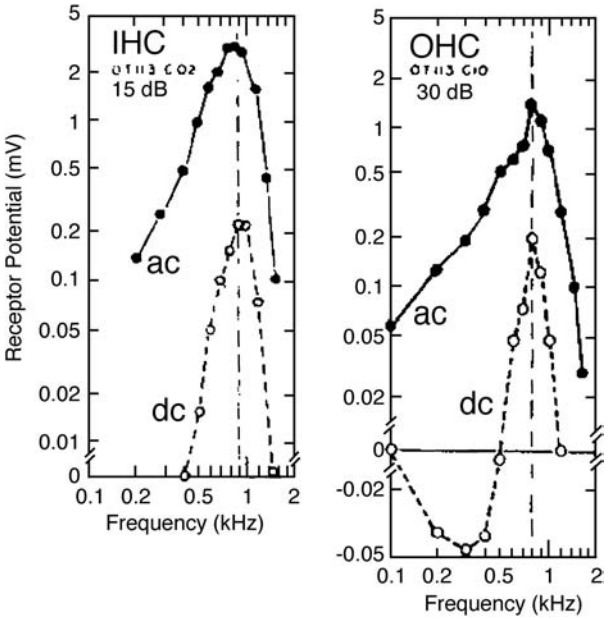

Figure 4.21 Intracellular AC and DC receptor potentials as a function of frequency at low levels of stimulation from an inner hair cell (*left frame*) and an outer hair cell (*right frame*) with comparable characteristic frequencies. *Source*: From *Hearing Research 22*, Dallos (Neurobiology of cochlear inner and outer hair cells: Intracellular recordings, 185–198, © 1986), with kind permission of from Elsevier Science Publishers—NL, Sara Burgerhartstraat 25, 1055 KV Amsterdam, The Netherlands.

elsewhere. The AVE SP and DIF SP components of the summating potential are probably produced by the same underlying processes (Cheatham and Dallos, 1984).

As we have seen for the cochlear microphonic, intracellular recordings also reveal that the summating potential is derived from the hair cells, with the principal contribution coming from the OHCs (Russell and Sellick, 1983; Dallos, 1985, 1986). Figure 4.21 provides insight into this relationship. It shows **tuning curves** obtained at low levels of stimulation for the AC and DC intracellular receptor potentials (the intracellular versions of the CM and SP, respectively) of an IHC and an OHC having comparable best frequencies. The figure reveals that the polarity of the outer hair cell's DC receptor potential changes in both the positive and negative directions. In contrast, the DC receptor potential of the inner hair cell is positive only. Thus, the distribution of the SP is consistent with that of the OHCs as opposed to the IHCs.

This negative–positive distribution of the intracellular DC receptor potential is in agreement with what we have just seen for the SP, which is the gross extracellular potential representing the contribution of many cells. (The negative–positive shape of the DC receptor potential as a function of frequency at low stimulus levels becomes positive only at higher levels.)

The effects of increasing stimulus level upon the intracellular DC potential are largely similar to those observed above for the AC potential. Specifically, the magnitude of the potential increases with stimulus level, compressing once moderate levels are achieved, and as a function of frequency, the response is sharply tuned and the band-pass around the best frequency at low levels of stimulation becomes wider and low-pass at higher levels.

Several other observations might be made from Fig. 4.21. The data were obtained using the lowest stimulus levels, which allowed complete tuning curves to be generated. Note that this was 15 dB for the IHC and 30 dB for the OHC. This difference should not be surprising if one recalls that the IHCs are roughly 12 dB more sensitive than the OHCs. Second, notice that the tuning curves for the DC receptor potentials are sharper than those for the AC potentials. Finally, notice that these tuning curves obtained at low levels of stimulation are very sharp—much sharper than what we have seen for the traveling wave envelope.

COCHLEAR TUNING AND FREQUENCY SELECTIVITY

Basilar membrane displacement reaches a peak near the apex of the cochlea in response to low frequencies and near the base for higher frequencies. That is, the traveling wave causes a displacement pattern, which is tuned as a function of distance along the basilar membrane. One may say that the cochlea is tuned to frequency as a function of distance along the cochlear partition. This relationship between the tuning of a location along the cochlear partition and the distance from the base to apex is depicted in Liberman's (1982) **cochlear frequency map** shown in Fig. 4.22. This map was derived by determining the **characteristic** or **best frequencies** of auditory neurons labeled with horseradish peroxidase (HRP), and then tracing these neurons back to their respective hair cells along the cochlear

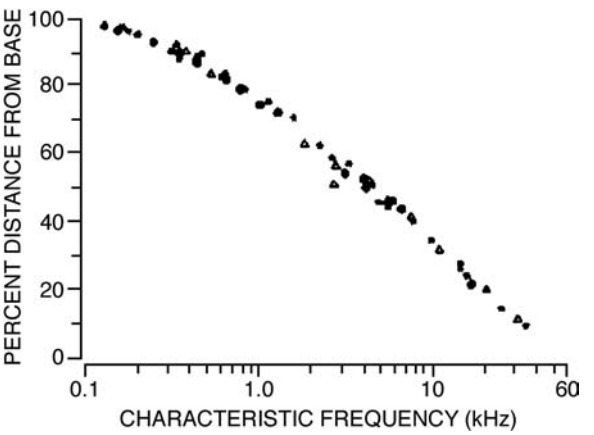

Figure 4.22 This cochlear map shows the relationship between frequency and distance in percent along the cochlear partition in the cat. *Source*: From Liberman (1982), with permission of *J. Acoust. Soc. Am.*

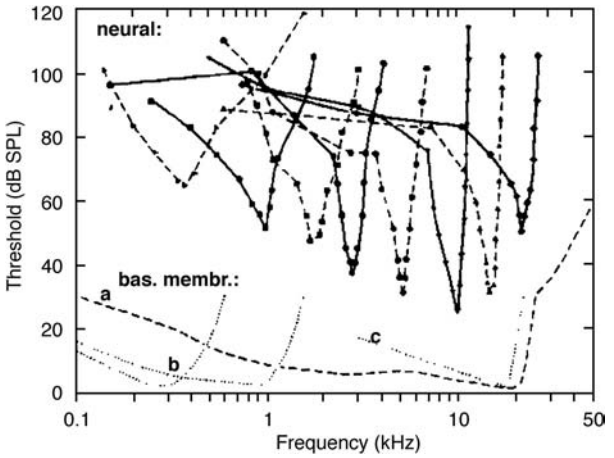

Figure 4.23 *Upper curves*: Neural tuning curves (guinea pig). *Lower curves*: Mechanical tuning (guinea pig) based on (a) Wilson and Johnstone, 1972, (b) Bekesy (1960/1989), and (c) Johnstone et al. (1970). *Source*: From Evans (1975), The sharpening of cochlear frequency selectivity. *Audiology*, 14, 419–442.

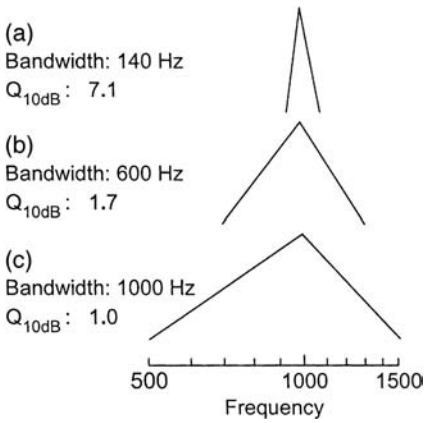

Figure 4.24 Q_{10dB} for three idealized "tuning curves" centered at 1000 Hz. These Q_{10dB} values were obtained as follows: (a) 1000/140 = 7.1, (b) 1000/600 = 1.7, and (c) 1000/1000 = 1.0.

duct (see Chap. 5). This method made it possible to precisely locate the places along the cochlea that correspond to particular frequencies. This cochlear map expresses distance along the cochlea in terms of percentage, thereby accounting for differences in cochlear length across specimens.

In the following chapters, we shall see that fine frequency discriminations are made in psychoacoustic experiments, and that auditory nerve fibers are very sharply tuned. Can the mechanical displacement pattern in the cochlea account for this remarkable degree of frequency selectivity?

A key question is whether the *sharpness* of **cochlear tuning** approaches that of the auditory nerve. The upper curves in Fig. 4.23 show a set of **response areas** or **tuning curves** for auditory nerve fibers in the guinea pig. Neural tuning curves will be discussed in Chapter 5. For now, note their sharp peaks, which indicate that auditory nerve fibers respond best to a limited range of frequencies around a characteristic frequency. The low-frequency slopes of the neural tuning curves range from about 100 to 300 dB per octave, and the high-frequency slopes are approximately −100 to −600 dB per octave in a variety of species (e.g., Kiang, 1965; Evans and Wilson, 1971, 1973; Evans, 1972a, 1972b; Geisler et al., 1974).

The sharpness of tuning can be described by a value **Q**, which is the ratio of the center frequency to the bandwidth. For a particular center (characteristic) frequency, the narrower the bandwidth, the larger is the Q value. This relationship is illustrated in Fig. 4.24. Recall that the half-power points are the usual cutoff values used to define a bandwidth. Since it is difficult to determine the half-power points of physiological tuning curves, it has become standard practice to use the points on the curve that are 10 dB down from the peak. For this reason, we use the value $\mathbf{Q_{10dB}}$ to summarize the sharpness of physiological tuning curves. Auditory neurons have Q_{10dB} values of about 2 to 10 for the midfrequencies (Evans and Wilson, 1973). With this in mind, let us proceed to examine the nature of frequency selectivity in the cochlea.

Bekesy (1949) was the first to describe **mechanical tuning** in the cochlea. He used a binocular microscope to observe **basilar membrane displacement patterns** in response to high-intensity signals. Figure 4.25 shows some of the basilar membrane tuning curves obtained by Bekesy. These curves are in terms of relative amplitude so that the peak is assigned a value of 1.0 and the displacements at other points along the curves are in proportions of the peak amplitude. The tuning curves tend to become sharper with increasing frequency, but the low-frequency slopes of about 6 dB per octave are far from the sharpness of neural tuning. This is illustrated in Fig. 4.23, in which Bekesy's curves (labeled b) are compared with neural tuning curves having similar characteristic frequencies.

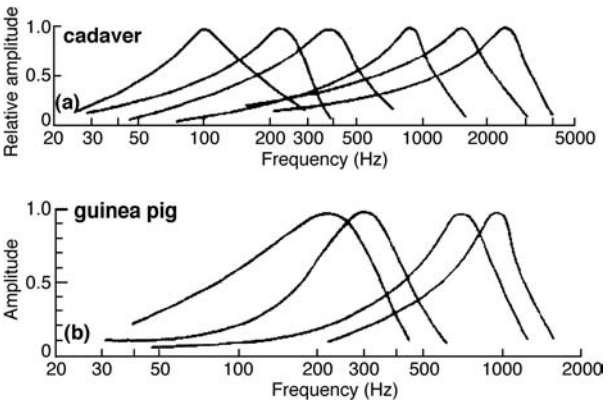

Figure 4.25 Basilar membrane tuning curves obtained in (a) cadaver (after Beksey, 1943/1949) and (b) guinea pig (after Bekesy, 1944).

Although Bekesy's data were of monumental significance, several experimental limitations make it difficult to compare these early findings with neural tuning data: Access to the cochlear partition was limited to the apical areas so that Bekesy's observations were restricted to relatively low frequencies. The observations were obtained visually. Absolute displacements were not specified (although they were in other contexts). Very high stimulus levels (roughly 120 dB SPL) were used, while neural data are available at much lower, including threshold, levels.

Subsequent studies investigated basilar membrane tuning using methods made possible by technological advances in the 1960s and 1970s (e.g., Johnstone et al., 1970; Rhode, 1971, 1978; Köhllofel, 1972; Wilson and Johnstone, 1972, 1975; Johnstone and Yates, 1974; Rhode and Robles, 1974). For example, Johnstone and Boyle (1967) measured tuning in the guinea pig cochlea by using the **Mössbauer technique**, which made it possible to use stimulus levels as low as 60 to 70 dB SPL. In this method, a radioactive source is placed on the basilar membrane and an absorber of the radiation is situated nearby. Vibration of the basilar membrane causes the amount of gamma rays absorbed to be modulated in a manner related to the vibration. Basilar membrane displacement is calculated based on these data. Mechanical tuning curves obtained with the Mössbauer method (e.g., curve ***c*** at the bottom of Fig. 4.23) were considerably sharper than what Bekesy found at low frequencies (e.g., curves labeled ***b*** in the figure).

Wilson and Johnstone (1972, 1975) measured basilar membrane tuning with a **capacitance probe**, which was a miniature version of the one used by Bekesy (1960/1989) (see Chap. 3). Their findings are of interest because they confirmed the Mössbauer data with another technique and also because the capacitance probe enabled them to measure basilar membrane vibrations for stimuli as low as 40 dB SPL (which is closer to the levels used to obtain neural tuning curves). Curve ***a*** in lower part of Fig. 4.23 shows an example. Comparing the upper and lower sections of Fig. 4.23 makes it clear that these measurements cannot account for the sharpness of the neural tuning data.

It was once thought that a **"second filter"** existing between the basilar membrane and neural responses might account for the sharpness of neural tuning. The main evidence for this idea was that neural tuning curves become wider when the metabolism of the cochlea is disturbed by interference with its oxygen supply or by chemical influences (Evans, 1972a, 1972b, 1974, 1975; Evans and Wilson, 1971, 1973). The appeal of the second filter concept to bridge the gap from broad mechanical to sharp neural tuning led to the proposal of several theories about its location and mechanism. One example involved **lateral inhibition**, which involves the suppression of activity in weakly stimulated neural units by more intense stimulation of adjoining units (e.g., Bekesy, 1960/1989), although other possible mechanisms were also proposed (e.g., Khanna et al., 1968; Duifhuis, 1976; Zwislocki, 1974, 1975, 1985; Manley, 1978; Crawford and Fettiplace, 1981). An example of lateral inhibition from common experience is the sharply defined border that is seen between adjoining black and white bars known as Mach bands. However, we shall see that *active processes* are at work that provide for mechanical tuning just as sharp as neural tuning. Thus, a "second filter" is not necessary. Interested readers should refer to Pickles (1982) and Gelfand (1981) for reviews of second filter theories.

That sharp tuning already exists prior to the neural response was demonstrated by Russell and Sellick (1977a, 1977b, 1978a, 1978b). They measured the intracellular DC receptor potential (summating potential) in guinea pig IHCs as a function of stimulus frequency and level. Typical findings are shown in Fig. 4.26. Each curve shows the sound pressure level needed to reach a certain magnitude of DC potential within the IHC as a function of frequency. These curves are called *isoamplitude contours* because each point on a given curve represents the SPL needed to achieve the same amplitude of SP. The smallest intracellular SP response that could elicit a response from the auditory nerve was about 2.0 mV. At high stimulus levels (SPLs that result in larger SP amplitudes), the SP tuning is more or less like that of the mechanical data we have previously reviewed. However, as the stimulus level decreases, the reduction in SP amplitude (A in mV) comes with a clear increase in the frequency selectivity of IHC intracellular tuning curves. For example, when SP amplitude is 2.7 mV (within 10 dB of threshold), Q_{10dB} is 9.2. This is as sharp as neural tuning. Similarly sharp tuning of intracellular potentials has also been reported for the OHCs (e.g., Dallos et al., 1982). One might note in this context that Cheatham and Dallos (1984) showed that tuning curves for the SP are consistent with those of the basilar membrane and the auditory nerve action potential.

These findings demonstrate that frequency selectivity as sharp as what is found in the auditory neuron already exists within the hair cell and *before* it transmits to the nerve fiber. Clearly, the acuity of neural tuning does not require an intervening filter between the hair cell and the neuron.

What (and where), then, is the origin of the sharp tuning that is already seen in the hair cell? The answer comes from studies of the in vivo mechanical responses of virtually undamaged cochleas at stimulus levels as low as those used to generate neural tuning curves.

In 1982, Khanna and Leonard demonstrated sharp basilar membrane tuning in the cat by using **laser inferometry**. A detailed discussion of this technique and its applications may be found in an informative series of papers by Khanna and colleagues (Khanna and Leonard, 1982, 1986a, 1986b; Khanna, 1986; Khanna et al., 1986). The sharpness of mechanical tuning in the cochlea has been repeatedly corroborated (e.g., Sellick et al., 1982a; Robles et al., 1986; Ruggero et al., 1997).

Figure 4.27a shows three cat basilar membrane tuning curves. These curves show the sound pressure levels needed to yield a certain threshold amplitude of basilar membrane vibration as a function of frequency. The sharpest of these three curves is

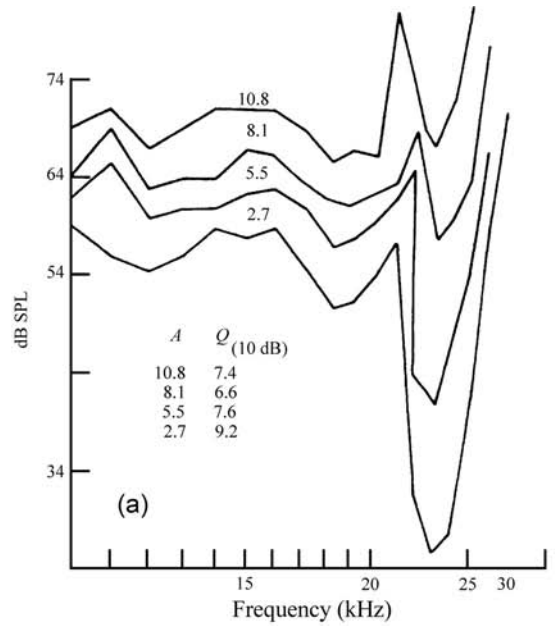

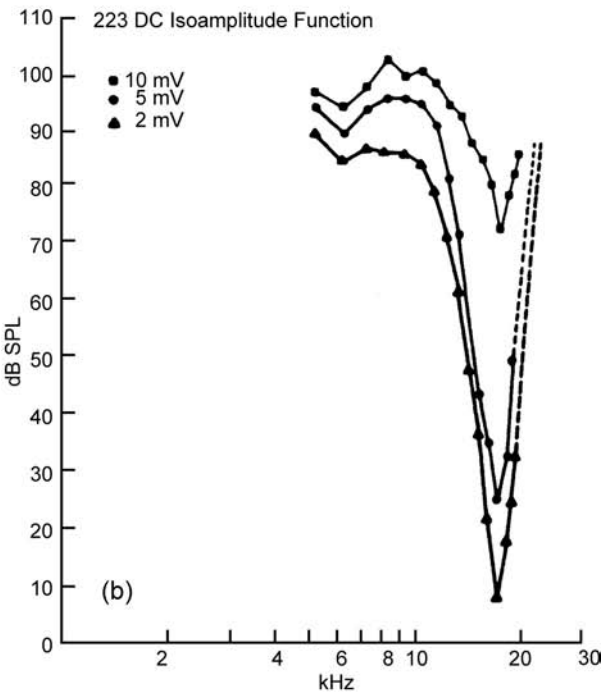

Figure 4.26 Intracellular DC receptor potentials (summating potentials) from guinea pig inner hair cells as a function of frequency: (a) Receptor potential amplitude (A in mV) is shown with corresponding values of Q_{10dB}. *Source*: From Russell and Sellick (1977a), courtesy of *Nature*. (b) Isoamplitude curves are shown for 2, 5, and 10 mV intracellular potentials. *Source*: From Russell and Sellick, Intracellular studies of cochlear hair cells: Filling the gap between basilar membrane mechanics and neural excitation, in *Evoked Electrical Activity in the Auditory Nervous System* (Naunton and Fernandez, eds.), © 1978 by Academic Press.

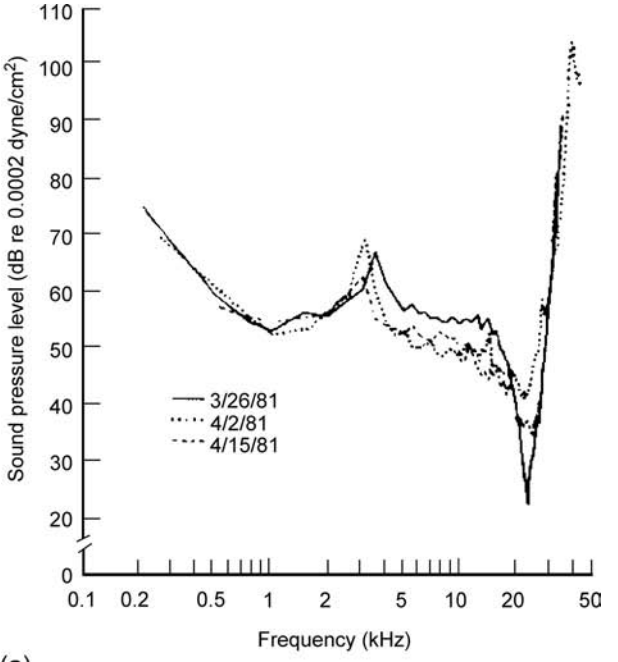

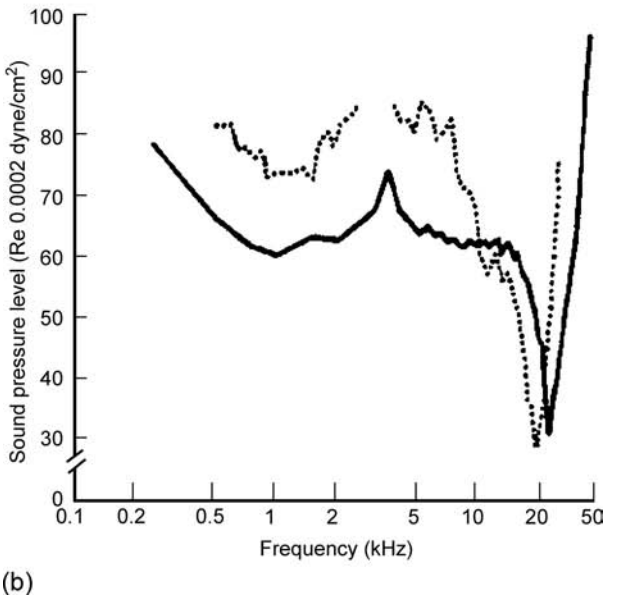

Figure 4.27 (a) The SPL necessary to achieve equal amplitudes of basilar membrane movements in three cats. (b) Comparison of the sharpest basilar membrane curve (3/26/81) with a neural tuning curve. *Source*: From Khanna and Leonard, Basilar membrane tuning in the cat cochlea, *Science*, 215, 305–306 (1982). Copyright © 1982. Reprinted with permission from American Association for the Advancement of Science.

shown redrawn in Fig. 4.27b along with a neural tuning curve. The basilar membrane curve is strikingly similar to that of the neuron in the sharply tuned tip of the tuning curve, but deviates from the neural response at lower frequencies. These graphs reveal that the basilar membrane's mechanical response is as sharp as that of the neural tuning curve in the region of the most sensitive response (where Q_{10dB} is 5.9 for both curves in this example).

Similar findings for the guinea pig cochlea were obtained by Sellick et al. (1982a, 1982b). Recall that the IHCs are activated by the velocity rather than the displacement of basilar membrane movement. As a consequence, they expressed the mechanical response of the basilar membrane in terms of the velocity of its motion. Figure 4.28a shows that the basilar membrane isovelocity curve (crosses) is remarkably similar to a representative neural tuning curve. Figure 4.28b shows the SPLs needed to yield an isoamplitude response of the basilar membrane. As in the previous figure, the isoamplitude response is similar to the neural response in the sharply tuned tip of the curve, but deviates at lower frequencies.

Sellick, Pauzzi, and Johnstone (1982a, 1982b) used the stimulus SPL needed to evoke an auditory nerve action potential (see Chap. 5) as a measure of the health of the cochlea over the course of their measurements. Examples of their results are shown in Fig. 4.29. They found that these thresholds worsened as time passed, revealing that the experimental invasion of the inner ear itself caused progressive damage to the cochlea. Khanna and Leonard (1982) also reported that trauma to the cochlea due to the experimental manipulations caused a loss of sharp mechanical tuning.

It is now clear that the mechanical tuning within the cochlea accounts for the sharpness of neural tuning; but what is the nature of this mechanical tuning process? We must recall at this juncture that the real concern is with the sharpness of the mechanical stimulus actually transmitted to the hair cells. The tuning of the cochlea involves more than just the passive traveling wave response of the basilar membrane. There also are **active processes** associated with the outer hair cells and their connections to surrounding structures.

Let us view the tuning curve somewhat differently in order to appreciate why the mechanical tuning of the cochlea involves active processes. The cochlea's mechanical response may be described as having two components (Khanna and Leonard, 1982, Leonard and Khanna, 1984; Kelly and Khanna, 1984a): One of these components has a broad low-pass response. The other is a sharply tuned band-pass filter. Together, the two components reveal the neural tuning curve's familiar sharp tip and broad tail. Injuries that affect the tip do not particularly affect the broad, low-pass component. In particular, injuries affecting the OHCs have been shown to affect the tip component but not the tail of the tuning curve, and the condition of the OHCs is correlated with the affect upon the tip of the tuning curve (Khanna and Leonard, 1986b; Leonard and Khanna, 1984; Liberman and Dodds, 1984). These changes in the tip of

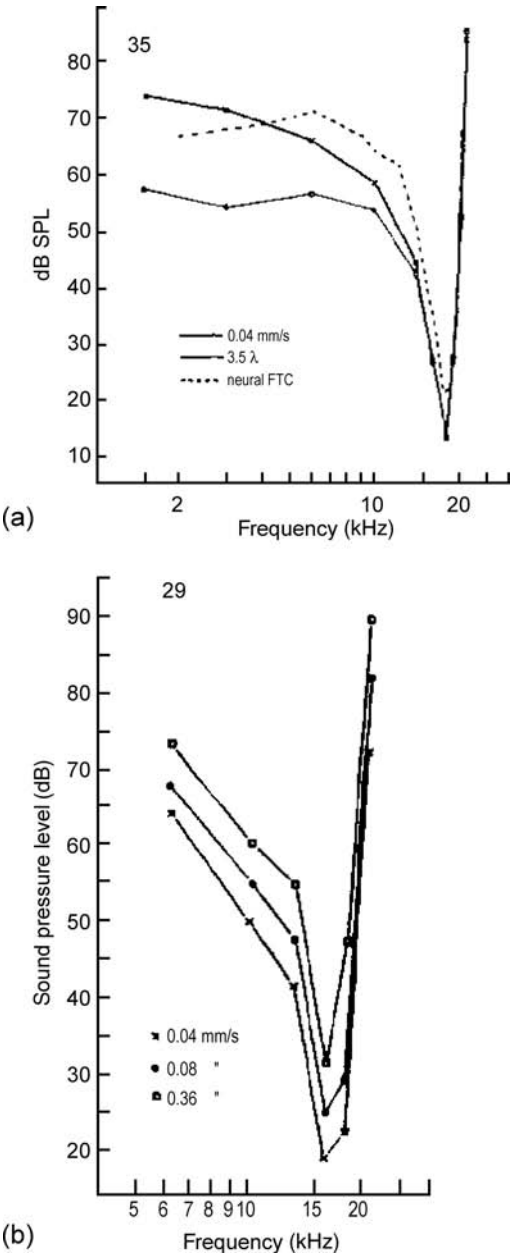

Figure 4.28 (a) The SPL necessary to achieve equal velocities (*crosses*) and amplitudes (*circles*) of basilar membrane vibration, and a comparable neural tuning curve (*dotted line*) in the guinea pig. (b) The SPL needed to achieve three velocities of basilar membrane vibration in the same guinea pig. *Source:* From Sellick et al. (1982), with permission of *J. Acoust. Soc. Am.*

the tuning curve are found in the absence of basilar membrane abnormalities (Kelly and Khanna, 1984a, 1984b). The tip component of the cochlea's mechanical tuning curve is associated with the outer hair cells.

One might note in this context the classic observation that thresholds become about 30 to 40 dB poorer when ototoxic

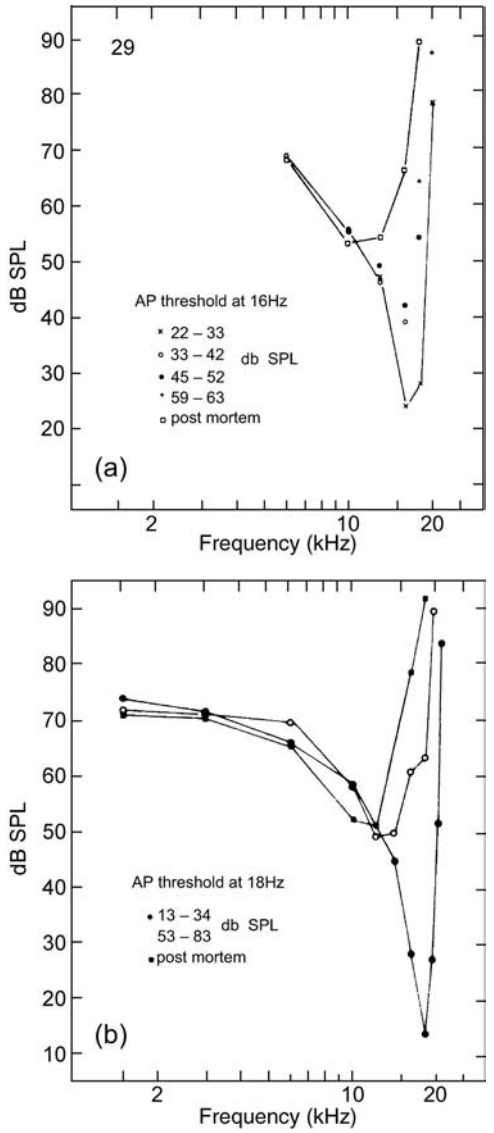

Figure 4.29 The loss of sharp mechanical tuning of the basilar membrane is observed as thresholds become elevated, revealing progressive damage to the cochlea over the course of the measurements, and post mortem, for two guinea pigs (a and b). From Sellick et al. (1982a, 1982b), with permission of *J. Acoust. Soc. Am.*

drugs have destroyed the *outer* hair cells (Dallos et al., 1972a, 1972b). The long-held interpretation of this observation was that the *inner* hair cells, which survived the ototoxic assault, are not as sensitive as the outer hair cells. However, we now know that the drop in thresholds is due to the loss of the sensitizing effects of the OHCs (Dallos and Harris, 1978). In fact, as previously noted and in contrast to previously held notions, intracellular recordings have established that the IHCs are on the order of 12 dB more sensitive than the OHCs (Dallos, 1985).

The two-component nature of cochlear tuning has also been demonstrated by Liberman and colleagues, who determined how various cochlear manipulations affected the associated auditory neurons' responses (Liberman, 1984; Liberman and Dodds, 1984; Liberman and Kiang, 1984; Kiang et al., 1986). They demonstrated that while both the IHCs and OHCs are needed to yield a normal neural tuning curve, the presence of the sharply tuned component of the response depends upon the presence and condition of the outer hair cells.

Smith et al. (1987) provided behavioral support for the contribution of the OHCs to the sensitivity and fine-tuning of the cochlea. They obtained **psychoacoustic tuning curves (PTCs)**, a behavioral measure of frequency selectivity (see Chap. 10), from patas monkeys before and after producing OHC damage with the drug dihydrostreptomycin. The drug caused elevations of threshold sensitivity of 50 dB or more, and the sharp tips of the PTCs to be obliterated, leaving only the broad, low-pass filter characteristic of the curves. Histological examination of the cochleas revealed that there was complete loss of OHCs but complete retention of the IHCs in the regions corresponding to the changes of the PTCs.

COCHLEAR NONLINEARITY

One of the seminal contributions to our knowledge of cochlear functioning was Rhode's (1971) demonstration that the mechanical response of the basilar membrane is **nonlinear**. The nonlinearity is seen in Fig. 4.30 as a lack of overlapping of the tuning curve peaks obtained at different stimulus levels. The three curves in the figure would have overlapped exactly if the basilar membrane's vibration was linear because the amplitude (in dB) is derived from the ratio of basilar membrane-to-malleus displacement. In a linear system, this ratio would stay the same for different stimulus levels. This nonlinearity, originally observed in the squirrel monkey, used to be the subject of controversy because other researchers at that time did not find it in the guinea pig. However, as we have seen for the sharpness of cochlear tuning, nonlinearity in the vicinity of the peak is the *normal* response (e.g., Rhode, 1971, 1978; Rhode and Robles, 1974; Sellick et al., 1982a, 1982b; Robles et al., 1986; Ruggero et al., 1997) (see Figs. 4.26, 4.28b, and 4.31).

Figure 4.31 provides a detailed illustration of this nonlinearity. Here, we see a set of tuning curves obtained from a healthy chinchilla cochlea by Ruggero et al. (1997), who used a wide range of stimulus levels and modern measurement techniques (a form of laser inferometry). Notice that the mechanical response is nonlinear around the characteristic frequency (tuning curve peak) and at higher frequencies, again indicated by the lack of overlapping). However, this does not occur at lower frequencies, where the curves are superimposed.

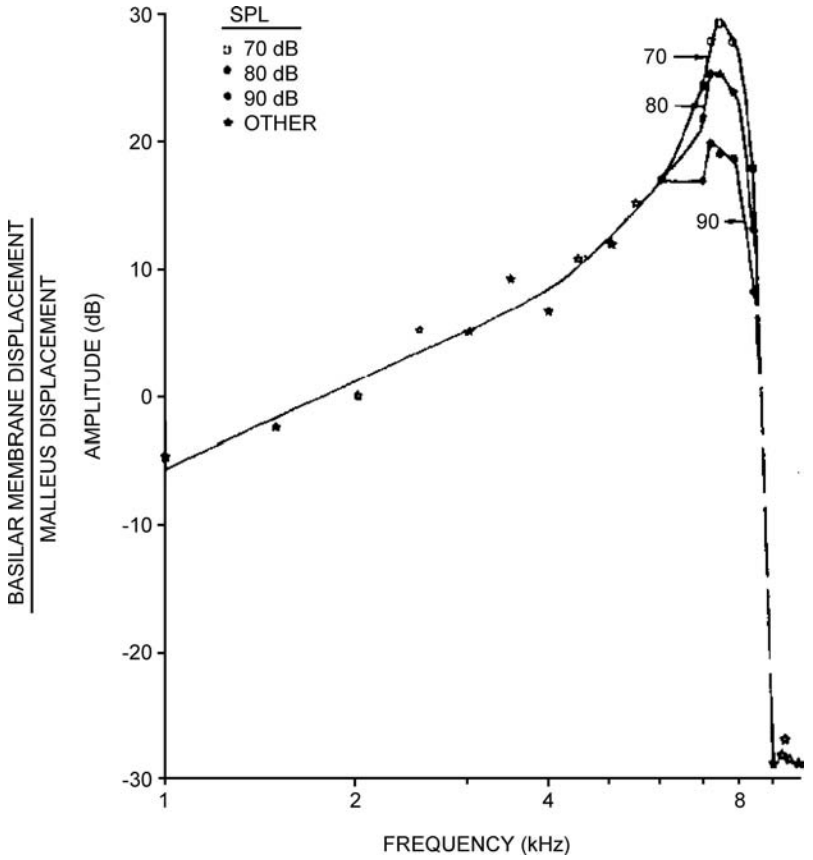

Figure 4.30 Basilar membrane tuning curves obtained in the squirrel monkey using stimulus levels of 70, 80, and 90 dB SPL. Notice that the peaks obtained at different stimulus levels do not overlap, indicating that the response is nonlinear. *Source*: From Rhode (1971), with permission of *J. Acoust. Soc. Am.*

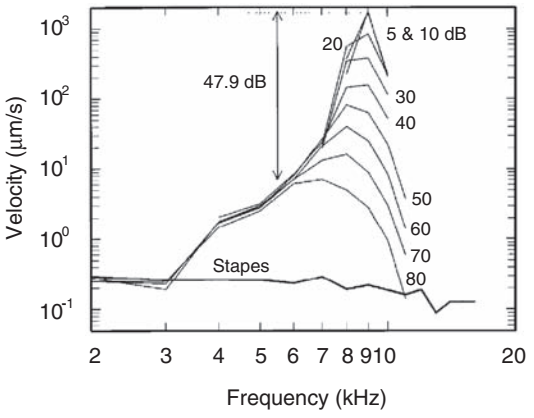

Figure 4.31 Basilar membrane tuning curves (gain in response velocity divided by stimulus level as a function of frequency) in the chinchilla cochlea, using a wide range of stimulus levels (indicated by the numbers next to each curve). The response is nonlinear for frequencies in the vicinity of the peak and above (revealed by the lack of overlapping), but is linear for lower frequencies (where the curves overlap). *Source*: Adapted from Ruggero et al. (1997), by permission of *J. Acoust. Soc. Am.*

The *compressive* nature of the nonlinear response of the basilar membrane is clearly seen in Fig. 4.32, which shows data from six essentially healthy chinchilla cochleas. Each curve shows how the magnitude of the basilar membrane response at the tuning curve peak is related to the sound pressure level of the stimulus. The straight line in the graph illustrates linear growth. The tipping-over of these curves shows that the growth of response magnitude slows down as the stimulus level rises. The nonlinear nature of these curves is highlighted by comparing them with the straight line representing linear growth.

As for sharp tuning, the sensitivity and nonlinear nature of the basilar membrane response depend on the health and integrity of the cochlea (e.g., LePage and Johnstone, 1980; Sellick et al., 1982a, 1982b; Yates et al., 1990). For example, Sellick et al. (1982a, 1982b) showed that sharp turning and the nonlinear response deteriorated as thresholds worsened, and that they were present early during experimental testing when the cochlea was still reasonably healthy, but were lost as the experiment proceeded and at postmortem (Fig. 4.29).

The nonlinearity of the cochlea also can be observed in the production of distortion products and by two-tone suppression.

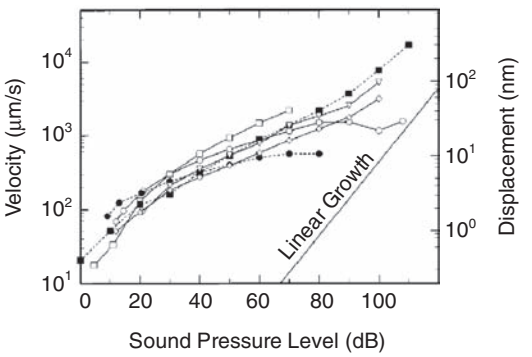

Figure 4.32 Magnitude of the basilar membrane response at the characteristic frequency (tuning curve peak) as a function of stimulus level from six chinchillas with essentially healthy cochleas. The compressive nature of the basilar membrane response is seen by comparing these curved lines with the straight line representing linear growth. (Filled circles indicate the function for the animal whose tuning curves are shown in Fig. 4.31.) *Source*: Adapted from Ruggero et al. (1997), by permission of *J. Acoust. Soc. Am.*

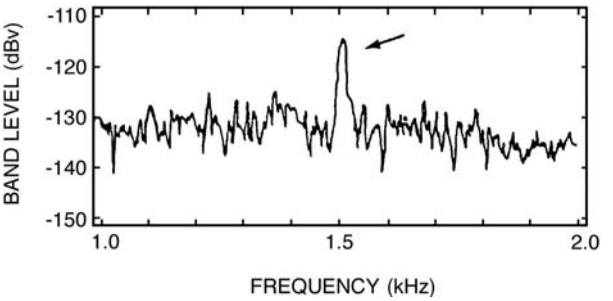

Figure 4.33 Example of a spontaneous otoacoustic emission at approximately 1500 Hz (*arrow*) detected above the noise floor in an occluded ear canal. Its level corresponds to about 11 dB SPL. *Source*: From Zurek, 1985, with permission of *J. Acoust. Soc. Am.*

Distortion products occur when the output of a system includes components that were not present at the input. For example, if two tones with frequencies f_1 and f_2 are presented to the ear (input), the basilar membrane's vibratory response (output) might include the *primaries* f_1 and f_2 plus *distortion products* such as f_2-f_1 and $2f_1$-f_2 (e.g., Nuttall et al., 1990; Nuttall and Dolan, 1993; Robles et al., 1991, 1997; Rhode and Cooper, 1993; Cooper and Rhode, 1997; Robles and Ruggero, 2001). The first example, $\mathbf{f_2}$-$\mathbf{f_1}$, is sometimes called the **quadratic difference tone** and is produced when f_1 and f_2 are presented at high levels. On the other hand, the **cubic difference tone $2\mathbf{f_1}$-$\mathbf{f_2}$** occurs when f_1 and f_2 are presented at low levels and is rather sensitive to the proximity of the primary tones. We will return to f_2-f_1 and $2f_1$-f_2 in the context of otoacoustic emissions below, and will discuss their perception in Chapter 12.

Two-tone suppression in the cochlea occurs when the response of the basilar membrane produced by one tone (at the characteristic frequency) is weakened by the presence of a second (suppressor) tone at a different frequency, and is the most likely origin of two-tone suppression in the auditory nerve, discussed in Chapter 6 (see, e.g., Ruggero et al., 1992; Cooper, 1996; Geisler, 1998; Robles and Ruggero, 2001). The effect is greatest when the characteristic frequency and suppressor tones are very close in frequency and decreases as their frequencies become further apart.

OTOACOUSTIC EMISSIONS

Kemp (1978, 1979) demonstrated that the cochlea can *produce* sounds as well as receive them. He found that when a click is directed into the ear, it is followed by an echo that is emitted back from the cochlea. This *cochlear echo* can be detected roughly 5 ms or more after the click, typically peaking at latencies in the vicinity of approximately 5 to 15 ms. This phenomenon was originally referred to as the *Kemp echo* and has come to be know as the **evoked or stimulated otoacoustic emission**. **Spontaneous otoacoustic emissions** occur as well (Kemp, 1979; Zurek, 1981; Strickland et al., 1985). These signals generated in the cochlea are measurable with a probe microphone in the ear canal. Figure 4.33 shows an example of a spontaneous otoacoustic emission at about 1500 Hz. However, we will concentrate upon evoked otoacoustic emissions here. The interested student will find a growing number of informative reviews and discussions about the nature, parameters, and applications of otoacoustic emissions in the literature (e.g., McFadden and Wightman, 1983; Zurek, 1985; Lonsbury-Martin et al., 1991; Probst et al., 1991; Dekker, 1992; Berlin, 1998; Robinette and Glattke, 2002).

It is worthwhile to review how the stimulated or evoked otoacoustic emission is obtained. Suppose a probe device like the one represented in Fig. 4.34a is inserted into someone's ear. This probe contains both a sound source (an earphone) and a microphone, and it occludes the ear when inserted. A click is presented to the ear and the sound pressure in the occluded ear is measured over time.

Before putting the probe into a human ear, let's first see what happens when it is inserted into a *Zwislocki coupler*, which is a metal cavity that has the same impedance characteristics as the human ear. In this case, there would be a damped oscillation like the one shown in the *upper* tracing of Fig. 4.34b. Now let's put the coupler into a human ear. In this case, the resulting waveform will resemble the *middle* tracing in Fig. 4.34b. Here we see an initial damped oscillation lasting about 6 ms and also a much smaller oscillation occurring after a latency of roughly 6 to 7 ms. The *initial* oscillations are the *impulse response* of the ear and are similar to what we just saw in the metal coupler. The *later* and smaller oscillations constitute the *cochlear echo*, or the evoked otoacoustic emission. The lower tracing in Fig. 4.34b shows just the evoked otoacoustic emission after the response has been amplified and displaced by 5 ms to remove the initial part of the response.

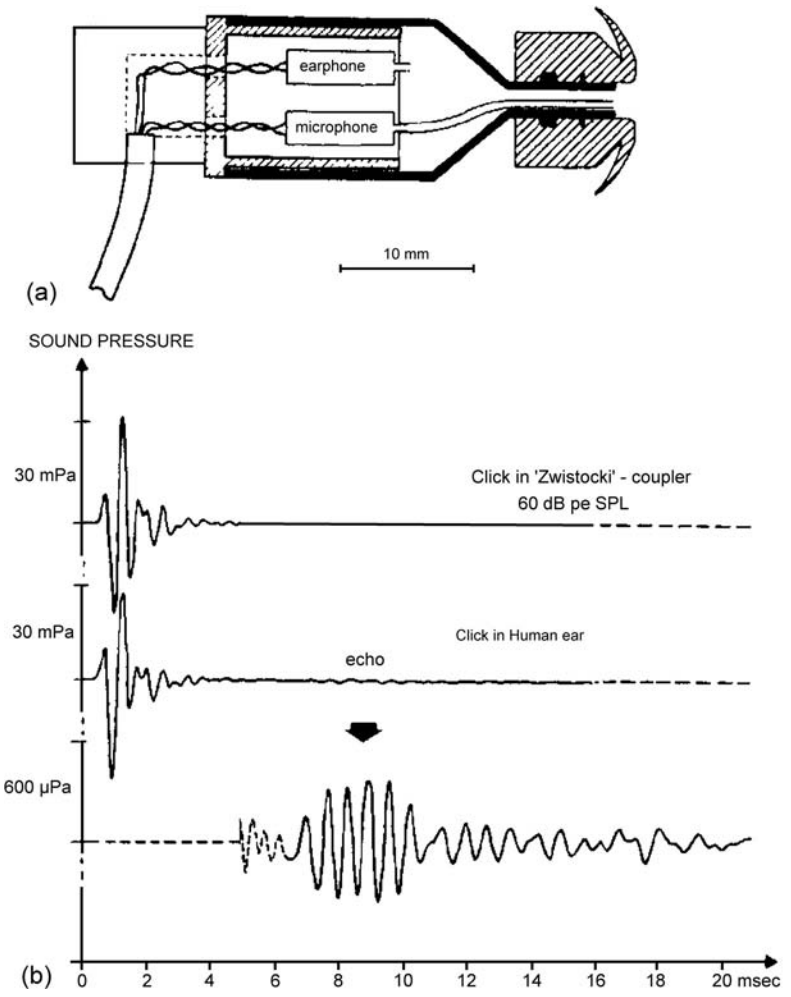

Figure 4.34 (a) The probe for eliciting and measuring otoacoustic emissions is inserted into the ear canal. The sound source is provided by the earphone and the microphone measures the sound pressure in the ear canal, which is occluded by the ear tip. (b) Responses to a click stimulus: *Upper tracing*: Damped oscillation in a metal cavity (Zwislocki coupler). *Middle tracing*: Responses in a human ear consisting of initial damped oscillations followed by the evoked otoacoustic emission (echo). *Lower tracing*: Amplified echo response displaced by 5 ms. *Source*: From Johnsen and Elberling (1982), with permission of *Scandinavian Audiology*.

Many studies of evoked otoacoustic emissions were undertaken within a short period after its original description and it continues to be the topic of extensive investigation (see, e.g., reviews by Wit and Ritsma, 1979, 1980; McFadden and Wightman, 1983; Zurek, 1985; Lonsbury-Martin et al., 1991; Probst et al., 1991; Dekker, 1992; Robinette and Glattke, 2002). A number of generalities have been derived from these and other studies. To begin with, virtually all normal hearing humans appear to have a stimulated acoustic emission in response to clicks and/or tone bursts. A given ear's emission is extraordinarily reproducible; however, the details of evoked emissions differ widely from ear to ear, just as we have seen with respect to the sharpness and nonlinearity of the cochlea's mechanical tuning. The evoked acoustic emission is also vulnerable to such insults as ototoxicity and noise exposure and is obliterated by any substantive degree of sensorineural hearing loss.

The latency and magnitude of the echo depend on the level of the stimulus. Latency tends to decrease as the stimulus levels become greater. Although the magnitude of the evoked emission gets larger with increasing stimulus level, this relationship is linear only for low stimulus levels, above which the input-output curve becomes compressed, and saturates by the time the emission reaches about 20 dB SPL.

The latency of the emission decreases with increasing frequency. This association is important because it is consistent with the idea that the location within the cochlea from which the echo originates moves closer to the base with increasing frequency, as one would expect. An apparent problem with this

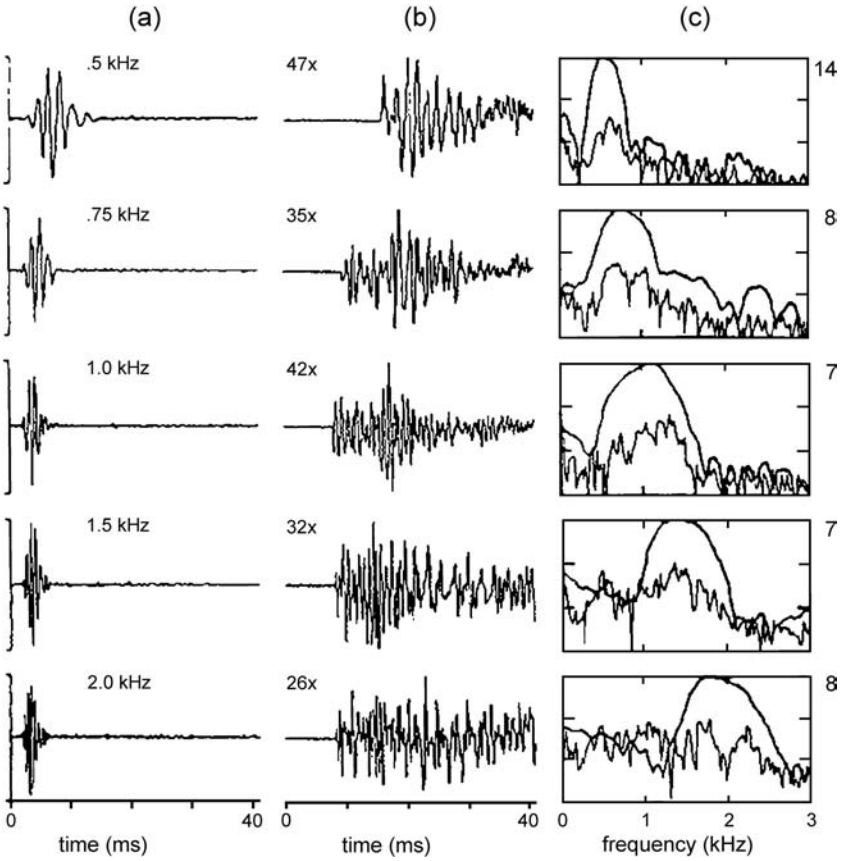

Figure 4.35 Effect of frequency from 500 to 2000 Hz on the evoked otoacoustic emission for one subject. Columns (a) and (b) show evoked otoacoustic emission waveforms before and after processing. Column (c) compares the spectra of the stimuli (*smoother curves*) to those of the otoacoustic emissions. *Source*: From Norton and Neeley (1987), by permission of *J. Acoust. Soc. Am.*

point has been the observation that the actual latencies of the echo seem to be two or three times longer than the estimated time it would take for the signal to reach and then return from a given place along the cochlear duct. However, it has been pointed out that otoacoustic emission latencies fall within the expected round-trip travel time when the latter is based upon data obtained at low stimulus levels, similar to those employed in acoustic emissions work (e.g., Neeley et al., 1986; Norton and Neeley, 1987).

The spectral characteristics of click-evoked otoacoustic emissions do not exactly match those of the click used to elicit them. Instead, they tend to show energy concentrations in fairly narrow frequency ranges. Norton and Neeley (1987) using tone-bursts showed that the frequency concentrations in the spectra of otoacoustic emissions follow those of the stimuli, as exemplified in Fig. 4.35. The third column of the figure compares the spectra of the otoacoustic emissions to those of the stimuli (represented by the smooth lines). Notice that there is an orderly change in the spectra of the otoacoustic emissions with the changes in the stimulus spectra.

Distortion product otoacoustic emissions (DPOAEs) occur at frequencies corresponding to the **f_2-f_1 difference tone** and the **$2f_1$-f_2 cubic difference tone**. Here f_1 and f_2 are the frequencies of the lower and higher **primary tones**, respectively. The level of f_1 is L_1, and L_2 is the level of f_2. The cubic difference tone otoacoustic emission is the most interesting and widely studied of the DPOAEs. Its level tends to be about 60 dB weaker than the levels of the primary tones. Several examples of DPOAEs are provided in Fig. 4.36 from an experiment by Bums et al. (1984). In the *lower* tracing, we see *spontaneous* otoacoustic emissions (SOAEs) at 1723 and 2049 Hz. These behave as primary tones to produce a cubic difference tone ($2f_1$-f_2) SOAE of 1397 Hz. In the *upper* tracing of the figure, we see that the introduction of an external tone masks (see Chap. 10) the higher primary. As a result, this leaves only the lower primary SOAE, and the cubic difference tone, which previously resulted from the interaction of f_1 and f_2, is now obliterated. These findings provide further evidence of active processes in the cochlea.

It is generally accepted that DPOAEs are best observed when (1) the primaries are in the 1000- to 4000-Hz region with an f_2/f_1

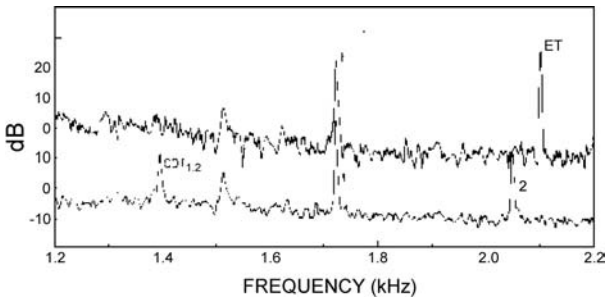

Figure 4.36 *Lower tracing*: Primary (1, 2) spontaneous otoacoustic emissions (SOAEs) at 1723 and 2049 Hz yield a cubic difference tone SOAE at 1397 Hz (CDT1,2). *Upper tracing*: Adding an external tone (ET) masks tone 2, leaving only tone 1, thus obliterating the distortion product. *Source*: From *Hearing Research 24*, Burns, Strickland, Tubis, and Jones (Interactions among spontaneous otoacoustic emissions. I. Distortion products and linked emissions, 271–278, ©1984), with kind permission of from Elsevier Science Publishers—NL, Sara Burgerhartstraat 25, 1055 KV Amsterdam, The Netherlands.

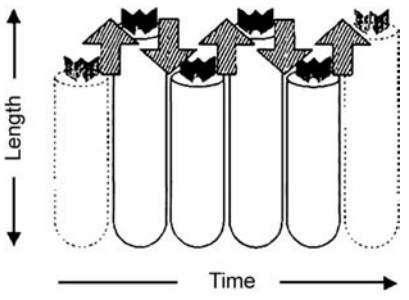

Figure 4.37 The electromotile response of an outer hair cell (changing length over time) acts as a positive-feedback mechanism, providing the force for active cochlear processes. The magnitude of the length, which is actually on the order of about 1% to 4%, is highly exaggerated in the drawing for illustrative purposes.

frequency ratio approximating 1.2, and (2) the $\mathbf{L_1}$ is the same as $\mathbf{L_2}$ for low stimulus levels, and $\mathbf{L_1}$ is 10 to 15 dB greater than $\mathbf{L_2}$ for high stimulus levels. However, more complicated relationships among the frequencies and levels of the primaries have been shown to optimize DPOAE levels (e.g., Johnson, Neely, Garner, and Gorga, 2006).[3]

When continuous tones are presented to the ear, the acoustic emission has the same frequency as the stimulus but is delayed by its latency. The stimulus and emission will interact, resulting in peaks and valleys at frequencies where they are in and out of phase. This effect is seen at low levels of the stimulus, becoming less apparent and finally disappearing when the stimulus level exceeds 40 to 50 dB SPL. This level dependency is expected because of the emission's very low amplitude. That is, interference between the stimulus and emission can only occur when their levels are relatively similar; the low level of the emission means that this condition can only be met at lower levels of the stimulus.

These phenomena are consistent with the concept that the evoked acoustic emissions monitored in the ear canal are cochlear in origin. It is apparent that active processes enable the cochlea to produce as well as receive acoustical signals.

ACTIVE PROCESSES AND THE COCHLEAR AMPLIFIER

We have seen that the outer hair cells have an significant impact upon the sharpness and nonlinearity of cochlear processes. This influence involves **active processes** that contribute to the cochlear response above and beyond the passive vibratory response of the basilar membrane (the traveling wave) and transmission of the transduced signals to the nervous system. This **cochlear amplifier** enhances the vibratory stimulus delivered to the inner hair cells, results in the cochlea's sharply tuned and nonlinear response, and generates otoacoustic emissions. The active mechanism relies on **outer hair cell electromotility**, which is the unique ability of the OHCs to rapidly contract and expand (by up to about 4%) in response to the sound stimulus, and thereby to affect cochlear micromechanics (e.g., Brownell et al., 1985; Brownell, 1990; Kalinec and Kachar, 1995; Holley, 1996; Patuzzi, 1996; Brownell and Popel, 1998; Geisler, 1998; Santos-Sacchi, 2003).

The prevalent explanation of OHC electromotility may be summarized as follows: Recall from Chapter 2 that there is positive hydrostatic pressure (turgor) within the OHC due to its cytoplasm, while its test tube–like shape is maintained by the tension of the matrix of structures in its lateral "walls" (see Figs. 2.29 and 2.30). The arrangement of these forces is such that changing the cell's surface area will change its length and girth. The surface area of the OHC is altered by conformational changes of components in the cell membrane, which, in turn, is controlled by the cell's polarization. Depolarization causes the OHCs to contract and hyperpolarization causes them to expand. As we have already seen, sound stimulation eventuates the bending of the OHC stereocilia, varying the ion currents through the opening and closing transduction channels, and thus varying the receptor potential. The changing polarization activates the cycle-by-cycle electromotile responses of the OHCs, which is able to occur fast enough to operate at all audible frequencies. Recalling that the OHCs are "mounted" between the Deiter's cells below and the reticular lamina above, this pushing-and-pulling motile response (Fig. 4.37) operates like a positive-feedback mechanism, which provides the forces that drive the cochlear amplifier.

Outer hair cell electromotility, which drives the cochlear amplifier, appears to be generated by the interaction of two

[3] Specifically, Johnson et al. (2006) found that, on average, normal DPOAEs were largest when

(a) $f_2/f_1 = 1.22 + \log_2(9.6/f_2) \cdot (L_2/415)^2$, and
(b) $L_1 = 80 + 0.137 \cdot \log_2(18/f_2) \cdot (L_2 - 80)$.

mechanisms or "motors" (Dallos, Zheng, and Cheatham, 2006; Kennedy, Evans, Crawford, and Fettiplace, 2006; Fettiplace and Hackney, 2006). The **somatic motor** relies on **prestin**, which has been identified as the *motor protein* of the OHC (Zheng et al., 2000; Oliver et al., 2001; Santos-Sacchi et al., 2001; Dallos and Fakler, 2002; Liberman et al., 2002; Dallos et al., 2006). The prestin motor is believed to operate by shuttling chloride ions back and forth between the inner and outer parts of the cell membrane (Fig. 4.38). Shortening is triggered by depolarization, which causes the prestin molecule to transport the chloride ion toward its inner side (Fig. 4.38a), and lengthening is triggered by hyperpolarization, which causes the prestin molecule to move the chloride ion toward its outer side (Fig. 4.38b). The **hair bundle motor** relies on the force generated by the changing compliance of the stereocilia bundle that occurs with the opening and closing of the transduction pores (Fettiplace, 2006; Fettiplace and Hackney, 2006; Kennedy et al., 2006).

In addition to the fast electromotile response just discussed, slower motile responses are also produced when OHCs are exposed to chemical agents and efferent neurotransmitter acetylcholine and electrical stimulation (e.g., Brownell et al., 1985; Zenner et al., 1985; Flock et al., 1986; Kachar et al., 1986; Ashmore, 1987; Ulfendahl, 1987; Slepecky et al., 1988a, 1988b; Zajic and Schacht, 1991; Holley, 1996). Figure 4.39 shows an example for a guinea pig OHC, which was removed from the cochlea and exposed to potassium gluconate (Slepecky et al., 1988b).

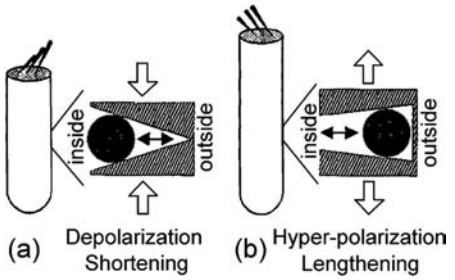

Figure 4.38 Artist's conceptualization of the somatic (prestin) motor of OHC electromotility. (a) Depolarization causes the prestin molecule to transport the chloride ion toward the inner side (shortening). (b) Hyperpolarization causes the prestin molecule to transport the chloride ion toward the outer side (lengthening).

The central nervous system influences the active processes of the cochlea via the efferent innervation of the OHCs from the medial efferent (olivocochlear) system (e.g., Guinan, 1996, 2006; Robles and Ruggero, 2001; see Chaps. 2 and 6). For example, activation of the medial efferent system has been found to reduce the magnitude and nonlinearity of basilar membrane vibrations in the vicinity of the characteristic frequency (e.g., Murugasu and Russell, 1996; Dolan et al., 1997; Russell and Murugasu, 1997; see Chap. 6).

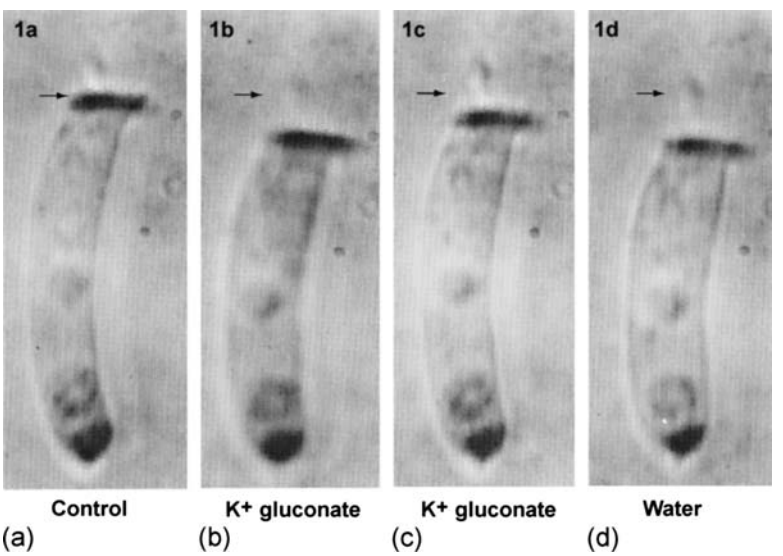

Figure 4.39 Effects of potassium gluconate on an isolated outer hair cell. (a) Original length of the hair cell. (b) The cell is shortened when exposed to potassium gluconate for 1 minute. (c) Cell returned to its original length after 4 minutes of contact. (d) The cell became swollen and shorter when the chemical medium was diluted with water (indicating that the cell membrane stayed intact during the experiment because it retained its normal osmotic characteristics). Arrows shown original length of the cell for comparison. *Source*: From *Hearing Research 24*, Slepecky, Ulfendahl, and Flock (Shortening and elongation of isolated outer hair cells in response to application of potassium glucomate, acetylcholine, and cationed ferritin, 119–126, ©1988), with kind permission of from Elsevier Science Publishers—NL, Sara Burgerhartstraat 25, 1055 KV Amsterdam, The Netherlands. Photograph courtesy of Dr. Norma Slepecky.

REFERENCES

Adrian, ED. 1931. The microphonic action of the cochlea: An interpretation of Wever and Bray's experiments. *J Physiol* 71, 28–29.

Ashmore, JE. 1987. A fast motile response in guinea-pig outer hair cells: The cellular basis of the cochlear amplifier. *J Physiol* 388, 323–347.

Bekesy, G. 1928. Zur Theorie des Hörens: Die Schwingungsform der Basilarmembran. *Physik Zeitschrchr* 29, 793–810.

Bekesy, G. 1944. Über die mechanische Frequenzanalyse in der Schnecke verschiedener Tiere. *Akust Zeitschr* 9, 3–11.

Bekesy, G. 1947. The variations of phase along the basilar membrane with sinusoidal vibrations. *J Acoust Soc Am* 19, 452–460.

Bekesy, G. 1948. On the elasticity of the cochlear partition. *J Acoust Soc Am* 20, 227–241. [Original in German: *Akust Zeitschr* 6: 265–278, 1941.]

Bekesy, G. 1949. On the resonance curve and the decay period at various points on the cochlear partition. *J Acoust Soc Am* 21, 245–254. [Original in German: *Akust Zeitschr*, 8: 66–76, 1943.]

Bekesy, G. 1950. D-C potentials and energy balance of the cochlear partition. *J Acoust Soc Am* 22, 576–582.

Bekesy, G. 1952. D-C resting potentials inside the cochlear partition. *J Acoust Soc Am* 24, 72–76.

Bekesy, G. 1953. Description of some mechanical properties of the organ of Corti. *J Acoust Soc Am* 25, 770–785.

Bekesy, G. 1960/1989. *Experiments in Hearing*. New York, NY: McGraw-Hill. [Republished by the Acoustical Society of America].

Berlin, CI (ed). 1998. *Otoacoustic Emissions: Basic Science and Clinical Applications*. San Diego, CA: Singular.

Brownell, WE. 1990. Outer hair cell electromotility and otoacoustic emissions. *Ear Hear* 11, 82–92.

Brownell, WE, Bader, CR, Bertrand, D, deRibaupierre, Y. 1985. Evoked mechanical response of isolated cochlear outer hair cells. *Science* 227, 194–196.

Brownell, WE, Popel, AS. 1998. Electrical and mechanical anatomy of the outer hair cell. In: AR Palmer, A Rees, AQ Summerfield, R Meddis (eds.), *Psychophysical and Physiological Advances in Hearing*. London, UK: Whurr, 89–96.

Burns, EM, Strickland, EA, Tubis, A, Jones, K. 1984. Interactions among spontaneous otoacoustic emissions. I. Distortion products and linked emissions. *Hear Res* 16, 271–278.

Cheatham, MA, Dallos, P. 1984. Summating potential (SP) tuning curves. *Hear Res* 16, 189–200.

Cooper, NP. 1996. Two-tone suppression in cochlear mechanics. *J Acoust Soc Am* 99, 3087—3098.

Cooper, NP, Rhode, WS. 1997. Mechanical responses to two-tone distortion products in the apical and basal turns of the mammalian cochlea. *J Neurophysiol* 78, 261–270.

Corey, DP. 2006. What is the hair cell transduction channel? *J Physiol* 576, 23–28.

Crawford, AC, Fettiplace, R. 1981. An electrical tuning mechanism in turtle cochlear hair cells. *J Laryngol* 312, 377–422.

Dallos, P. 1973. *The Auditory Periphery*. New York, NY: Academic Press.

Dallos, P. 1984. Some electrical circuit properties of the organ of Corti. II. Analysis including reactive elements. *Hear Res* 14, 281–291.

Dallos, P. 1985. Response characteristics of mammalian cochlear hair cells. *J Neurosci* 5, 1591–1608.

Dallos, P. 1986. Neurobiology of cochlear inner and outer hair cells: Intracellular recordings. *Hear Res* 22, 185–198.

Dallos, P, Billone, MC, Durrant, JD, Wang, C-Y, Raynor, S. 1972a. Cochlear inner and outer hair cells: Functional differences. *Science* 177, 356–358.

Dallos, P, Cheatham, MA. 1976. Production of cochlear potentials by inner and outer hair cells. *J Acoust Soc Am* 60, 510–512.

Dallos, P, Cheathan, MS, Ferraro, J. 1974. Cochlear mechanics, nonlinearities, and cochlear potentials. *J Acoust Soc Am* 55, 597–605.

Dallos, P, Fakler, B. 2002. Prestin, a new type of motor protein. *Nat Rev Mol Cell Biol* 3, 104–111.

Dallos, P, Harris, D. 1978. Properties of auditory-nerve responses in the absence of outer hair cells. *J Neurophys* 41, 365–383.

Dallos, P, Popper, AN, Fay, RR. (eds.), 1996. *The Cochlea*. New York, NY: Springer-Verlag.

Dallos, PJ, Santos-Sacchi, J, Flock, A. 1982. Intracellular recordings from cochlear outer hair cells. *Science* 218, 582–584.

Dallos, P, Shoeny, ZG, Cheatham, MA. 1970. Cochlear summating potentials: Composition. *Science* 170, 641–644.

Dallos, P, Shoeny, ZG, Cheatham, MA. 1972b. Cochlear summating potentials: Descriptive aspects. *Acta Otol Suppl* 302, 1–46.

Dallos, D, Zheng, J, Cheatham, MA. 2006. Prestin and the cochlear implifier. *J Physiol* 576(1), 37–42.

Davis, H. 1957. Biophysics and physiology of the inner ear. *Physiol Rev* 37, 1–49.

Davis, H. 1958. A mechano-electrical theory of cochlear action. *Ann Otol* 67, 789–801.

Davis, H. 1961. Some principles of sensory receptor action. *Physiol Rev* 4, 391–416.

Davis, H. 1965. A model for transducer action in the cochlea. *Cold Spring Harb Symp Quant Biol* 30, 181–190.

Davis, H, Deatherage, BH, Eldredge, DH, Smith, CA. 1958. Summating potentials of the cochlea. *Am J Physiol* 195, 251–261.

Davis, H, Deatherage, B, Rosenblut, B, Fernandez, C, Kimura, R, Smith, CA. 1958. Modificatiaon of cochlear potentials by streptomycin poisoning and by extensive venous obstruction. *Laryngoscope* 68, 596–627.

Davis, H, Derbyshire, A, Lurie, M, Saul, L. 1934. The electric response of the cochlea. *Ann Otol* 68, 665–674.

Davis, H, Eldridge, DH. 1959. An interpretation of the mechanical detector action of the cochlea. *Ann Otol Rhinol Laryngol* 68, 665–674.

Davis, H, Fernandez, C, McAuliffe, DR. 1950. The excitatory process in the cochlea. *Proc Natl Acad Sci U S A* 36, 580–587.

Dekker, TN, (ed). 1992. Otoacoustic emissions. *Sem Hear* 13(1), 1–104.

Dolan, DF, Guo, MH, Nuttall, AL. 1997. Frequency-dependent enhancement of basilar membrane velocity during olivocochlear bundle stimulation. *J Acoust Soc Am* 102, 3587–3596.

Duifhuis, H. 1976. Cochlear nonlinearity and second filter: Possible mechanisms and implications. *J Acoust Soc Am* 59, 408–423.

Eggermont, JJ, Odenthal, DW, Schmidt, PN, Spoor, A. 1974. Electrocochleography: Basic principles and clinical application. *Acta Otol Suppl* 316, 1–84.

Evans, EF. 1972a. The frequency response and other properties of single nerve fibers in the guinea pig cochlea. *J Physiol* 226, 263–287.

Evans, EF. 1972b. *Does frequency sharpening occur in the cochlea?* In: Symposium on Hearing Theory. Eindhoven, The Netherlands: Institute for Perception Research.

Evans, EF. 1974. The effects of hypoxia on tuning of single fibers in the cochlear nerve. *J Physiol* 238, 65–67.

Evans, EF. 1975. The sharpening of cochlear frequency selectivity in the normal and abnormal cochlea. *Audiology* 14, 419–442.

Evans, EF, Wilson, JP. 1971. *Frequency resolving power of the cochlea: The effective bandwidth of cochlear nerve fibers*. In: Proceedings of the 7th International Congress on Acoustics, Vol. 3. Budapest, Hungary: Akademiai Kiado, 453–456.

Evans, EF, Wilson, JP. 1973. Frequency selectivity of the cochlea. In: AR Møller (ed.), *Basic Mechanisms in Hearing*. New York, NY: Academic Press, 519–554.

Eybalin, M. 1993. Neurotransmitters and neuromodulators of the mammalian cochlea. *Physiol Rev* 73, 309–373.

Fettiplace, R. 2006. Active hair bundle movements in auditory hair cells. *J Physiol* 576 (1), 29–36.

Fettiplace, R, Hackney, CM. 2006. The sensory and motor roles of auditory hair cells. *Nat Rev Neurosci* 7(1), 19–29.

Flock, A. 1971. Sensory transduction in hair cells. In: WR Lowenstein (ed.), *Principles of Receptor Physiology*, Vol. I. New York, NY: Springer-Verlag, 396–441.

Flock, A, Flock, B, Ulfendahl, M. 1986. Mechanisms of movement in outer hair cells and a possible structural basis. *Arch Otorhinolaryugol* 243, 83–90.

Geisler, CD. 1998. *From Sound to Synapse: Physiology of the Mammalian Ear*. New York, NY: Oxford University Press.

Geisler, CD, Rhode, WS, Kenedy, DT. 1974. Responses to tonal stimuli of single auditory nerve fibers and their relationship to basilar membrane motion in the squirrel monkey. *J Neurophysiol* 37, 1156–1172.

Gelfand, SA. 1981. *Hearing: An Introduction to Phychological and Physiological Acoustics*. New York, NY: Marcel Dekker.

Grundfest, H. 1971. The general electrophysiology of input membrane in electrogenic excitable cells. In: WR Lowenstein (ed.), *Handbook of Sensory Physiology. Vol. 1: Principles of Receptor Physiology*. New York, NY: Springer-Verlag, 136–165.

Guinan, JJ Jr. 1996. Physiology of olivocochlear efferents. In: P Dallos, AN Popper, RR Fay (eds.), *The Cochlea*. New York, NY: Springer-Verlag, 435–502.

Guinan, JJ Jr. 2006. Olivocochlear efferents: Anatomy, physiology, function, and the measurement of efferent effects in humans. *Ear Hear* 27, 589–607.

Helmholtz, H. von. 1870. *Die Lehre von den Tonempfindungen als physiologische Grundlage für die Theorie der Musik. Dritte umgearbeitete Ausgabe.* Braunschweig: Vieweg.

Holley, MC. 1996. Cochlear mechanics and micromechanics. In: P Dallos, AN Popper, RR Fay (eds.), *The Cochlea*. New York, NY: Springer-Verlag, 386–434.

Honrubia, V, Ward, PH. 1968. Longitudinal distribution of the cochlear microphonics inside the cochlear duct (guinea pig). *J Acoust Soc Am* 44, 951–958.

Honrubia, V, Ward, PH. 1969a. Dependence of the cochlear microphonic and summating potential on the endocochlear potential. *J Acoust Soc Am* 46, 388–392.

Honrubia, V, Ward, PH. 1969b. Properties of the summating potential of the guinea pig's cochlea. *J Acoust Soc Am* 45, 1443–1449.

Hudspeth, AJ. 1982. Extracellular current flow and the site of transduction by vertibrate hair cells. *J Neurosci* 2, 1–10.

Hudspeth, AJ. 1985. The cellular basis of hearing: The biophysics of hair cells. *Science* 230, 745–752.

Hudspeth, AJ, Corey, DP. 1977. Sensitivity, polarity, and conductance change in the response of vertibrate hair cells to controlled mechanical stimulation. *Proc Natl Acad Sci U S A* 74, 2407–2411.

Hudspeth, AJ, Jacobs, R 1979. Stereocilia mediate transduction in vertibrate cells. *Proc Natl Acad Sci U S A* 76, 1506–1509.

Johnsen, NJ, Elberling, C. 1982b. Evoked acoustic emissions from the human ear I. Equipment and response parameters. *Scand Audiol* 11, 3–12.

Johnson, TA, Neely, ST, Garner, CA, Gorga, MP. 2006. Influence of primary-level and primary-frequency ratios on human distortion product otoacoustic emissions. *J Acoust Soc Am* 119, 418–428.

Johnstone, BM, Boyle, JE. 1967. Basilar membrane vibration examined with the Mossbauer technique. *Science* 15S, 389–390.

Johnstone, BM, Taylor, KJ, Boyle, AJ. 1970. Mechanics of the guinea pig cochlea. *J Acoust Soc Am* 47, 504–509.

Johnstone, BM, Yates, GK 1974. Basilar membrane tuning curves in the guinea pig. *J Acoust Soc Am* 55, 584–587.

Kachar, B, Brownell, WE, Altschuler, R, Fex, J. 1986. Electrokinetic shape changes of cochlear outer hair cells. *Nature* 322, 365–368.

Kalinec, F, Kachar, B. 1995. Structure of the electromechanical transduction mechanism in mammalian outer hair cells. In: A Flock, D Ottoson, M Ulfendahl (eds.), *Active Hearing*. Kidlington, UK: Pergamon, 181–193.

Kazmierczak, P, Sakaguchi, H, Tokita, J, Wilson-Kubalek, EM, Ronald, A, Milligan, RA, Muller, U, Bechara Kachar, B. 2007. Cadherin 23 and protocadherin 15 interact to form tip-link filaments in sensory hair cells. *Nature* 449(7158), 87–92.

Kelly, JP, Khanna, SM. 1984a. Ultrastructural damage in cochleae used for studies of basilar membrane mechanics. *Hear Res* 14, 59–78.

Kelly, JP, Khanna, SM. 1984b. The distribution of darnage in the cochlea after removal of the round window membrane. *Hear Res* 16, 109–126.

Kemp, DT. 1978. Stimulated acoustic emissions from within the human auditory system. *J Acoust Soc Am* 64, 1386–1391.

Kemp, DT. 1979. Evidence of mechanical nonlinearity and frequency selective wave amplification in the cochlea. *Arch Otol Rhinol Laryngol* 224, 37–45.

Kennedy, HJ, Evans, MG, Crawford, AC, Fettiplace, R. 2006. Depolarization of cochlear outer hair cells evoked active hair bundle motion by two mechanisms. *J Neurosci* 26, 2757–2766.

Khanna, SM. 1986. Homodyne interferometer for basilar membrane measurements. *Hear Res* 23, 9–26.

Khanna, SM, Johnson, GW, Jacobs, J. 1986. Homodyne interferometer for basilar membrane vibration measurements. II. Hardware and techniques. *Hear Res* 23, 27–36.

Khanna, SM, Leonard, DGB. 1982. Basilar membrane tuning in the cat cochlea. *Science* 215, 305–306.

Khanna, SM, Leonard, DGB. 1986a. Measurement of basilar membrane vibrations and evaluation of the cochlear condition. *Hear Res* 23, 37–53.

Khanna, SM, Leonard, DGB. 1986b. Relationship between basilar membrane tuning and hair cell condition. *Hear Res* 23, 55–70.

Khanna, SM, Sears, RE, Tonndorf, J. 1968. Some properties of longitudinal shear waves: A study by computer simulation. *J Acoust Soc Am* 43, 1077–1084.

Kiang, NYS. 1965. *Discharge Patterns of Single Nerve Fibers in the Cat's Auditory Nerve*. Cambridge, MA: MIT Press.

Kiang, NYS, Liberman, NC, Sewell, WF, Guinan, JJ. 1986. Single unit clues to cochlear mechanisms. *Hear Res* 22, 171–182.

Kim, DO. 1986. Active and nonlinear cochlear biomechanics and the role of outer-hair-cell subsystem in the mammalian auditory system. *Hear Res* 22, 105–114.

Klink, R. 1986. Neurotransmission in the inner ear. *Hear Res* 22, 235–243.

Kohllofel, LUE. 1972. A study of basilar membrane vibrations. *Acustica* 27, 49–89.

Konishi, T, Butler, RA, Fernandez, C. 1961. Effect of anoxia on cochlear potentials. *J Acoust Soc Am* 33, 349–356.

Kros, CJ. 1996. Physiology of mammalian cochlear hair cells. In: P Dallos, AN Popper, RR Fay (eds.), *The Cochlea*. New York, NY: Springer-Verlag, 318–385.

Leonard, DGB, Khanna, SM. 1984. Histological evaluation of damage m cat cochleae used for measurement of basilar membrane mechanics. *J Acoust Soc Am* 75, 515–527.

LePage, EL, Johnstone, BM. 1980. Nonlinear mechanical behavior of the basilar membrane in the basal turn of the guinea pig cochlea. *Hear Res* 2, 183–192.

Liberman, MC. 1982. The cochlear frequency map for the cat: Labeling auditory-nerve fibers of known characteristic frequency. *J Acoust Soc Am* 72, 1441–1449.

Liberman, MC. 1984. Single-neuron labeling and chronic cochlear pathology. I. Threshold shift and characteristic-frequency shift. *Hear Res* 16, 33–41.

Liberman, MC, Dodds, LW. 1984. Single-neuron labeling and chronic cochlear pathology. II. Stereocilia damage and alterations of spontaneous discharge rates. *Hear Res* 16, 43–53.

Liberman, MC, Gao, J, He, DZZ, Wu, X, Jia, S, Zuo, J. 2002. Prestin is required for electromotility of the outer hair cell and for the cochlear amplifier. *Nature* 419, 300–304.

Liberman, MC, Kiang, NYS. 1984. Single-neuron labeling and chronic cochlear pathology. IV. Stereocilia damage and alterations in rate- and phase-level functions. *Hear Res* 16, 75–90.

Lim, DJ. 1986. Cochlear micromechanics in understanding otoacoustic emission. *Scand Audiol* 25, 17–25.

Lonsbury-Martin, BL, Whitehead, ML, Martin, GK. 1991. Clinical applications of otoacoustic emissions. *J Speech Hear Res,* 34, 964–981.

Manley, GA. 1978. Cochlear frequency sharpening—A new synthesis. *Acta Otol* 85, 167–176.

Manoussaki, D, Dimitriadis, EK, Chadwick, RS. 2006. Cochlea's graded curvature effect on low frequency waves. *Phys Rev Lett* 96, 088701.

McFadden, D, Wightman, EL. 1983. Audition: Some relations between normal and pathological hearing. *Ann Rev Psychol* 34, 95–128.

Misrahy, GS, Hildreth, KM, Shinabarger, EW, Gannon, WJ. 1958. Electrical properties of the wall of endolymphatic space of the cochlea (guinea pig). *Am J Physiol* 194, 396–402.

Murugasu, E, Russell, IJ. 1996. The effect of basilar membrane displacement in the basal cochlea. *J Neurosci* 16, 325–332.

Naidu, RC, Mountain, DC. 1998. Measurements of the stiffness map challenge a basic tenet of cochlear theories. *Hear Res* 124, 124–31.

Neeley, ST, Norton, SJ, Gorga, MP, Jesteadt, W. 1986. Latency of otoacoustic emissions and ABR wave V using tone-burst stimuli. *J Acoust Soc* Am 79(suppl. 1), S5.

Norton, SJ, Neeley, ST. 1987. Tone-burst-evoked otoacoustic emissions from normal-hearing subjects. *J Acoust Soc Am* 81, 1860–1872.

Nuttall, AL, Brown, MC, Masta, RI, Lawrence, M. 1981. Inner hair-cell responses to velocity of basilar membrane motion in the guinea pig. *Brain Res* 211, 171–174.

Nuttall, AL, Dolan, DF. 1993. Intermodulation distortion (f2-f1) in inner hair cell and basilar membrane responses. *J Acoust Soc Am* 93, 2061–2068.

Nuttall, AL, Dolan, DF, Avinash, G. 1990. Measurements of basilar membrane tuning and distortion with laser velocimetry. In: P Dallos, JW Matthews, CD Geisler, MA Ruggero, CR Steele, (eds.), *The Mechanics and Biophysics of Hearing*. Berlin, Germany: Springer-Verlag, 288–295.

Oliver, D, He, DZZ, Klöcker, N, Ludwig, J, Schulte, U, Waldegger, S, Ruppersberg, JP, Dallos, P, Fakler, B. 2001. Intracellular anions as the voltage sensor of prestin, the outer hair cell motor protein. *Science* 292, 2340–2343.

Patuzzi, R. 1996. Cochlear mechanics and micromechanics. In: P Dallos, AN Popper, RR Fay (eds.), *The Cochlea*. New York, NY: Springer-Verlag, 186–257.

Peake, WT, Sohmer, HS, Weiss, TE. 1969. Microelectrode recordings of intracochlear potentials. *MlT Res Lab Electron Quart Prog Rep* 94, 293–304.

Pickles, JO. 1982. *An Introduction to the Physiology of Hearing*. London, U.K.: Academic Press.

Pickles, JO, Corey, DP. 1992. Microelectrical transduction by hair cells. *Trends Neurosci* 15(7), 254–259.

Pickles, JO, Comis, SD, Osborne, MP. 1984. Cross-links between stereocilia in the guinea pig organ of Corti, and their possible relation to sensory transduction. *Hear Res* 15, 103–112.

Probst, R, Lonsbury-Martin, BL, Martin, GK. 1991. A review of otoacoustic emissions. *J Acoust Soc Am* 89, 2027–2067.

Rhode, WS. 1971. Observations of the vibration of the basilar membrane in squirrel monkey using the Mossbauer technique. *J Acoust Soc Am* 49, 1218–1231.

Rhode, WS. 1978. Some observations on cochlear mechanics. *J Acoust Soc* Am 64, 158–176.

Rhode, WS, Cooper, NP. 1993. Two-tone suppression and distortion production on the basilar membrane in the hook region of cat and guinea pig cochleae. *Hear* Res 66, 31–45.

Rhode, WS, Robles, L. 1974. Evidence from Mossbauer experiments for nonlinear vibration in the cochlea. *J Acoust Soc Am* 55, 588–596.

Roberts, WM, Howard, J, Hudspeth, AJ. 1988. Hair cells: Transduction, tuning, and transmission in the inner ear. *Ann Rev Cell Biol* 4, 63–92.

Robinette, MS, Glattke, TJ, (eds.). 2002. *Otoacoustic Emissions: Clinical Applications*, 2nd ed. New York, NY: Thieme Medical Publishers.

Robles, L, Ruggero, MA. 2001. Mechanics of the mammalian cochlea. *Physiol Rev* 81, 1305–1352.

Robles, L, Ruggero, MA, Rich, NC. 1986. Basilar membrane mechanics at the base of the chinchilla cochlea: I. Input-output functions, tuning curves, and response phase. *J Acoust Soc Am* 80, 1363–1374.

Robles, L, Ruggero, MA, Rich, NC. 1991. Two-tone distortion in the basilar membrane of the cochlea. *Nature* 349, 413–414.

Robles, L, Ruggero, MA, Rich, NC. 1997. Two-tone distortion on the basilar membrane of the chinchilla cochlea. *J Neurophysiol* 77, 2385–2399.

Ruggero, MA, Rich, NC, Recio, A, Narayan, SS, Robles, L. 1997. Basilar membrane responses to tones at the base of the chinchilla cochlea. *J Acoust Soc Am* 101, 2151–2163.

Ruggero, MA, Robles, L, Rich, NC. 1992. Two-tone suppression in the basilar membrane of the cochlea: Mechanical basis of auditory nerve rate suppression. *J Neurophysiol* 68, 1087–1099.

Russell, IJ, Murugasu, E. 1997. Medial efferent inhibition suppresses basilar membrane responses to near characteristic frequency tones of moderate to high intensities. *J Acoust Soc Am* 102, 1734–1738.

Russell, IJ, Sellick, PM. 1977a. Tuning properties of cochlear hair cells. *Nature* 267, 858–860.

Russell, IJ, Sellick, PM. 1977b. The tuning properties of cochlear hair cells. In: EF Evans, JP Wilson (eds.), *Psychophysics and Physiology of Hearing*. London, UK: Academic Press, 71–87.

Russell, IJ, Sellick, PM. 1978a. Intracellular studies of hair cells in the mammalian cochlea. *J Physiol* 284, 261–290.

Russell, IJ, Sellick, PM. 1978b. Intracellular studies of cochlear hair cells: Filling the gap between basilar membrane mechanics and neural excitation. In: RF Naunton, C Fernandez (eds.), *Evoked Electrical Activity in the Auditory Nervous System*. London, UK: Academic Press, 113–139.

Russell, IJ, Sellick, PM. 1983. Low frequency characteristics of intracellularly recorded potentials in guinea pig cochlear hair cells. *J Physiol* 338, 179–206.

Rutherford, W. 1886. A new theory of hearing. *J Anat Physiol* 21, 166–168.

Santos-Sacchi, J. 2003. New tunes from Corti's organ: The outer hair cell boogie rules. *Cur Opin Neurobiol* 13, 1–10.

Santos-Sacchi, J, Shen, W, Zheng, J, Dallos, P. 2001. Effects of membrane potential and tension on prestin, the outer hair cell lateral membrane motor protein. *J Physiol* 531, 661–666.

Sellick, PM, Patuzzi, R, Johnstone, BM. 1982a. Measurement of basilar membrane motion in the guinea pig using the Mossbauer technique. *J Acoust Soc Am* 72, 131–141.

Sellick, PM, Patuzzi, R, Johnstone, BM. 1982b. Modulation of responses of spiral ganglion cells in the guinea pig by low frequency sound. *Hear Res* 7, 199–221.

Sellick, PM, Russell, IJ. 1980. The responses of inner hair cells to basilar membrane velocity during low frequency auditory stimulation in the guinea pig cochlea. *Hear Res* 2, 439–445.

Sewell, WF. 1996. Neurotransmitters and synaptic transmission. In: P Dallos, AN Popper, RR Fay (eds.), *The Cochlea*. New York, NY: Springer-Verlag, 503–533.

Slepecky, N, Ulfendahl, M, Flock, A. 1988a. Effects of caffeine and tetracaine on outer hair cell shortening suggest intracellular calcium involvement. *Hear* Res 32, 11–32.

Slepecky, N, Ulfendahl, M, Flock, A. 1988b. Shortening and elongation of isolated outer hair cells in response to

application of potassium gluconate, acetylcholine and cationized ferritin. *Hear Res* 34, 119–126.

Smith, DW, Moody, DB, Stebbins, WC, Norat, MA. 1987. Effects of outer hair cell loss on the frequency selectivity of the patas monkey auditory system. *Hear Res* 29, 125–138.

Steel, KR. 1983. The tectorial membrane of mammals. *Hear Res* 9, 327–359.

Strickland, EA, Burns, EM, Tubis, A. 1985. Incidence of spontaneous otoacoustic emissions in children and infants. *J Acoust Soc Am* 78, 931–935.

Tasaki, I, Davis, H, Eldredge, DH. 1954. Exploration of cochlear potentials in guinea pig with a microelectrode. *J Acoust Soc Am* 26, 765–773.

Tasaki, I, Davis, H, Legouix, JP. 1952. The space–time pattern of the cochlear microphonic (guinea pig) as recorded by differential electrodes. *J Acoust Soc Am* 24, 502–518.

Tasaki, I, Spiropoulos, CS. 1959. Stria vascularis as a source of endocochlear potential. *J Neurophysiol* 22, 149–155.

Tonndorf, J. 1960. Shearing motion in scale media of cochlear models. *J Acoust Soc Am* 32, 238–244.

Tonndorf, J. 1975. Davis-1961 revisited: Signal transmission in the cochlear hair cell-nerve junction. *Arch Otol* 101, 528–535.

Ulfendahl, M. 1987. Motility in auditory sensory cells. *Acta Physiol Scand* 13Q, 521–527.

Vollrath, MA, Kwan, KY, Corey, DP. 2007. The micromachinery of mechanotransduction in hair cells. *Ann Rev Neurosci* 30, 339–365.

von Helmholtz, H. 1870. *Die Lehre von den Tonempfindugen* als physiologische Grundlage fur die Theorie der Musik. Dritte umgearbeitete Ausgabe. Braunschweig, Germany: Vieweg.

Wangemann, P, Schacht, J. 1996. Homeostatic mechanisms in the cochlea. In: P Dallos, AN Popper, RR Fay (eds.), *The Cochlea*. New York, NY: Springer-Verlag, 130–185.

Wever, EG. 1949. *Theory of Hearing*. New York. NY: Dover.

Wever, EG. 1966. Electrical potentials of the cochlea. *Physiol Rev* 46, 102–126.

Wever, EG, Bray, CW. 1930. Action currents in the auditory nerve in response to acoustic stimulation. *Proc Natl Acad Sci U S A* 16, 344–350.

Wever, EG, Lawrence, M. 1950. The acoustic pathways to the cochlea. *J Acoust Soc Am* 22, 460–467.

Wever, EG, Lawrence, M. 1954. *Physiological Acoustics*. Princeton, NJ: Princeton University Press.

Wilson, JP, Johnstone, JR. 1972. *Capacitive probe measures of basilar membrane vibration*. In: Symposium on Hearing Theory. Eindhoven, The Netherlands: Institute for Perception Research, 172–181.

Wilson, JP, Johnstone, JR. 1975. Basilar membrane and middle ear vibration in guinea pig measured by capacitive probe. *J Acoust Soc Am* 57, 705–723.

Wit, HP, Ritsma, RJ. 1979. Stimulated acoustic emissions from the human ear. *J Acoust Soc Am* 66, 911–913.

Wit, HP, Ritsma, RJ. 1980. Evoked acoustical emissions from the human ear: Some experimental results. *Hear Res* 2, 253–261.

Yates, GK, Winter, IM, Robertson, D. 1990. Basilar membrane nonlinearity determines auditory nerve rate-intensity functions and cochlear dynamic range. *Hear Res* 45, 203–220.

Zajic, G, Schacht, J. 1991. Shape changes in isolated outer hair cells: Measurements with attached microspheres. *Hear Res* 407–411.

Zenner, HP, Zimmerman, U, Schmitt, U. 1985. Reversible contraction of isolated mammalian cochlear hair cells. *Hear Res* 18, 127–133.

Zheng, J, Shen, W, He, DZZ, Long, K, Madison, LD, Dallos, P. 2000. Prestin is the motor protein of cochlear outer hair cells. *Nature* 405, 149–155.

Zurek, PM. 1981. Spontaneous narrow-band acoustic signals emitted by human ears. *J Acoust Soc Am* 69, 514–523.

Zurek, PM. 1985. Acoustic emissions from the ear: A summary of results from humans and animals. *J Acoust Soc Am* 78, 340–344.

Zwislocki, J. 1974. A possible neuro-mechanical sound analysis in the cochlea. *Acustica* 31, 354–359.

Zwislocki, J. 1975. Phase opposition between inner and outer hair cells and auditory sound analysis. *Audiology* 14, 443–455.

Zwislocki, J. 1985. Cochlear function—An analysis. *Acta Otol* 100, 201–209.